Analyzing the Transcriptional Landscape of Glial Cells Across the Human Lifespan Using Single Cell RNA Sequencing

Moein Yaqubi

Faculty of Medicine, Integrated Program in Neuroscience (IPN), McGill University, Montreal, Quebec, Canada
August 2021

A thesis submitted to McGill University in partial fulfillment of the requirements of the degree of Doctor of Philosophy (Ph.D.)

Table of Contents

Abstract:

Glial cells of the central nervous system including oligodendrocyte (OL) lineage cells and microglia are non-neuronal cells which are critically important for the maintenance of brain homeostasis. Loss of these homeostatic functions or gain of toxic functions can underlie a wide range of neurological disorders including multiple sclerosis. The majority of glia research has been carried out using model organisms with a particular focus on the rodent system. Consequently, a detailed understanding of glia origin and function in the human brain is lacking. In-depth transcriptomic analysis of glia can provide an opportunity to understand the molecular mechanisms governing the activity of these cells in health, and this may inform our understanding of how these cells contribute to disease. In this study, we accessed human OL lineage cells and microglia from resected brain tissue and studied these cells using high throughput techniques such as microarray and single cell RNA sequencing. We characterized different cell types of the OL lineage including early OL progenitor cells (e-OPCs), late-OL progenitor cells (l-OPCs) and mature oligodendrocytes (MOLs) in humans at different developmental ages. A critically important time point included in our study was that of early post-natal age in which a peak of myelination occurs. At the functional level we revealed progenitor cells have great capacity to ensheath nanofibers, an in vitro model of myelination potential. We also explored spatial heterogeneity of MOLs across three anatomical location of CNS and showed there were transcriptionally distinct sub-types of MOLs which showed region specific distribution pattern. Our analysis indicated that spinal cord MOLs have a distinct expression signature which provide them more immunogenic features compared to brain cells. Microglia were subjected to a detailed single cell RNA sequencing analysis, here we showed that pre-natal microglia have a distinct transcriptional and regulatory signature relative to its post-natal counterpart that includes an upregulation of phagocytic pathways. Trajectory analysis indicated that the transcriptional signatures adopted by microglia throughout development are in response to changing microenvironments and do not reflect predetermined developmental states. Finally, having compared our human microglia dataset to an equivalent mouse dataset we found that post-natal human microglia acquire a mature signature more quickly than their mouse counterparts. This analysis imparts unique insights into the development of human microglia and provides a reference for understanding the contribution of microglia to developmental and age-related human disease. In all, the results presented in my study, for the first time, provide data on glia cell development at a single cell level across the human lifetime including from an early post-natal age, previously not examined by the scientific community.

Résumé:

Les cellules gliales du système nerveux central, y compris les cellules de la lignée oligodendrocytes et la microglie, sont des cellules non neuronales qui sont d'une importance critique pour le maintien de l'homéostasie cérébrale. La perte de ces fonctions homéostatiques ou le gain de fonctions toxiques peuvent être à l'origine d'un large éventail de troubles neurologiques, y compris la sclérose en plaques. La majorité des recherches sur la glie ont été réalisées à l'aide d'organismes modèles avec un accent particulier sur le système des rongeurs. Par conséquent, une compréhension détaillée de l'origine et de la fonction de la glie dans le cerveau humain fait défaut. Une analyse transcriptomique approfondie de la glie peut fournir une opportunité de comprendre le mécanisme moléculaire régissant l'activité de ces cellules en bonne santé, et cela peut éclairer notre compréhension de la façon dont ces cellules contribuent à la maladie. Dans cette étude, nous avons accédé à des cellules de la lignée des oligodendrocytes humains et à des microglies à partir de tissus cérébraux réséqués et avons étudié ces cellules à l'aide de techniques à haut débit telles que le séquençage de puces à ADN et d'ARN à cellule unique. Nous avons caractérisé différents types cellulaires de lignées d'oligodendrocytes, y compris les cellules progénitrices d'oligodendrocytes précoces (e-OPC), les cellules progénitrices d'oligodendrocytes tardifs (l-OPC) et les oligodendrocytes matures (MOLs) chez l'homme à différents âges de développement. Un point de temps d'une importance critique inclus dans notre étude était celui de l'âge post-natal précoce au cours duquel un pic de myélinisation se produit. Au niveau fonctionnel, nous avons également révélé que les cellules progénitrices ont une grande capacité à envelopper des nanofibres, un modèle in vitro du potentiel de myélinisation. La microglie a été soumise à une analyse détaillée du séquençage de l'ARN monocellulaire. Nous avons également exploré l'hétérogénéité spatiale des MOL sur trois emplacements anatomiques du SNC et avons montré qu'il existait des sous-types de MOL distincts sur le plan transcriptionnel qui présentaient un modèle de distribution spécifique à la région. Notre analyse a indiqué que les MOL de la moelle épinière ont une signature d'expression distincte qui leur confère plus de caractéristiques immunogènes que les MOL du cerveau. Nous avons montré ici que la microglie prénatale a une signature transcriptionnelle et régulatrice distincte par rapport à son homologue postnatale qui comprend une régulation positive des voies phagocytaires. L'analyse de trajectoire a indiqué que les signatures transcriptionnelles adoptées par la microglie tout au long du développement sont en réponse à des microenvironnements changeants et ne reflètent pas des états de développement prédéterminés. Enfin, après avoir comparé notre/mon ensemble de données sur la microglie humaine à un ensemble de données équivalent sur la souris, nous constatons/je constate que la microglie humaine post-natale acquiert une signature mature plus rapidement que ses homologues murins. Cette analyse donne des informations uniques sur le développement de la microglie humaine et fournit une référence pour comprendre la contribution de la microglie aux maladies humaines liées au développement et à l'âge. Dans l'ensemble, les résultats présentés dans mon étude, pour la première fois, fournissent des données sur le développement des cellules gliales à un niveau cellulaire unique tout au long de la vie humaine, y compris à partir d'un âge postnatal précoce, qui n'avaient pas été examinées auparavant par la communauté scientifique.

Acknowledgements:

I would like to express my deepest gratitude to my supervisors, Dr. Luke Healy and Dr. Jack Antel for their mentorship and never ending patience. They graciously accepted me as their graduate student in the middle of a crisis in my graduation journey in which I had to change my lab. Through their unwavering support they thought me how to think critically, and more importantly how to do research in a collaborative way. I specifically thank them for always being available to meet despite their busy schedule. I found them extraordinarily professional and supportive supervisors.

I would like to thank all my colleagues in Healy and Antel lab who made my PhD a great and fun experience. Specifically, to our amazing lab manager Manon Blain and all other research assistants, graduate, undergraduate and visiting students of the lab including Nicholas Kieran, Julia Luo, Kelly Perlman, Marie-France Dorion, Jinar Rostami, Florian Pernin, Qiao-Ling Cui, Mahshad Kolahdouzan, Naomi Futhey, Sara Sedaghat, Milton Fernandes for their help, advice, support stimulating discussions.

Thank to my committee members Dr. Timothy Kenedy and Dr. Ioaniss Ragoussis whose input and constructive guidance helped me to shape my projects.

Thanks to all neuro-immunology unit members by making lab to such a lovely place to work. I would also like to thank Dr' Jo Anne Straton and her team particularly Adam Groh for all constructive advices and supports.

Last, but not least, I am grateful of my wife Niusha, my friend Shakour and all my family back in Iran who supported me in every single step of my graduation. I never could have finished my PhD without their help.

Preface and Contribution of authors

Contribution to original knowledge and contribution of authors

All concepts, analyses, results, text, and interpretations presented in this thesis represent original scholarship.

Preface:

I joined Integrated Program in Neuroscience (IPN) at McGill University in January 2016. I started my PhD under the supervision of Dr. Michael Meaney. After 2.5 years and due to reasons outside of my control I had to change my lab. In this regard, I joined the labs of Dr. Luke Healy and Dr. Jack Antel in May 2018 and started my PhD from scratch in the new field of neuro-immunology, I was given 3.5 years to complete my PhD degree. The content of this thesis is as a result of my research efforts during the past 3 years.

Contribution of authors:

My thesis is presented in 2 main results chapters. The first chapter (chapter 2) is dedicated to characterizing human oligodendrocyte progenitor cells at expression and functional levels (2.1) in addition to a study of the temporal (2.2.1) and spatial characterization (2.2.2) of oligodendrocyte lineage cells in human development at single cell level. The second chapter (chapter 3) is dedicated to characterizing microglia during human development.

Chapter 2.1: Distinct function-related molecular profile of adult human A2B5-positive pre-oligodendrocytes versus mature oligodendrocytes

The result of this sub-part is published in the form of following paper in Journal of Neuropathology & Experimental Neurology. *I am a co-first author on this manuscript.

Caroline Esmonde-White, Moein Yaqubi*, Philippe A. Bilodeau, Qiao Ling Cui, Florian Pernin, Catherine Larochelle, Mahtab Ghadiri, Yu Kang T Xu, Timothy E. Kennedy, Jeffery Hall, Luke M. Healy, Jack P. Antel (2019) Distinct function-related molecular profile of adult human A2B5-positive pre-oligodendrocytes versus mature oligodendrocytes. Journal of Neuropathology & Experimental Neurology, 78, 468–479.*

When I joined to the lab, I got involved in an ongoing project in which all the cellular experiments were done by my colleagues in the lab. My contribution to this work, was analyzing all the gene expression data, running all the subsequent bioinformatics analyses such as biological pathway analysis, interpreting the findings, and providing figures and corresponding text for the paper. Overall author contributions are as follow:

Caroline Esmonde-White: Involved in conception of the study, data analysis, data interpretation drafting of the manuscript
Philippe A. Bilodeau: Drafting of the manuscript, data interpretation
Qiao Ling Cui: Performed in vitro experiment including immunocytochemistry, flow cytometry, qPCR.
Florian Pernin: Performed cell isolation from brain tissue
Catherine Larochelle: Data interpretation
Mahtab Ghadiri: Statistical support and graph generation
Yu Kang T Xu: Analyzed axon ensheathment data
Timothy E. Kennedy: Provided scientific guidance for data interpretation
Jeffery Hall: Designed protocol to provide adult surgical samples.
Luke M. Healy: Provided scientific guidance for data interpretation.
Jack P. Antel: Designed the experiment, provided scientific guidance for data interpretation and writing the draft

Chapter 2.2: Temporal (2.2.1) and spatial (2.2.2) transcriptional landscape of oligodendrocyte lineage cells in the human CNS revealed by single cell RNA sequencing
In the first section of this chapter the result of the study of the temporal heterogeneity of oligodendrocyte lineage cells is represented (2.2.1). The content of this section is published in the form of following paper in Glia journal in which I am the third author. In the second section of this chapter (2.2.2), I present the results of an exploration of the spatial heterogeneity of mature oligodendrocyte cells. **I am the primary contributor to this section**. The results from these analyses are under preparation to be submitted in the coming weeks.

Kelly Perlman, Charles P. Couturier, Moein Yaqubi, Arnaud Tanti, Qiao-Ling Cui1, Florian Pernin, Jo Anne Stratton, Jiannis Ragoussis, Luke Healy, Kevin Petrecca, Roy Dudley, Myriam Srour, Jeffrey A. Hall, Timothy E. Kennedy, Naguib Mechawar, Jack P. Antel (2020) Developmental trajectory of oligodendrocyte progenitor cells in the human brain revealed by single cell RNA sequencing. Glia, 68, 1291-1303.

2.2.1 I was involved in single cell RNAseq data analysis, transcription factor binding site and gene regulatory network analysis, providing figures for these parts and write corresponding parts of draft. Overall author contributions are as follow:

Kelly Perlman: Analyzing single cell RNAseq data, Diffusion pseudotime analysis, RNAscope and proving the figures of corresponding parts.
Charles P. Couturier: Developing the pipeline for analyzing single cell RNAseq data
Arnaud Tanti: Technical guidance for RNAscope
Qiao-Ling Cui: Performed cell isolation from brain tissue
Florian Pernin: Performed cell isolation from brain tissue
Jo Anne Stratton: Provided scientific guidance for data interpretation
Ioannis Ragoussis: Sample sequencing, technical advice
Luke Healy: Provided scientific guidance for data interpretation
Kevin Petrecca: Designed protocol, provided adult surgical samples
Roy Dudley: Designed protocol, provided pediatric surgical samples
Myriam Srour: Designed protocol, provided pediatric surgical samples
Jeffrey A. Hall: Designed protocol, provided adult surgical samples
Timothy E. Kennedy: Provided scientific guidance for data interpretation
Naguib Mechawar: Technical guidance for RNAscope.
Jack P. Antel: Designed the experiment, provided scientific guidance for data interpretation and writing the draft

Chapter 3: Analysis of the microglia transcriptome across the human lifespan using single cell RNA sequencing

Data from this chapter is currently under review in Cell Reports with a manuscript number of CELL-REPORTS-D-21-04040. I am the first author of this paper.

Moein Yaqubi, Julia Xiao Xuan Luo, Hadi Hashemi, Sarthak Sinha, Nicholas W. Kieran, Marie-France Dorion, Manon Blain, Qiao-Ling Cui, Jeff Biernaskie, Myriam Srour, Roy Dudley, Jeffery A. Hall, Jack Antel, Luke M. Healy

For this chapter, I conceived the project, conducted all analyses, interpretated the results, produced the figures and wrote the manuscript with the guidance of Dr. Luke Healy and Dr. Jack Antel. Overall author contributions are as follow:

Julia Xiao Xuan Luo: Assisted with pseudo-time trajectory analysis.

Hadi Hashemi: Technical guidance for generation of bioinformatics script

Sarthak Sinha: Assisted with gene regulatory network analysis

Nicholas W. Kieran: Drafting the manuscript and data interpretation

Marie-France Dorion: Performed cell isolation from brain tissue

Manon Blain: Performed cell isolation from brain tissue, technical support

Qiao-Ling Cui: Performed cell isolation from brain tissue, technical support

Jeff Biernaskie: Assisted with gene regulatory network analysis

Myriam Srour: Designed protocol to provide pediatric surgical samples

Roy Dudley: Designed protocol, provided pediatric surgical samples, critical revision of manuscript

Jeffery A. Hall: Designed protocol, provided adult surgical samples

Jack Antel: Provided scientific guidance for data interpretation and financial support

Luke M. Healy: Designed the experiment, provided scientific guidance for data interpretation, figure presentation and writing the draft.

Chapter 1

Introduction and literature Review

Introduction:

Glial cells such as microglia, astrocytes, and oligodendrocyte (OL) lineage cells are major cell types in the central nervous system (CNS). Multiple lines of evidence have revealed that besides supporting neurons, they are critically important for normal brain function and are extensively involved in the pathophysiology of neurological disorders. Even though many biological aspects of these cell have been uncovered in the past decade, a detailed understanding of their functions under physiological conditions has yet to be determined. Understanding the function of glial cells requires a deep understanding of the mechanisms controlling their activity at a molecular level. In this regard, analyses of the transcriptomic content of these cells provides direct insight into the diverse functions of glial cells.

Animal studies have played a central role in the development of lifesaving medical interventions, with virtually every pharmaceutical on the market having gone through a pre-clinical animal testing phase. Animals have taught us a huge amount about human physiology and cellular function. Their genetic continuity, low cost and huge array of well-validated reagents and behavioral testing paradigms have thus given rodents a centralized role in basic science research [1,2]. However, it has been shown that only one out of ten studies showing positive results in animals will subsequently lead to an approved therapy for the treatment of human disease [3].
In evolutionary terms, rodents and humans diverged over 65 million years ago. Factors that contribute to the poor predictive value of findings in animals include their development in a semi-sterile environment, their extensive in-breeding, the sterility, and the lack of variety in their diet. In particular, the immune system may be the most sensitive to evolutionary change, with human subjects receiving exposure to a wide array of pathogens throughout life, while lab rodents are raised in a highly controlled environment. Concerns regarding the failure of translation for animal model findings go beyond efficacy and permeate into the realm of safety. Famous cases include that of thalidomide, which was an antiemetic that was deemed safe for use in humans following toxicity testing in animals [4]. Prescribed to pregnant mothers to treat morning sickness, it eventually led to death of an estimated 2,000 children and serious birth defects in a further 10,000. This critical interspecies different was attributed to an enhanced metabolic breakdown of the compound in rodents, to enhanced antioxidant defenses in rodent embryos and to a vastly different

'critical period' with respect to thalidomide sensitivity between the two species. This difference also goes the other way, with corticosteroids having widespread teratogenic effects in animals but not in humans [4]. It is also not just rodents that display considerable species differences with humans, leading to major safety concerns. Leukemia drug TGN1412, successfully completed testing in non-human primates and was well tolerated. It subsequently entered a human phase I clinical trial where 1/500th of the safe monkey dose was given to 6 healthy volunteers. Within hours it had caused life-threatening morbidity in all 6 volunteers characterized by massive cytokine storm and multiple organ failure [5]. Differences between the species are not just pharmacological: a comprehensive study on the basic genomic changes caused by common inflammatory conditions such as trauma, endotoxemia and burns showed very poor correlation between rodents and humans [6].

There is an ongoing interest in neuro-immunological and neurodegenerative disease and how glial cells play a role in both contributing to, and driving, the progression of such conditions. To have a better understanding about the role of human glial cells in CNS, we require a clear understanding of their development and their heterogeneity in resting and disease states. The majority of human studies on CNS tissue has so far focused on either post-mortem fixed tissues or human fetal tissue, [7] with limited studies on human adult brain tissue [8,9]. However, there is an important missing stage in the development of cells, which is the 'pediatric' or early life stage. Early life is not just an important time for the development of an organism as a whole, but is an equally crucial time for the development of glial cells. This is especially the case for OL development, since the peak of myelination occurs during this time period [10]. There is no study to date that has considered the developmental trajectory of human microglia and OL lineage all the way from fetal to early life and into adulthood.

To provide more accurate insight into the pathology of complex neurological diseases, we first need to understand the development of basic signatures of primary human glia from the human CNS. The main two cell types that we have access to in our lab are OL lineage cells and microglia. Therefore, the result of my thesis is separated into two major chapters: one of which is dedicated to the OL lineage cells and the other to microglia.

Literature review

History of the oligodendrocyte

Oligodendrocytes (OLs) are myelin-forming cells of the central nervous system (CNS) which function to insulate the axonal segments of neurons, which is required for the saltatory conduction of electrical impulses. The study of these cells began in the early years of 20th century by Pío Del Río Hortega who revolutionized the study of neuroglial cells by developing specific staining techniques to study non-astrocytic cells of the CNS [11]. During this time, CNS cells were broadly categorized into three main groups: the first and second groups were called "first and second element", corresponding to neurons and astrocytes, respectively [12]. OLs and microglia belonged to a group referred to as the "third element" [12]. Del Río Hortega later modified the classic staining methods, and for the first time proposed that the OL and astrocyte belong to the same group of cells whereas microglia have a separate origin – although he mistakenly suggested mesodermal origin for this cell type [13,14]. The concept of the "third element" was further confirmed and expanded by the studies of Wilder Penfield who was a visiting scientist in the lab of Del Río Hortega at that time [15].

Development of oligodendrocyte lineage cells

Transcription regulation machinery of the OL lineage development is primarily determined by the cross-regulation of different transcription factor (TF) families. During development, the generation of OL lineage cells starts with the differentiation of neuroepithelial progenitors (NEPs), which are capable of making OL lineage cells, in addition to neurons and astrocytes [16]. Since these cells undergo neuronal differentiation under default conditions, these neuronal development pathways must first be blocked in order for them to differentiate towards OL lineage fate (Figure 1A). One of the most important regulators of this process is the OL lineage transcription factor (OLIG) family which mainly exerts its function by the activity of OL lineage transcription factor 2 (*OLIG2*) and OL lineage transcription factor 1 (*OLIG1*). This TF family and more specifically *OLIG*2 have been studied extensively and it has been indicated that *OLIG2* activity is critically important for OL generation and its deficiency leads to OPCs loss in the spinal cord and brain [17,18]. In contrast to *Olig2*, more recent studies show that *Olig1* plays a minor and non-essential role in OL development and that its deficiency might be compensated by over-activation of *Olig2* [19]. *Olig2* represses the activity of the NK2 Homeobox 2 (*Nkx2.2*) which has a pro-neuronal function at the

NEPs stage (figure 1A) [20]. Pro-neuronal pathways are also inhibited by activity of Achaete-Scute Family BHLH Transcription Factor 1 (*Ascl1*) which is called *Mash1* as well. *Ascl1* exerts its function by repressing neuronal TF like Distal-Less Homeobox 1 (*Dlx1*) and Distal-Less Homeobox 2 (*Dlx2*) (Figure 1A) [21]. It has been indicated that *Ascl1* operates in conjugation with *Olig2* during OPC specification in the embryonic telencephalon, and the loss of *Ascl1* function reduces embryonic oligodendrogenesis [22]. Even though earlier studies confirms *Ascl1* has a role in specification of OPC and also terminal differentiation of OLs by its interaction with *Olig2* and *Nkx2*.2 [23], a recent study has shown that *Ascl1* is an intrinsic regulator of proliferative properties of OPC and not its differentiation (Figure 1A).

In order to fully commit to OL lineage, other TFs need to be recruited to make pre-OPC/committed OPCs which are also classified as NG2-positive cells [24]. A critical function of *Olig2* at this stage is regulating expression of SRY-Box Transcription Factor 10 (*Sox10)* which is mandatory for specification of committed OPCs (Figure 1B) [25]. *Sox10* controls the expression of a set of canonical TFs whose function is crucial for the proper development of OLs. Once expression of *Sox10* is established, there is extensive cross-regulation between this factor and *Olig2,* forming a positive feedback loop (Figure 2B) [26]. Moreover, alternative mechanisms control the activity of *Sox10* and *Olig2*. For example, *Sox10* has inhibitory effects on *Olig2* by activating expression of *Nfat2c* [26]. To keep the OPCs at their progenitor state, there is an extensive cooperation between *Olig2*, *Sox10* and other factors. Such factors include: inhibitor of differentiation (ID) proteins, Hes Family BHLH Transcription Factor 5 (*HES5*), SOXD family of TF like SRY-Box Transcription Factor 5 (*Sox5*), SRY-Box Transcription Factor 6 (*Sox6*) and SRY-Box Transcription Factor 13 (*Sox13*) (Figure 1B).

Id2 and *Id4* negatively regulate differentiation of OLs by keeping the OPCs in their progenitor state [27]. These proteins exert their function by directly interacting with OLIG1/2 proteins and indirectly by sequestering Transcription Factor 3 (*E2A/TCF3)* gene splice products E12 and E47 which are OLIG1/2-associated proteins [27]. *Hes5* has high expression at the early stage of OPC formation and interacts with *Sox10* to prevents expression of genes that are mandatory for starting OPC differentiation and therefore retains the OPC at their progenitor state (Figure 1B) [28]. SoxD family of TFs and more specifically *Sox6* and *Sox5* have been shown to interact with *Sox10* to promote expression of pdgf receptor alpha (*Pdgfra*) in the OPC and therefore keep that at its

progenitor state [29]. SRY-Box Transcription Factor 9 (*Sox9*) on the other hand, is a well-established factor which determines the early fate determination of glial cell by promoting NSCs to differentiate into OLs (Figure 1B) [30]. Recent studies using more computational and advanced technique like single-cell RNA-seq and pseudotime analysis confirmed that expression of *Sox9* reduces during development of OLs. This highlights the role of this factor in the early phase of OL development [31]. To accomplish this function, *Sox9* cooperates with Nuclear Factor I A (*NFIA*) to control expression of genes that are required for early phase of gliogenesis [32]. SRY-Box Transcription Factor 8 (*Sox8*) is another factor which is demonstrated to be a critical factor in maintaining myelination state in the differentiated OLs by cooperating with *Sox10*. Conditional deletion of both *Sox8* and *Sox10* results in loss of *Plp1*+ mature OL [33]. *Sox8* targets a wide range of the genes, but myelin oligodendrocyte glycoprotein *Mog* has been shown to be the main target gene for this TF [33].

While the factors that maintain OPC progenitor states are crucial, other stage-specific factors remain needed to produce fully differentiated OLs. SRY-Box Transcription Factor 8 (*Sox17)* is required to control expansion of OPCs and promote its maturation toward pre-OLs and finally mature OLs. Notch signaling pathway is the main signaling pathway, which is regulated by *Sox17* and helps expansion of the OPCs (Figure 1C) [34]. Furthermore, one major TF that is also regulated by *Sox17* is Transcription Factor 7 Like 2 (*Tcf7l2*) [34], which removes the inhibitory effect of Wnt signaling pathway on OPCs at the onset of differentiation [35,36], and thus facilitates differentiation of OPCs to pre-OLs. Later on, *Tcf7l2* binds to *Sox10* and *Olig2* to promote the final stage of OL maturation [35,36]. *Tcf7l2* changes the interacting partners to regulate OL formation during development. At the OPC state, *Tcf7l2* in conjugation with beta-catenin represses expression of myelin-related genes through Wnt signaling pathway. However, upon onset of differentiation, *Tcf7l2* begins to partner with Zinc Finger And BTB Domain Containing 33 (*Zbtb33*) and *Sox10* to facilitate differentiation toward mature OL (Figure 1C) [35]. *Zbtb33* is a transcriptional repressor of the Wnt signaling pathway which has an oscillatory expression pattern during OL development. The expression of *Zbtb33* increases at the onset of OPC differentiation and reaches the highest expression at the stage of pre-OL, and finally decreases at the end stage stage of OL maturation [35]. Moreover, *Tcf7l2* expression is affected by *Yy1* transcription factor, which regulates transition from progenitors into myelinating OLs by facilitating the cell cycle exit for the OPCs [37]. Conditional deletion of the *Yy1* results in blocking the transition from OPC

toward mature OL. It seems *Yy1* along with Zinc Finger E-Box Binding Homeobox 2 (*Zeb2*) inhibit the activity of *Id4* and *Tcf7l2* which keeps the OPCs in their proliferative states (Figure 1) [37,38]. *Tcf7l2* and *Sox10* activate expression of an important gene for the final stage of OL maturation, called Myelin Regulatory Factor (*Myrf*). *Myrf* induces the expression of genes that are necessary for myelin formation (Figure 1C) [39]. Once induced by *Sox10, Myrf* represses expression of *Sox10* in the form of negative feedback loop and therefore represses expression of genes that keep OPCs in their progenitor state [39]. Furthermore, *Myrf*, and *Sox10* have interaction with another critically important factor called Zinc Finger Protein 24 (*Zfp24*) which binds to the promotor region of *Sox10* and Myelin Basic Protein (*Mbp*) genes and thus is required for their expression [40]. However, the main factor which modulates the function of *Zfp24* is *Myrf* (figure 1C), because it is indicated that over-expression of *Myrf* in *Zfp24*-null-derived OL lineage cells, results in over-expression of *Mbp* (as a maker of mature OLs) which had been decreased four fold in Zfp24-null OLs [40]. *Sox10* targets another important group of proteins called Nuclear factor of activated T-cells (NFAT) proteins, for which their activity depends on calcium signaling and act to positively regulate differentiation of OL lineage cells [26]. Among various proteins of this family, NFAT2C has the most obvious effect on OL differentiation. The main function of *Nfat2c* is removing the reciprocal repression of *Olig2* and *Nkx2.2* which is a mandatory step for OL differentiation and myelination (Figure 1C) [26].

NKX homeobox family of TFs have a significant role in establishing the correct timing of OL development. For example, at the later stage of OPC differentiation it has been indicate that Nkx2.2 repress expression of Pdgfra and accelerate maturation of OLs (figure 1D). To do that, Nkx2.2 recruits transcriptional co-repressors such as Histone Deacetylase 1 (HDAC1) and DNA Methyltransferase 3 Alpha (DNMT3A) which already being expressed at the OPC [41]. Another member of this family of TFs is NKX6.2, whose overexpression helps commitment of progenitor cells to OL lineage during differentiation of helps induced pluripotent stem cells toward mature OLs (Figure 1D) [42]. Furthermore, it has been indicated that Nkx6.2 and Nkx2.2 are both up-regulated in mature myelinating OLs at the later stages of development, which supports their collaborative mode of action in gene expression regulation for the final stage of development [43]. Nkx6.2 represses the expression of the Sox10 at specification and differentiation steps of OL development and therefore keeps activity of Sox10 limited to the OPC state. By inhibiting the

activity of Sox10 at the maturation step, Nkx6.2 facilitates expression of genes that are mandatory for final stages of OL development [25].

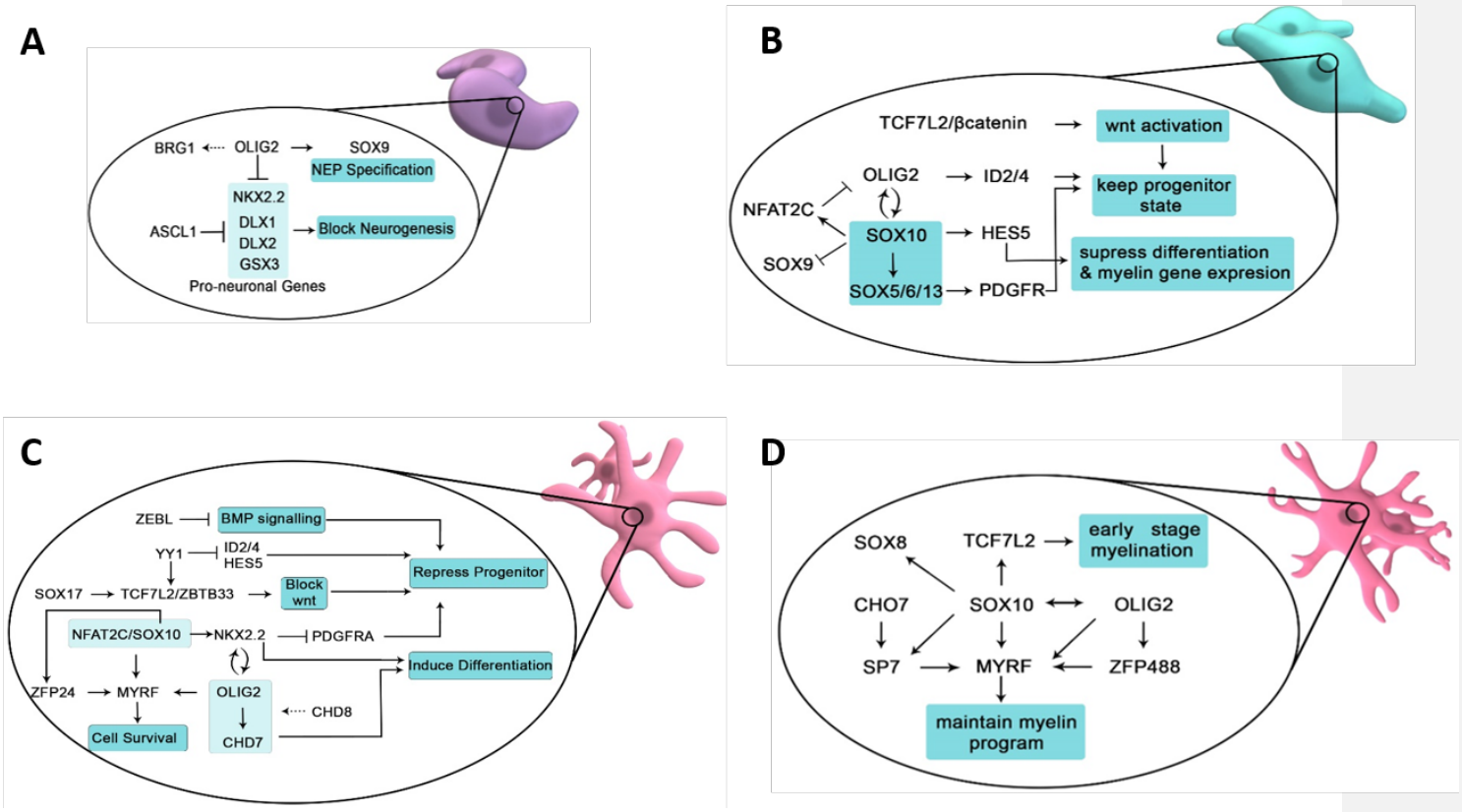

Figure 1:
Schematic overview of gene expression regulation during development of oligodendrocyte (OL) lineage cells. Development of OL lineage contain four distinct cellular stages including start with specification of neuroepithelial (NEP) cells (A), appearance of OL progenitor cells (OPCs) (B), specification of OPCs to pre-OLs (C) and finally appearance of mature myelinating OLs (D). The dashed line arrows indicate the factors are being recruited to the site of expression regulation. The light blue box around TFs indicates those proteins exert their function in the form of a complex

Myelination and remyelination

The myelination of axons is one of the crucial developmental steps to facilitate cognitive, sensory and motor development throughout the lifespan of individuals. Dynamic expansion and activity of OL populations in the first few years after birth is responsible for neuron insulation in the human brain, which is especially important given that humans are born with unmyelinated axons [44]. The process of axon myelination continues into the adolescent stage in a spatiotemporal manner which is correlated with emergence and maintenance of proper circuit function [45]. It has been indicated that the sheath number, length, and thickness of myelin differs between and within different parts of the same axon, thereby greatly affecting the speed of signal conductance [46]. It has recently been indicated that myelin abundance can be influenced by neuronal activity. For example, it has been shown that learning a new skill can change myelination pattern of axons in white matter parts of brain in human and rodent [47,48]. Furthermore, it is currently believed that neural activity influences the proliferation of OPCs, the differentiation of mature OLs, and the formation of myelin sheaths around axons [49,50].

Remyelination of axons which have lost their myelin sheath is a regenerative process through which demyelinated axons become newly ensheathed [51]. Demyelination of axon tracts can occur through two primary mechanisms: genetic abnormalities can cause malfunctions of glial cells (leukodystrophy), or inflammatory damage can damage the myelin and OLs. Adult-onset leukoencephalopathies and Multiple Sclerosis (MS) are prime examples of these two major types of demyelination. The focus of remyelination research relies on its role as an important outcome determinant of neurodegenerative diseases like MS, for which demyelination is a hallmark.

One significant outcome of demyelination is changing the ionic balance across the neuronal membrane by exposing ion channels which had previously been covered by myelin [52]. One suggested mechanism to compensate for the ionic imbalance is to upregulate voltage-gated sodium channels along their length [53]. However, such mechanisms cannot fully recover the efficacy of neurons for salutatory conductance [54]. The functional outcomes of demyelination are dictated primarily by two factors: the extent and the severity of demyelination sites [55,56].

A critical outcome of remyelination is maintaining the integrity of the axons. It has been indicated that ablating OPC populations in mice results in slowing down the remyelination and therefore

promoting axonal degeneration [57]. Furthermore, accelerating remyelination by promoting OL differentiation in a cell-specific manner results in preserving more axons [58]. Myelin protects axons through multiple mechanisms. One such mechanism is through the potassium ion channel KIR4.1; conditional knockout of KIR4.1 in OLs has been shown to result in axonal degeneration [59]. The myelin sheath is a platform to deliver metabolic products generated by OLs to the axons [60,61]. Of the produced metabolites, insulin-like growth factors have been shown to be of great importance for protecting axons [62]. Myelin sheaths provide a protective barrier by shielding the axon from reactive oxygen species [63,64].

Currently there are two major opinions regarding the molecular mechanisms and cell types controlling the remyelination process. It has traditionally been believed that the first source of new myelin is produced by newly generated OLs following the recruitment and development of OPCs at the site of injury [51,65]. Transplantation of OPCs into the demyelinated regions can restore the myelin layer of axons [66,67]. Following an injury to the myelin layer around axons, OPCs migrate to the site of insult and start to express necessary TFs for their differentiation, which includes *Nkx2.2, Olig2, Sox2* and *Myrf* [68–70]. A combination of TFs and growth factors like IGF1 and FGF present in the lesion microenvironment are thought to regulate migration and proliferation of OPCs toward the lesion site [71]. High-throughput technologies like single-cell and single-nuclear RNA-sequencing have shown that remyelinating OLs in MS lesions have a unique phenotype [72]. This difference might be attributable to the different transcriptomic profiles of these cells and those found in healthy brain tissue [72]. The second suggested source of new myelin is through the activity of those mature OLs that survived demyelination. This mechanism was originally underestimated due the fact that these cells are post-mitotic and therefore cannot divide nor can they effectively migrate since their myelin sheaths are engaged with neuronal membranes [73]. Transplantation and fate mapping experiments show that mature OLs do not engage in remyelination in rodents [65,74]. Surprisingly, newer studies have shown that mature cells can participate in myelination in larger animals in the form of thin and thick myelin layers [56]. The shape and thickness of the myelin layer can provide information about the myelinating cells in the lesion. For instance, the thick myelin layer around remyelinated regions might suggest that there are OLs that survived an insult and can re-extend their processes and remyelinate adjacent denuded axons [56]. In a recent study, Yeung et al. (2019) investigated oligodendrogenesis in humans with

MS using a specific carbon dating strategy [75]. Using this strategy, the authors measured new OL production in regions that are considered intermediate remyelinated and are called “shadow plaques”. Interestingly, the amount of newly generated OLs in the shadow plaques is proportionate to the non-diseased brain, suggesting that in humans, the mature OLs can remyelinate denuded axons [75]. However, these findings need to be approved on a cohort with larger sample sizes and the technique must be optimized for application in younger MS patients. Therefore, the question of whether adult OLs can remyelinate will require further validation in future studies.

Physiological function of different oligodendrocyte lineage cell

Among all glial cells in CNS, NG2-positive cells are relatively young cells which were discovered in 1986 years prior to the identification of other glia cells [76]. An array of studies elucidated their OL lineage and their key role in generating mature myelinating OL throughout life [77,78]. The most important biological feature of these cells is that they are multipotent stem cells, capable of constantly replenishing the mature OL population that is susceptible to cell death [79]. Another key hallmark of these cells is their ability to unidirectionally synapse with neurons in a spatiotemporal specific manner at different brain regions [80,81]. The existence of these cells in brain regions partially myelinated, such as gray matter of the cerebral cortex, raise the intriguing possibility that OL lineage cells may confer more specific biological function in addition to its canonical role in myelination. In this regard, ablating NG2-positive cells, which is rather challenging as opposed to other glial cells, has been proposed to dissect the role of OL lineage cells in the brain. The difficulty in studying these progenitor cells lies in their tight homeostatic control and rapid replenishing capacity in response to cellular ablation [79].

First ablation studies highlighted the repopulation capacity of the NG2-positive cells. However, more recent studies have shown that these cells have a direct influence on the activity of the neuronal network of the CNS by secreting fibroblast growth factor 2 (FGF2) which influences transmission of glutamatergic neurons. Furthermore, FGF2 affects glutamate uptake capacity of the astrocyte [82].The role of NG2-positive cells in the maintenance of the thalamic energy metabolism was evidenced by a separate study using three distinct approaches of NG2 ablation [83]. In this study, the authors indicated that under the physiological condition NG2-positive cells synapse with the leptin-expressing neurons [83], which are implicated in integrative circadian

control of feeding and energy metabolism in the dorsomedial hypothalamic nucleus [84]. Therefore, through direct signaling to leptin-expressing neurons, NG2-positive cells modulate energy metabolism of the brain. In the case of mature OLs, as expected, ablation studies reported a common observation in which the death of mature myelinating OLs leads to primary demyelination of the axons, reviewed comprehensively in the study of Jakel and Dimou [85] .

Transcriptome analysis of oligodendrocyte lineage cells at bulk and single cell level

The accessibility of the human whole genome sequence since 2001 render large-scale transcriptomic analysis a powerful tool to study cell biology at a greater depth [86]. The output of the different transcriptomic technologies is a list of genes differentially expressed between two conditions. Such list can be used to determine if a similar pattern in publicly available dataset exists, to highlight key markers; and to perform pathway enrichment analyses which will associate the differentially expressed genes with known gene ontology (GO) terms in each of these categories: biological cellular processes, molecular function and subcellular compartment expression. Over the past decade, transcriptomic analyses of OL lineage cells have been studied using microarray technique and RNA sequencing both at bulk and single cell levels. One of the first attempt to profile gene expression signatures of different CNS cell types including OL was from Ben Barres group using microarray [87]. The same group expanded the idea of characterizing different cell types of OL lineage cell using bulk RNA sequencing and characterized post-natal OPCs, newly-formed OLs and myelinating OLs [88]. More importantly, more recent microarray studies aimed to understand OPCs biology in a diseased context using mouse models [89]. Hence, microarray and bulk RNAseq techniques have been pivotal in shedding light regarding particular cell type of interest. However, they are restricted at quantifying the average signal of a bulk cell population. Advent of single cell RNA sequencing has enabled researchers to explore the granularity between cells of the same cell population. Thus, in the following part I will mainly review literature of transcriptional profiling of OL lineage cells in mouse and human using single cell technology.

Transcriptomic analysis of oligodendrocyte lineage cells in mouse

One of the first studies that explored transcriptional heterogeneity of the CNS cells including OL lineage cells was conducted by Linnarsson's *et al*.[90]. In this study, the authors applied Fluidigm

C1 STRT-seq and unraveled the heterogeneity of the cells in the mouse hippocampus and somatosensory cortex; they identified 47 distinct cell identities, including six OL lineage clusters [90]. These six clusters are composed of OL lineage cells at different stages of development such as, immature, pre-myelinating, myelinating, and terminally differentiated post-myelination OLs. Due to the tight quality control parameters taken into consideration and given that these cells presented lower level of RNA compared to other OL lineage cells, they did not identify classic signature of the OL progenitor cells [90]. Afterwards, a seminal study performed by Marques and colleagues explored transcriptome of 5072 OL lineage cells from 10 regions of mouse juvenile and adult CNS [91]. In this study the authors identified 13 clusters consisting of cells expressing progenitor cell marker (*Pdgfra*+) continuously up to mature cells. Among the mature OL populations they found six distinct clusters [91]. They reported that the initial stages of differentiation of OL lineage cells are similar between various brain regions in juvenile mice while the more mature cells exhibit a regional heterogeneity. The same group in a separate study showed how transitional states between different stages of OPC generation occurs in mice. They also revealed that post-natal OPC from the brain and spinal cord present a similar transcriptional signature [92]. Transcriptional heterogeneity of the OL lineage cells in mouse visual cortex using lineage tracing approaches identified *Pdgfra*+ and *Cspg4*+ OPCs along with two classes of mature OLs.

In parallel, Chen and colleagues captured more than 14000 single cells from the whole hypothalamus of mice [93]. In their study, they identified 11 non-neuronal clusters with distinct transcriptional signatures. The authors confirmed the heterogeneity of OL lineage cells observed by Marques *et al.* in 2016 and showed the cells express different level of OL lineage markers form progenitor cells to the mature one [93]. Single nuclear sequencing of OL lineage cells also revealed that in the adult mouse spinal cord, 44% OPC, 28% OLs and 19% immature neurons have been identified which emphasizes the importance of resident cycling cells in the OL lineage cells.

Transcriptomic analysis of oligodendrocyte lineage cells in human

Having access to human brain tissue provide a unique opportunity to study the OL lineage cells. The pioneering studies on human OL lineage cells originated with the work of Goldmann *et al.* , shedding light on the gene signature of adult white matter progenitor cells using microarray [94].

In this paper, the authors compared the transcriptional profile of freshly isolated adult human white matter progenitor cells to those of white matter from which the progenitors were derived [94]. The main marker that they used to characterize the progenitor cells was *A2B5*, a ganglioside expressed at the cell surface [94]. *A2B5* is not restricted to the OPCs, and this marker also identifies lineage-restricted astrocyte and immature neurons [95]. In this regard, the same group used *PDGFRA* to specifically isolate fetal OPC. It has been indicated that these *PDGFRA*-positive cells could be instructed to either mature OL or astrocyte *in vitro*. A significant similarity was found between the transcriptional signature of human fetal and adult OPC with the reported signature for the mouse cells [95].

Following initial studies, mainly focused on characterizing OPCs using microarray technique [94,95] advent of bulk RNAseq studies allowed for exploring the cellular identity of all OL in more detail. The first being the group of Darmanis et al. in which he characterized 332 cells from dissociated adult human cerebral cortex and 134 cells from fetal brain tissue using Fluidigm C1 technology [96]. In their study, they identified mature OL and OPC as distinct clusters [96]. Later on, Spaethling and colleagues sequenced around 300 single cells of healthy adult human brain cells. Surprisingly, in their study they could not find an independent and separate OL cluster [97]. The major reason for this observation might be the small number of cells that were sequenced. With sequencing of 19550 single nuclei from adult human post-mortem frozen brain tissue, Habib and colleagues identified OPC as *PDGFRA*-positive cells and mature OL as *PLP1*-positive cells [98]. The detected genes in OL populations were fewer than those identified in neurons [98] consistent with previous finding [90]. In a cross-species study in which the authors examined mouse and human ventral midbrain development expression of specific cell types identities including OPCs and radial glial like cells were identified [99]. The authors of the paper suggested that according to the expression signature of the cells, the radial glial cells could be considered as a cell type in the OL lineage cells [99]. Recently, in a comprehensive study, Jakel and colleagues analyzed 16 262 single nuclei from the visual cortex and 9794 nuclei from the frontal cortex of post-mortem frozen brain tissue. The authors identified 6 clusters belonging to non-neuronal cells including OPCs and mature OLs [100].

History of microglia:

The discovery of microglia begins in early 19th century when anatomists decipher cellular heterogeneity of the CNS using different dyes. The first person to describe the presence of a non-neuronal connective-like tissue in the CNS was Rudolf Virchow in 1856. He applied the word "glia" to this connective-like tissue derived from the Greek word meaning "glue". However, the existence of microglial cells within the CNS was only demonstrated a century ago in 1919 by del Rio-Hortega, now considered to be "the father of microglia" Initially, microglia had been considered as static bystanders of the CNS without any specific function. However, over the course of time, scientists proposed several physiological function of microglia. The earliest identified role was immune surveillance of the CNS. Later, they were considered to be the prototypic tissue-resident macrophage-like innate immune cells of the CNS equipped with memory-like function which enables them to act in a context-dependent manner. In the current era of multi-omics, it is now clear that microglia are multifunctional cells that interact with other cells in the CNS including neurons, astrocyte and OL lineage cells. In this regard, during the past decade, they have taken center stage in the emerging field of neuroimmunology; novel sequencing techniques revealed their active involvement in multiple CNS disorders. In addition, genome wide association studies (GWAS) have indicated that microglia express genes with risk alleles for various neurodegenerative disorders like Alzheimer's disease (AD), Parkinson's disease (PD), schizophrenia, autism, and MS. Furthermore, it has been indicated that microglia dysfunction during development is associated with several monogenetically inherited microgliopathies which cause severe brain abnormalities. As such, microglia have become a major therapeutic target for the treatment of numerous neuropsychiatric diseases. Despite significant improvements in the methods to study microglia, most of our understanding comes from studying microglia of model organism like zebrafish and rodents. Unfortunately, there is a lack of understanding regarding primary human microglia, and thus warrants a more in-depth characterization. In the following section, I will describe the origin, biology and function of microglia described to date.

Ontogeny and origin of microglia

Understanding the origin of microglia have been a subject of various studies even prior to their identification as unique and independent cells of the CNS. In the late 19th century W. Ford Roberston, introduced the term “mesoglia" to describe the mesodermal origin of microglia, which was distinct from origin of neuronal and neuroglial cells. Later, it was indicated that the cells that Robertson had been referring to were actually OL. The concept of the “third element” was introduced by Ramon y Cajal by which he distinguished microglia from neurons and neuroglia and stated that these cells might have a mesodermal origin. This concept was further clarified by del Rio-Hortega based on the morphological and functional properties of the cells and he subsequently proposed the term “microglia cell” to describe a population of cells that are distinct from neuroectodermal oligodendroglia or OLs [101].

Despite all these seminal studies, the origin of microglia remained controversial and there were two broad opinions about the origin of microglia. The first group of scientists believed in the concept of neuroectodermal origin of microglia, supported by other studies indicating a shared neuroectodermal origin for both microglia and other glial cells. For example, a study of Fujita and colleagues proposed a common, matrix-derived progenitor for microglia, astrocytes, and OLs [102]. This concept was further verified by Kitamura who showed microglia and astrocyte originated from neuroectoderm derived glioblasts [103]. In parallel, a separate study showed that donor bone marrow cells failed to contribute to the adult microglial population in either newborn [104] or adult rodents [105] suggesting that the majority of microglia had a local neuroectodermal origin. However, further studies updated this concept and claimed that microglia are highly resistant to radiotherapy, a feature unique to microglia in contrast to blood leukocyte population and CNS macrophages [106]. Subsequent studies confirmed this concept by indicating majority of microglia remained of host origin up to 15 weeks after bone marrow transplantation [107].

In contrast to the studies which focused on neuroectodermal origin of microglia, a separate line of study emphasized their mesodermal origin. Morphological similarity of microglia to macrophages at different times of development along with their positive reaction to antigens were the main source of such speculation [108,109]. Indeed, immunohistochemical studies confirmed that microglia express macrophages markers in both mouse and human [110,111]. Finally, a genetic study revealed that mice deficient in the transcription factor PU.1, which is crucial for the development of myeloid cells, were also devoid of microglia [112]. Such observations highlighted

the myeloid nature of microglia and provided evidence that microglia and macrophage might have same ontogeny. Historically, it was believed that the maintenance and replenishment of different macrophage populations in the body including microglia depend on mobile circulating monocytes [113]. However, it is now firmly understood that monocytes and tissue resident macrophages develop from three distinct developmental pathways [114].

Microglia and border associated macrophages (BAM) which consist of macrophages in the perivascular space, choroid plexus, dura matter and subdural meninges develop from the first wave of macrophages development which is known as transient primitive wave [115]. In this regard, they are the first glial cells to seed the brain. Microglia and BAM originate from c-Kit^{lo} CD41^{lo} early myeloid progenitor (EMP) around embryonic day 7.25 (E7.25) from the embryonic yolk sac (YS) in mouse [116,117]. In this wave, it is thought that EMPs first give rise to pre-macrophages (pre-MF) which then subsequently become microglia and BAM in the embryonic CNS. The main route that directs these progenitors to the CNS is the developing vasculature, this wave of hematopoiesis is independent of monocyte intermediates [116] and the activity of the *Myb* transcription factor [118,119]. It has been shown that macrophages of the choroid plexus is replaced by monocyte-derived cells of the hematopoietic stem cell origin over time which make them to be distinct from the rest of the BAM population [119]. It has also been indicated that infiltration of microglia progenitors into the brain is not uniform and their morphology, density and varies by location [120]. Furthermore, microglia acquire specific gene expression signature according to the different brain region that they localize [121]. Besides direct migration of the YS progenitors to the brain, a potential alternative in microglia development is the initial expansion of progenitors in the fetal liver before seeding the brain at E112.5 [122]. In human, microglia-like cells with different morphologies can be seen as early as gestational weeks 3-5 [123,124]. Continued microglia development was depicted with the colonization in the spinal cord starting at GW 9 and the peak of microglia influx and distribution at GW 16 and finally appearance of ramified morphologies by GW 22 [125]. Recent studies at the single cell resolution also confirmed the timeline of microglia development; they acquire a mature phenotype by GW 18 [126].

Gene expression regulation of microglia development and maintenance

The development and maintenance of microglia are tightly controlled by a gene expression regulation program. In addition, local CNS factors significantly affect microglia maintenance, with evidence that CSF1R signaling is critical for microglia survival [127]. IL34 and CSF1 are the two ligands of CSF1R which are transcriptionally enriched in the CNS both embryonically and during post-natal life [128]. However, it has been observed that these two signaling molecules have differential spatial distribution in the CNS [129]. Another signaling molecule which is critically involved in microglia maintenance is *TGFB*. This growth factor mainly affects microglia homeostasis in the late embryonic and early post-natal developmental stages during which the proliferation capacity of microglia is high [130]. Upon birth, microglia face an active proliferation pattern across different CNS regions, albeit in a sporadic manner [131,132].

It is believed that the size of adult microglia population is kept in a steady state condition through self-renewal [133]. Following conditional and local elimination of microglia through pharmacological means such as the application of diphtheria toxin or *CSF1R* inhibition (PLX3397), microglia number is restored by the proliferation of rare surviving populations [127,134]. A balanced regulation between microglia proliferation and apoptosis is involved in this process of renewal [131]. Furthermore, fate mapping experiments indicated that microglia are not replaced by bone-marrow derived progenitors [135]. This feature of microglia resembles the physiology of lung and liver resident macrophage populations which also depend on self-renewal for their maintenance and proliferation [136]. Altogether, even though it has been shown that the microglia turnover rate is controversial and depends on the brain microenvironment [137], self-renewal is the primary mechanism for their proliferation.

Microglia function during embryonic stage and early post-natal stage

The early colonization of the brain by microglia that occurs prior to the appearance of any other glial cells suggests that these cells play an important role in aiding developmental processes such as neurogenesis and neuronal migration. Microglia acquire distinct morphological and transcriptomic signatures at different stages of development [133,138]. Such unique signatures are driven by different microenvironment that microglia come across during development from embryonic stages to adulthood [133]. Perturbation of microglia environment has a significant effect on the physiology and maintenance of microglia [139]. At the embryonic and very early

post-natal stages, microglia lack the ramified morphology of adult microglia. Instead, they adopt an amoeboid shape indicative of cellular activation [133]. In addition, it has been shown that microglia have a higher proliferative capacity at this time of development [131,140].

The simultaneous appearance of microglia with neurons in the CNS indicates a possible contribution of microglia in forming the neuronal architecture [141]. Microglia affect neurogenesis by controlling the number and fate of neural progenitors; induction of neural progenitor cell apoptosis and phagocytosis of dying cells limit neurogenesis [142]. This property of microglia is not restricted to the embryonic stage. The brain architecture is also highly plastic during the first two weeks of post-natal development in mouse, during which neurons form extensive connections together. The number of generated synapses exceeds the final number of synapses in the adult healthy brain and therefore the extra synapses need to be eliminated. It has been indicated that microglia have a critical function in regulating and fine-tuning the number of synapses, in a process called synaptic pruning. CX3CR1-deficient mice which show significant reduction in microglia number have abnormal synaptic networks, suggesting an active role for microglia in synaptic remodeling [143]. Malfunction of microglia in removing unnecessary synapses is associated with variety of neurological diseases including epilepsy [144], autism [145] and schizophrenia [146]. On the other hand, microglia can stimulate neurogenesis by secreting neurotrophic molecules like insulin-like growth factor 1 (IGF-1) [147]. Besides their classical role in regulating the neurogenesis process, it has been shown that microglia support other CNS cells such as OL progenitor cells and vasculature development. A specific subpopulation of microglia which cluster in the white matter-surrounding regions such as the corpus callosum and cerebellum promotes myelin production by OL lineage cells [148]. These cells are Cd11c+ cells and are the main source of IGF1; their depletion results in primary myelination impairment [149]. In addition, it has been shown that a balance between pro-inflammatory and anti-inflammatory microglia states is required for efficient myelin regeneration following damage to the myelin layer [150].

Microglia function during adulthood

Microglia have been traditionally considered to be static cells in the CNS. However, through a combination of imaging [151] and genetically engineered mouse studies [152] it has been shown that microglia protrusions constantly monitor the CNS environment and have significant interactions with other cell types. Even though the exact molecular mechanism underlying

microglia interaction with the environment is not clear, purinoreceptors, ion channels, and neurotransmitters have been shown to be involved in the processes [153]. Microglia are specialized phagocytic cells of the CNS which efficiently clear bacteria, cellular debris, and excessive cells [154]. Among the most well studied molecular mechanisms underlying the control of microglia phagocytic activity are those involving tyrosine receptor kinases such as AXL and MER [155]. Mice lacking *Axl* and *Mer* genes are characterized by an accumulation of apoptotic cells in the neurogenic CNS regions [155].

Molecular heterogeneity of microglia during development

Earlier microglia characterization works were based on their morphology, density and electrophysiological properties, in addition to the expression of a small panel of marker genes [120,156]. Considering the variety of function that microglia undertake during CNS development, there emerged the hypothesis that subpopulations of microglia which perform specific functions exist. In addition, later works demonstrated that microglia can easily change their transcriptomic signature and become activated in the context of neurodegenerative diseases [157].

Microglia are now widely considered to be a heterogeneous cell population within the CNS [158]. The most significant factor which hindered undersetting microglia biology at the single cell level was the scarcity of appropriate techniques to capture microglia at the single cell level. A few studies which have evaluated microglia biology at the single cell level employed techniques such as flow cytometry, *in situ* hybridization, or immunocytochemistry. However, these techniques only allow the evaluation of a small number of proteins and RNA molecules and are therefore not appropriate for a comprehensive study of microglia biology.

Studies attempting to identify distinct microglia subpopulations started with bulk evaluation of the transcriptome [121] and proteome [159]. The focus of these studies was to unravel the spatial heterogeneity of microglia across different brain regions. For example, it has been shown that microglia acquire distinct expression signature in different brain regions, and cerebellar and hippocampal microglia exist in more immune-vigilant state compared to other brain regions of adult mice [121]. Hippocampal microglia have been shown to have a higher expression of *Tnf* and *Fcgr2,* which again implies a state of heightened pro-inflammatory activity compared to other

brain regions [160]. Region-specific expression of key markers was also characterized, further supporting that microglia have different molecular function across CNS regions. Expression of the phagocytic marker *CD68* differs across various brain regions, which implies unequal phagocytic capacity of microglia in adult mice [161,162]. Another example is the *Usp18* gene, which can be used to distinguish microglia of the deep white matter of CNS from those of the cortices [163]. Higher expression of *Usp18* in the white matter is indicative of a higher activation state of microglia in that region [163]. One limitation of these bulk studies is that their approach, while yielding informative data about microglia on a population level, does not provide information regarding the existence of small subpopulations of specialized microglia.

Single cell RNA seq studies of microglia

Since the emergence of single cell RNA sequencing, mouse and human microglia have been subjected to a wide range of analysis in healthy and diseased CNS states [8,138,164–167]. Understanding the molecular diversity of microglia during development has been a major focus of research. For example, studies have evaluated different timepoints of microglia development in mice and showed that microglia are more heterogenous (i.e. can be categorized in larger number of subpopulations) at the embryonic and early post-natal developmental stages compared to adulthood [8,164,165]. The common findings of these seminal studies were that embryonic microglia represent a distinct cell population from the post-natal microglia [8,164,165]. Each of these studies also reported specific subpopulations of microglia with unique functions. For example, Hammond and colleagues found two interesting sub-populations of microglia including axon tract-associated microglia (ATM) and microglia which express both microglia and BAM markers [164]. The first subpopulation appeared transiently at the early post-natal developmental stages around the axonal tract of the corpus callosum and disappeared later during development. These cells were *Spp1* positive, highly activated, and clustered around pre-myelinated axon tracts [164]. It has been shown that these cells have crucial roles in maintaining the faithful myelination of the CNS [148,149]. Another specific subpopulation which was identified at the early post-natal stages was the subpopulation of cells expressing the following markers: *Clec7a, Gpmbp, Spp1, Lgals3* and *Igf1*. These cells were mainly found in the white matter of mouse brain [148,164,165] and had similar expression signature to disease associated microglia (DAM) previously identified by Karen Shaul in 2017 [166]. Yet another subpopulation is a cluster of microglia which is

significantly enriched in the embryonic stages and express both canonical microglia markers like *Tmem119* and BAM markers like those encoding the MS4A family of proteins [164]. The authors concluded that these cells may act as progenitor cells of the microglia and BAM. However, it has been shown that cells expressing both microglia and BAM marker could be microglia derived from the second wave of microglia development which seeds the fetal liver prior to seeding the brain [122]. Even though the exact molecular function of these distinct subpopulations is unknown, the presence of these clusters may indicate distinct maturation stages of these cells across different regions. Li and colleagues also considered spatial heterogeneity to be responsible for the different subpopulations of microglia, but observed that microglia of adult mice do not have significant heterogeneity across brain regions, contrasting previous findings made using bulk techniques [165].

Spatial heterogeneity of microglia across CNS regions

The concept of the presence of different microglia subtypes across CNS regions was put in light with bulk RNAseq studies in which researchers reported clear difference between the microglia present in the cerebellum and those located in the cortex, hippocampus and striatum [121]. However, more recent studies which have explored heterogeneity at the single cell level at these anatomical locations could not find the same heterogeneity as it was reported at the bulk level [8,164,165]. All these studies found a transcriptional continuum between microglia across different anatomical locations. Cerebellar microglia-specific gene expression signature introduced by Garbert and colleagues was shown to be present in BAM as well, and was not just restricted to microglia [165]. The only anatomical location that have a specific microglia signature seems to be the olfactory bulb where microglia have been shown to be more proliferative [137,165]. Apart from anatomical location across CNS region, there is one more source of microglia variation was introduced by Sankowski and colleagues in which grey matter microglia express canonical markers of microglia higher than the white matter in which microglia express more inflammatory and MHC-II genes [9].

Summary, Hypothesis and Aims:

Oligodendrocyte (OL) lineage cells and microglia have crucial roles in the normal development of the CNS and in maintaining brain homeostasis throughout the entire human lifespan. Failure in their normal function of either cell at any stage of development can contribute to an array of neurological disorders including multiple sclerosis, epilepsy, schizophrenia, and autism spectrum disorders. Studying the transcriptomic content of these cells provides a valuable source of data that sheds light on the potential function of the cells. The transcriptional landscape of primary human OL lineage cells and microglia is understudied due to the limited availability of brain samples from various ages of human development. In this regard, our understanding of these two cell types is based on the analyses of cells from rodent model organisms. Of the studies carried on the transcriptome content of human cells only pre-natal and adult tissue samples have been studied, neglecting the pediatric and adolescent age range. Having access to human brain tissues which allows us to perform transcriptional and functional experiments on primary human glial cells led to the aims of current study which was to fill the existing gap in the knowledge of transcriptome content of human glial cells at the single cell level.

Aim 1: Characterizing temporal and regional transcriptomic profile of primary human oligodendrocyte lineage cells using high-throughput techniques (Chapter 2)

We hypothesized by that by applying microarray and single cell RNA sequencing technologies along with functional testing to primary human OL cells which we have gathered across different developmental ages we can characterize different cell identities of OL lineage over time and explore their function. Furthermore, we hypothesized that mature adult OL across various CNS regions including the brain parenchyma, spinal cord and sub-ventricular zone have distinct transcriptional landscapes. Thus, by performing single cell RNA sequencing on the isolated cells from these regions we can explore their spatial heterogeneity.

Aim 2: Characterizing the transcriptomic profile and gene regulatory network of primary human microglia across development at single cell level (Chapter 3)

We hypothesized that the application of high throughput sequencing to primary human microglia and downstream bioinformatics analysis would reveal previously unappreciated temporal heterogeneity of human microglia. Moreover, transcription factor binding site analysis would reveal gene regulatory networks responsible for microglia development over time.

Chapter 2

This chapter is divided into two sub-parts:

Part 2.1:
Distinct function-related molecular profile of adult human A2B5-positive pre-oligodendrocytes versus mature oligodendrocytes

Part 2.2:
Temporal and spatial transcriptional landscape of oligodendrocyte lineage cells in the human CNS revealed by single cell RNA sequencing

Part 2.1:

Distinct function-related molecular profile of adult human A2B5-positive pre-oligodendrocytes versus mature oligodendrocytes

Preface:

The result of this sub-part is published in the form of following paper in Journal of Neuropathology & Experimental Neurology. *I am a co-first author on this manuscript.

Caroline Esmonde-White, Moein Yaqubi*, Philippe A. Bilodeau, Qiao Ling Cui, Florian Pernin, Catherine Larochelle, Mahtab Ghadiri, Yu Kang T Xu, Timothy E. Kennedy, Jeffery Hall, Luke M. Healy, Jack P. Antel (2019) Distinct function-related molecular profile of adult human A2B5-positive pre-oligodendrocytes versus mature oligodendrocytes. Journal of Neuropathology & Experimental Neurology, 78, 468–479.*

When I joined to the lab, I got involved in an ongoing project in which all the cellular experiments were done by my colleagues in the lab. My contribution to this work was analyzing all the gene expression data, running all the subsequent bioinformatics analyses such as biological pathway analysis, interpreting the findings, and providing figures and corresponding text for these parts.

Abstract

Remyelination in the human CNS is ascribed to progenitor cells rather than previously myelinating oligodendrocytes (OLs). The ganglioside-recognizing antibody A2B5 has been used to isolate putative progenitor cells, whose in vitro features resemble cells labeled as "pre-oligodendrocytes." Here, we compare the transcriptional profiles of adult human brain-derived A2B5 antibody-selected cells (A+) after initial isolation (day in vitro (DIV1)) and after DIV6, with non-selected (A–) cells (mature OLs), with regard to their differentiation state and functional properties. While a number of previously recognized progenitor associated genes, specifically PTPRZ1 and PDGFRA, were upregulated in the A2B5+ population, a number of such genes were comparably expressed in the mature OLs, as were mature myelin genes. Additional progenitor-related genes were upregulated in the A+ population. We show that A2B5+ cells have greater capacity to ensheath nanofibers, a model of myelination potential; consistent with this, ingenuity pathway analysis indicated that A+ cells had upregulated expression of genes within cell growth and cell signaling pathways. Differential expression of cell death/survival pathways complements previous functional studies showing their increased susceptibility to metabolic stress. At DIV6, we observed significantly fewer differentially expressed genes; suggestive of cell maturation occurring in vitro, indicating the complexity in comparing in vitro and in situ cell properties.

Methodology

Isolation of the human adult oligodendrocyte progenitor cells from brain tissue

For the first part of this chapter the adult OL progenitor cells were isolated as follow. The Human brain samples obtained from subcortical white matter enriched tissue resected from patients undergoing surgery for the treatment of nontumor related intractable epilepsy (specimens from 28 individuals [33% female], mean age 35 years, range 20–60 years). Use of adult tissues was approved by the Montreal Neurological Institute and Hospital (MNI/H) Neurosciences Research Ethics Board. Tissue was subjected to trypsin digestion followed by Percoll gradient centrifugation. Cells were collected from the nonmyelin and non-red blood cell layer fraction. Total brain cells were cultured in DMEM/F12 medium (Sigma, Oakville, ON) containing N1 (Sigma), 0.01% bovine serum albumin, and 1% penicillin-streptomycin (Invitrogen, Burlington, ON) overnight which we call it day in vitro 1 (DIV1) and the floating cell fraction was collected. A2B5 antibody conjugated microbeads (Miltenyi Biotec, Auburn, CA) were used to select A2B5+ cells. Aliquots of A2B5-selected (referred to as A+) and non-selected cells (referred to as A–) were cultured for 6 days in DMEM/F12 + N1 medium supplemented with platelet-derived growth factor (PDGF)-AA (10 ng/mL), basic fibroblast factor (10 ng/mL), and triiodothyronine (T3, 2 nM) (Sigma) (DIV6).

Immunocytochemical Studies

For flow cytometry analysis, cells at DIV1 before or after immune-magnetic bead selection were stained with LIVE/DEAD fixable Aqua Dead Cell Stain kit (ThermoFisher Scientific, Eugene, OR), blocked for 15 minutes at +4°C with human FcR blocking reagent, and immunostained with A2B5, O4 (Miltenyi, Somerville, MA), PDGFRA (Cell Signaling, Whitby, Ontario), and/or IL-7 receptor (IL-7R) antibodies (BioLegend, San Diego, CA). Data were acquired on a BD LSR II (BD Biosciences, San Jose, CA) and analysis carried out with FlowJo software. For some studies, cells growing on chamber slides were immunostained with A2B5, O4, or IL-7R antibodies and assessed by fluorescence microscopy.

Nanofiber Ensheathment Assay

A+ and A– cells were plated in multi-well aligned Nanofiber plates (The Electrospinning Company Ltd., Didcot, Oxfordshire, UK) and cultured for 4 weeks in DMEM/F12 + N1 medium supplemented with B27 (Life Technologies, Grand Island, NY) and T3, followed by immunostaining with O4 (R&D Systems, Oakville, ON) and MBP (Sternberger Monoclonals, Lutherville, MD) primary antibodies and corresponding secondary antibodies conjugated with either Alexa Fluor 488 (Thermo Fisher Scientific) or Texas Red (Biosource, Camarillo, CA). Images were acquired with a Zeiss fluorescence microscope; measurement of percentage of ensheathment by A+ or A– cells was analyzed by MATLAB software using a heuristic approach [168]. This heuristic approach targets the general morphological characteristics of OL sheaths, such as the presence of thick elongated structures. In this way, the algorithm provides rapid approximations for accurate measurements of individual ensheathed segments.

RNA-Based Analyses

Total RNA was extracted from cell samples at DIV1 and DIV6 using a standard Trizol protocol followed by DNase treatment according to manufacturer's instructions (Qiagen, Valencia, CA). RNA from DIV1 cells derived from 3 independent surgical samples were hybridized to the GeneChip Human Transcriptome 1.0 Arrays (Affymetrix; Genome Québec Innovation Centre). RNA from DIV6 cells derived from 3 other independent surgical samples were hybridized to the GeneChip Human Transcriptome 2.0 Arrays (Affymetrix; Genome Québec Innovation Centre). Limitations of cell numbers precluded using the same tissue samples to obtain DIV1 and DIV6 cell samples. The CEL data files were normalized using the RMA algorithm in the FlexArray software. Comparisons in the study were made between the 2 cell types, that is, A+ versus A– at DIV1 and DIV6, using paired analysis. Genes upregulated or downregulated with p values <0.05 were considered in the final analysis. Selected gene expression was confirmed using qPCR.

Ingenuity Pathway Analysis

Total differentially expressed genes (DEGs) at DIV1 and DIV6 were selected based on false discovery rate (FDR) <0.2 for the pathway analysis, as determined by IPA (Qiagen, https://www.qiagenbioinformatics.com/products/ingenuitypathway-analysis). This threshold was considered to expand the list of affected biological processes. Core analysis was

performed on the data using filters to restrict pathways to human CNS cells and to display categories considered relevant to molecular and cellular function. The FDR < 0.2

Results:

Immunocytochemical Analyses of A2B5+ (A+) and A2B5– (A–) Cells

To document the frequency of A2B5+ cells in our initial cell isolates, the effectiveness of our immune-magnetic bead selection, procedure, and the persistence of A2B5+ cells in vitro, we combined flow cytometry and immunostaining on chamber slides. Figure 1A–C provides an example of the composition of the total nonadherent cell pool recovered after the initial 24-hour period (DIV1) as determined by flow cytometry. Overall, A+ cells comprised ∼5%–15% of the cell population (Figure 1A; confirmed by immunostaining Figure 1D), of which ∼60%–70% were O4+ confirmed by immunostaining (Figure 1F), compared with 90+% of A2B5– (A–) cells. Less than 2% of cells expressed the myeloid cell marker CD11b (Figure 1B). PCR-based analysis of our Percoll gradient based isolation technique indicated that astrocytes (glial fibrillary acidic protein (*GFAP*) and aquaporin 4 (*AQP4*) expressing cells) were depleted during the initial cell isolation procedure (Figure 2).

The immunomagnetic bead selection process resulted in ∼10% of cells being recovered from the column (A+ fraction), whereas 90% of cells comprised the A– fraction. Analysis of cells on chamber slides showed that a high percentage of cells in the A2B5+ selected population were A2B5+ (∼90%; Figure 1E). At this time these cells have limited process extension (Figure 1D-F). Flow cytometry-based analysis confirmed that A2B5+ cells were predominant in the positively selected population (Figure 3A). Flow cytometry could not account for all the cells in the 2 populations, suggesting that detection of A2B5-reactive cells faced technical limitations. In the non-selected cell fraction, <5% of cells were A2B5+ (Figure 3B). The overall percentage of myeloid cells present did not differ between selected and non-selected populations (<1%–2%). We did not detect CD3+ cells in either the A2B5+ or A2B5– populations as determined by FACS analysis; in comparison, the initial unfractionated population contained up to 4% of CD3+ cells.
Following 6 DIV, immunostaining of cultures showed that both A+ and A– initiated cultures contained >90% O4 cells. At this time, both cell types have extensive process outgrowth (illustrated for A+ cells in figure 1H). There was a significant reduction in relative proportion of A2B5+ cells in the A+ cultures (<5%, Figure 1G) compared with DIV1-selected cells (>90%, Figure 1E). Isotype control values with an IgM antibody were 4%–8% (Figure 1I).

Immunostaining of cells with microglia (Iba-1) and astrocyte (GFAP) directed antibodies indicated that such cells comprise <1% of the total cells at both DIV1 and DIV6.

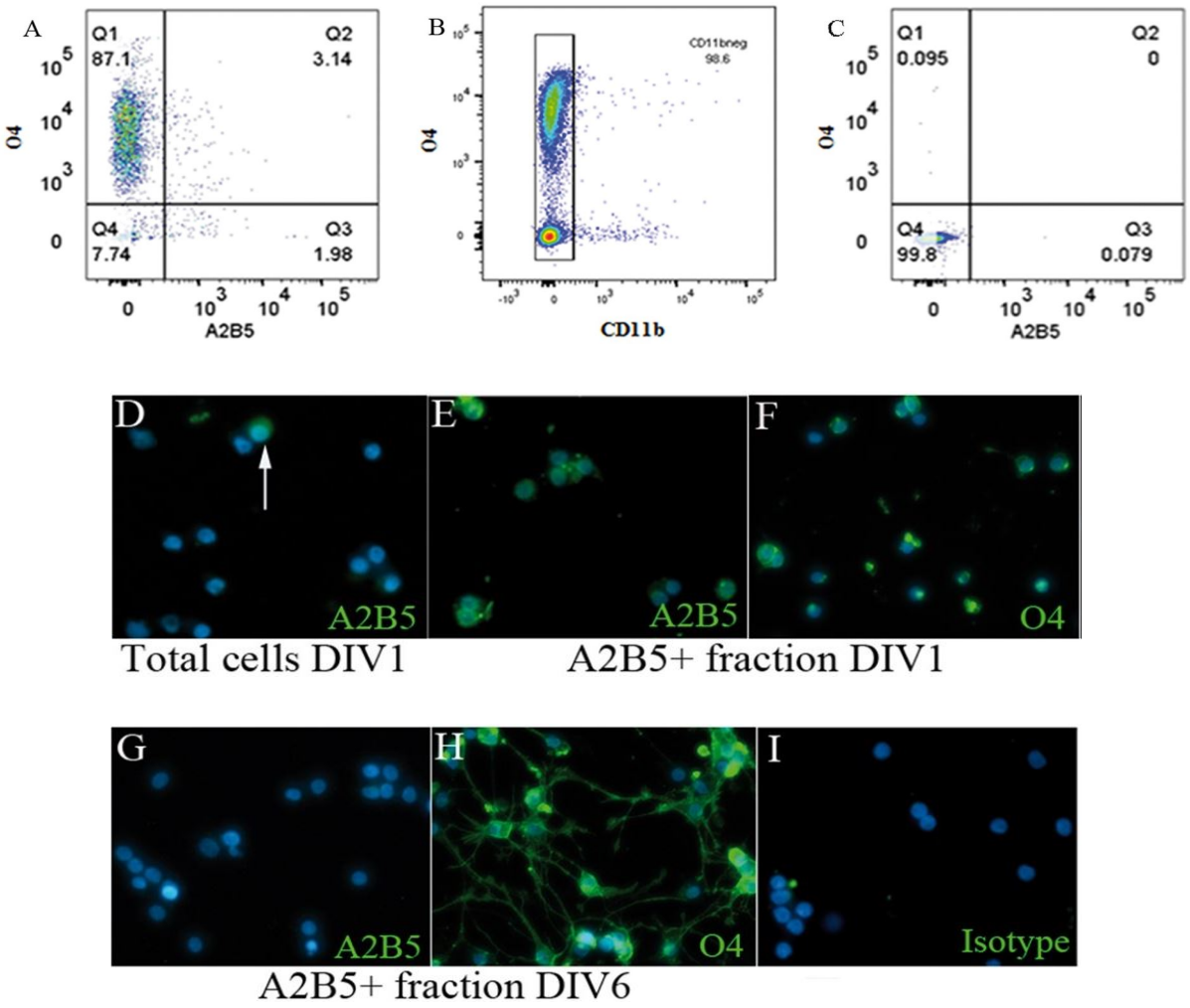

Figure 1. Detection of A2B5+ cells. (A–C) Flow cytometry-based detection of A2B5+ cells in unfractionated adult brain-derived nonadherent cell ("floating cell") population at DIV1. (A) A2B5-reactive cells comprise ~5% of the total cell population with ~60% of these cells (3.14%/5.12%) being O4+ compared with 92% (87.1%/94.84%) of A2B5– (A–) cells. (B) Double negative fraction (O4–/A2B5–) did not contain significant numbers of myeloid (CD11b+) cells. (C) Isotype control for A2B5 and O4 staining; <1% of cells are O4 or A2B5+. (D–I) Immunostaining of cells on chamber slides at DIV1and DIV6 with either A2B5 or O4 antibodies (green); (D) shows the total floating cell fraction on DIV1 (15%–20% of cells are A2B5+ [arrow]); (E) shows the A2B5-selected cell fraction on DIV1; 90+% of cells are A2B5+; (F) shows the A2B5-selected cell fraction immunostained with O4 antibody on DIV1, note the lack of processes; (G) shows the A2B5-selected cell fraction immunostained on DIV6, <1% of cells are A2B5+; (H) shows the A2B5-selected cell fraction immunostained with O4 antibody on DIV6, >90% of cells are O4+ and have extensive processes; (I) shows the isotype control staining of A2B5-selected cell fraction on DIV1; <1% of cells are A2B5+.

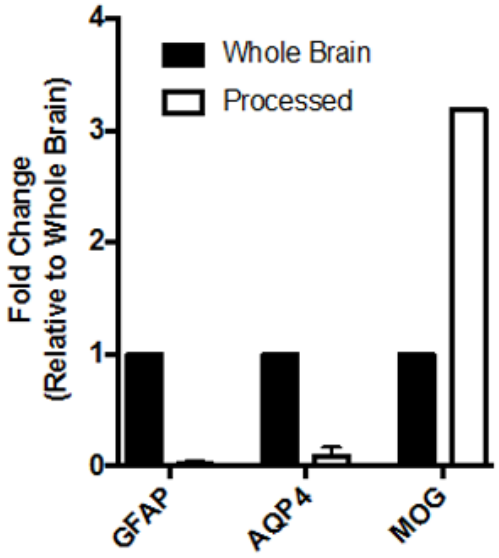

Figure 2. PCR analysis illustrating loss of astrocytes (GFAP and AQP4 expression) during Percoll gradient based isolation procedure. Individual bars indicate CT values for GFAP, AQP4, and MOG (representing oligodendrocytes) in a tissue preparation pre- and post Percoll gradient (referred to as "whole brain" and "processed" respectively). For GFAP, n = 4; AQP, n = 3; MOG, n = 1.

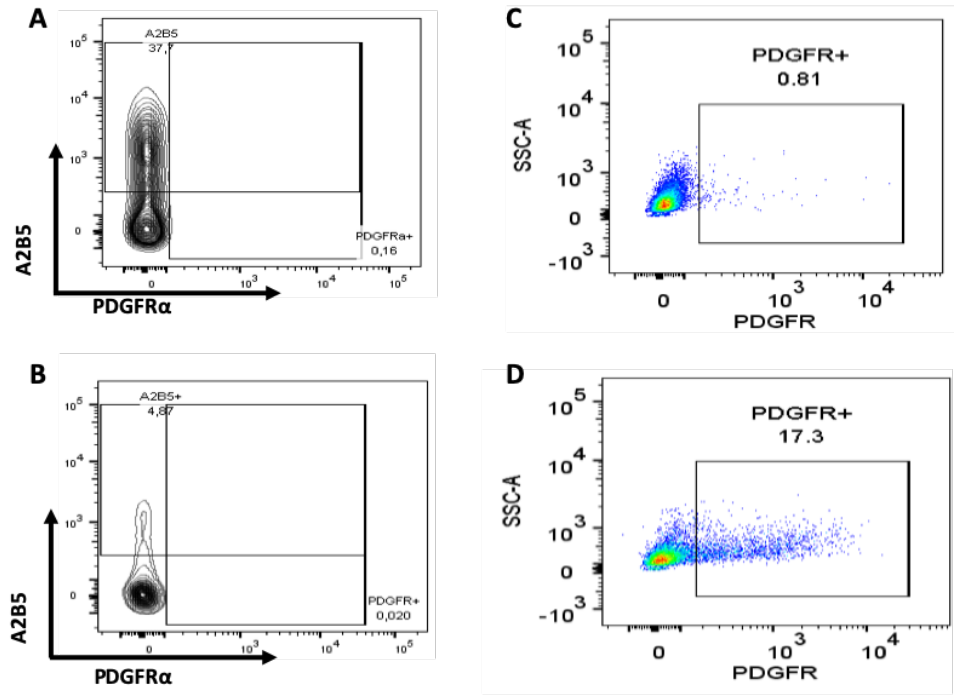

Figure 3. (A, B) Flow cytometry-based detection of A2B5 and PDGRα expression in A2B5 antibody immuno-magnetic bead selected (A+) (A) and non-selected (A-) cell fractions (B) at DIV1. A2B5+ cells are predominantly in A2B5 antibody selected fraction. Immunostaining showing no significant population of PDGFRA+ cells in the A+ or A- fractions. (C, D) Immunostaining of mid-2nd trimester fetal brain-derived cells with isotype control (C) or PDGFRA antibody (D) showing specific PDGFRA reactivity (17% of PDGFRA+ cells). Representative of n = 3 experiments.

Nanofiber Assay

To determine whether A+ and A– cells differed in their potential to contribute myelination, we used a quantitative analysis system to compare their relative capacities to ensheath artificial nanofibers [168]. As illustrated in Figure 4A-D and quantified in Figure 4E-H, the proportion of O4 expressing cells within the A+ population that ensheathed nanofibers was significantly greater compared with the A– population (Figure 4E). Moreover, the mean length of ensheathed segments formed by A+ cells was longer (Figure 4F and G), although the mean number of segments formed per A+ cell was not significantly more than the mean number of segments formed per A– cell (figure 4H).

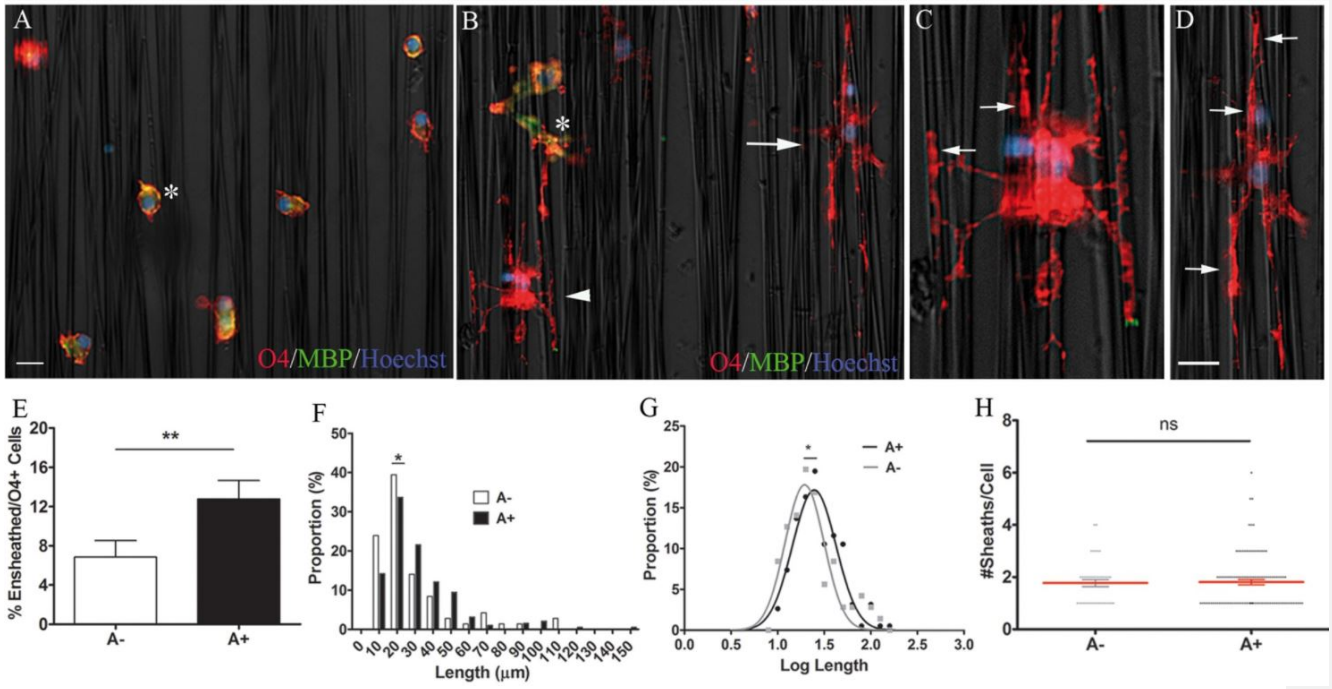

Figure 4. Increased ensheathment capacity of A2B5+ versus A2B5– cells. A2B5– cells (A) and A2B5+ cells (B) were cultured on nanofiber multi-well plates for 4 weeks, followed by immunostaining with O4 (red), MBP (green), and Hoeschst (blue). Images were merged with nanofibers under phase contrast. (C, D) Enlargements of individual cells from panel (B) as indicated by arrowhead (C) or arrow (D). Examples of ensheathed segments are indicated by arrows in panels C and D. Asterisk (*) indicates cells that co-express MBP and O4 in panels A and B. (E) The percentage of O4+ cells ensheathing nanofibers was increased for A+ versus A– cells as analyzed by t-test, $^{**}p < 0.01$, $n = 4$. The distribution of segment lengths for each cell fraction was graphed in panels F and G, the difference between A+ and A– fractions was analyzed by Mann Whitney test, $^{*}p < 0.05$. The number of ensheathed segments per cell was graphed in panel H, the difference between A+ and A– fractions was analyzed by Mann Whitney test. Scale bars = 20 μm (bar in panel A applies for A and B; bar in panel D applies for C and D).

Gene Expression Studies

DIV1 Studies

Our initial aim was to compare the A+ and A– cells at our earliest possible time point (DIV1). Figure 5A presents Volcano plots comparing total gene expression between A2B5-selected (A+) and non-selected (A–) cells at the initial time point (DIV1). Data in volcano plots are expressed relative to A– cells. There are more upregulated than downregulated genes in A+ cells when compared with A– at DIV1. As documented in the Venn diagram (Figure 5B and Table 1), there were 2094 genes differentiating the A+ from A– cell types, based on p-value <0.05. A majority (80%) of these DEGs are upregulated in the A+ population compared with A– cells.

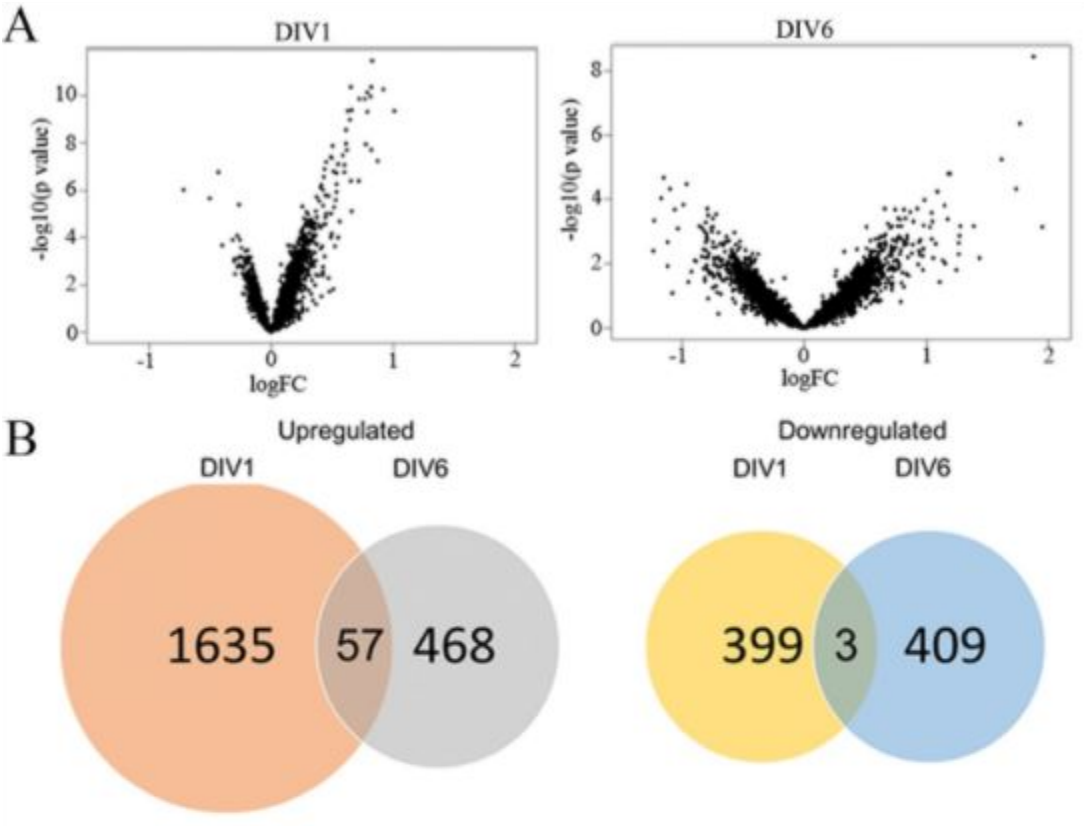

Figure 5. (A) Volcano plots comparing total gene expression between A2B5-selected (A+) and non-selected (A–) cells at the initial time point (DIV1) and after 6 days in vitro (DIV6). Data in volcano plots are expressed relative to A– cells. There are more upregulated than downregulated genes in A+ cells when compared with A– at DIV1 but not at the DIV6. n = 3 for each time point. (B) Venn diagrams of differentially expressed genes (DEGs) in initial cell population (DIV1) and following 6 days in vitro (DIV 6) indicating numbers of differentially upregulated genes in A+ versus A– at DIV1 (orange circle) and DIV 6 (grey circle); downregulated genes in A+ versus A– at DIV1 (yellow circle) and DIV 6 (blue circle). Fewer than 2% of DEGs are in common between the 2 time points.

A+ Versus A–	Upregulated	Downregulated	Total
DIV1	1692	402	2094
DIV6	525	412	937

Table 1. Summary of Genes Significantly (p-value < 0.05) Differentially Expressed (Up or Downregulated) Between Cell Types (A+ vs A–) Initially or After 6 Days in Vitro

OL Lineage Relevant Gene Expression

To identify differential expression of OL lineage genes between A+ and A– cells, we derived gene lists from the following studies: (i) Sim et al compared A2B5+ cells upon immediate isolation from adult human brain with tissue from which cells were isolated [94,169]; (ii) Dugas et al compared rat OL precursor cells (OPCs) and OLs using selection procedures that derived OPCs (GalC–/O4+ cells) from 7 day postnatal rats (P7) and OLs (A2B5–/GalC+ cells) from P10–P12 rats [170]; (iii) Cahoy et al compared postnatal (P1–P30) mouse forebrain-derived OPCs (*PDGFRA*-selected), recently developed OLs, and mature OLs using immune-panning based purification [171]; and (iv) Marques et al used murine lineage tracing studies using juvenile and adult mouse brain tissues [91].

As regards a comparison of differentially expressed OL lineage genes by A+ versus A– cells with those derived by Sim et al, for the 3 OL progenitor "marker" genes overexpressed in A2B5+ versus whole tissue, we also found increased expression of *PDGFRA* at DIV1 (fold change = 1.53) but no difference in *ST8SIA1* or *NG2* (Table 2). However, no *PDGFRA* population could be identified by flow cytometry in either the A2B5-selected or non-selected populations (Figure 3A & B) in contrast to what can be observed using dissociated human fetal brain cells (Figure 3D; panel C shows isotype control on fetal cells). There were no differences in the neural progenitor/stem cell associated genes, *DCX*, *ASCL1 (MASH1)*, or *HES1*. For the "functionally relevant genes" (Table 3), we observed significant upregulation of 16 out of a total of 78 such genes in DIV1 A+ versus A– cells including protein tyrosine phosphatase receptor type Z1 (*PTPRZ1*). *PTPRZ1* was the fifth most overall upregulated gene in our analysis as shown in table 4. This table presents a list of the 25 most significantly up or downregulated genes in the A+ versus A– cell populations. None of the "marker genes" and "functionally relevant genes" was upregulated in our A– fraction.

Using the overall OL differentiation gene lists derived from murine based studies [170–172], we identified 19 additional lineage genes that were overexpressed in the A+ population as indicated in Table 3 that were not listed in the previous human studies [94]. As regards the comparison of our data with the murine based studies, 11 out of a total of 80 genes from mouse forebrain-derived OPCs (*PDGFRA*-selected) [171], 9 out of 50 genes in OPCs from murine lineage tracing studies [170], and 10 out of 46 genes from rat OPCs [172] are significantly upregulated in DIV1 A+ versus

A– cells. As in the Sim et al study, we found that late myelin genes (*MBP, MAG, MOG*) were comparably expressed in the A– and A+ fractions (Table 2). We had insufficient cell numbers to compare relative gene expression in A2B5+O4– (putative early progenitors) and A2B5+O4+ cells (putative late progenitors that comprise the majority of our A2B5+ cells).

Table 2 Differential Expression at DIV 1 and DIV 6 by A+ Versus A– Cells of "Marker Genes" (Ref 16)

	DIV 1		**DIV 6**	
	F.C.	***p-value***	**F.C.**	***p-value***
Oligodendrocyte progenitor				
CSPG4 (NG2)	–1.13	0.25	1.02	0.85
PDGFRA	1.53	0.003	1.56	0.02
ST8SIA1 (GD3 synthase)	1.11	0.4	–1.25	0.11
Neural progenitor cells				
ASCL1 (MASH1)	1.06	0.68	–1.23	0.39
DCX (doublecortin)	–1.18	0.17	1.25	0.08
HES1	–1.09	0.35	1.20	0.20
Oligodendrocyte				
CNP (CNPase)	1.20	0.09	–1.03	0.79
NKX2-2	–1.14	0.19	1.05	0.7
OLIG2	–1.1	0.4	–1.06	0.61
PLP1 (PLP/DM20)	–1.09	0.38	1.13	0.27
QKI	1.17	0.11	1.06	0.47
SOX10	–1.09	0.47	1.05	0.67
Myelinating oligodendrocyte				
GALC	1.2	0.2	1.08	0.44
MAG	–1.03	0.73	1.11	0.14
MAL	–1.00	0.96	1.11	0.16
MBP	–1.22	0.11	1.14	0.26
MOBP	–	–	–1.09	0.46
MOG	1.21	0.18	1.32	0.02
Microglia				
CD11b	1.03	0.79	1.08	0.60
CD68	–1.01	0.89	–1.20	0.15
CD86	1.27	0.12	1.10	0.47
Astrocyte				
AQP4	–1.13	0.32	–1.17	0.31
GFAP	1.00	0.97	3.66	3.55E–09
GLUL	1.05	0.57	1.02	0.78
Lymphocyte				
CD3D	6.16	7.23E–11	1.47	0.02
CD3G	4.40	1.04E–09	–1.05	0.68
CD3E	4.12	1.07E–08	1.08	0.51
TCR alpha	1.56	0.002	1.25	0.20

Table 3. Common and unique genes expressed at DIV 1 and DIV 6 in A+ versus A– cells in comparison with the "Functionally Relevant Genes" reported by Sim et al (Ref 16)

DIV 1						**DIV 6**					
Common Genes			**Unique Genes**			**Common Genes**			**Unique Genes**		
ID	**F.C.**	**p-Value**	**ID**	**F.C.**	**p-Value**	**ID**	**F.C.**	**p-Value**	**ID**	**F.C.**	**p-Value**
PTPRZ1	6.64	1.90E–08	*FABP7*	1.88	0.002	*PTPRZ1*	3.84	0.0006	*SLC35F1*	2.42	0.0006
SATB1	2.36	1.37E–05	*CALCRL*	1.86	0.0003	*CHL1*	2.69	0.006	*FABP7*	2.06	0.001
NELL2	2.37	0.0004	*ID2*	1.80	0.0009	*CNR1*	2.28	1.55E–05	*PTGFRN*	1.95	0.003
GMP6A	1.99	0.0004	*ZFP36L1*	1.70	0.0005	*NCAN*	2.25	1.57E–05	*CACNG4*	1.95	0.01
SCG2	1.76	0.0004	*S100A10*	1.66	0.0001	*VCAN*	2.15	0.03	*OLFM2*	1.91	0.005
PDGFRA	1.53	0.002	*KLF12*	1.61	0.0006	*TNR*	2.10	0.002	*TOP2A*	1.72	0.003
SERPINE2	1.59	0.003	*LPHN3*	1.61	0.049	*DOK5*	1.75	0.002	*CCND2*	1.69	0.001
DOK5	1.51	0.01	*MCM6*	1.57	0.0005	*C1orf61*	1.67	0.0002	*LHFPL3*	1.65	0.003
TSPAN7	1.46	0.01	*F2R*	1.49	0.007	*OPCML*	1.60	0.009	*MT3*	1.63	0.003
NRCAM	1.35	0.01	*GM2A*	1.43	0.008	*TIPM4*	1.60	0.02	*LPHN3*	1.46	0.04
FLRT2	1.40	0.02	*CCND2*	1.42	0.043	*PDGFRA*	1.56	0.02	*LRRTM3*	1.46	0.02
CHL1	1.34	0.02	*CCNG1*	1.42	0.029	*GRIA2*	1.54	0.01	*DDAH1*	1.46	0.01
GPR19	1.55	0.03	*NET01*	1.40	0.006	*CHRDL1*	1.52	0.002	*ENC1*	1.45	0.01
CNR1	1.44	0.04	*DDAH1*	1.38	0.008	*CLDN10*	1.45	0.04	*MTSS1L*	1.45	0.009
SLC1A2	1.37	0.04	*FNBP1L*	1.36	0.02	*SLC1A2*	1.45	0.01	*NETO1*	1.44	0.007
CASK	1.32	0.04	*RELN*	1.29	0.044	*THBS4*	1.42	0.01	*CCND1*	1.43	0.007
			ADORA2B	–1.30	0.038	*NR2F1*	1.38	0.01	*GPR37L1*	1.40	0.02
			SLITRK1	–1.53	0.034	*COL11A1*	1.36	0.02	*PCDH15*	1.39	0.01
			HBB	–5.25	9.38E–07	*ADCY8*	1.35	0.04	*SULF1*	1.37	0.02
						RAB31	1.27	0.02	*CNTN6*	1.33	0.04
									PRRX1	1.33	0.04
									PFKL	1.33	0.04
									HMOX1	–1.97	0.0001

Table 4. List of top 25 genes differentially expressed by A+ versus A– cells initially or after 6 days in vitro (paired sample analysis)

	DIV1						DIV6				
Upreg	**F.C.**	**p-value**	**Downreg**	**F.C.**	**p-value**	**Upreg**	**F.C.**	**p-value**	**Downreg**	**F.C.**	**p-value**
IL7R	10.2	4.30E–10	*HBB*	–5.25	9.38E–07	*PTPRZ1*	3.84	0.0006	*OR2L5*	–2.34	0.004
GIMAP7	8.29	5.41E–11	*IFNA17*	–3.19	2.16E–06	*GFAP*	3.66	3.55E–09	*MIR4320*	–2.33	0.0004
GIMAP2	7.51	5.84E–08	*OBP2B*	–2.71	1.78E07	*SPARCL1*	3.40	4.35E–07	*SNORD111*	–2.24	8.99E–05
GZMA	6.71	3.28E–12	*HIST1H2BI*	–2.50	0.0002	*ATP1B2*	3.32	4.73E–05	*SNORA38B*	–2.21	2.08E–05
PTPRZ1	6.64	1.90E–08	*OR2M7*	–2.07	0.0001	*CXCL14*	3.06	5.59E–06	*CCL8*	–2.16	0.002
KLRK1	6.57	4.38E–11	*C6orf124*	–2.00	0.0008	*CHL1*	2.69	0.006	*SLC7A11*	–2.16	0.01
AMICA1	6.53	1.07E–10	*LPA*	–2.00	0.0009	*RNA5SP395*	2.61	0.0006	*HIST2H4B*	–2.13	4.73E–05
CD3D	6.16	7.23E–11	*CYP2A6*	–1.98	0.003	*SLC35F1*	2.42	0.0006	*HIST1H2AH*	–2.08	0.0002
CD2	6.16	4.74E–10	*KRTAP10–7*	–1.88	8.18E–05	*UBD*	2.41	0.001	*MIR4266*	–2.04	0.0008
GIMAP4	5.95	1.17E–08	*KRTAP13–3*	–1.88	0.001	*MMP7*	2.40	0.005	*HMOX1*	–1.97	0.0001
GZMK	5.84	1.42E–10	*PVALB*	–1.87	0.0007	*ATRNL1*	2.40	0.002	*FAM45A*	–1.94	3.28E–05
SMAD3	5.31	1.35E–10	*MRGPRX1*	–1.85	0.001	*SCN3A*	2.36	0.01	*ANKRD30B*	–1.92	0.03
IFITM1	5.23	4.02E–07	*FKSG83*	–1.82	4.00E–06	*CNR1*	2.28	1.55E–05	*SNORA11*	–1.88	0.01
GBP5	4.58	7.84E–06	*SPAG11B*	–1.79	0.0001	*NCAN*	2.25	1.57E–05	*NPS*	–1.85	0.007
ANXA1	4.53	4.01E–10	*ATAD3C*	–1.79	0.0006	*TNC*	2.24	0.0003	*HIST1H2AK*	–1.83	0.008
IGFBP3	4.50	3.94E–07	*WFS1*	–1.75	0.001	*HIST1H3B*	2.22	0.009	*HSPA6*	–1.80	0.0006
TC2N	4.47	4.17E–11	*KRTAP4–12*	–1.74	0.0002	*CADPS*	2.21	0.0001	*FPR3*	–1.78	0.005
CD3G	4.40	1.04E–09	*C1orf180*	–1.74	0.003	*MOXD1*	2.19	0.007	*ZNF799*	–1.78	0.0007
CD52	4.21	4.23E–10	*CSH1*	–1.71	0.02	*VCAN*	2.15	0.03	*OR5B21*	–1.76	0.003
GPR171	3.97	1.66E–07	*MGC5590*	–1.70	0.003	*CNR1*	2.12	5.60E–05	*MIR4421*	–1.76	0.0009
CD3E	4.12	1.07E–08	*LCE1D*	–1.70	0.001	*IL23A*	2.12	5.91E–05	*IL8*	–1.75	0.02
CD96	4.08	2.77E–09	*C11orf44*	–1.68	0.002	*TNR*	2.10	0.002	*HTR2B*	–1.75	0.03
GPR176	3.97	1.66E–07	*OR10A2*	–1.68	0.001	*GRIK3*	2.07	0.006	*GTF2IRD2B*	–1.74	0.0005
FYB	3.97	8.83E–08	*LOC80054*	–1.68	0.004	*MXRA5*	2.06	0.0004	*GIPC2*	–1.74	0.003
CLEC2D	3.38	3.46E–08	*ABAT*	–1.67	0.02	*FABP7*	2.06	0.001	*RNU2–7P*	–2.34	0.002

Differential Pathway Regulation in A+ Versus A– Cells

An IPA analysis of the total DEGs based on FDR <0.2 in A+ cells compared with A– cells identified their main functional pathway categories (Figure 6A). The top 2 pathways identified at DIV1 were cellular growth/proliferation and cellular development. As indicated, all DEGs were upregulated in the A+ cells. Additional pathways included cell-to-cell signaling and interactions, cellular function and maintenance, and cell death and survival (highlighted) [173].

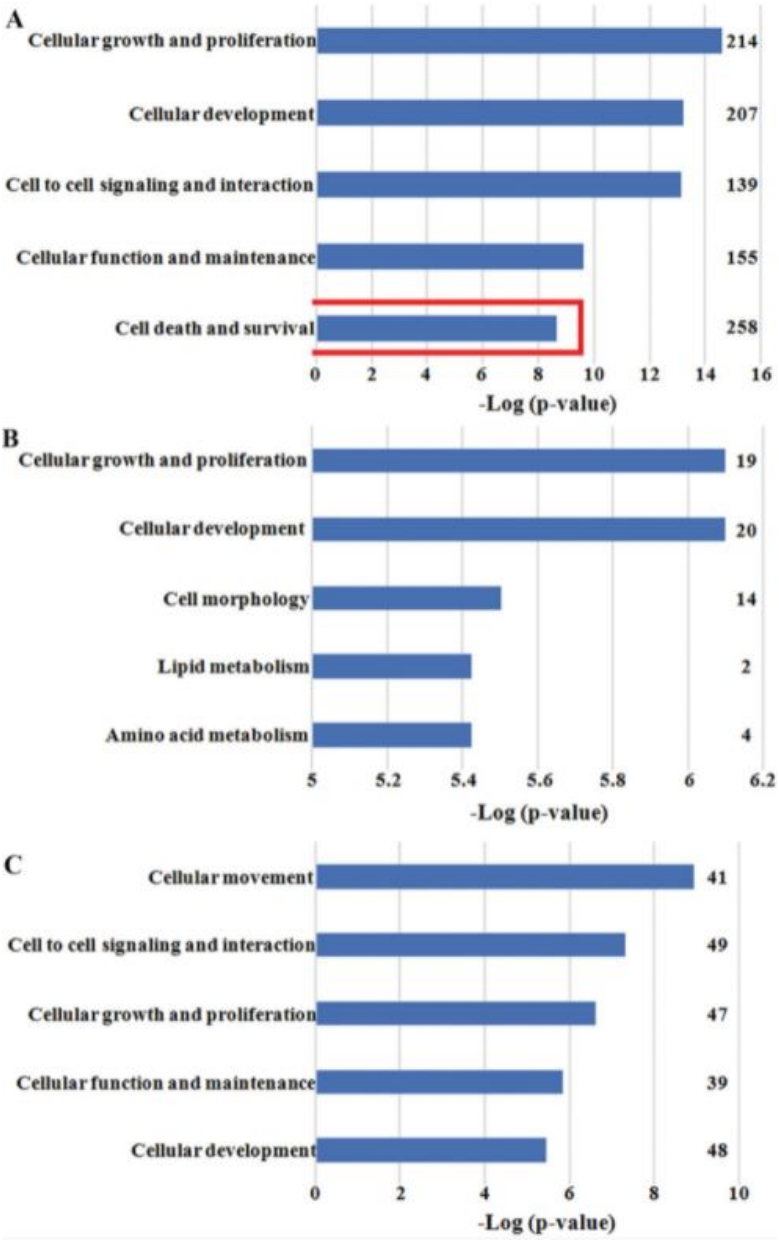

Figure 6. Distinct functional pathways between A+ and A– cells at DIV1 (A) and DIV6 (B) pathways were identified by IPA analysis of total differentially expressed genes of DIV1 and DIV6 based on FDR <0.2 in A+ cells compared with A– cells. Cell death pathway is highlighted in red. Number of differentially expressed genes are indicated for each pathway; all are upregulated in the A+ population except for 1 out of 139 cell-to-cell signaling and interaction genes and 11 out of 258 cell death/survival genes. (C) Distinct functional pathways derived by IPA analysis of genes differentially expressed at both time points (3 downregulated and 57 upregulated).

Non-OL Lineage Genes

We found no differences between A+ and A– cells in levels of expression of selected genes that characterize myeloid cells (*CD11b, CD68, CD86*) or astrocytes (*AQP4, GFAP, GLUL*); however, a select number of lymphocytes associated genes were upregulated (Table 2 and 4). *IL7* receptor (*CD127*) was the most upregulated gene in the DIV1 A+ cells (fold change = 10.2; Table 4). We confirmed increased mRNA expression patterns of *CD127*, as well as *PTPRZ1* and *PDGFRA* by qPCR (Figure 7A and B). We further documented increased expression of IL7 receptor on A+ cells by flow cytometry at DIV1 (Figure 8 A-C). Immunostaining showed significant co-staining by *IL-7R* and O4 antibodies of the large majority of OLs in culture (Figure 8 D-G). The small observed differences between microarray and qPCR might be due to the intrinsic differences which might exist between these two techniques.

A

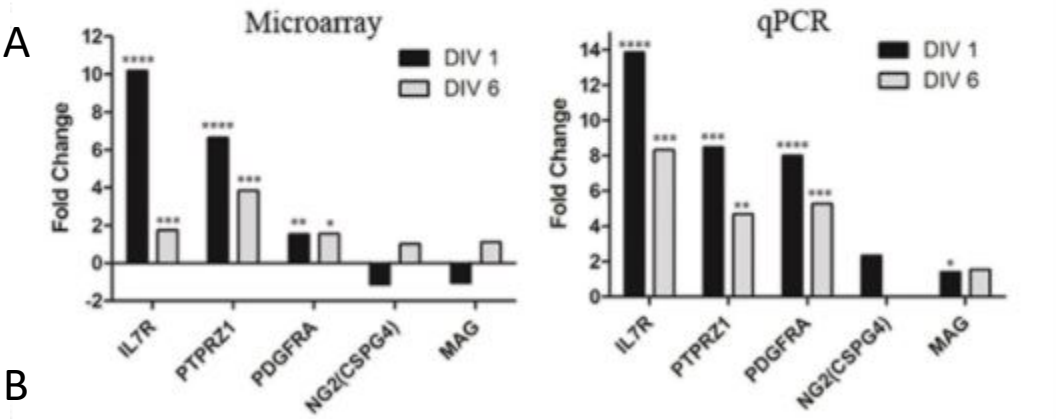

B

A+ vs A-	Microarray				qPCR			
	DIV 1		DIV 6		DIV1 (Mean ±SEM)		DIV6 (Mean ±SEM)	
	Fold Change	P-value	Fold Change	P-value	Fold Change	P-value	Fold Change	P-value
IL7R	10.20	4.30E-10	1.75	0.001	13.86 (2.87)	1.6E-6	8.33 (1.97)	0.0005
PTPRZ1	6.64	1.90E-08	3.84	0.0006	8.49 (2.40)	0.0002	4.68 (1.07)	0.005
PDGFRA	1.53	0.0029	1.56	0.02	8.0 (1.7)	8.3E-6	5.28 (1.49)	0.001
NG2 (CSPG4)	-1.13	0.246	1.02	0.85	2.33 (0.87)	0.17	-	-
MAG	-1.03	0.73	1.11	0.14	1.40 (0.06)	0.14	1.54 (0.79)	0.85

Figure 7. Fold change of CD127 (IL7R), PTPRZ1, and PDGFRα as well as NG2 and MAG in DIV1 and DIV6 A+ versus A– cells are illustrated by bar graph (A) and the values are listed by a table (B). (A) Microarray (left) and qPCR (right) data showing increased expression of CD127 (IL7R), PTPRZ1, and PDGFRα in DIV1 and DIV6 A+ versus A– cells. Each bar represents fold change of gene expression in A+ versus A– cells. Relative increases are lower at DIV6. PCR for DIV1 n = 5, DIV6 n = 3.

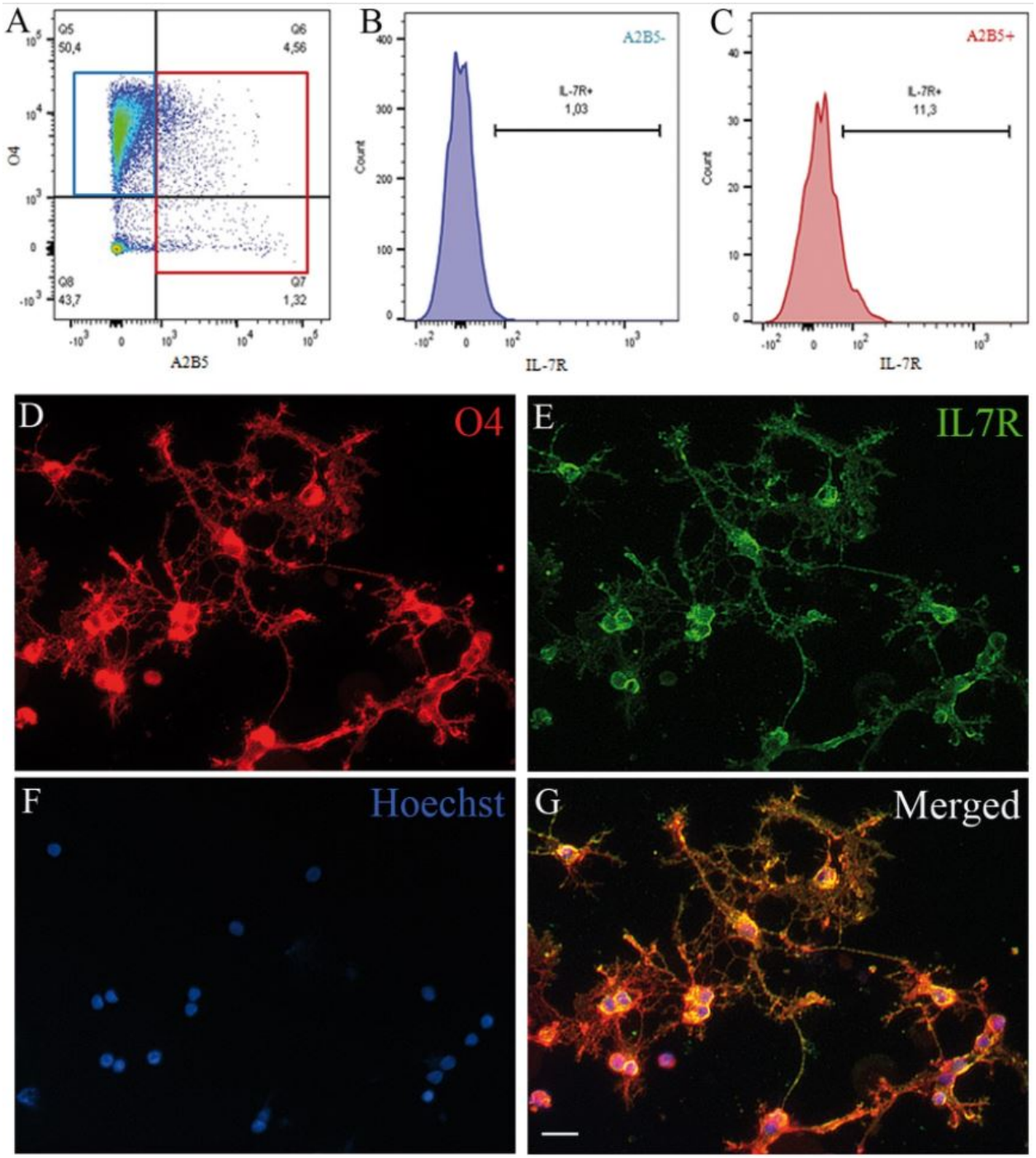

Figure 8. Increased frequency of IL-7R (CD127) on A2B5+ versus A2B5– cells at DIV1. Oligodendrocytes in the floating cell fraction were selected by gating on O4+ CD11b– cell fraction (Fig. 1B). A2B5+ and A2B5– populations were identified by double immunostaining with O4 and A2B5 antibodies (A). Immunostaining with IL7-R antibody demonstrates decreased frequency of IL-7R expression in A2B5– (B) versus A2B5+ (C) populations. Shown is an example of n = 3 experiments. Immunostaining of cells on chamber slides at DIV6 with O4 (red, D) and IL7R (green, E) antibodies shows IL7R expression on O4 + cells (merged, G). (F) Nuclear staining with Hoechst (blue). Scale bar = 20 µm.

DIV6 Studies

To examine the effects of tissue culture on gene expression in A+ cells, we acquired gene expression data on these cells after being maintained in dissociated culture for 6 days, a time when these cells express extensive processes. The total number of DEGs was lower (937) at DIV6 compared with DIV1 cells (2094) (Table 1). For the DIV6 cells, 44% of DEGs were downregulated in the A+ population (Figure 5B, Table 1). Table 4 provides a list of the 25 genes that are most significantly up or downregulated in the A+ versus A– cell populations. *PTPRZ1* is the most relatively upregulated gene in the A+ population; however, the extent of upregulation was relatively reduced at DIV6 as compared with DIV1 (fold change 3.84 vs 6.64) as was *IL-7R* (1.75 vs 10.20). These changes were confirmed by qPCR (Figure 7A and B). The upregulation of *PDGFRA* remained the same following 6 days in vitro (Table 4;1.56 vs 1.53); however, it was decreased in the qPCR analysis (8.0 vs 5.2; Figure 7A and B). *MOG* expression was increased at DIV6, $p = 0.01$ (Table 2). No OL differentiation process linked gene was found to be upregulated in the A– population at DIV6. There was no increase in microglia gene expression (*CD11b, CD68*, and *CD86*); the upregulation of lymphocyte associated genes noted at DIV1 was less apparent at DIV6 (Table 2). The microarray noted increase in the astrocyte related gene *GFAP* in A+ versus A– cells on DIV6, was not confirmed by PCR.

The DIV6 IPA analysis again identified cellular growth/development and cellular proliferation as the most upregulated biological processes (Figure 6B), although the number of genes involved in these pathways is decreased compared with DIV1 (Figure 6A). Figure 6C further presents pathway categories derived from IPA analysis of genes differentially expressed at both time points (57 upregulated genes and 3 downregulated genes, indicating that some features of A+ cells are retained at DIV6.

Part 2.2:

Temporal and spatial heterogeneity of oligodendrocyte lineage cells in the human CNS revealed by single cell RNA sequencing

Preface

This chapter is divided into two sections**.** In the first section, the result of the study of the temporal heterogeneity of oligodendrocyte lineage cells is represented (2.2.1). The content of this section is published in the form of following paper in Glia journal in which I am the third author. In this project I collaborated with Kelly Perlman who was an under graduate student in the lab. For detailed contribution of authors please refer to author contribution part.

Kelly Perlman, Charles P. Couturier, Moein Yaqubi, Arnaud Tanti, Qiao-Ling Cui1, Florian Pernin, Jo Anne Stratton, Jiannis Ragoussis, Luke Healy, Kevin Petrecca, Roy Dudley, Myriam Srour, Jeffrey A. Hall, Timothy E. Kennedy, Naguib Mechawar, Jack P. Antel (2020) Developmental trajectory of oligodendrocyte progenitor cells in the human brain revealed by single cell RNA sequencing. Glia, 68, 1291-1303.

The temporal heterogeneity is followed by a brief part of evaluating spatial heterogeneity of mature oligodendrocyte cells. I am the primary contributor to this section. The results from these analyses are under preparation to be submitted in the coming weeks.

For this project:
Single cell RNAseq data of human sub-ventricular zone was provided by Dr. Kevin Petrecca's lab. Human spinal cord tissue was harvested from organ donors through a collaboration with Transplant Quebec performed in Montreal General Hospital.

Abstract

Transcriptional profiling of oligodendrocyte (OL) lineage cells at single cell resolution heave greatly increased our understanding of molecular function of them in maintaining brain homeostasis and white matter diseases. However, due to the scarcity of human samples much of our knowledge regarding transcriptional content of OL lineage cells is restricted to rodent model organisms and human post mortem CNS samples. In this section, we explored both temporal and spatial heterogeneity of OL lineage cells using single cell RNA sequencing technique (scRNAseq). For the temporal characterization, scRNAseq was applied to viable whole cells isolated from brain parenchyma of individuals at various ages of human development including second-trimester fetal, 2-year-old pediatric, 13-year-old adolescent and adult samples. Downstream bioinformatics analysis revealed three distinct cellular subpopulations comprised of an early OPC (e-OPC) group, a late OPC group (l-OPC), and a mature OL (MOL) group. For each stage of development, we observed a specific enrichment of cell types with their specific function. According to our biological process analysis, e-OPCs were highly proliferative, l-OPCs showed great enrichment of extra cellular matrix re-organization and expectedly MOLs were heavily involved in myelination. For the spatial characterization scRNAseq was applied to viable whole cells isolated from human adult spinal cord, sub-ventricular zone (SVZ) and brain parenchyma. To explore the heterogeneity, we focused on MOLs and our results showed that the brain parenchyma and SVZ MOLs have more similar transcriptional content which is distinct from spinal cord MOL which have more immunogenic signature. These findings highlight the transcriptomic variability in OL lineage cells before, during, and after peak myelination and contribute to identify novel sets of genes and molecular pathways whose their activity can be used to understand the role of these cells in more detail for keeping brain homeostasis and during disease. Furthermore, these results provide the first comparison of human MOLs across spinal cord and CNS.

Methodology

Isolation and processing of the surgical brain parenchyma, sub-ventricular zone and spinal cord tissue

The brain tissues (telencephalon) of second-trimester human fetus (resulted from elective abortion) and the post-natal samples from different ages of human development who underwent brain surgeries (table 1) were collected by CUSA bag during the surgery and subjected to the preprocessing steps. For the post-natal samples, the brain tissue was obtained from normal superficial tissue that had to be removed to get to the area of underlying pathology. The fetal samples were obtained from University of Washington Birth Defects Research Laboratory. Use of pediatric, adolescent, and adult tissues was approved by the Montreal Neurological Institute and Hospital (MNI/H) Neurosciences Research Ethics Board; use of pediatric and adolescent samples were approved by the Montreal Children's Hospital Research Ethics Board. The tissues were digested using mechanical and enzymatic (trypsin and DNase) dissociation followed by a Percoll gradient to remove the myelin layer. The dissociated cells washed 3 times in PBS, and resuspended at a concentration of 106 cells per ml. Next, 100,000–200,000 cells were submitted for sequencing at Génome Québec. The viability of cells before sequencing was ~75-80% using trypan blue.

Human spinal cord tissue was harvested from organ donors through a collaboration with Transplant Quebec. All procedures are approved by and performed in accordance with the ethical review board at McGill University (IRB#s A04-M53-08B). Familial consent was obtained for each subject. The rapid autopsy spinal cord samples were processed within 2 hours of removal from the spinal column, tissue was kept on ice throughout. The samples were provided from the lumbar region of the cord (L1-L5) of three adults, two females and one male. For tissue processing, the meninges were carefully removed, and the tissue crosscut into small pieces of 1–2 mm3. The subsequent steps of processing were similar to brain parenchyma samples.

Human ventral sub-ventricular zone (SVZ) specimens were obtained from patients who underwent surgery to remove tumors. These samples were MRI negative for tumor and were collected from normal stissue that had to be removed to get to the area of underlying pathology. The tissue washed three times in sterile PBS containing penicillin and streptomycin. Specimens were then minced

into pieces of less than 1mm in size, before being digested in a collagenase solution containing DNAase (Cal Biochem EMD Chemicals) and MgCl2 for 1 hour at 37◦C. The digested specimens were washed with sterile PBS, and large debris were removed with a 70µm strainer. Residual RBCs were removed by density gradient using percoll (GE-Healthcare Bio-science AB). Samples were washed two more times in sterile PBS. An aliquot of cells was collected for sequencing Génome Québec.

Single cell library preparation and sequencing:

10x chromium technology was used to make the library of the cells. Briefly, single-cell RNA library was generated using the GemCode Single-Cell Instrument (10x Genomics, Pleasanton, CA, USA) and Single Cell 3' Library & Gel Bead Kit v2 and Chip Kit (P/N 120236 P/N 120237 10x Genomics). The user guide of Single Cell 3' Reagent Kits v2 was followed for this step (Ref number 34 Charles Nat. Commun. Paper). The sequencing ready library was purified with SPRIselect, quality controlled for sized distribution and yield (LabChip GX Perkin Elmer), and quantified using qPCR (KAPA Biosystems Library Quantification Kit for Illumina platforms P/N KK4824). Finally, the sequencing was done using Illumina HiSeq4000 PE75 instrument (Illumina) at the McGill University and Génome Québec Innovation Centre.

Single cell RNAseq data analysis

In this section, two approaches were used to analyze single cell RNAseq datasets of nine brain parenchymal samples as follow.

Analysis of single cell RNAseq data for brain parenchyma samples

All data demultiplexing and genome mapping was done using the Cell Ranger analysis pipeline (https://github.com/10XGenomics/cellranger). Reads were aligned to reference genome GRCh38. Multiple runs were aggregated and normalized to the same sequencing depth. For the downstream analysis we used a standard pipeline which is introduced by Couturier and colleagues at 2020 [174]. The following parameters were considered to filter the cells: Any cells found to express more than 12% of mitochondria were removed from the analysis to eliminate dying or low-quality cells [175]. Cells were excluded if they were found to express fewer than 1,000 genes. Moreover,

any cells with fewer than 1,800–2,000 unique molecular identifiers (UMI) were removed, with the minimum being dependent on the specific sample [174].

Genes with a zero count (i.e., genes that were not detected in the sample) were automatically removed and UMI counts were normalized for each cell. Principal component analysis (PCA) was used to reduce the high-dimensionality datasets to a lower dimensional space for visualization and to remove noise. Cell cycle scores were calculated by summing the expression of all cell cycle genes detected in each cell, which were then z-scored across all cells. Cell cycle scores ≤0 were considered to be noncycling. The principal component axes that were computed based on the noncycling cells were then projected onto the complete dataset. Each dataset was analyzed separately and the OL lineage cells from each individual dataset was further integrated for the downstream analysis. The identity of each cell types was identified using the relative expression of each cell types specific gene. The following gene list was used to identify each OL lineage cells: *PDGFRA* for OPC, *MBP, MOG, MAG* and *PLP1* for mature OL. The integrated cells were subjected to unbiased Louvain clustering with the resolution parameter 1.

Analysis of single cell RNAseq data for brain SVZ and spinal cord samples

In order to have the same analysis approach for regional heterogeneity part, in addition to analyzing SVZ, spinal cord samples, three adult brain parenchyma samples were also re-analyzed as follow: The 10XGenomics CellRanger pipeline was used to demultiplex the cells and their unique molecular identifier barcodes, and to align reads to the GRCh38 human reference genome. The subsequent analyses were done using the Seurat (v3.1) R package [176].

Individual datasets were subjected to standard Seurat pipeline for quality control, gene expression normalization, batch-effect correction, clustering, and differential expression analysis. Briefly, any cell with a genome that was comprised of 5 to 12 percent of mitochondrial genes was considered a dead cell and was removed from analysis. Similarly, any cell that contained less than 200 or more than 2500 unique feature counts was considered a low-quality cell and was removed from the downstream analysis. The gene expression levels of the cells were natural log normalized and scaled. The downstream analysis was restricted 2000 highly variable genes for each dataset. At this point individual datasets were integrated using the Seurat “FindIntegrationAnchors” and

"IntegrateData" functions, which perform canonical correlation analysis (CCA) to remove any possible batch effect between datasets. Highly variable genes of integrated object were identified and principle component analysis (PCA) was performed on them to reduce the dimensionality of the data. The first 20 principle components were selected for the clustering purpose. A shared-nearest neighbor graph was constructed based on the PCA analysis and the Louvain clustering algorithm was used several times to identify clusters at multiple different resolutions. Resolution 1 was selected for clustering purpose. Finally, the uniform manifold approximation and projection (UMAP) algorithm was used to visualize the clusters in two-dimensional space. The expression levels of cell-type marker genes were used to determine the identity of each cluster. Mature OL were subset using the expression of *MOG* and subjected to re-clustering with resolution 0.25. Differentially expressed genes between clusters and anatomical regions were identified using the "FindMarkers" function in Seurat based on Wilcox test scores for genes that were detected in at least 25% of cells in the populations compared. Heatmap plots of the top marker genes were generated using the DoHeatmap function.

Diffuse pseudotime analysis of brain parenchymal samples

We used diffusion pseudotime (DPT) created by Haghverdi et al. to track the patterns of expression of specific genes of interest, as identified by our differential expression analyses, over the developmental period [177]. To quantify how genes were differentially expressed across groups, population distributions for each gene were compared using the Mann–Whitney U test and adjusted for the false discovery rate (FDR). Genes were considered to be significantly differentially expressed between groups if they had an FDR-corrected p-value < 0.05 and a standard absolute fold change ≥ 2, which translates to an absolute log2 FC (LFC) ≥ 1. For the age-specific comparisons, any genes that were significantly differentially expressed between datasets within the same age group ($n = 10$ for pediatric, $n = 7$ for adult) were excluded to eliminate as much inter-subject variability as possible.

Pseudotime trajectory inference analysis of regional heterogeneity of mature oligodendrocytes

Pseudotime trajectory inference analysis was done using the PhateR (v1.0) package to order cells in "pseudotime" and visually highlight transitions between cells using dimensional reduction

methods that minimize gene expression difference between sequential cell pairs. PhateR uses the "potential of heat diffusion for affinity-based embedding" (PHATE) method created by Moon et al, 2019 [178]. Briefly, PHATE encodes local data via local similarities, encodes global relationships using potential distances based in diffusion probabilities, and embeds potential distance information into low dimensions via metric multi-dimensional scaling [178]. The phate algorithm was run on the integrated counts derived from the Seurat object with the gamma parameter set to gamma=0 and the remaining parameters set to default (knn=5, decay=40, optimal t was automatically selected to be t=8). PhateR was chosen for the trajectory inference analysis as it does not rely on prior assumptions of data structure.

Protein-Protein interaction network

The list of upregulated genes for each cell population were explored in the STRING database to retrieve protein-protein interactions [179]. To increase the confidence of obtained interactions from the STRING database, we set a confidence score of 0.7 (high confidence). These interactions were clustered using the MCL clustering algorithm with an inflation parameter equal to 3. The gene ontology (GO) feature in StringDB was utilized to generate a list of upregulated GO biological processes. Among the significantly enriched GO terms, we curated the most biologically relevant and informative subset.

Gene regulatory network construction and analysis

To make a gene regulatory network (GRN) the list of differentially expressed genes was searched in the Chip Enrichment Analysis (ChEA) data base and the list of TFs were obtained [180]. We matched our gene list with the entries of this database and retrieved TFs with FDR-corrected p-value <0.05 and $|LFC| > 1$. The list of TFs and its target genes was as input of Cytoscape software to construct and visualize the GRN [181]. Identification of the most central TF of the GRN was done using CentiScape plug-in of the cytoscape [182]. To identify the complete list of TFs, present in our study, we referenced the list of TFs provided by Lambert et al. (2018) [183]. Networks were formed with significant TFs in the network as well as with non-TFs with FDR corrected p-value <0.05 and $|LFC| > 2$ (in order to limit the number of connections).

Fluorescent in situ hybridization

Postmortem ventromedial prefrontal cortex of the adults (ages 39 and 61) without known neurologic disorders who dies suddenly without prolonged agonal period were used to perform in situ hybridization. To this end, at the first step the brain tissue was sliced to the 10 micro meter slide sections which were subsequently fixed in cold 10% neutral buffered formalin for 15 min at 4^{o}C, dehydrated by 2 min long successive ethanol baths of increasing concentration (70, 95, and 100%) and air dried for 5 min. Endogenous peroxidase activity was quenched with hydrogen peroxide reagent for 10 min, followed by protease digestion for 30 min at room temperature. The following probes were then hybridized for 2 hr at 40_C in a humidity-controlled oven (HybEZ II, ACDbio): Hs-VCAN (cat. no. 430071-C2), Hs-TNR (cat. no. 525811) and PDGFRα (cat. no. 604481-C3) to quantify VCAN and TNR expression in l-OPCs (PDGFRA+). Successive addition of amplifiers was performed using the proprietary AMP reagents, and the signal visualized through probe-specific HRP-based detection by tyramide signal amplification with Opal dyes (Opal 520, Opal 570 or Opal 690; Perkin Elmer) diluted 1:300. Slides were then coverslipped with Vectashield mounting medium with DAPI for nuclear staining (Vector Laboratories) and kept at 4_C until imaging. Image acquisition was performed on an Olympus FV1200 laser scanning confocal microscope. Images were taken using a 40X objective (NA = 0.95) and 60X (NA = 1.42). Images were processed with ImageJ.

Result

Characterizing the isolated cells of the brain tissues

To study transcriptional landscape of oligodendrocyte (OL) lineage cells, human brain samples were collected at different stages of development (Table 1). The post-natal samples were obtained though surgical procedures to resect CNS tissue. In all post-natal cases, the collected brain tissue was obtained from normal superficial tissue that had to be removed to get to the area of underlying pathology (i.e., the superficial surgical corridor on the way to the pathological tissue). Following tissue resection, they subjected to enzymatic and mechanical dissociation. The cell isolation procedure that was used, resulted in over representation of OL lineage cells and microglia in the final cell population. There was still a minor population of other cell types in the isolated cells including lymphocyte (*CCL5*+, *CD4E*+) and astrocyte (*GFAP*+ and *AQP4*+). In the table 2 we summarized the OL lineage cells across different developmental ages that we had in our study. There was a differential distribution of the OL lineage cells at each stage of development. While OL lineage cells were rare in the fetal population amounting to only ~1.6% of all detected cells (Table 2) they made majority of the cells among the post-natal cells. This differential distribution originated from the effect of Percoll treatment on the post-natal cells which were toxic for neuronal cells while in the fetal sample we did not use Percoll due to the fact there was no myelination in the fetal cells and therefore there was no need for Percoll treatment.

Age	Pathology	Location
Second trimester fetal (1-4)	-	Telencephalon
2-year-old (1)	Rasmussen encephalitis	Right central area taken during hemispherectomy
2-year-old (2)	Hemi-megalencephaly	Left central area taken during hemispherectomy
13-year-old	Intractable non-malignant epilepsy	Right Superficial Temporal cortex
58-year-old	Glioma	Supratentorial region
62-year-old	Non-tumor related epilepsy (hippocampal sclerosis)	Temporal cortex/subcortical

Table 1. Pathologies and location of tissue resected for subjects in each age group.

Age range	Group	n	Total cell	OL-lineage cell count	% OL-lineage in total count
Second trimester	Fetal	4	22,637	359	1.59
2 years	Pediatric	2	5,893	3,432	58.24
13 years	Adolescent	1	4,037	3,8086	76.44
58 and 62 years	Adult	2	5,418	3,510	64.78
Total	6.64	9	37,985	10,387	27.35

Table 2. Properties of cell yield from scRNA-seq organized by age group

OL lineage cells have distinct gene expression signature which is associated with their function

Unsupervised clustering of the cells based on the expression of the 5613 genes which were resulted from taking the union of the preprocessed gene sets from each age group led to identification of three distinct cell populations including an early progenitor group (e-OPC), a late progenitor group (l-OPC), and a mature oligodendrocyte (MOL) group (Figure 2). Accuracy of the clustering was verified by a cell-cell correlation heatmap which confirmed presence of three cell types in the analyzed cell population (Figure 3).

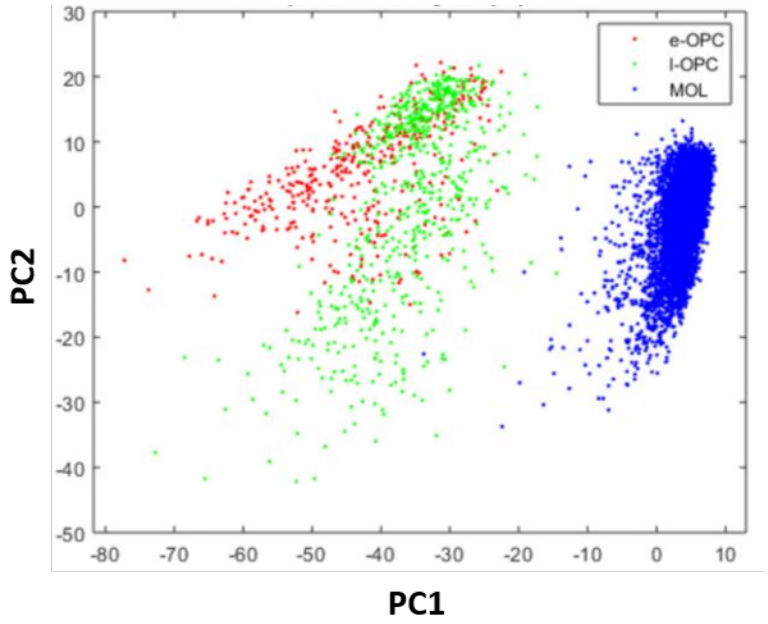

Figure 2. PCA plots of pooled sample colored by OL-subpopulation as determined by unbiased clustering algorithm. Red = early OPCs (e-OPC); Green = late OPCs (l-OPC); Blue = mature oligodendrocytes (MOL)

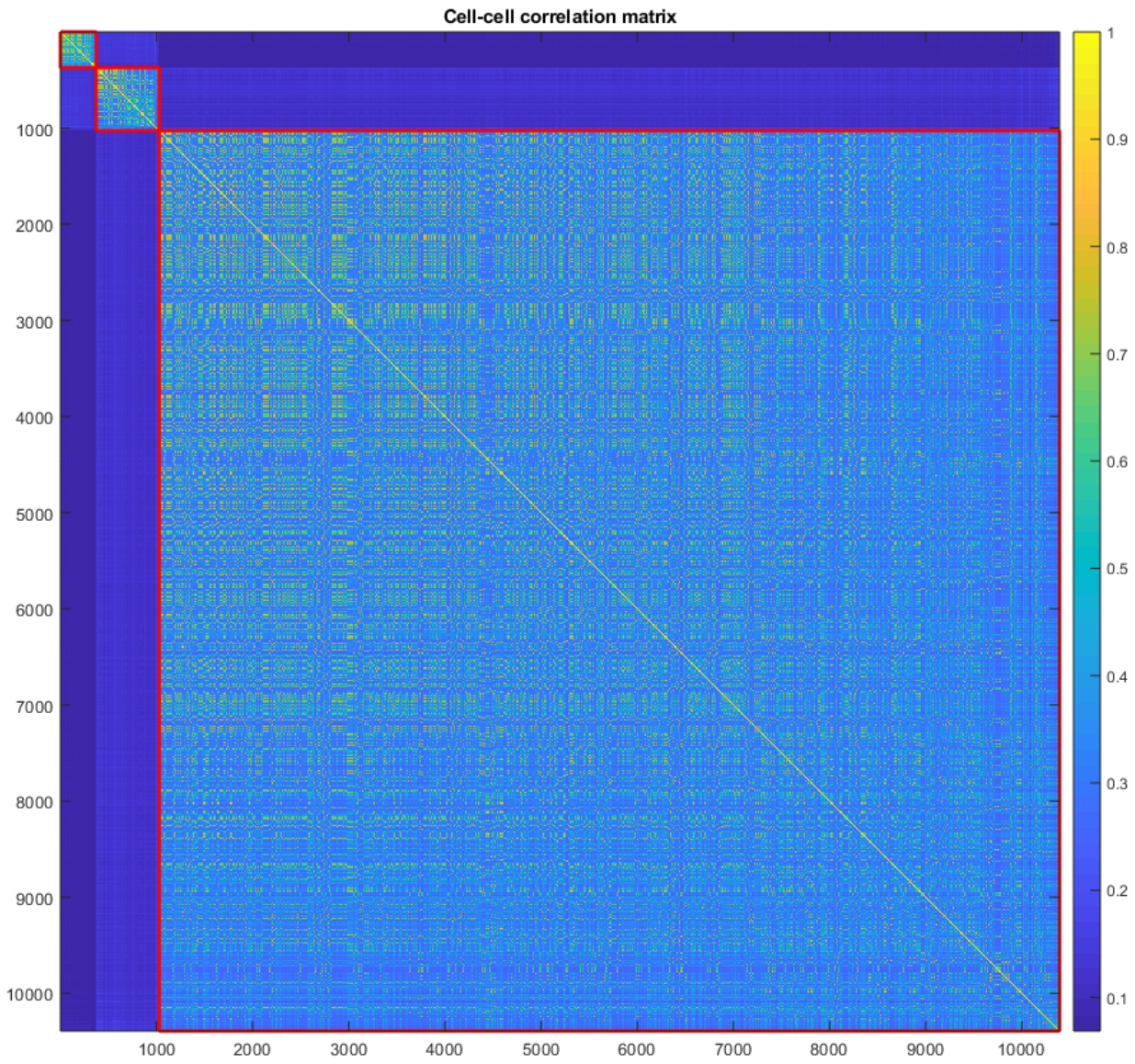

Figure 3. Cell-cell correlation diagram indicating the degree of correlation (color bar) of individual cell gene expression within clusters (red boxes).

Differential gene expression analysis between three cell types indicated that there were 500 up regulated genes and 103 down regulated genes in e-OPCs compared to l-OPCs and MOLs. For the l-OPC group we observed the same pattern of up and down regulated genes as e-OPCs. In this group there were 338 up regulated and 75 down regulated genes compared to e-OPC and MOL. Finally, in MOL group we noticed an opposite pattern in which there were 94 up regulated and 370 down regulated genes in MOL comparison versus e-OPC and l-OPC. The relative proportion of up and down regulated genes for each cell type is represented in figure 4. Heatmap showing the

differentially expressed genes between groups is displayed at figure 5. The most up regulated genes in each cell types were represented in figure 6 which confirmed gene expression signature of each cell type is associated with specific function (Figure 6). For instance, l-OPCs expressed genes specific to myelination at intermediate level compared to the fully mature cells which expressed these genes at highest level and e-OPC which expressed them at lowest level (Figure 6). This observation suggests there is graded rather than binary regulation of gene expression at OL lineage cells. Expression of these genes was specific to each cell types as it is indicated in the PCA plots which are colored according to expression of marker genes (Figure 7).

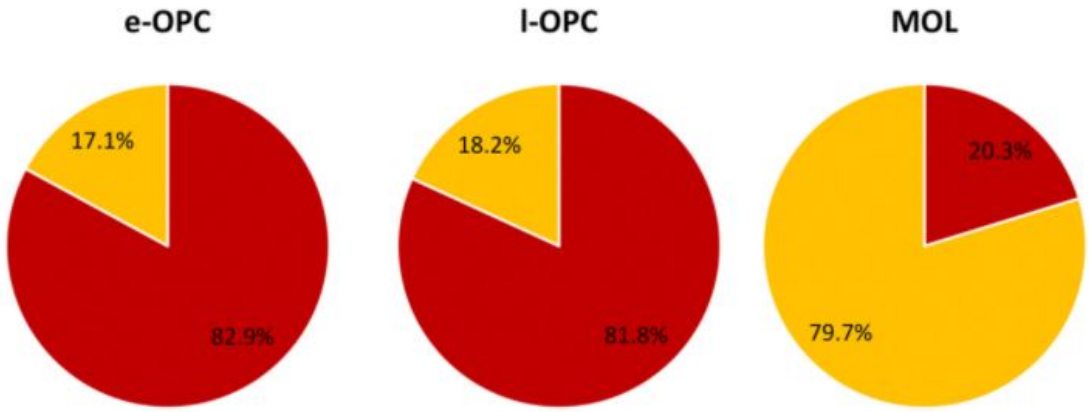

Figure 4. Pie charts presenting the relative percentage of upregulated (red) and downregulated (yellow) genes for each subpopulation.

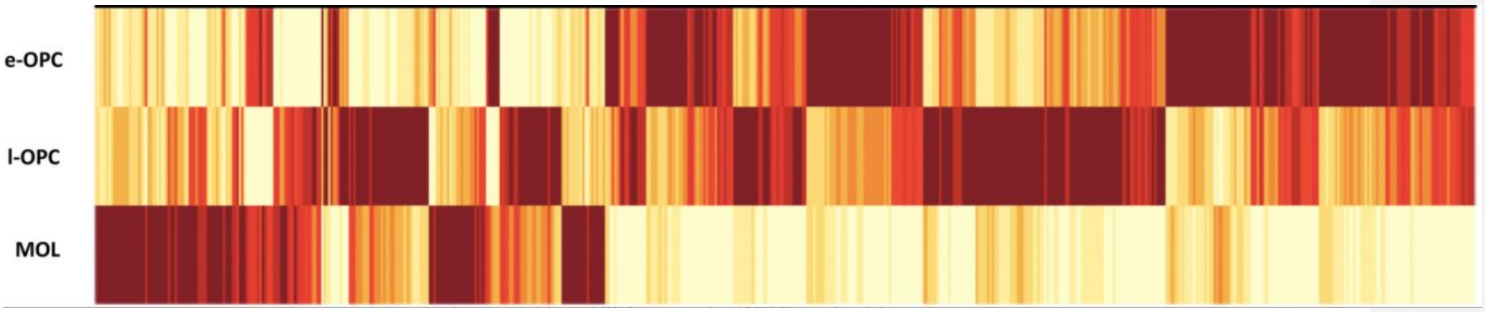

Figure 5. Heat map with corresponding dendrogram showing e-OPC, l-OPC, and MOL gene expression relative to each other. Darker colors represent higher expression levels

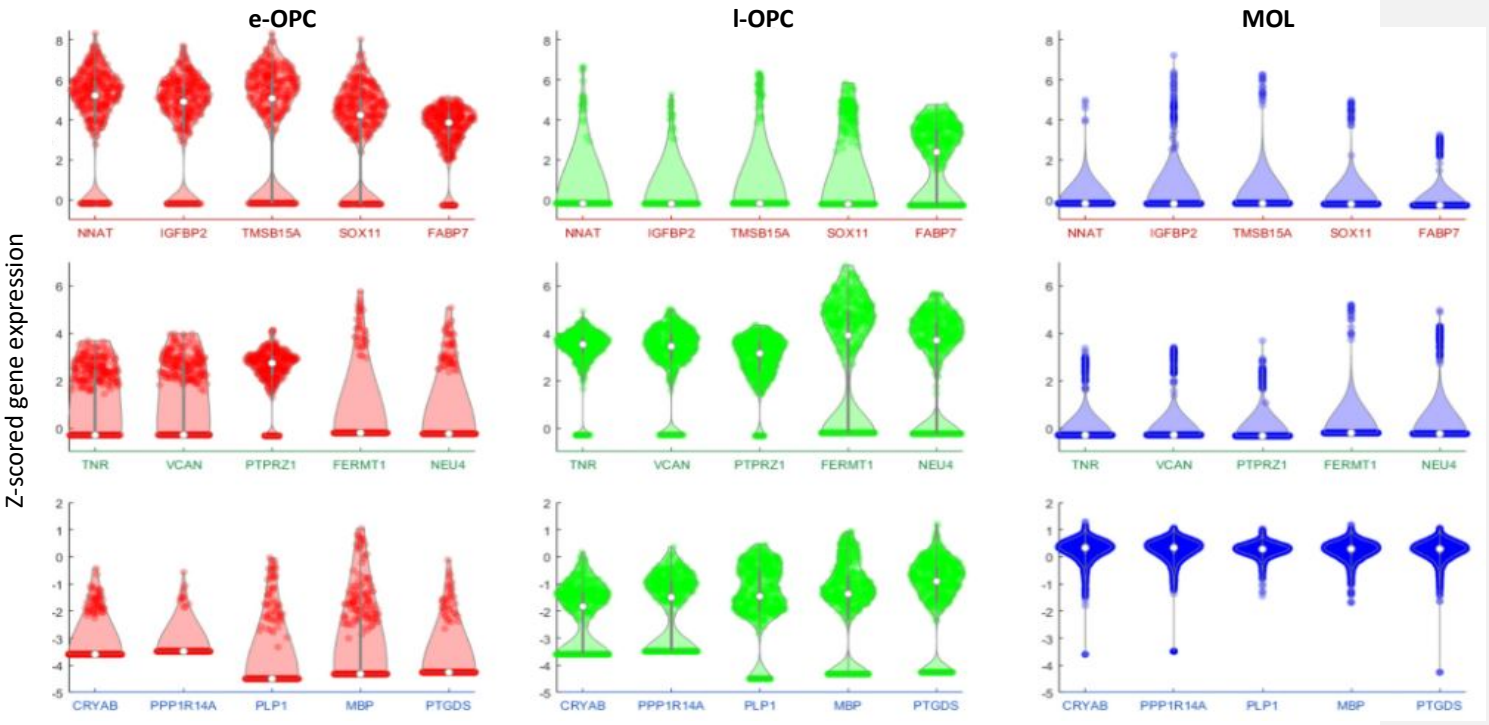

Figure 6. Violin plots comparing the expression of the top from five genes from each OL-lineage subpopulation as defined by top log fold change.

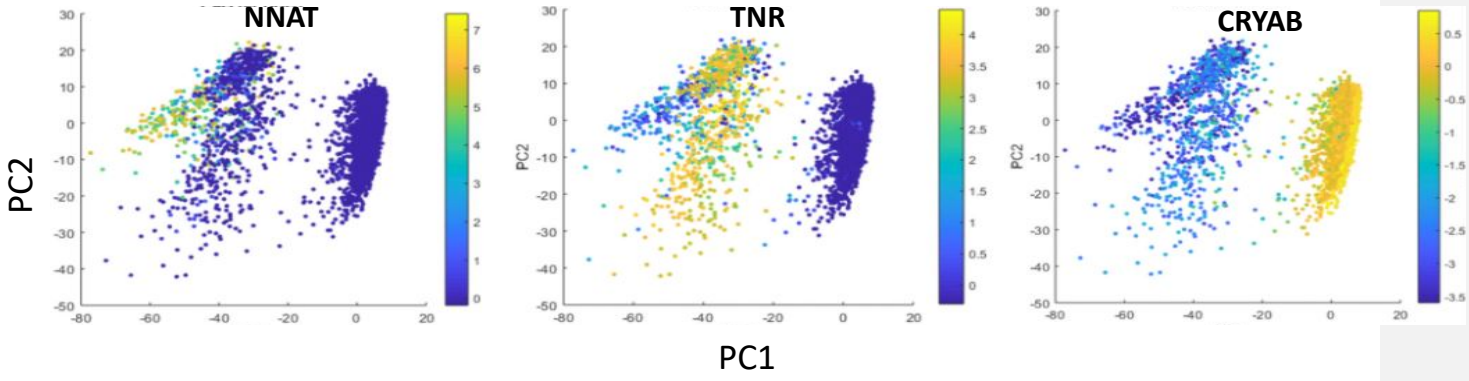

Figure 7. Representation of the expression of the top gene from each subpopulation as defined by log fold change on PCA plots, with each top gene showing high specificity to its respective cluster. Color bar represents expression on a z-scored log base 2 scale

Distribution of the three OL-lineage subpopulations was different at various stage of development (Table 2, Figure 8). For example, fetal cells made the whole population of the e-OPC population, while pediatric samples (less than 5 years of age) contained both l-OPC and MOL. On the other hand, adolescent and adult samples were significantly composed of MOLs and a small amount of l-OPCs (Table 3, Figure 8). To assess the dynamic of gene expression changes over differentiation of OL lineage cells, expression of top 5 differentially expressed genes from each sub population plotted across the stages of differentiation revealed subpopulation-specific patterns of gene expression (Figure 9). Expectedly, expression of e-OPC specific genes peaks at the earliest pseudotime time points which is followed by expression of l-OPC markers and finally expression of MOL markers (Figure 9). At the next step, expression of canonical marker genes of each cell types were plotted across pseudotime to evaluate whether the pattern of gene expression changes matches with the prediction form previous literature or not [184] (Figure 10). Our result showed that expression of each gene not only followed the expected pattern, but also unraveled more fine-tuning changes for the overall gene expression regulation. For instance, even though *PDGFRA* and *CSPG4* are both considered as markers of progenitor cells, but we showed expression *CSPG4* peaks when the cells are more committed toward mature cells (Figure 10).

Furthermore, to check the correlation of our findings in human OL lineage cells with murine single cell RNAseq studies we compared our results with the murine scRNA-seq study conducted by Artegiani et al. (2017) [185] (Figure 11). Importantly, this murine clustering analysis also identified 3 distinct OL-lineage subpopulations of differing maturity states (OPC, COP, MFOL), so a direct comparison with our clusters was readily possible. All identified clusters in terms of maturity level display the highest percentage of overlapping genes, as would be expected (Figure 11).

	% e-OPC	% l-OPC	% MOL
Fetal	100	0	0
Pediatric	0.38	17.37	82.35
Adolescent	0	1	99
Adult	0	0.77	99.23

Table 3. Distribution of OL-lineage subpopulations within each age group. The frequency of cells in a given subpopulation for a given age is expressed by % of total OL-lineage cell count.

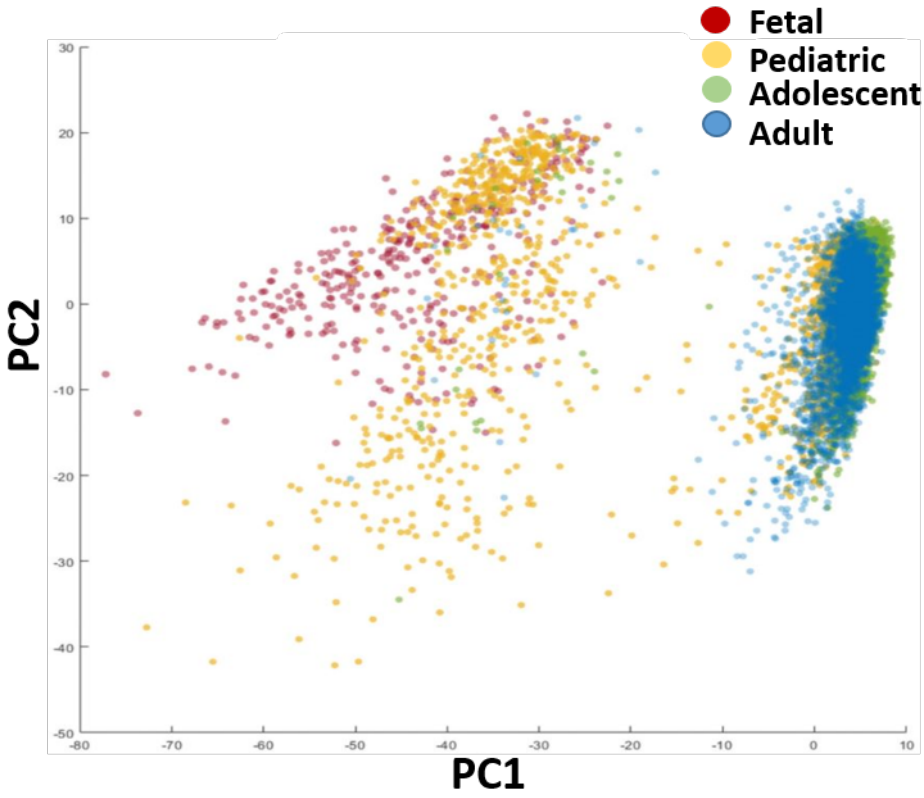

Figure 8. Distribution of OL-lineage subpopulations within each age group. (a) Graphical representation of the age-specific differences in subpopulation distribution on a PCA plot, with points colored by age.

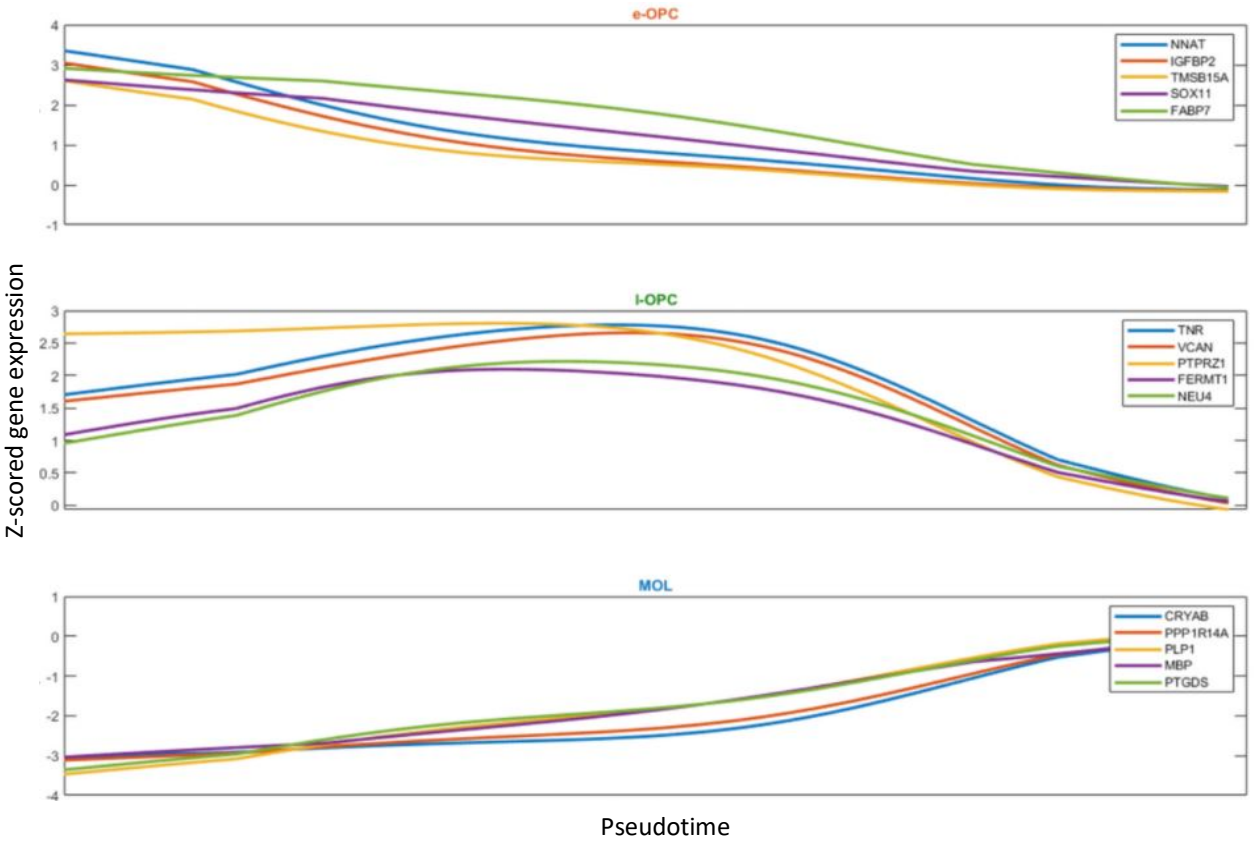

Figure 9. Expression of top five genes from each subpopulation tracked across pseudotime to reveal population-specific expression patterns.

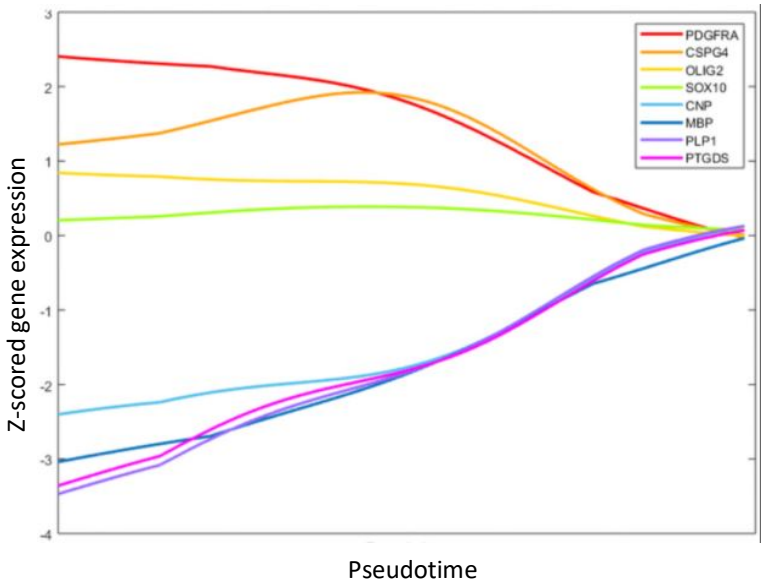

Figure 10. Expression of canonical OL-lineage genes tracked across pseudotime to assess that their expression matches the expected patterns

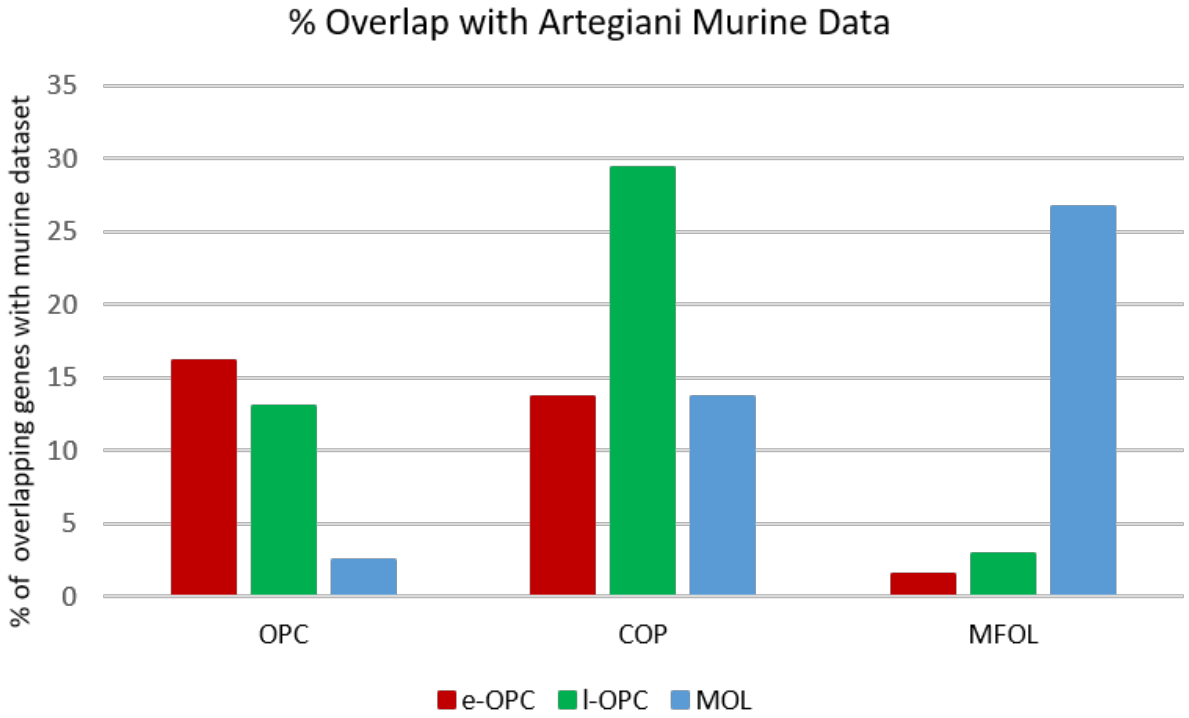

Figure 11. Changes in gene expression found to be significant in our differential expression analyses were then compared to the results of the murine scRNA-seq study conducted by Artegiani et al. (2017). Percentage of overlapping genes with murine dataset is represented over Y axis and the cell types are shown on the X axis.

Biological pathways and molecular functions which are associated with each cell type in OL lineage

In order to get an insight regarding the biological processes which were associated with cell types in OL lineage we performed gene ontology analysis for the most up regulated genes for each cell types (Figure 12A and B). The most affected biological process in the MOLs were myelination, regulation of transport, organelle organization and intracellular iron sequestration (Figure 12A). For the early and late OPCs we performed a differential expression analysis between these two cell types to get a more accurate expression signature. Biological pathway analysis for the up regulated genes in e-OPCs showed that regulation of the cell cycle, microtubule cytoskeletal organization, and chromatin conformation were among the most affected pathways. On the other hand, for the l-OPCs we found upregulated pathways included extracellular matrix (ECM) metabolism, lipid metabolism, and myelination. (Figure 12B). We further analyzed protein-protein interaction network of up regulated genes for each cell type in which we identified presence of protein clusters which are associated with more specific function (Figure 13-15). For example, in the l-OPCs we discovered modules of genes coding for the ECM and collagens, axon guidance molecules, ionotropic glutamate receptors, g-coupled protein receptors, and synaptic proteins. These modules are interlinked with each other via highly interconnected nodes that include the genes *GPR17, GRM5, NTN1, FYN, TRIO, SDC3, GRIA2*, and *GRIA3* (Figure 15).

A

GO term	Description	-log(FDR)
GO:0000278	mitotic cell cycle	12.70
GO:0051301	cell division	11.75
GO:0051726	regulation of cell cycle	7.71
GO:0071103	DNA conformation change	6.65
GO:0006323	DNA packaging	6.36
GO:0034508	centromere complex assembly	4.85
GO:0006333	chromatin assembly or disassembly	4.79
GO:0042127	regulation of cell population proliferation	4.30
GO:0071824	protein-DNA complex subunit organization	4.29
GO:0051383	kinetochore organization	4.27
GO:0006029	proteoglycan metabolic process	8.08
GO:0030204	chondroitin sulfate metabolic process	7.12
GO:0050655	dermatan sulfate proteoglycan metabolic process	6.60
GO:0007155	cell adhesion	6.35
GO:0006024	glycosaminoglycan biosynthetic process	6.32
GO:0051963	regulation of synapse assembly	6.22
GO:0007411	axon guidance	6.01
GO:0043269	regulation of ion transport	5.74
GO:0016477	cell migration	5.09
GO:0030111	regulation of Wnt signaling pathway	2.39
GO:2000311	regulation of AMPA receptor activity	1.95
GO:0042552	myelination	4.48
GO:0031109	microtubule polymerization or depolymerization	3.06
GO:0097435	supramolecular fiber organization	2.74
GO:0048709	oligodendrocyte differentiation	2.66
GO:0007017	microtubule-based process	2.51
GO:1904062	regulation of cation transmembrane transport	2.26
GO:0006633	fatty acid biosynthetic process	2.11
GO:0051050	positive regulation of transport	1.88
GO:0032271	regulation of protein polymerization	1.86
GO:0006880	intracellular sequestering of iron ion	1.79
GO:0032879	regulation of localization	1.72

Figure 12A. Top biological pathways enriched each OL-lineage subpopulation as determined by gene ontology.

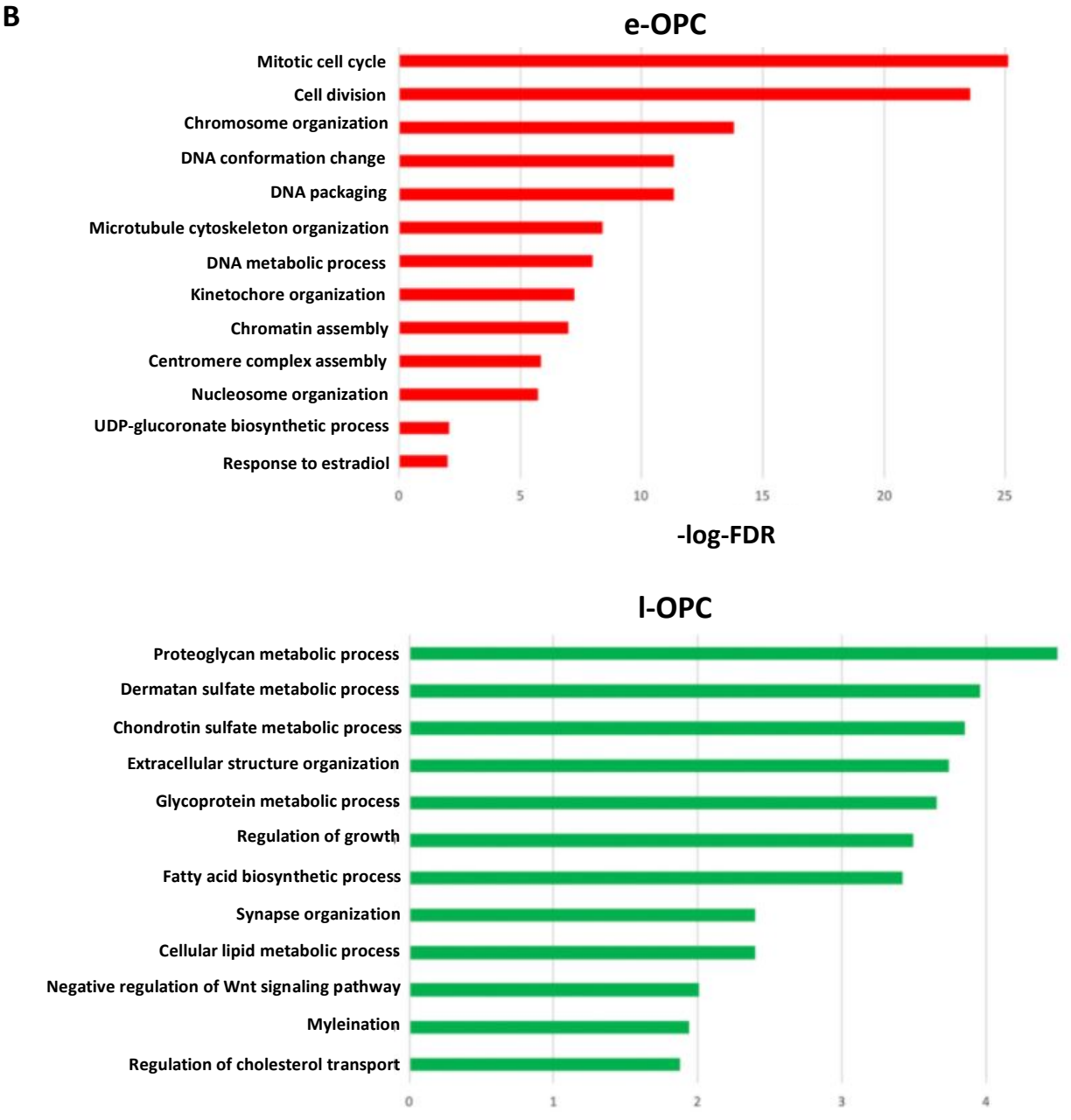

Figure 12B. Top biological pathways enriched in e-OPC and l-OPC derived from two-way differentially expressed genes as determined by gene ontology

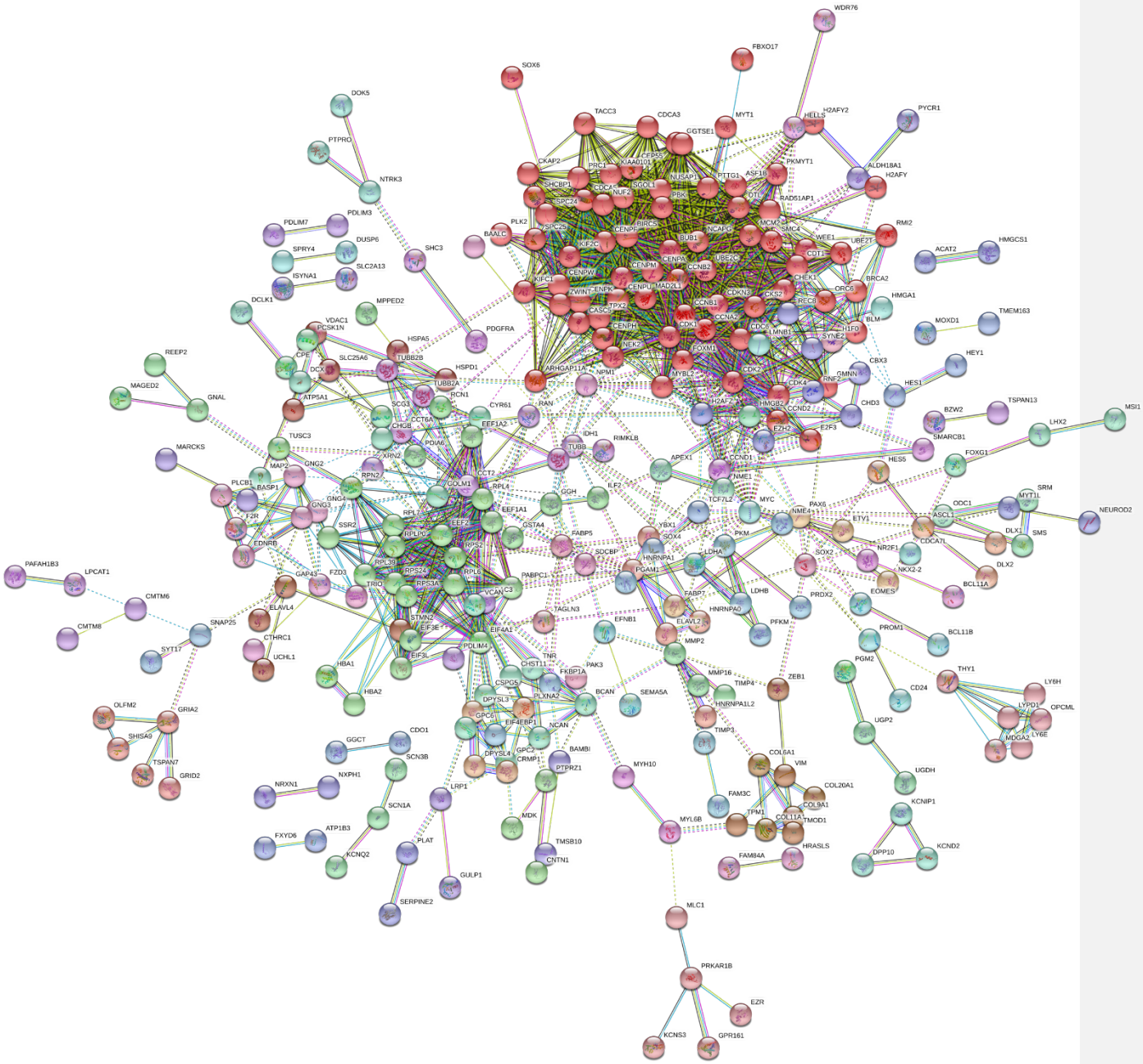

Figure 13. e-OPC protein-protein interactions network

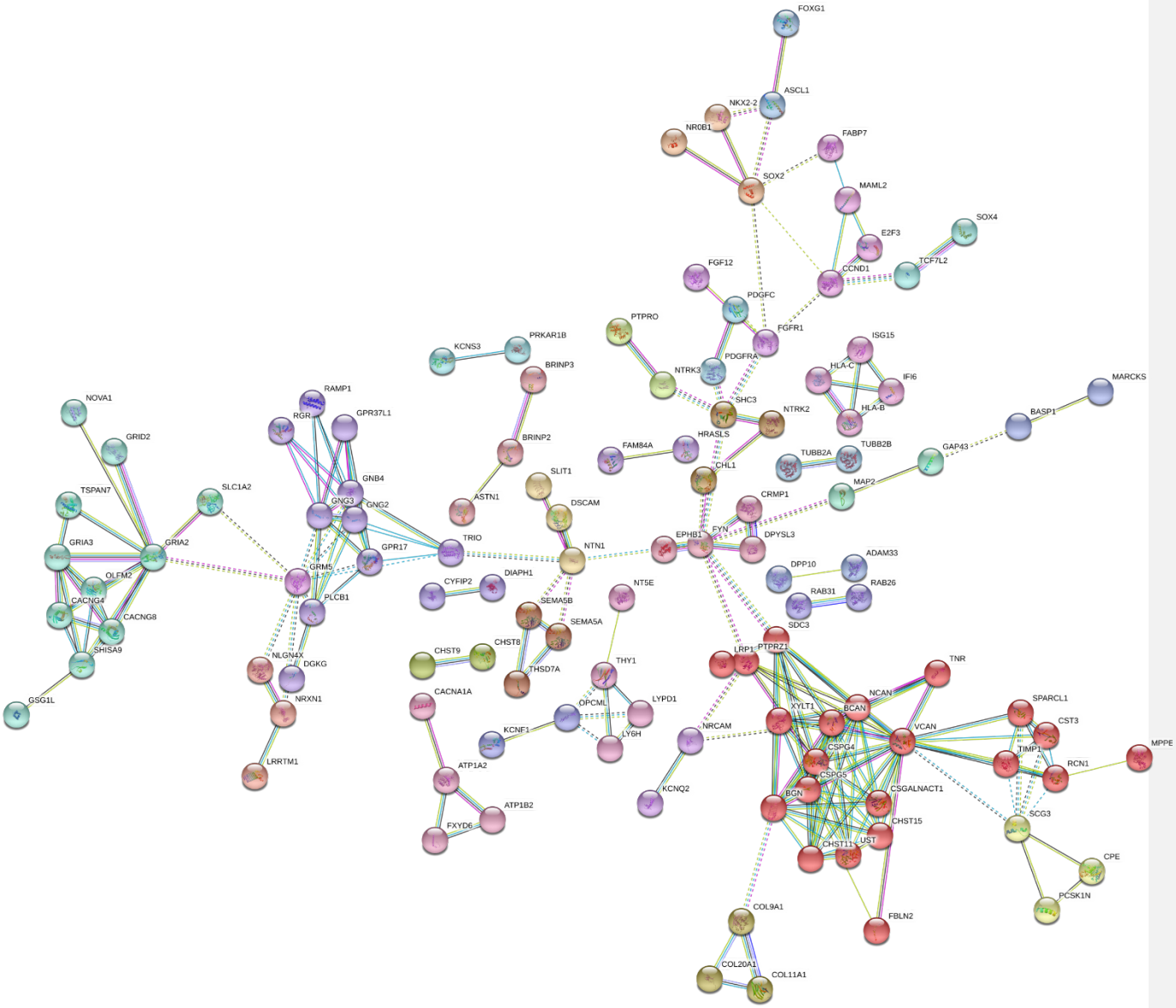

Figure 14. l-OPC protein-protein interactions network

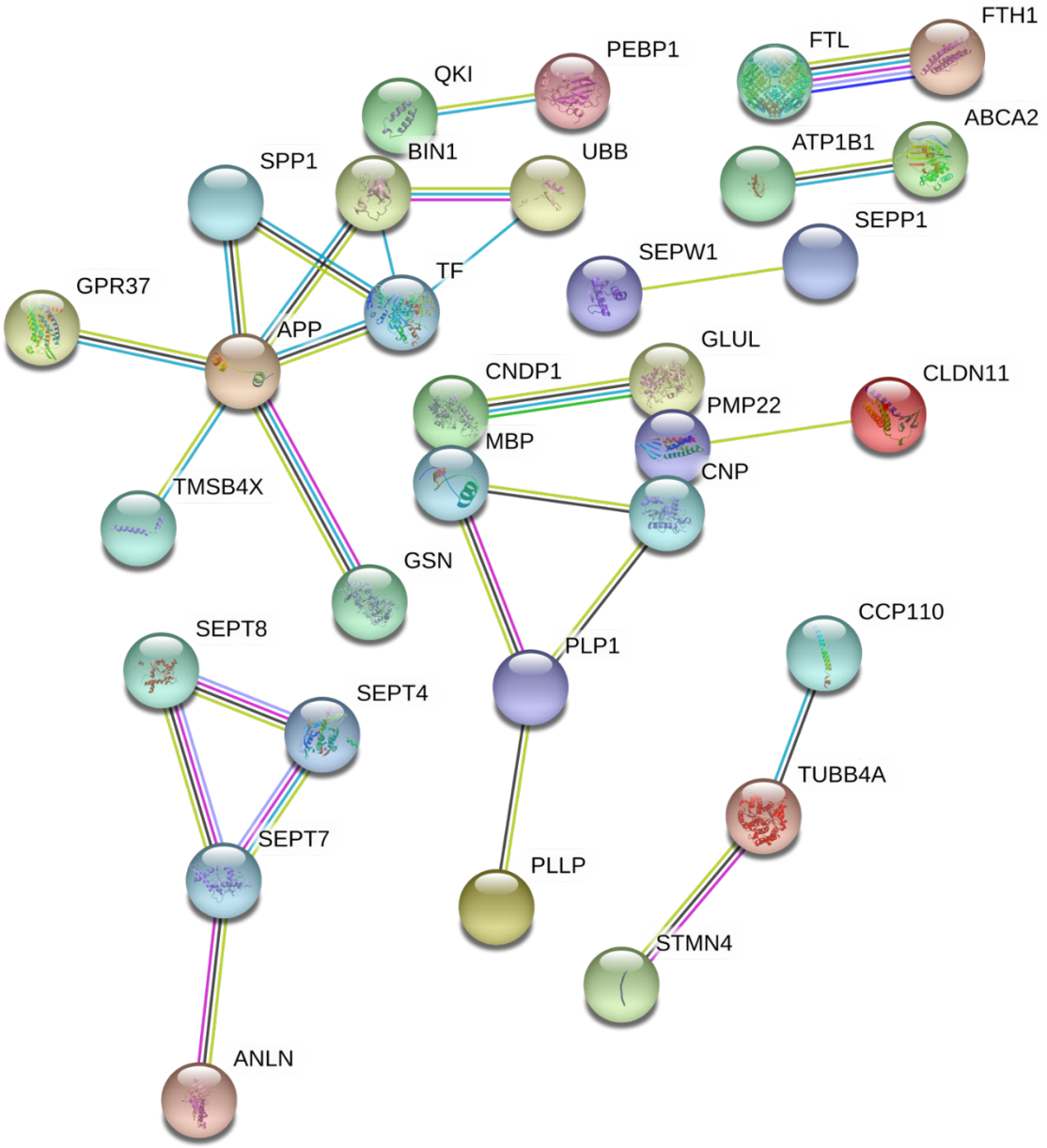

Figure 15. MOL protein-protein interactions network

Transcription factors associated with the OL-lineage cell subset

In order to unravel profile of transcription factors (TFs) which underlie differentiation of cell types in the OL lineage, the list of gene expression data of each cell type was filtered based on a list of human transcription factors reported by Lambert et al. (2018) [183]. We inly kept those TFs that were differentially expressed between cell types (log fold change >1 and FDR corrected p-value <0.05). Using this criteria, fifty transcription factors were identified that are differentially expressed in at least one subpopulation (Figure 16). TFs that were selectively expressed in one subpopulation as compared to the other two include: *MYC, ZNG385D, MYT1L, DLX1, HES4, FOXM1* in e-OPCs; *HMGA1, PRRX1, E2F3, SOX21, HIF3A, ZNF469,* and *SOX8* in l-OPCs; and *CREB5, MYRF, JUND* in MOLs. At the next step we wanted to see which TF might be the most central factor by considering the direct number of their target genes. By browsing the list TFs in Enricher database that contains the data of verified TF binding site, we obtained the list of target genes of each TF. Centrality analysis indicated that *SOX2* was the most highly connected TF in e-OPC, l-OPC, and MOL (Figure 17A-C), consistent with its key role in regulating the OL lineage [186].

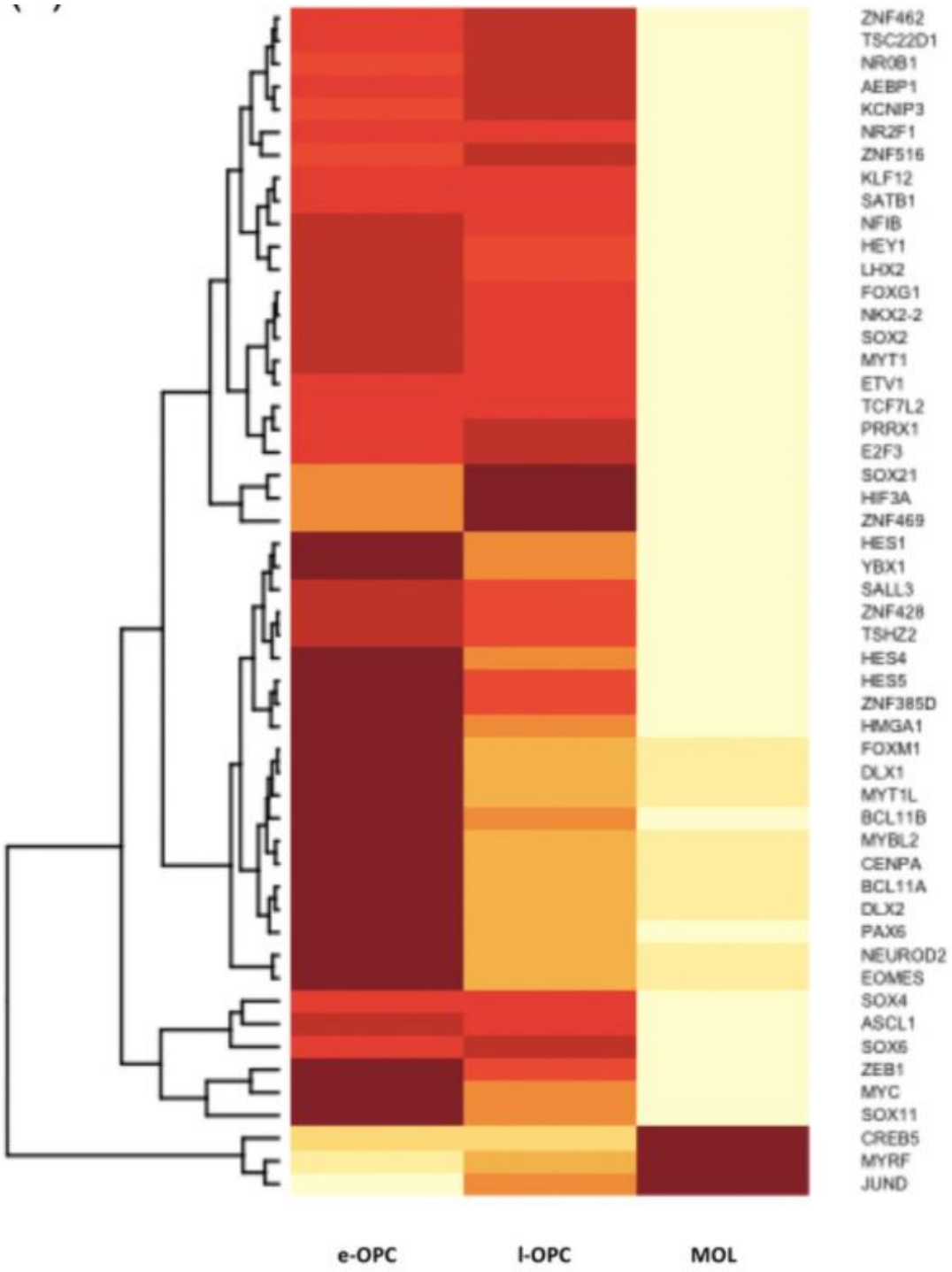

Figure 16. Heatmap comparing expression of transcription factors across subpopulations. Darker color donates higher expression.

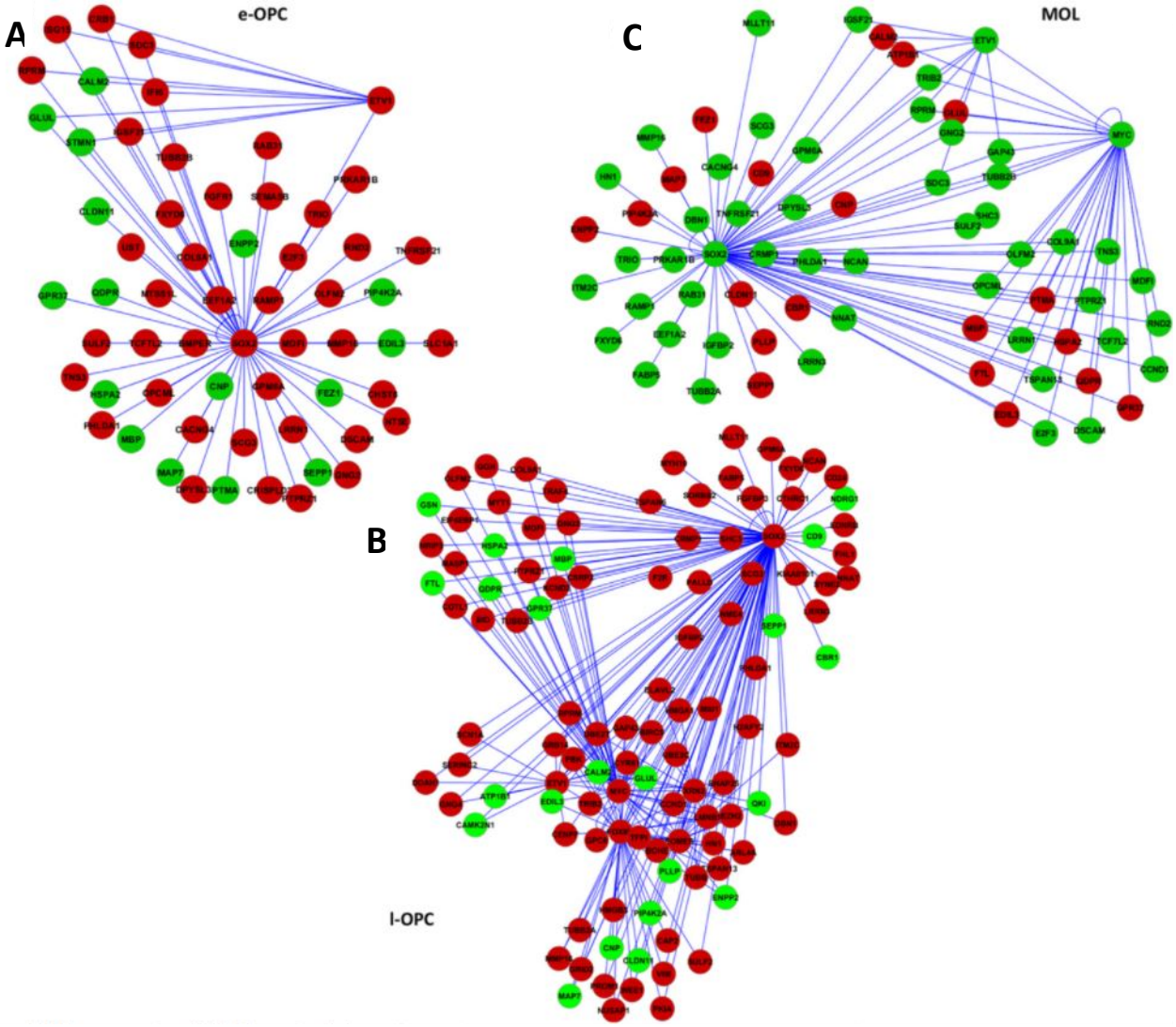

Figure 17. SOX2 hub gene networks for (b) e-OPCs, (c) l-OPC, and (d) MOLs. Red nodes = upregulated gene, green node = downregulated gene

Age specific differences between cell types in the OL lineage

At the next step we wanted to compare gene expression profile of cells within age groups. For the e-OPCs since we could not find this cell type in post-natal cells we could not do direct comparison between ages. However, for the l-OPC and MOL we directly compared populations for the pediatric and adult samples. MOL populations between pediatric and adult samples were significantly similar, with only two genes being significantly differentially expressed (log fold change >1 and FDR corrected p-value <0.05). In contrast, the expression signature of l-OPC between pediatric and adult samples were significantly different. We found 60 differentially up genes in pediatric l-OPC and 244 up genes in adult l-OPC (Figure 18A). Biological pathway analysis revealed that the most affected biological processes by the up regulated genes in pediatric l-OPC included differentiation, axon guidance, and metabolism of ECM components, and in adult l-OPCs, the GO terms were related to regulation of cell projections, dynein arm assembly, and supraoxide metabolism (Figure 18B). Protein-protein interaction network of the up regulated genes of l-OPC within each age group identified relationships between the genes within each age-specific signature. Notably, *MBP* and *CNP* genes, both characteristic of myelination, were upregulated in the pediatric l-OPCs compared to the adult l-OPC. Genes encoding transcription factors that were significantly upregulated in l-OPCs in pediatric and adults are listed in Figure 18C.

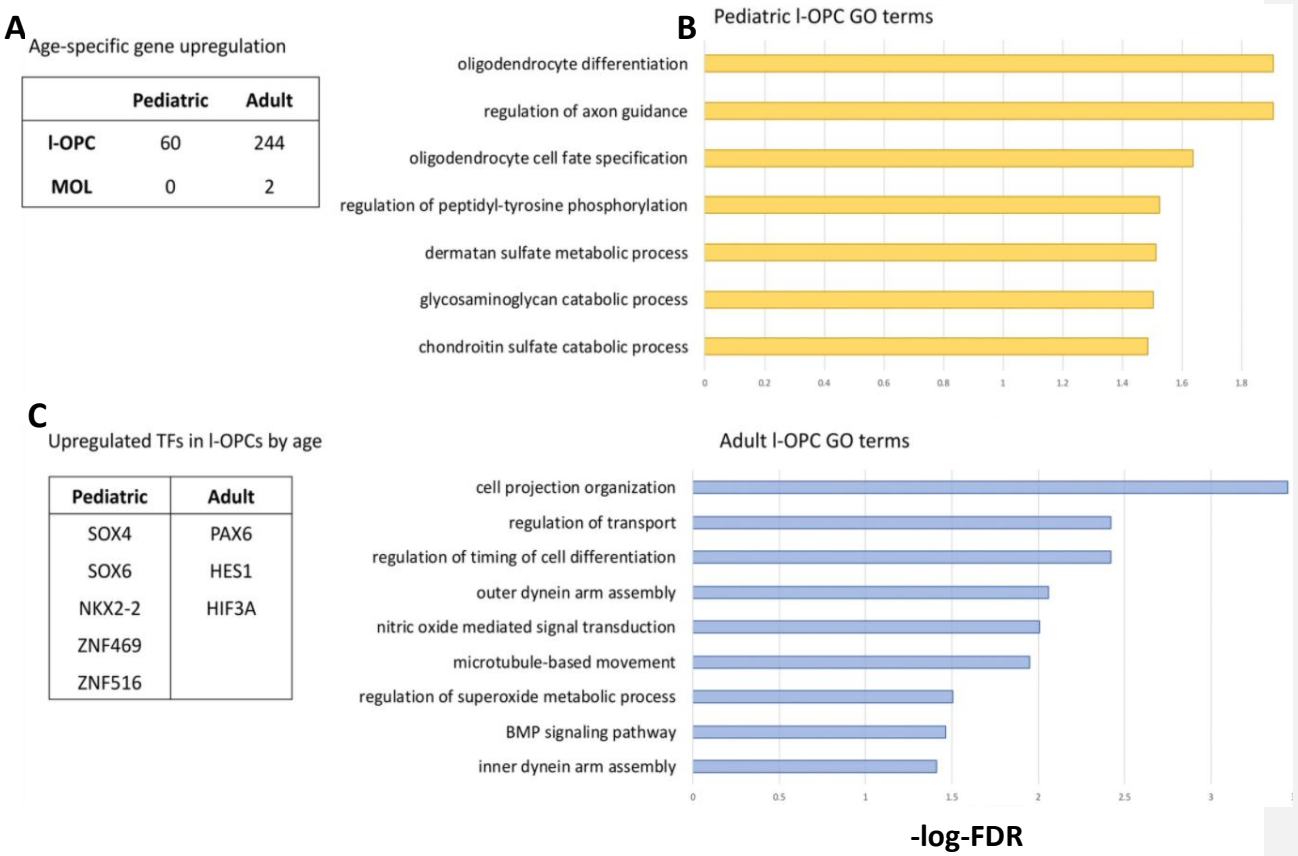

Figure 18. A) Number of significantly upregulated genes in pediatric and adult cells for l-OPCs and MOLs. (B) Top biological pathways enriched in pediatric l-OPCs and adult l-OPCs, as determined by gene ontology, based on their respective significantly upregulated genes. (c) Significantly upregulated transcription factors specific to pediatric and adult l-OPCs

In situ validation

To assess whether any cells with the signature of the relatively abundant l-OPCs present at ages associated with peak myelination could be detected in situ in the adult brain, we used RNAScope fluorescent in situ hybridization. Given that no e-OPCs were identified in our adult samples, we considered all *PDGFRA*+ cells to be l-OPCs. In Figure 19, *PDGFRA*+ cells were found to express (a) *TNR* and (b) *VCAN* in sections of adult postmortem ventromedial prefrontal cortex (98.3% *TNR*+/*PDGFRA*+; 100% *VCAN*+/*PDGFRA*+) (Figure 19A and B). This expression pattern was highly specific to OPCs, as these genes were not detected in *PDGFRA*- cells, thus providing validation of our l-OPC signature. Many of the significantly upregulated genes in the l-OPCs are central to ECM-related biological processes (Figure 20), with *TNR* and *VCAN* being the two top genes as determined by highest LFC.

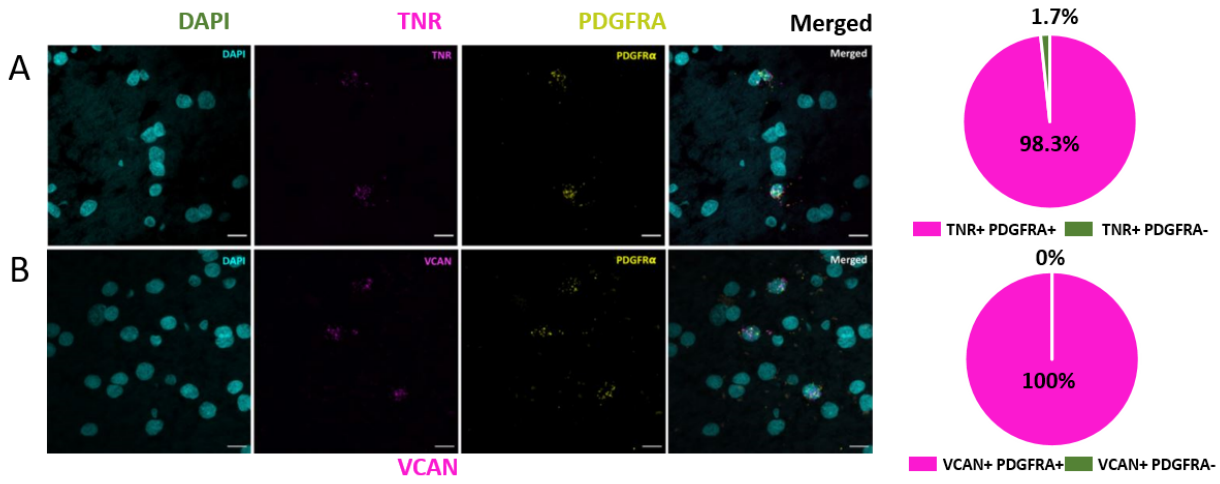

Figure 19. Enrichment of extracellular matrix gene expression in late OPCs was validated using single molecule fluorescent in situ hybridization (RNAscope). Representative confocal images of l-OPCs identified based on PDGFRA expression (yellow) and showing co-expression with (a) TNR and (b) VCAN (magenta). Pie charts illustrate that 98.3% of TNR-expressing cells are l-OPCs (N = 60 cells), while 100% of VCAN-expressing cells are l-OPCs (N = 60 cells), indicating a strong enrichment of those genes in l-OPCs. Scale bar = 10 µm. Pie charts illustrate that 98.3% of TNR-expressing cells are l-OPCs (N = 60 cells), while 100% of VCAN-expressing cells are l-OPCs (N = 60 cells), indicating a strong enrichment of those genes in l-OPCs. Scale bar = 10 µm.

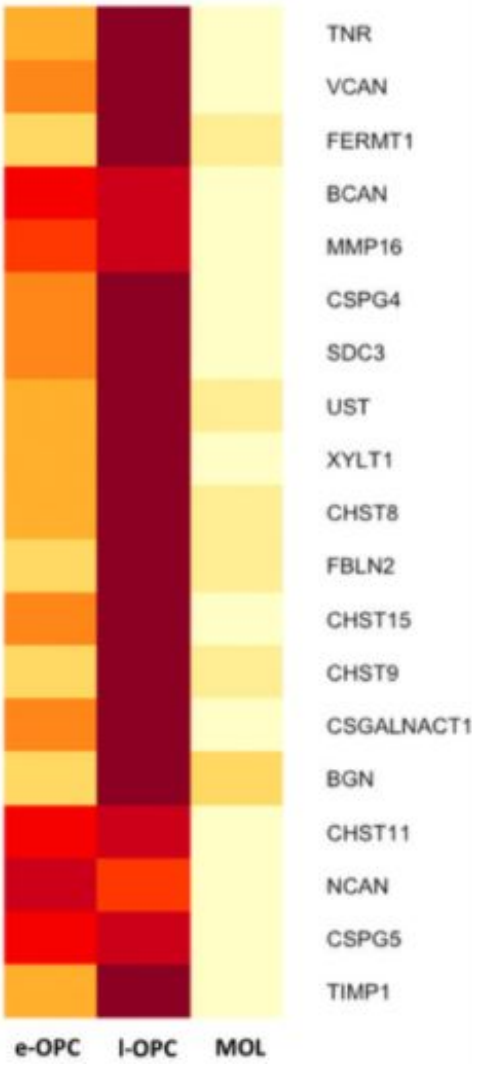

Figure 20. Heatmap illustrating the z-scored expression of key extracellular matrix genes in each OL-lineage subpopulation. Genes are ordered in decreasing LFC for l-OPC. Darker colors indicate higher expression of genes.

Regional heterogeneity of mature oligodendrocytes

In the previous section we explored the temporal heterogeneity of OL lineage cells during human development. In this part we sought to uncover whether mature oligodendrocytes (MOLs) are regionally heterogeneous across several distinct anatomical regions of the human CNS. Typically, MOLs were classified into four distinct sub-types according to their morphology [14], with later studies providing additional morphological MOL sub-types [187,188]. The activity of MOLs including the pattern and number of myelin sheaths formed by them also could be used to categorize into different sub-types [189]. However, the advent of newer techniques such as single cell RNA sequencing provided the opportunity to explore MOL diversity in a more comprehensive way. One of the most important studies to explore the temporal and regional heterogeneity of mouse OL lineage cells under homeostatic condition was performed by Marques and colleagues [91]. In this paper the authors were unable to identify region- or age specific subpopulations of OPCs, but they identified six transcriptionally distinct MOL subtypes across ten anatomical location of the CNS which showed region specific pattern [91]. Even though these sub-types shared a core gene expression signature, they showed their own specific signature as well. For instance, there were clusters enriched in lipid biosynthesis and myelination genes and clusters enriched for synaptic component genes and glutamate receptors [91]. In two follow-up studies the authors confirmed the presence of these transcriptionally distinct MOL subtypes in vivo using RNAscope in situ hybridization (ISH) and in situ sequencing (ISS) [190,191]. Moreover, the authors showed that the existence of distinct MOL populations is independent of their developmental origin and instead environmental cues are the main driving force for their generation [190,191]. In contrast to rodent models' studies, the regional heterogeneity of human MOLs is understudied.

Here, we explored the spatial heterogeneity of MOLs from three CNS regions including i) adult brain parenchyma, ii) adult spinal cord and the iii) adult sub-ventricular zone (SVZ) (table 4). Tissues from three independent donors per region were subjected to single cell RNA sequencing. Following quality control and the removal of dead or low-quality cells the remaining cells were integrated into single object for downstream analysis. Among different cell identities which were captured during the experiment, MOLs were selected for further analysis based on expression of

the canonical MOL marker gene myelin OL glycoprotein (*MOG*) (Figure 21). The isolated MOLs were down-sampled and re-clustered to unravel more detailed differences between each anatomical location according to transcriptome of MOLs. A minor population of the isolated cells were expressing microglia markers like *AIF1*, these cells were considered contaminants and excluded for downstream analysis resulting in 1,264 cells per region. Re-clustering of these cells resulted in identification of five distinct sub-types of MOL with differential distribution patterns between anatomical regions (Figure 22). Hierarchal clustering of cells according to expression of top up regulated genes in each cluster indicates that each cluster has a specific gene expression signature (Figure 23). Gene ontology analysis of the upregulated genes per cluster indicated specific function associated with MOL clusters. Expectedly, myelinogenesis and lipid related terms are among the most affected biological processes as revealed by our over representation analysis (Figure 24). Interestingly, we observed an enrichment of immune related terms among the most affected biological processes in clusters 1 and 4 (Figure 24). These clusters were expressing high levels of histocompatibility genes like *HLA-DRA, HLA-B* and *HLA-C* (Figure 25). These clusters were mainly occupied by spinal cord MOLs. We also observed a clear difference between MOLs from the spinal cord and those from the brain parenchyma and SVZ (Figure 26). Highly expressed genes of the spinal cord MOL in comparison to parenchyma and SVZ cells are *HLA-DRA* and *CD74* and *APOE* genes which might suggest more immune vigilant state of cells in the spinal cord (Figure 27). Looking the most affected biological processes of the highly expressed genes in each region we see significant similarity between parenchymal and SVZ cell (Figure 28). Among the most affected biological process we identified myelination, ensheathment of neuron, gliogenesis. On the other hand, for the spinal cord we observed terms such as antigen processing and presentation, leukocyte degranulation (Figure 28). Among all observed affected biological processes both at the cluster level and also at the region level we observed the presence of cell metabolism related pathways. It has been indicated that there are subtypes of OL which may play a role in metabolic support of axons [192].We suggest in all three anatomical locations there is this specific sub-population which controls the metabolism activity of neuronal cells.

In the next step we wanted to know if MOLs of different CNS regions are developmentally different or not. Therefore, we performed a pseudotime trajectory analysis using Potential of Heat-diffusion for Affinity-based Trajectory Embedding (PHATE) [178]. Our analysis revealed that

OLs from different anatomical locations did not align on the trajectory plot according to their regions. Instead the majority of observed differences between the cells were driven by differential clustering (Figure 29).

Altogether, our results confirmed the presence of multiple MOLs sub-types across three independent CNS regions. Whether these transcriptionally distinct sub-types perform specific functions requires further experimentation. In addition, we showed that MOLs of brain parenchyma and SVZ have homogenous transcriptional landscape which is distinct from spinal cord ones in which the cord cells have more immunogenic signature. Furthermore, our trajectory observations suggest that the observed differences between MOLs is not due to a developmental difference but instead reflects interactions of these cells within their local and unique tissue environment.

Region	**Sample**	**Age (Y.O)**
Brain Parenchyma	HA801	41
	HA800	51
	HA738	62
Sub ventricular zone	SVZ	53
	SVZ350	51
	SVZ444	71
Spinal cord	SC004	68
	SC005	39
	SC010	53

Table 4. Information of the samples that were used for spatial heterogeneity analysis

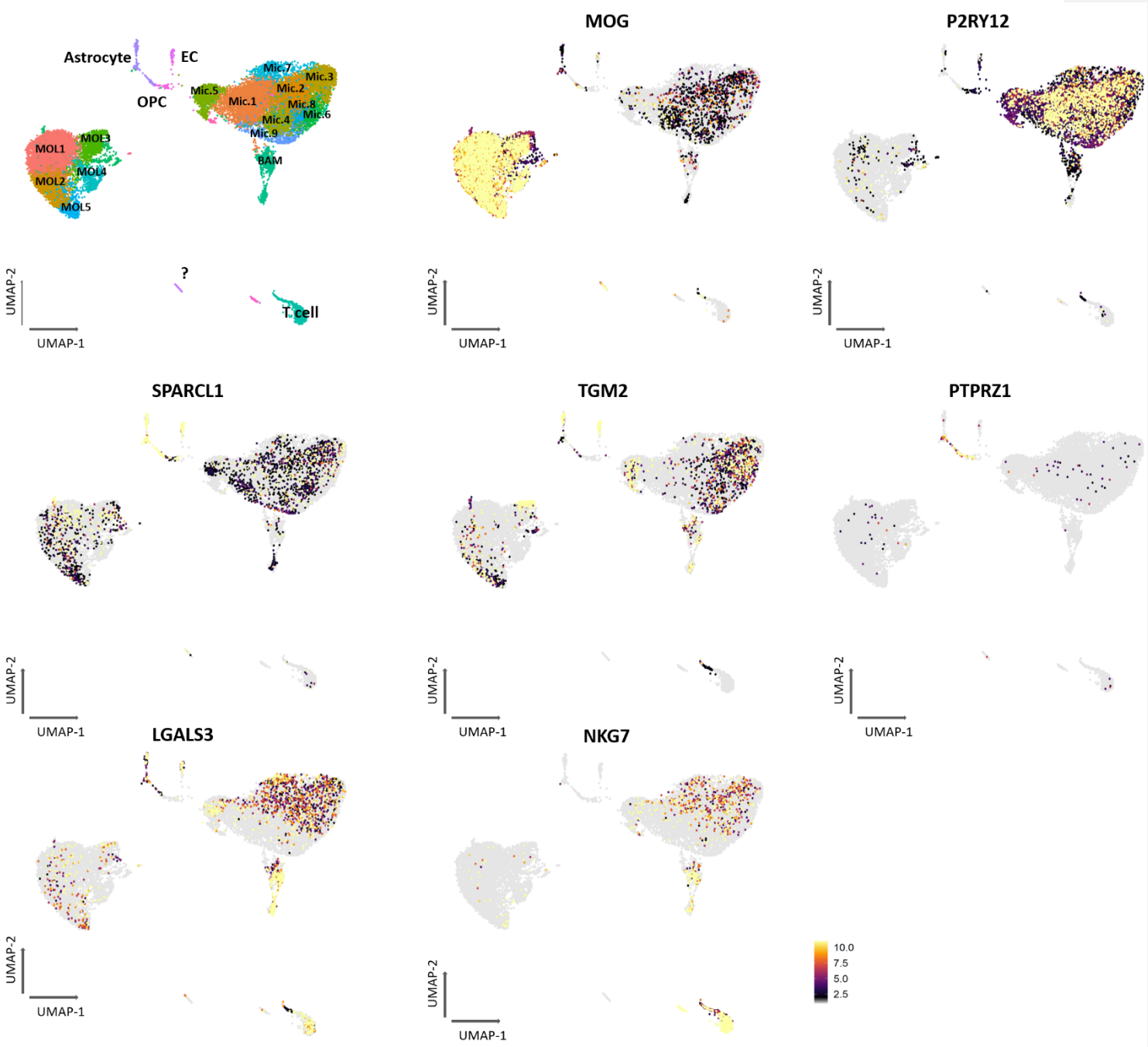

Figure 21. UMAP plot representing the identity of the captured cells from single cell RNAseq data. Normalized average expression of cell type specific markers genes is represented. MOG+ = MOL, P2RY12+ = microglia, SPARCL1+ = astrocyte, TGM2+ = endothelial cells (ECs), PTPRZ1+ = OPCs, LGALS3+ = BAM and NKG7+ = T cells.

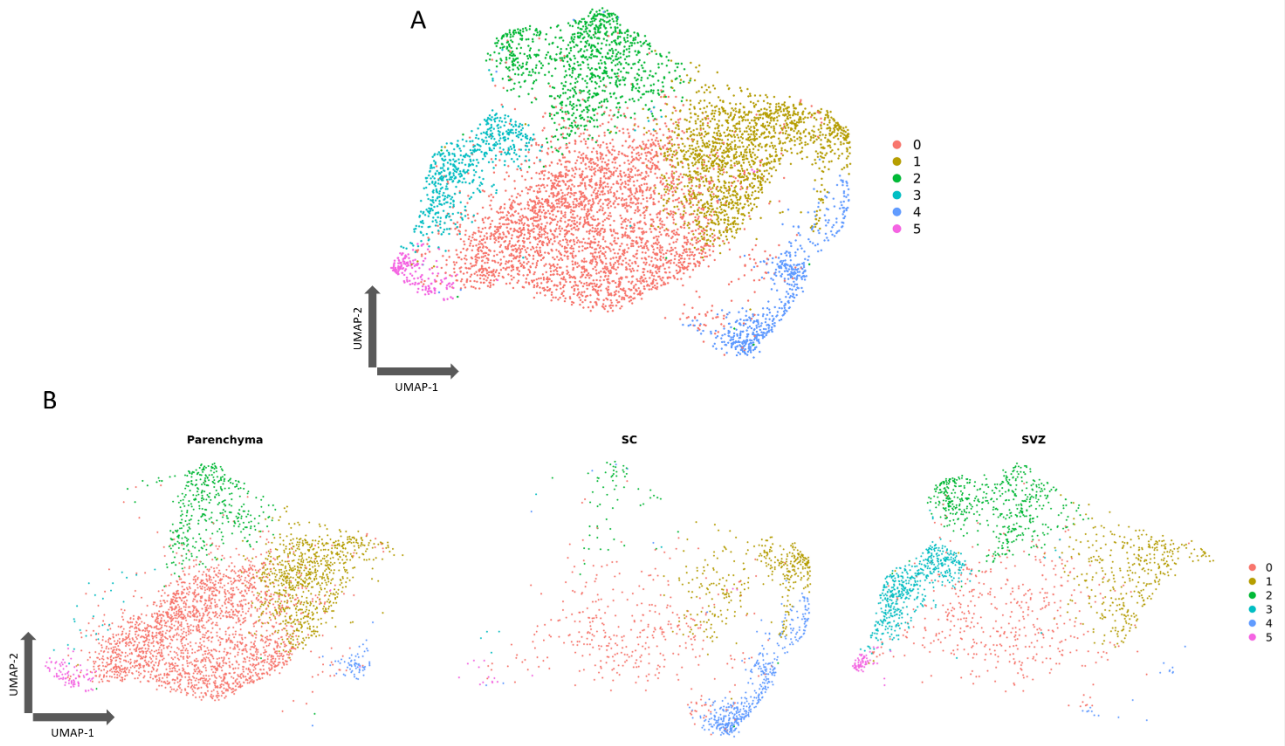

Figure 22. A) UMAP plot representing identified clusters of MOLs which is separated by region in panel B.

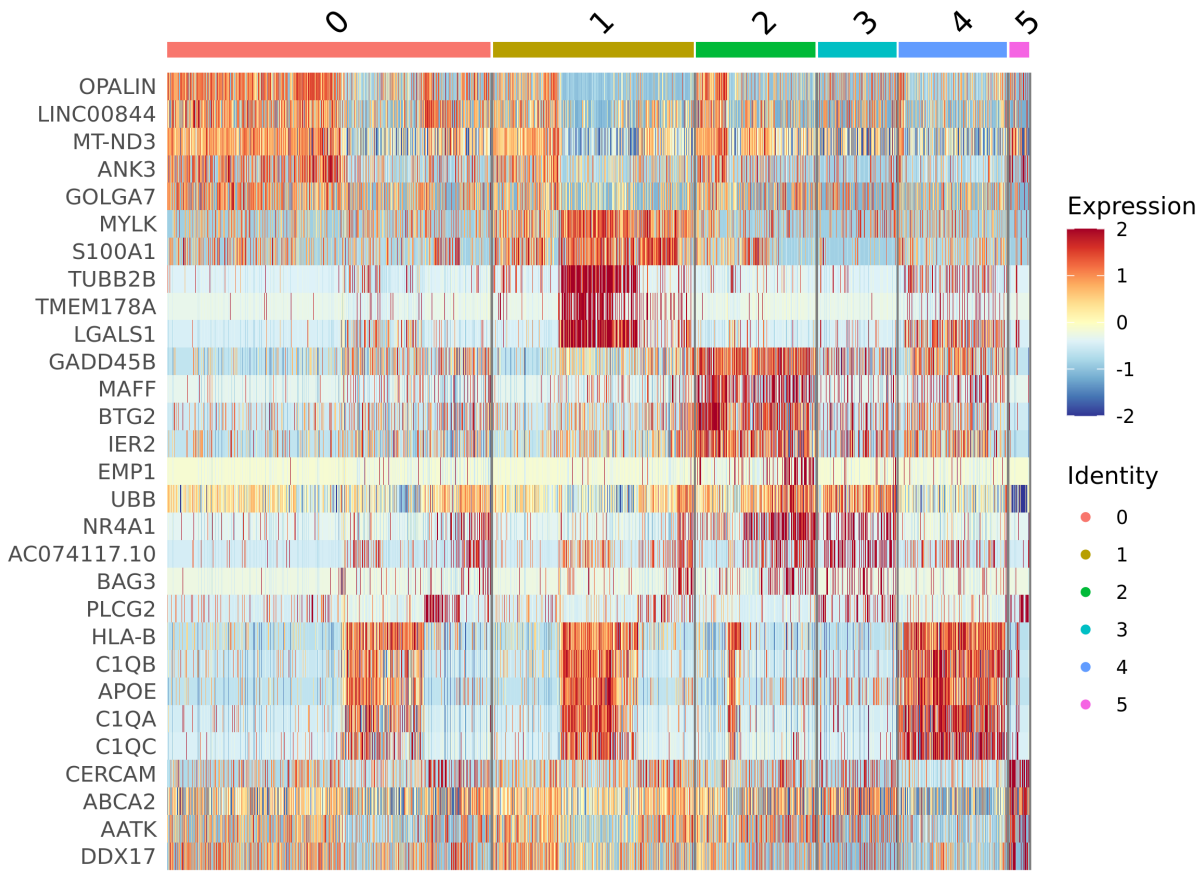

Figure 23. Heatmap of top 10 DEGs per cluster. Gene expression is represented by a color-coded z-score. Up and down regulated genes are shown by red and blue color respectively.

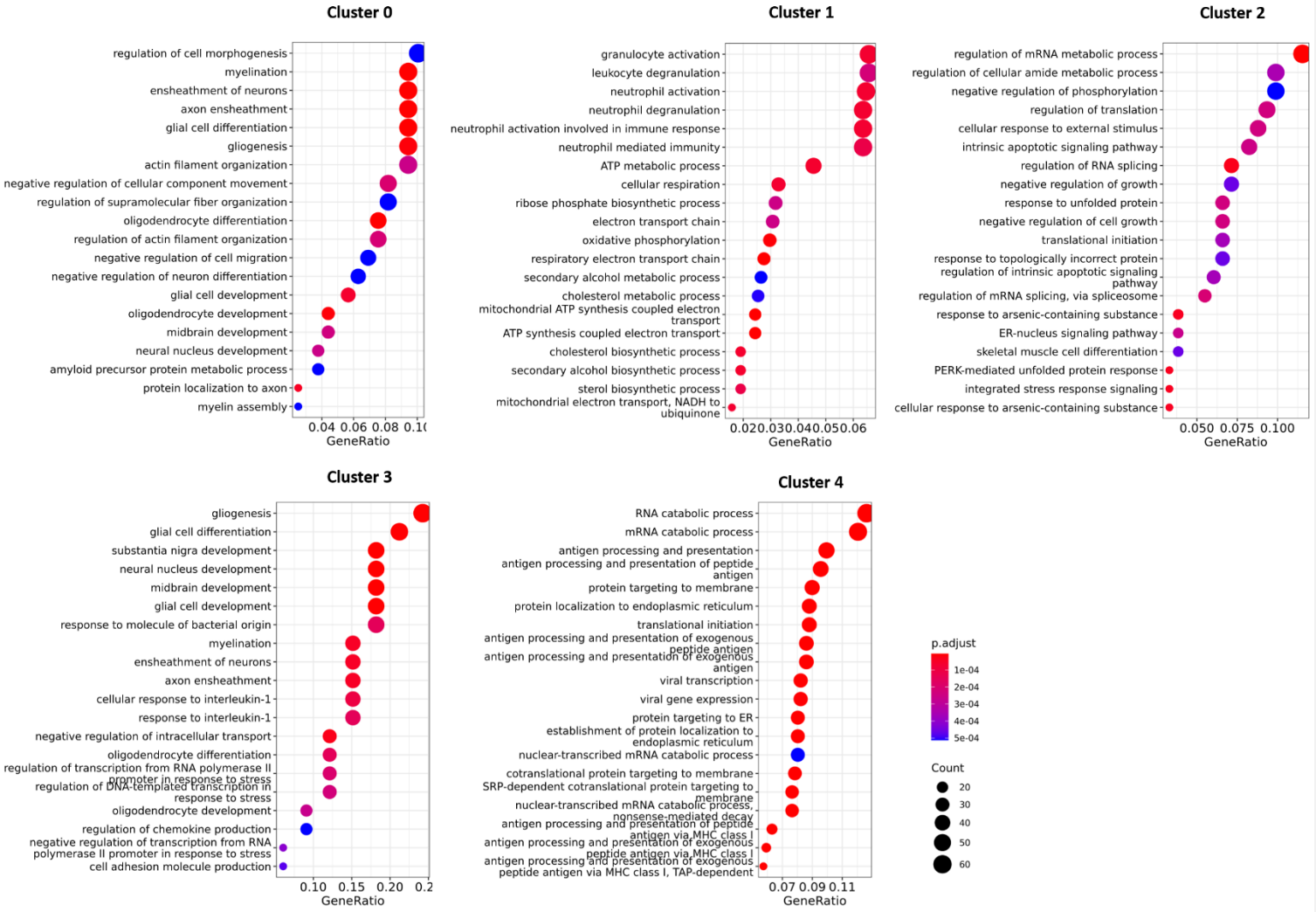

Figure 24. Over representation analysis results. The most represented biological processes for each cluster are represented (cluster 5 did not have enough genes to be represented). The statistical significance of the terms is represented by color coded p-value. Circle size donates the number genes present in each cluster.

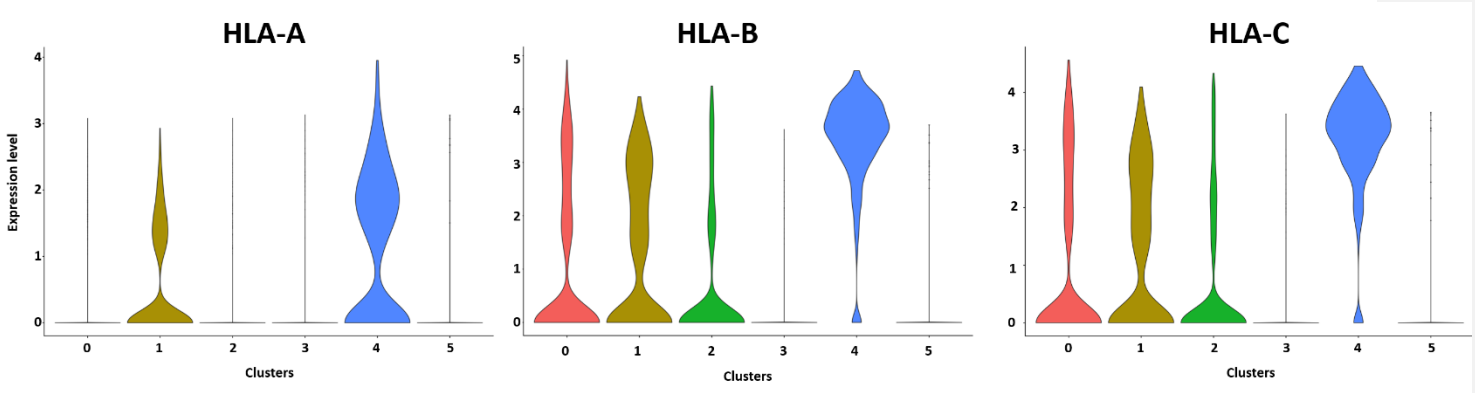

Figure 25. Violin plots depicting expression of histocompatibility genes across all clusters. The expression level of genes are represented in Y axis and the clusters are shown on the X axis.

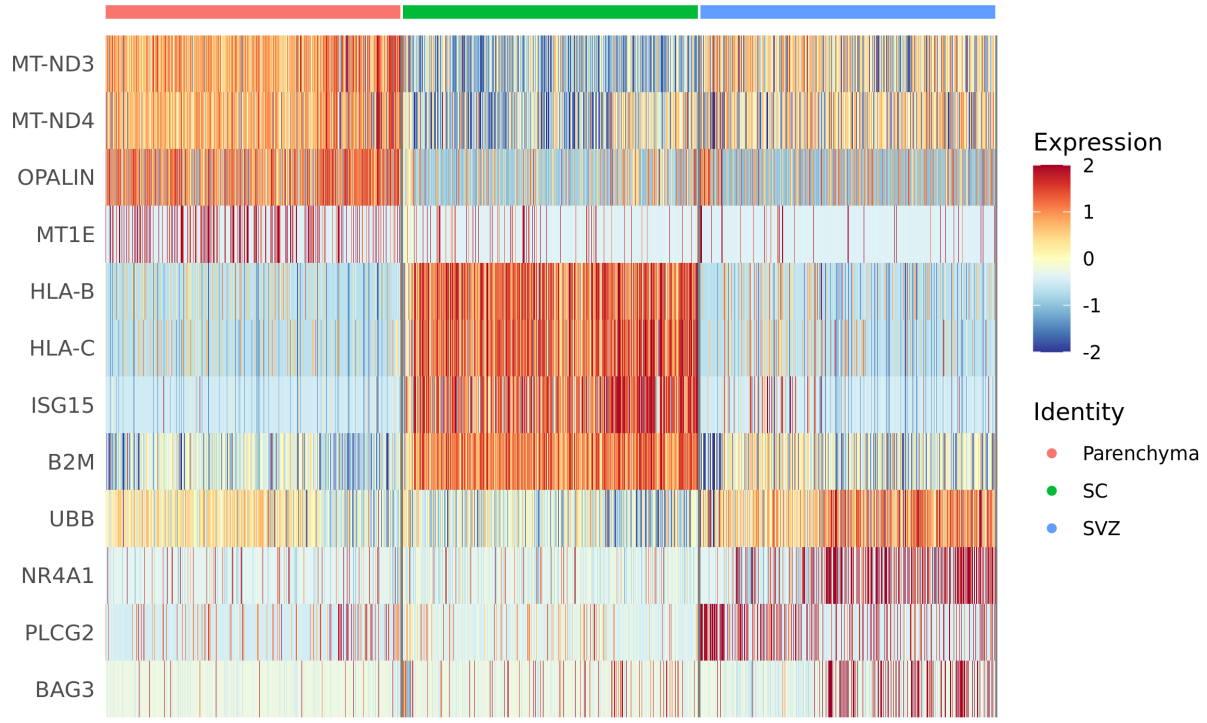

Figure 26. Heatmap of top 10 DEGs per anatomical location. Gene expression is represented by a color-coded z-score. Up and down regulated genes are shown by red and blue color respectively.

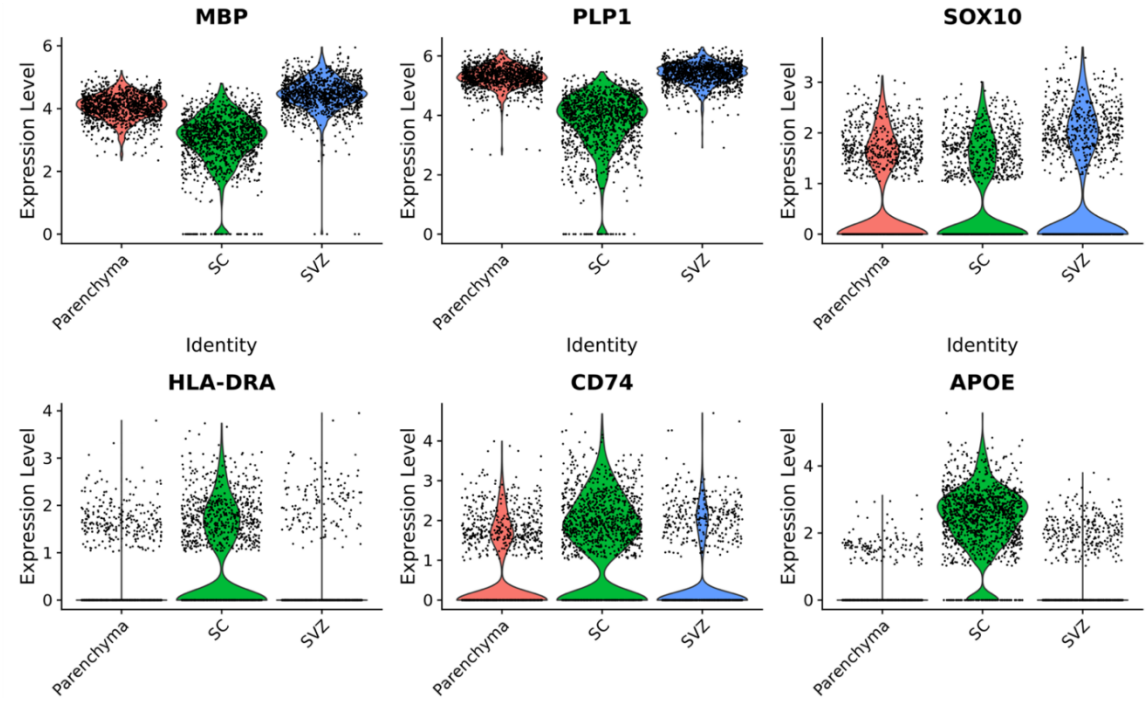

Figure 27. Violin plot showing expression of marker genes across three distinct CNS regions. Gene expression level is represented in Y axis and anatomical location in X axis.

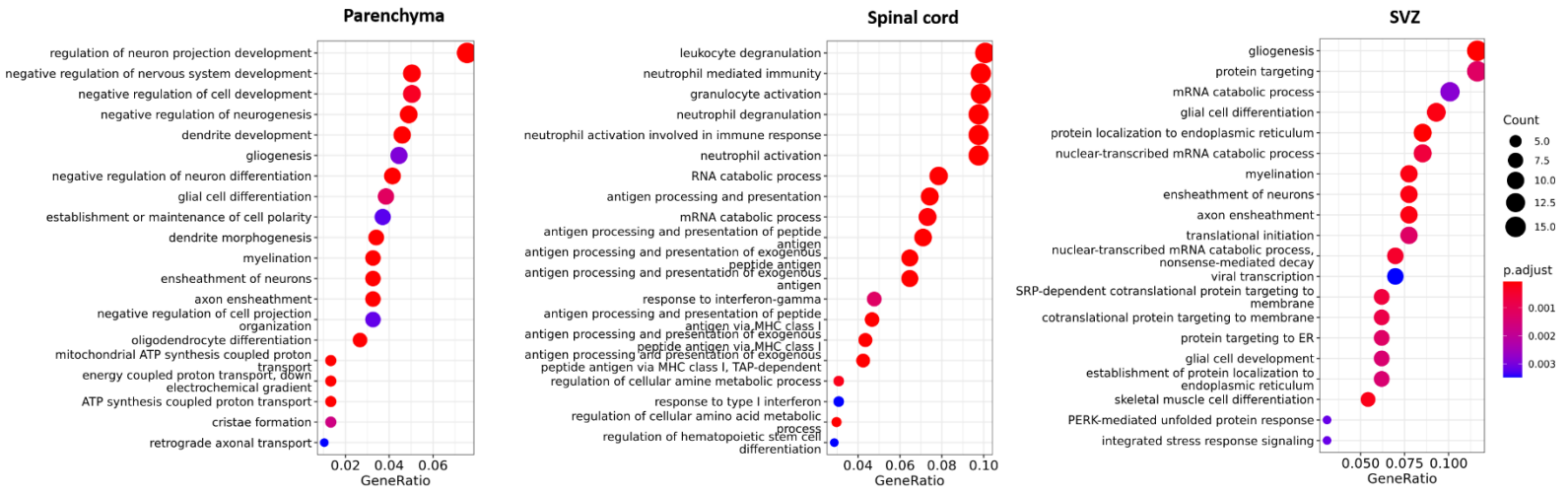

Figure 28. Over representation analysis results of the most up regulated genes in each anatomical location. The most represented biological processes for each region are represented. The statistical significance of the terms is represented by color coded p-value. Circle size donates the number genes present in each cluster.

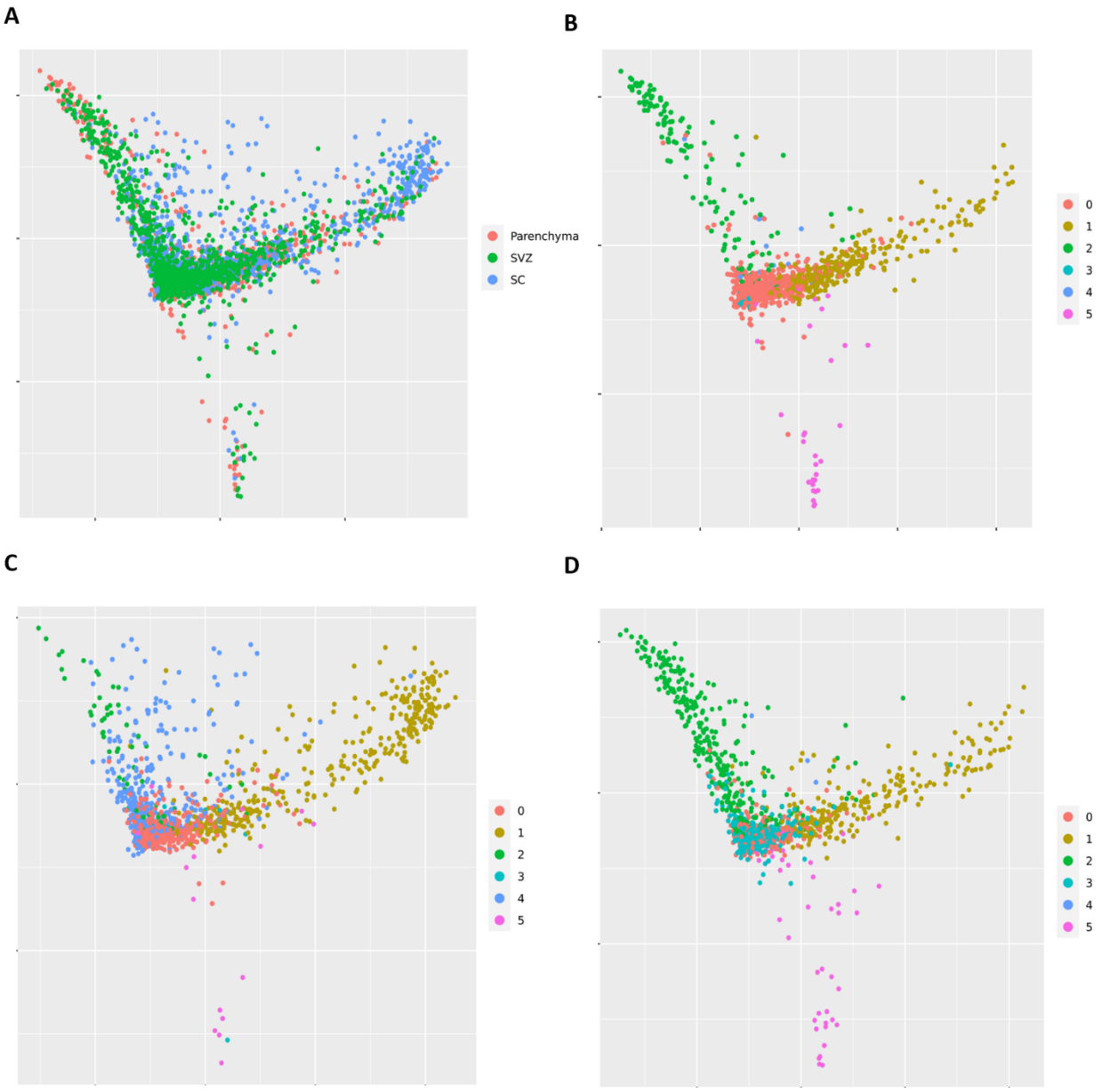

Figure 29. A) PHATE visualization for MOL by region. B-D) PHATE visualization for primary human MOLs by cluster in parenchyma, spinal cord and SVZ respectively.

Chapter 3:

Analysis of the microglia transcriptome across the human lifespan using single cell RNA sequencing

Preface:

In this part we will explore transcriptional landscape of microglia during human across the human lifespan. Data of this chapter is currently under review in Cell Reports with a manuscript number of CELL-REPORTS-D-21-04040. I am the first author of this paper. For contribution of other people for this chapter please refer to the author contribution chapter.

Abstract:

Microglia are tissue resident macrophages with a wide range of critically important functions in central nervous system development and homeostasis. In this study, we aimed to characterize the transcriptomic signature of primary human microglia at different times of development using cells derived from pre-natal, pediatric, adolescent, and adult brain samples. We show that pre-natal microglia have a distinct transcriptomic signature compared to post-natal microglia that includes an upregulation of phagocytic pathways. Trajectory analysis indicates that the transcriptional signatures adopted by microglia throughout development are a response to a changing brain microenvironment and are not predetermined developmental states. Finally, we find that post-natal human microglia acquire a mature signature more quickly than their mouse counterparts. In all, this study provides a unique insight into the development of human microglia and will provide a useful reference for understanding the contribution of microglia to developmental and age-related human disease.

Methodology:

Human brain samples:

Human brain tissues were obtained after surgeries from the Department of Neuropathology at the Montreal Neurological Institute and Hospital (MNI) and the Montreal Children's Hospital with written consent from families. Use of pediatric and adult tissues where approved by the MNI Neurosciences Research Ethics Board (Protocol ANTJ 1988/3) and the use of pediatric tissues approved by the Montreal Children's Hospital Research Ethics Board. The initial diagnoses of the post-natal samples were different, but in all cases the tissues were obtained from normal superficial tissue that had to be removed to get to the area of underlying pathology (i.e., the superficial surgical corridor on the way to the pathological tissue). Second-trimester pre-natal human brain samples were obtained from the University of Washington Birth Defects Research Laboratory (MP-37-2014-540; 13-244-PED; eReviews_3345). Complete sample information is reported in Supplementary table 1.

Tissue processing and preparation of single cell suspension:

Post-natal brain samples were collected in Cavitron Ultrasonic Surgical Aspiration (CUSA) bag during the surgeries and were subjected to enzymatic (0.05 % Trypsin (ThermoFisher) and 50 ug/ml DNAase (Roche) treatment and mechanical dissociation once brought to the laboratory. The resulting cell suspension was subjected to Percoll gradient to remove the myelin layer. The total cell population, which was mainly composed of microglia and OL lineage cells, was subjected to library preparation using 10x chromium technology for single cell RNA-sequencing for each post-natal sample. The pre-natal samples also underwent enzymatic and mechanical dissociation, however, because there is no myelin at the pre-natal time point, the Percoll gradient step was skipped and the total cell population was sent for single cell RNA-sequencing.

Fluorescent activated cell sorting (FACS)

One of the pre-natal samples was subjected to FACS. For this sample, following enzymatic and mechanical dissociation, the cells were resuspended in FACS buffer containing CD11b and CD45 antibodies. Samples were kept on ice and sorted by a BD FACSAria Solution. The resulting sorted cells were used for single cell RNA-sequencing.

Single cell RNA-sequencing data analysis:

All samples were sequenced at McGill University and the Génome Québec Centre. 10X Chromium v2.0 technology was used for cell single cell capturing and library preparation. Single cell RNA-sequencing (scRNAseq) was performed on the Illumina HiSeq4000 PE75 sequencer. The 10XGenomics CellRanger pipeline was used to demultiplex the cells and their unique molecular identifier barcodes, and to align reads to the GRCh38 human reference genome. The subsequent analyses were done using the Seurat (v3.1) R package [176].

Individual datasets were subjected to standard Seurat pipeline for quality control, gene expression normalization, batch-effect correction, clustering, and differential expression analysis. Briefly, any cell with a genome that was comprised of 5 to 12 percent of mitochondrial genes was considered a dead cell and was removed from analysis. Similarly, any cell that contained less than 200 or more than 2500 unique feature counts was considered a low-quality cell and was removed from the downstream analysis. Moreover, genes that have been shown to be artefacts of cell isolation procedures were deleted from the gene-barcode matrix [9,193]. The expression of sorted pre-natal sample was normalized according to expression of housekeeping genes of non-sorted prenatal samples. After these quality control steps, the gene expression levels of the cells were natural log normalized and scaled. In order to come over single cell RNA sequencing drop-out, we limited our analysis to a subset of 2000 highly variable genes for each dataset. Principle component analysis (PCA) was performed on the highly variable genes to reduce the dimensionality of the data. The first 20 principle components were selected for the clustering purpose. A shared-nearest neighbor graph was constructed based on the PCA analysis and the Louvain clustering algorithm was used several times to identify clusters at multiple different resolutions. Individual datasets were analyzed using a resolution of 0.6. Finally, the uniform manifold approximation and projection (UMAP) algorithm was used to visualize the clusters in two-dimensional space. The expression levels of cell-type marker genes were used to determine the identity of each cluster. Microglia from each individual dataset were subset using the expression of *TREM2* and *C1QA*. Microglia selected from each individual dataset were subjected to dataset integration as follows: Following down sampling of post-natal microglia according to the number of pre-natal cells (3500 cells per developmental stage), all datasets were integrated using the Seurat "FindIntegrationAnchors" and "IntegrateData" functions, which perform canonical correlation

analysis (CCA) to remove any possible batch effect between datasets. The integrated object was then re-clustered. For PCA plotting, cell cycle related genes were regressed out using the Seurat cell-cycle scoring and regression pipeline. The optimum resolution for clustering was determined using "clustree" R package [194]. This package measures the stability of clusters at different resolutions, and a high degree of movement between clusters is considered over clustering. We chose a resolution of 1 for our clustering purpose. Differentially expressed genes were identified using the "FindMarkers" function in Seurat based on Wilcox test scores for genes that were detected in at least 25% of cells in the populations compared. Heatmap plots of the top marker genes were generated using the DoHeatmap function.

Pseudotime trajectory inference

Pseudotime trajectory inference analysis was done using the PhateR (v1.0) package to order cells in "pseudotime" and visually highlight transitions between cells using dimensional reduction methods that minimize gene expression difference between sequential cell pairs. PhateR uses the "potential of heat diffusion for affinity-based embedding" (PHATE) method created by Moon et al, 2019 [178]. Briefly, PHATE encodes local data via local similarities, encodes global relationships using potential distances based in diffusion probabilities, and embeds potential distance information into low dimensions via metric multi-dimensional scaling. The phate algorithm was run on the integrated counts derived from the Seurat object with the gamma parameter set to gamma=0 and the remaining parameters set to default (knn=5, decay=40, optimal t was automatically selected to be t=8). PhateR was chosen for the trajectory inference analysis as it does not rely on prior assumptions of data structure.

Mouse single cell RNAseq data analysis

Raw expression matrices of 12 single cell RNA-sequencing samples were downloaded from Gene Expression Omnibus (GEO) with the accession number 121654 [164]. Each dataset was subjected to Seurat analysis in the same way as was done for the human samples. The average expression of genes from each developmental stage was measured using the "AverageExpression" function in Seurat.

Jaccard similarity matrix

The weighted Jaccard similarity index calculates the similarity between two or more numeric vectors. In our study, we use a Jaccard similarity matrix to measure the similarity between the average expression of genes between developmental stages. The average expression levels of genes for the whole population of microglia at each developmental stage were calculated using the "AverageExpression" function in Seurat. The range of this similarity is from 0 to 1, in which 1 is highest similarity and 0 is lowest similarity between samples. The Jaccard similarity index is calculated using the sum of minimum values in two vectors at a time (the intersection of two RNA-seq data samples) divided by the sum of the maximum values in both vectors (the union of each). We used MATLAB to calculate the Jaccard similarity index automatically.

Gene regulatory network analysis

Single cell regulatory network inference and clustering (SCENIC) [195] was employed to infer transcription factor (TF) activity by identifying target genes that were co-expressed with TFs using a random forest model. Analysis was performed using default and recommended parameters as suggested on the SCENIC vignette (https://github.com/aertslab/SCENIC) using the hg19 mc9nr (Version 9) RcisTarget database (https://resources.aertslab.org/cistarget). Kernel density histograms that plotted the differential AUC distribution across microglia of different developmental stages and the targetome of individual TFs were queried using previously described modifications [196]. Briefly, histograms were plotted using the regulon activity matrix ('3.4_regulonAUC.Rds'), in which columns represent cells and rows represent the AUC regulon activity and the targetome of individual TFs, both which were queried using the regulon data frame ('2.6_regulons_asGeneSet.Rds').

PCA analysis for pseudo-bulk analysis and batch effect correction:

The average expression of microglia genes from each developmental stage was measured using the "AverageExpression" function in Seurat. Following batch effect correction, these values were used to measure the principal component scores using the built-in function of R called prcomp, and the results were visualized using the ggplot2 in R. The batch effect between human and mouse samples was removed using ComBat function in the SVA package using default parameters [197].

Pearson correlation

Pearson correlation analysis was employed to check the similarity of the human and mouse samples. The correlation coefficient was measured and visualized using MATLAB's built-in functions.

Gene Set Enrichment Analysis (GSEA) and Ontology analysis

GSEA was performed by pre-ranked GSEA option using GSEA tool [198]. Gene ontology analysis was performed using gProfiler web tool. Only significant terms with adjusted p-value < 0.05 were presented.

Results:

Isolation and characterization of human microglia

To study changes in the transcriptional profile of microglia over time, human brain samples were collected at different developmental stages. Pre-natal samples were obtained from second trimester fetal brain tissue, (Figure 1, Table 1). Post-natal brain samples were obtained from patients undergoing surgical resection of CNS tissue, with neuropathology reports indicating that all collected tissue samples were located distal from the site of pathology. Post-natal samples were collected from individuals grouped into three age brackets: pediatric (1.5 – 2 years), adolescent (10 – 14 years) and adult (41 – 61 years) (Figure 1, Table 1).

Post-natal tissue was enzymatically and mechanically digested, followed by cell separation using a Percoll gradient. The cell suspension was subjected to single cell RNA-sequencing (scRNA-seq) using droplet-based sequencing through a 10x chromium technology (Figure 1). Isolated cells were predominantly microglia and oligodendrocytes, with minor populations of border associated macrophages (BAM), OPCs, astrocyte and lymphocytes (Figure 2). Microglia were selected for further analysis based on expression of canonical microglia markers complement c1q A chain (*C1QA*) and triggering receptor expressed on myeloid cells 2 (*TREM2*) (Figure 3). Following removal of low-quality cells, 14,520 post-natal microglia were retained for downstream analysis. Pre-natal samples were enzymatically and mechanically digested as described above, due to the absence of myelin in the pre-natal brain a Percoll separation was not carried out. Of the three pre-natal samples obtained two were processed as above and one sample was subjected to fluorescence-activated cell sorting (FACS) (live, *CD45*+/*CD11B*+). In total 4,211 pre-natal microglia expressing canonical microglia markers of *TREM2* and *C1QA* were obtained (Figure 4). Prior to downstream analysis a population of highly proliferative microglia expressing proliferation markers cyclin dependent kinase (*CDK1*) and DNA topoisomerase II alpha (*TOP2A*) were excluded (Figure 4).

Following quality control checks and removal of the proliferative cluster 3,400 pre-natal microglia were obtained for further analysis. The post-natal microglia population was down sampled to match that of the pre-natal samples. Following integration of pre- and post-natal microglia populations, 13,583 cells with an average of 91,879 reads and 1,234 genes per cell were obtained.

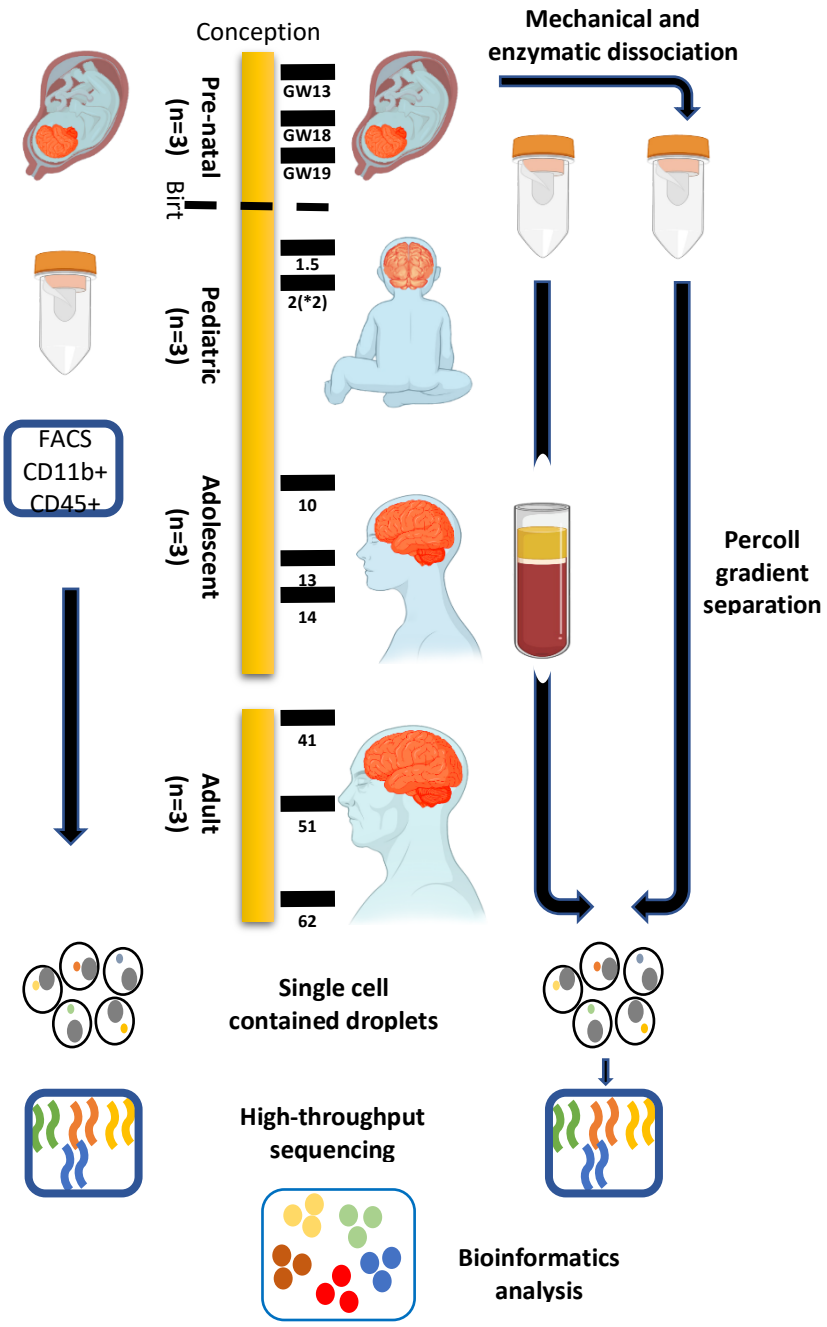

Figure 1. A) Microglia were isolated from brain tissue at different ages, followed by tissue processing, single cell RNA sequencing and bioinformatics analysis. Three biological replicates per developmental stage (n=12 in total) were used for downstream analysis.

Age	Sex	Pathology
GW13	Male	-
GW18	Male	-
GW19	Female	-
18 months old	Male	Focal cortical dysplasia
2-year-old (1)	Male	Rasmussen encephalitis
2-year-old (2)	Female	Hemi-megalencephaly
10-year-old	Female	Focal epilepsy
13-year-old	Female	Focal epilepsy
14-year-old	Female	Congenital stroke
41-year-old	Female	Focal epilepsy
51-year-old	Female	Mesial Temporal sclerosis
62-year-old	Male	Non-tumor related epilepsy (hippocampal sclerosis)

Table 1. Age, sex and pathology of samples which were used in our study.

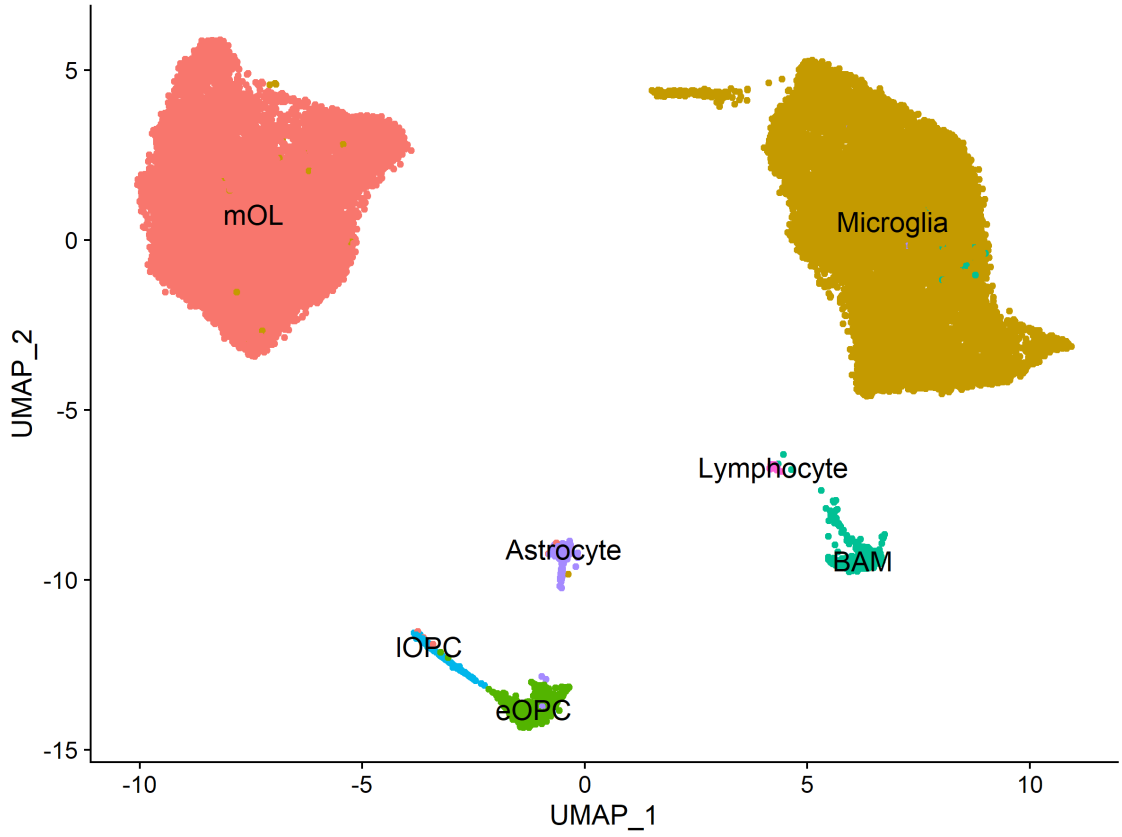

Figure 2. UMAP plot showing the cell identities captured by single cell RNA sequencing in the post-natal datasets. mOL = mature oligodendrocyte, eOPC = early oligodendrocyte progenitor cell, eOPC = late oligodendrocyte progenitor cell, BAM= Border associated macrophage.

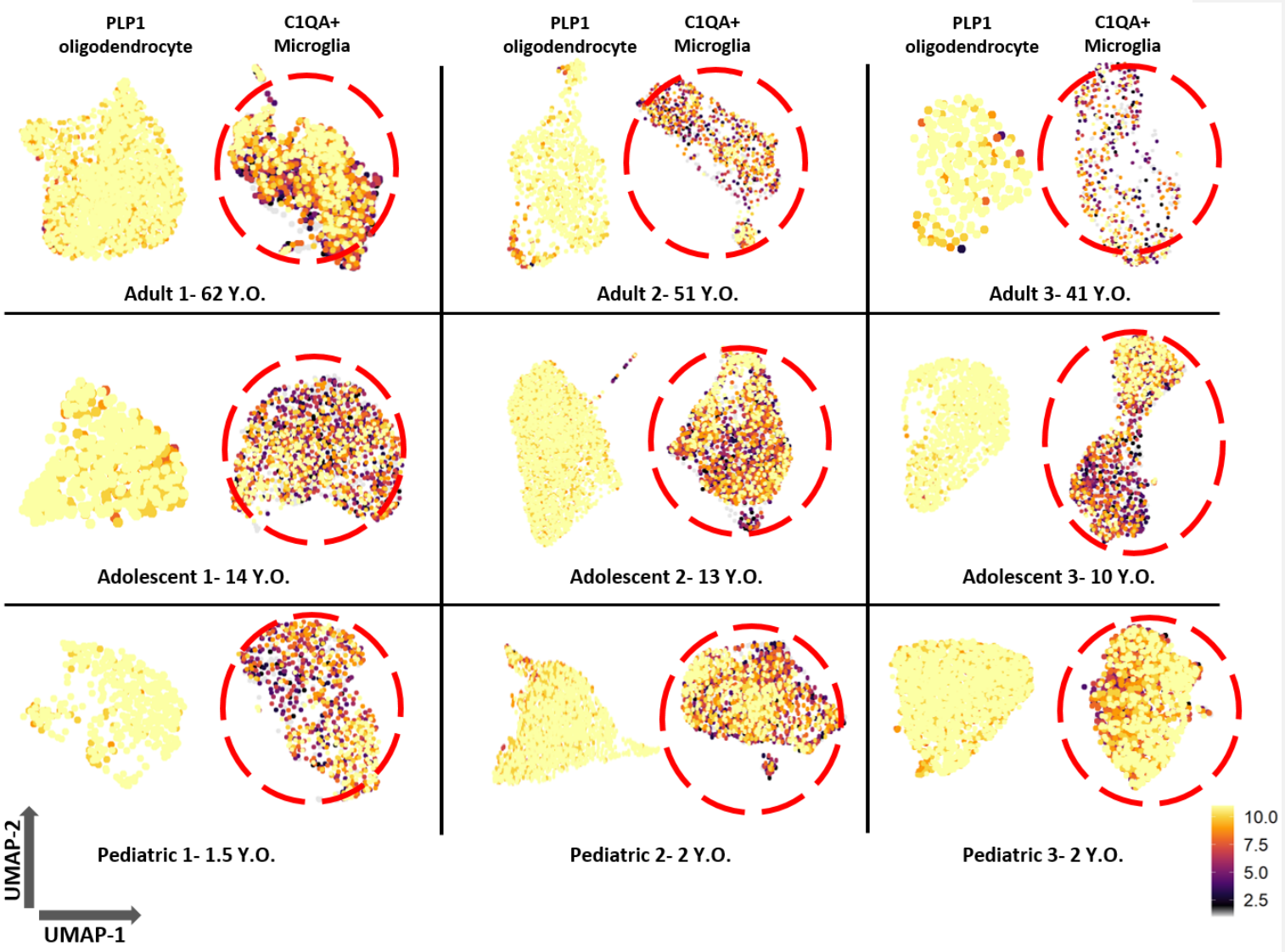

Figure 3. UMAP plot of nine individual postnatal datasets highlighting C1QA (microglia) and PLP1 (mature oligodendrocyte) expression. C1QA+ cells were used for downstream cell integration. Expression of genes is represented by color coded z-score.

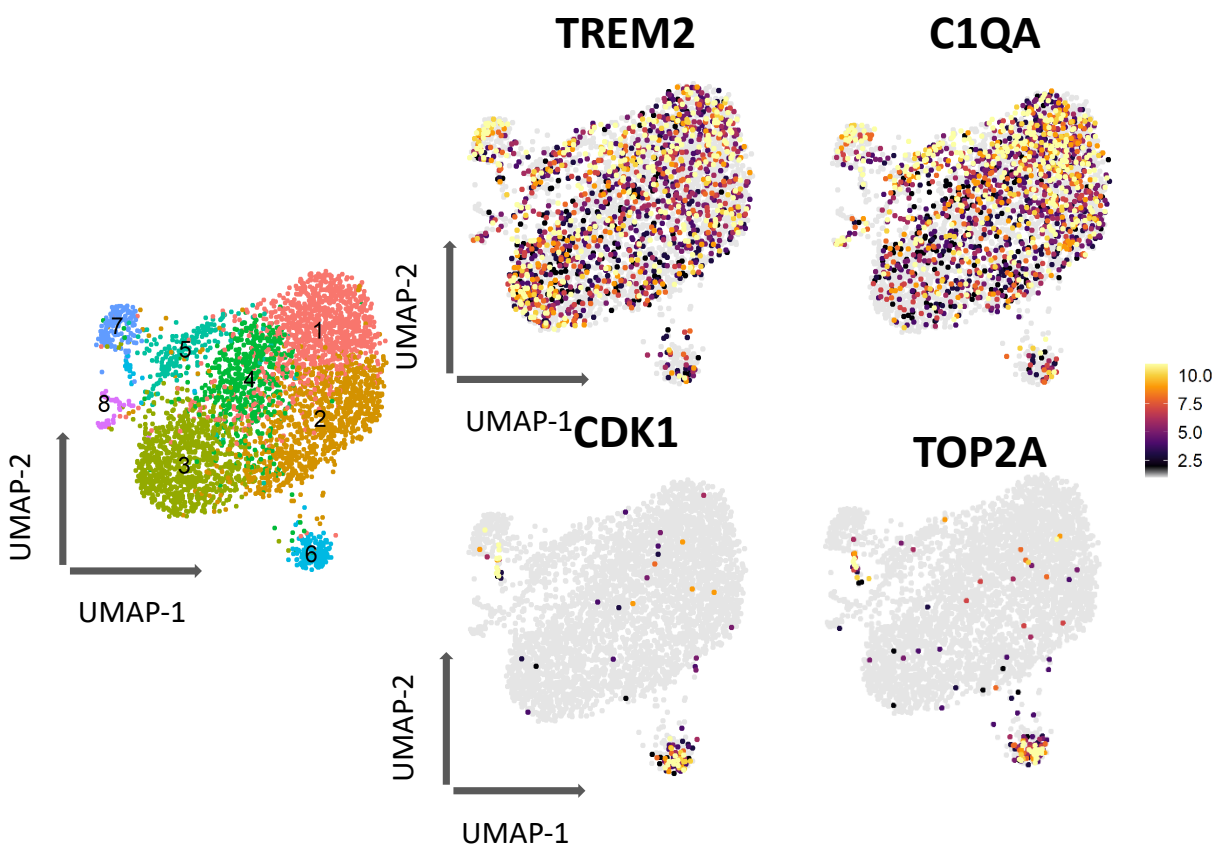

Figure 4. UMAP plot showing clusters of pre-natal microglia after tissue processing and single cell RNA sequencing. Normalized average expression of microglia canonical marker genes and cell proliferation marker genes.

We next aimed to determine the extent of microglia transcriptional heterogeneity at different points of human development. To do this we integrated all cells and performed unsupervised clustering, generating 13 clusters (Figure 5A) grouped into two primary clouds. One cloud was composed primarily of pre-natal microglia and the other post-natal microglia (Figure 5B). Analysis revealed a continuum of gene expression between post-natal developmental stages, resulting in diffuse localization as opposed to compact clustering within the larger cloud of cells (Figure 5B). Additionally, we confirmed that all cells from all clusters expressed canonical microglia markers including *C1QA* and *TREM2* (Figure 5C). The size of each clusters varied, ranging from the largest cluster 1 (18% of total cells) to the smallest cluster 13 (0.3% of total cells) (Figure 6A). Our analysis showed that each age group made a differential contribution to each cluster (Figure 6B). For instance, clusters 4 and 10 were comprised of predominantly pre-natal cells, cluster 12 predominantly adult cells, and cells from each age contributed in equal proportion to cluster 2 (Figure 6B).

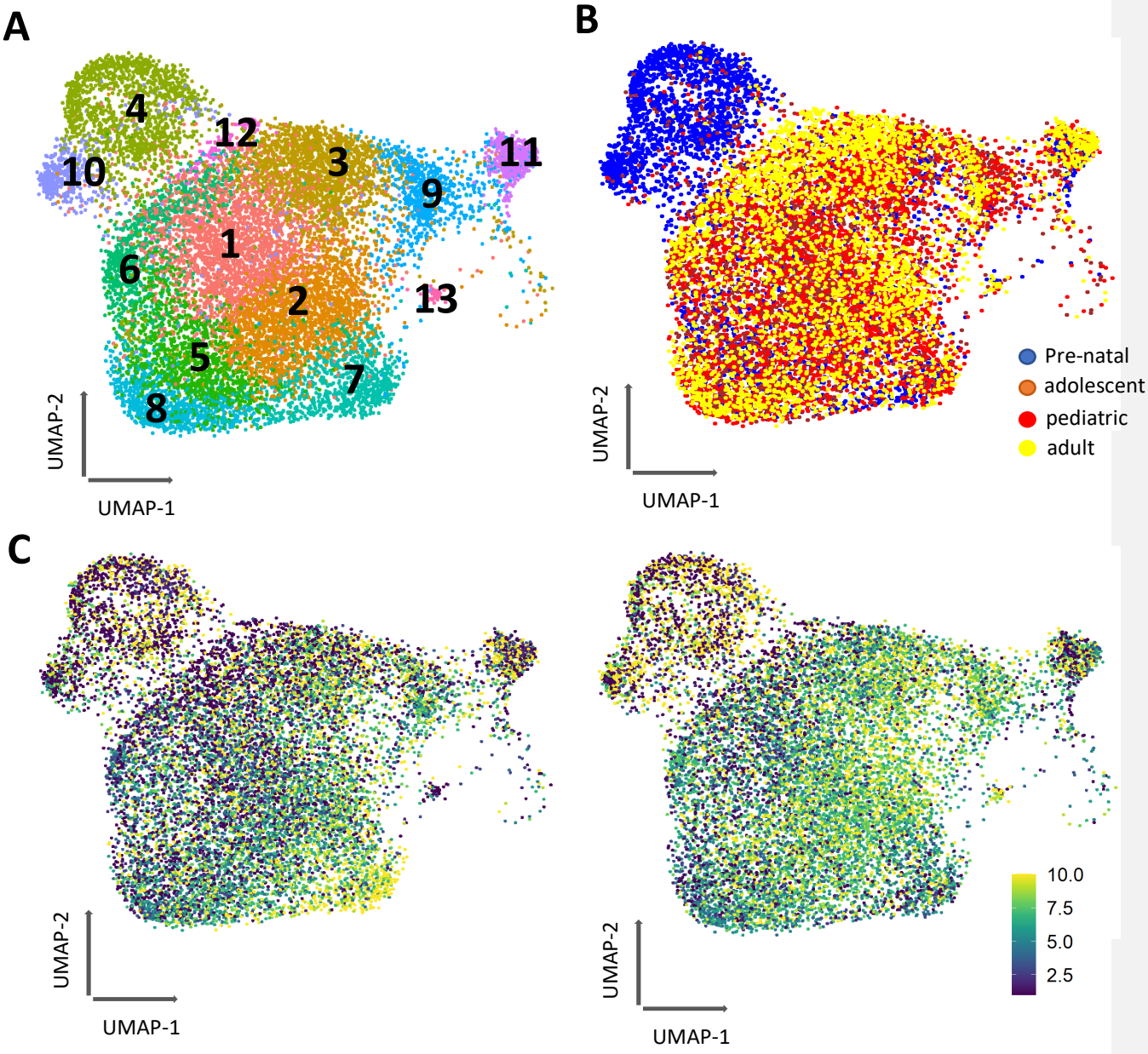

Figure 5. A) UMAP plot of 13 clusters of 13,583 isolated microglia. B) UMAP plot representing pre-natal microglia have distinct expression profile compared to post-natal cells. Each age is represented by a separate color. C) UMAP plot showing normalized average expression of canonical microglia genes in all cells.

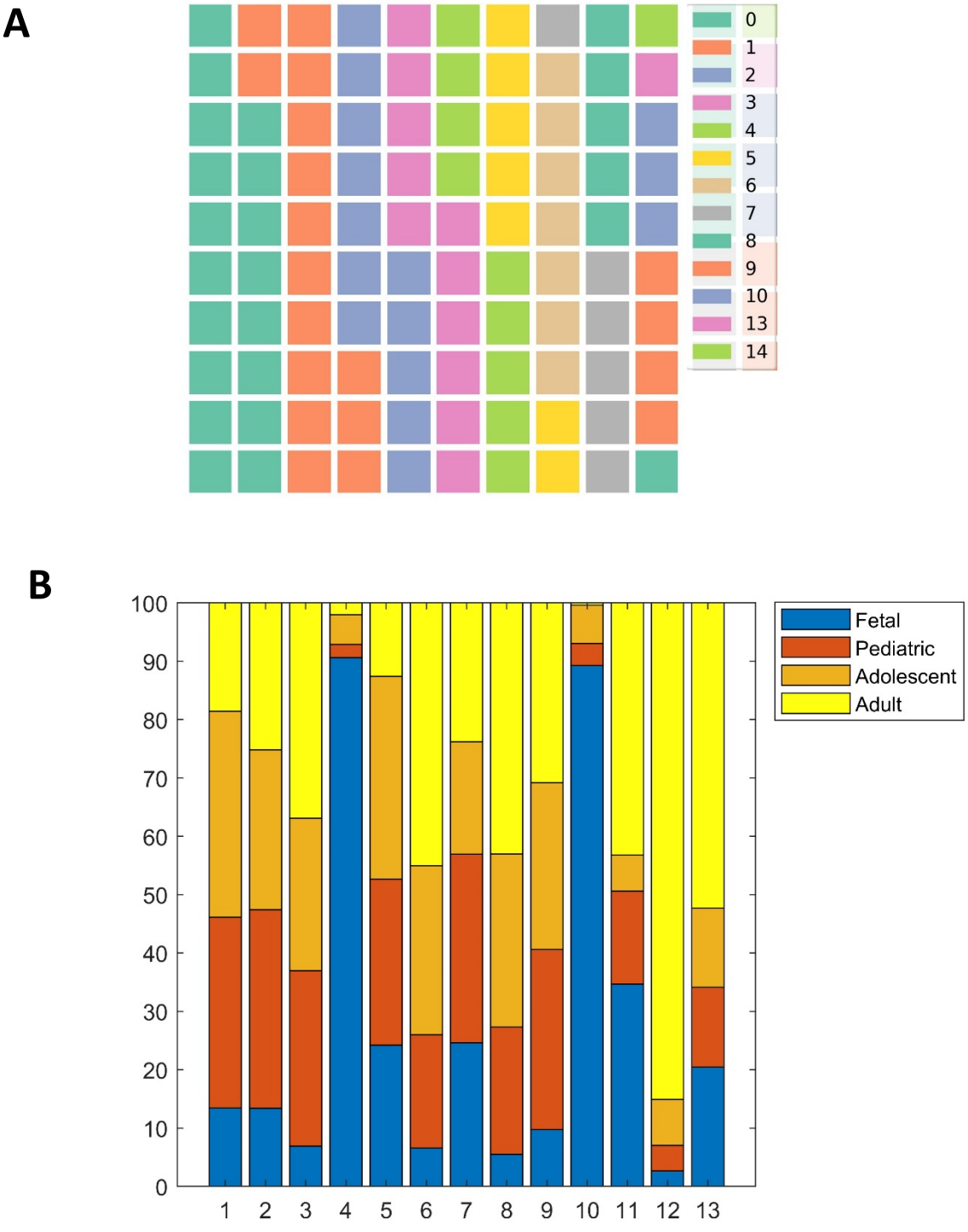

Figure 6. A) Waffle chart showing the contribution of each cluster to the total population, each cluster is represented by a distinct color. B) Stack bar plot showing the contribution of microglia from each age in each cluster. Different ages are represented by a distinct color.

Hierarchal clustering using the top differentially expressed genes (DEGs) between each cluster revealed different transcriptomic signatures (Figure 7). Certain microglia clusters were associated with specific functions (Figure 8). Clusters 6, 8, and 12, were constituted of post-natal microglia (specifically adult microglia), expressing interleukin 1 beta (*IL1B*), macrophage scavenger receptor 1 (*MSR1*) well known mediators of the inflammatory response. The most up regulated gene of cluster 8 was C-C motif chemokine ligand 4 (*CCL4*) which is involved in the recruitment of peripheral immune cells in the CNS (Figure 9). The most significant biological processes associated with these three clusters were inflammatory processes, leukocyte activation, and apoptotic processes (Figure 8). The upregulation of inflammatory-associated pathways by adult cells suggests that human microglia acquire a more inflammatory phenotype over time.

In cluster 13 we found an upregulation of genes belonging to the membrane-spanning 4A (*MS4A*) family, specifically *MS4A4A* and *MS4A7*, commonly considered to be macrophages markers (Figure 10) [199]. Hammond et al previously reported a group of mouse microglia that express both classical microglia markers and *MS4A* macrophage markers [164]. They found that these cells were present during embryogenesis and proposed that they act as a progenitor pool for both microglia and macrophages. In contrast, we found that microglia expressing the *MS4A* family genes were derived from adult tissue (Figure 10). It has recently been proposed that in addition to the canonical microglia developmental pathway a second wave of microglia development occurs in mice. The resulting microglia have been shown to express both microglia and macrophage markers and persist into adulthood [122].

Altogether, our data indicate that the transcriptional signature of human microglia during development can be divided into two distinct phases of pre- and post-natal development. Further, we show that there are subtle yet potentially significant differences in microglia at different stages of post-natal life, including the upregulation of inflammatory pathways in adult microglia.

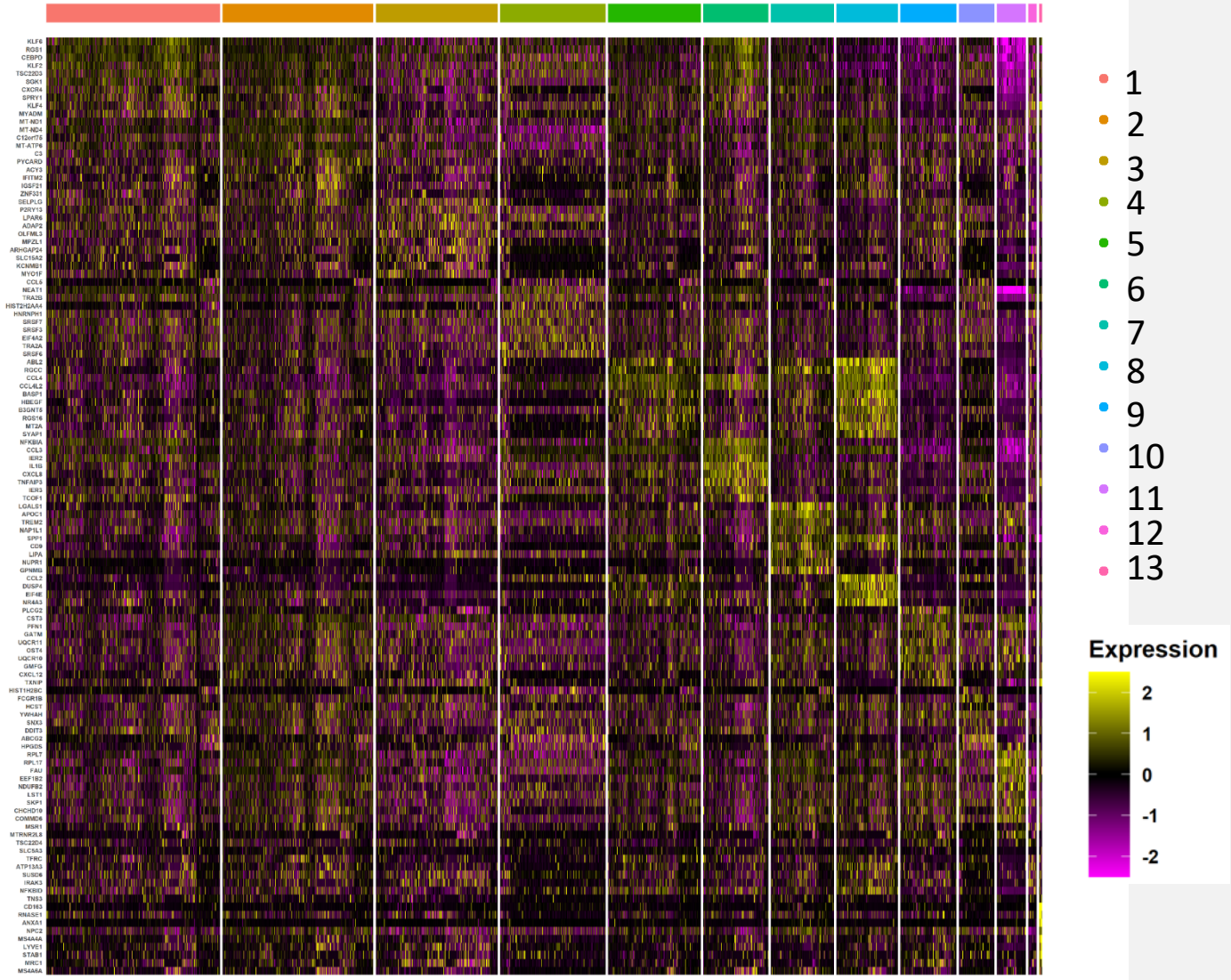

Figure 7. Heatmap of top 10 DEGs per cluster. Gene expression is represented by a color-coded z-score. Up and down regulated genes are shown by yellow and violet color respectively.

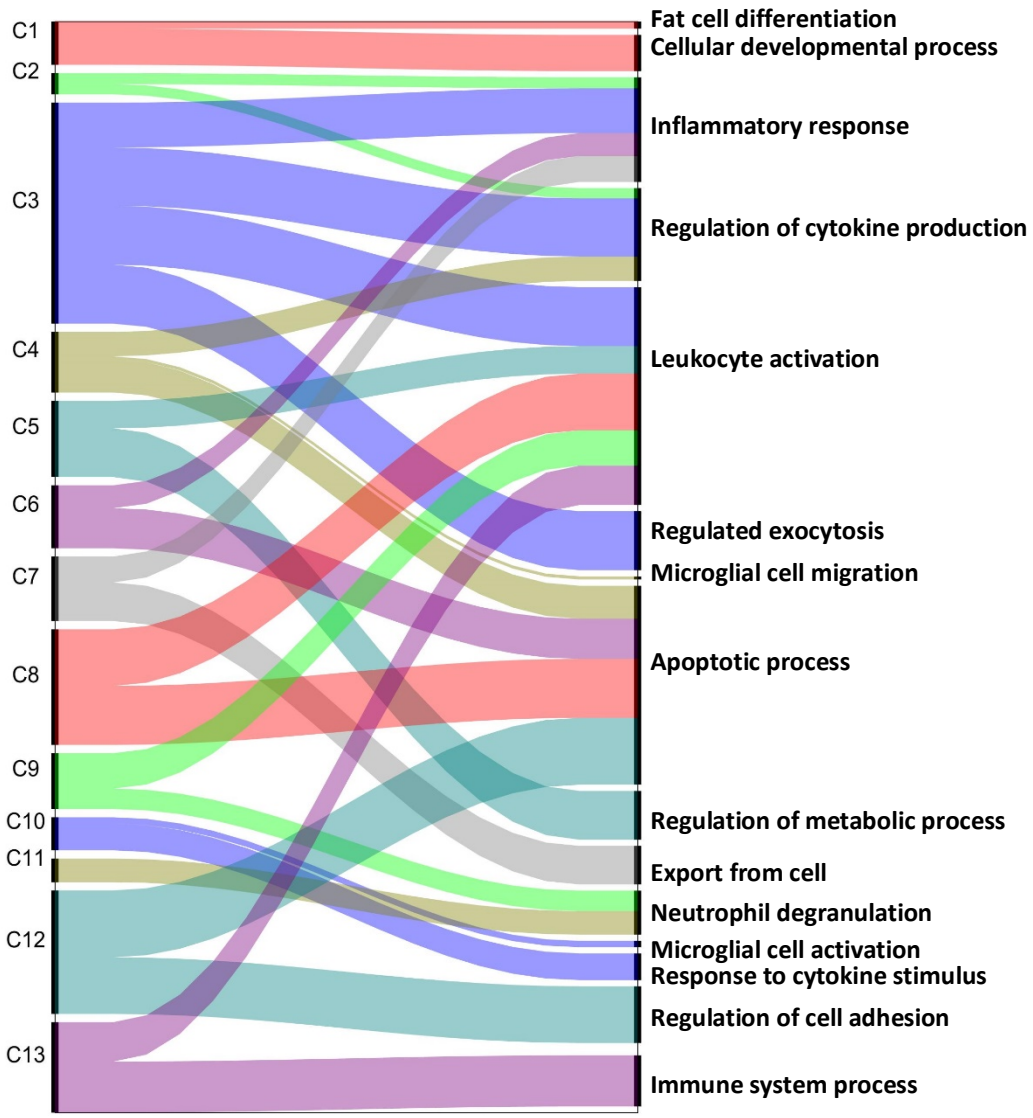

Figure 8. Alluvial plot representing the most affected biological processes by upregulated genes of each cluster. Ribbon thickness indicates the number of genes per biological process.

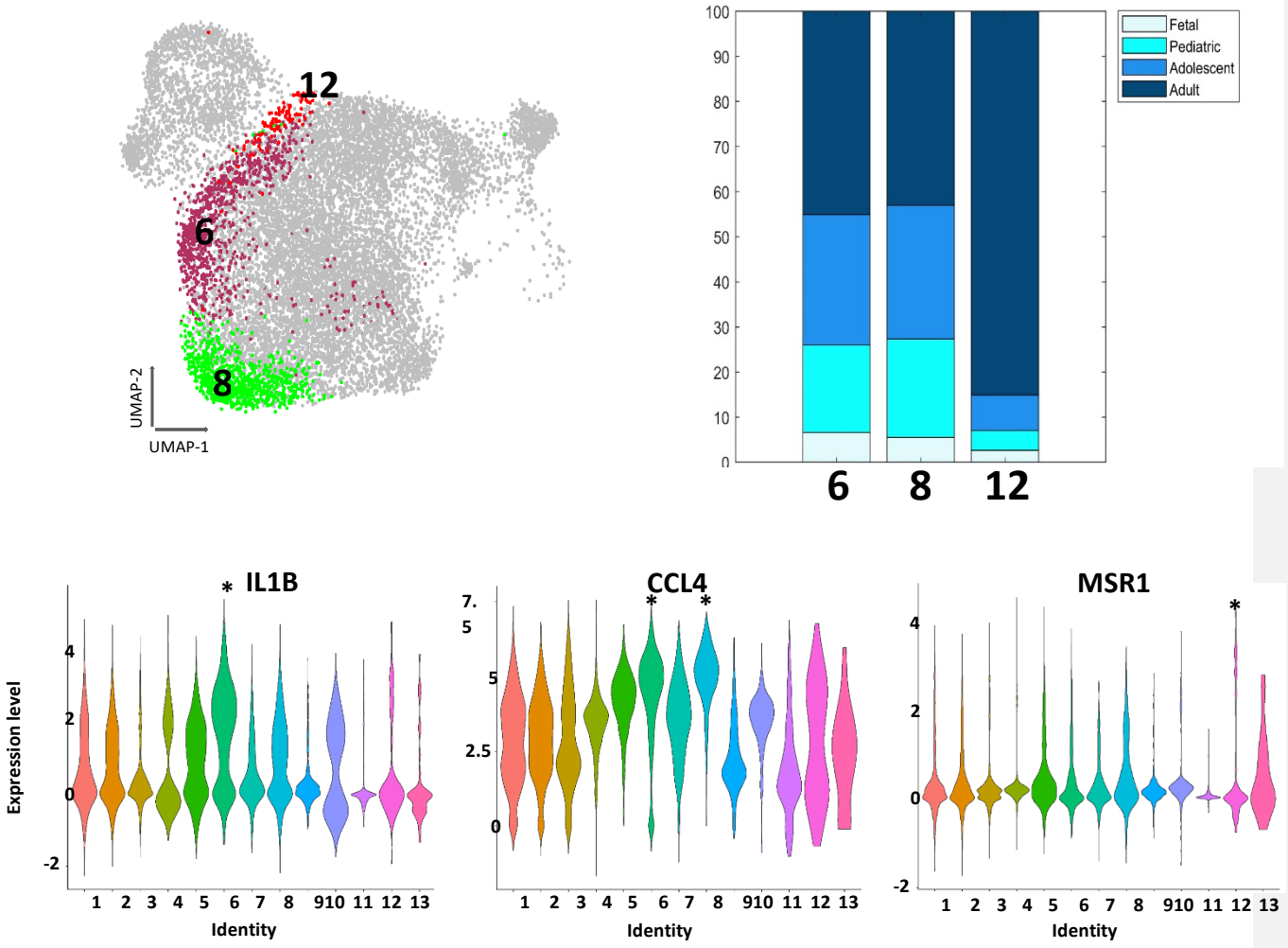

Figure 9. UMAP plot highlighting three microglia clusters associated with inflammatory phenotypes. Stack bar plot showing contribution of each age to these three clusters. Each age is represented by a distinct color. Violin plot depicting expression of significantly upregulated gene in these three clusters *adjusted p-value < 0.05 (Wilcox test).

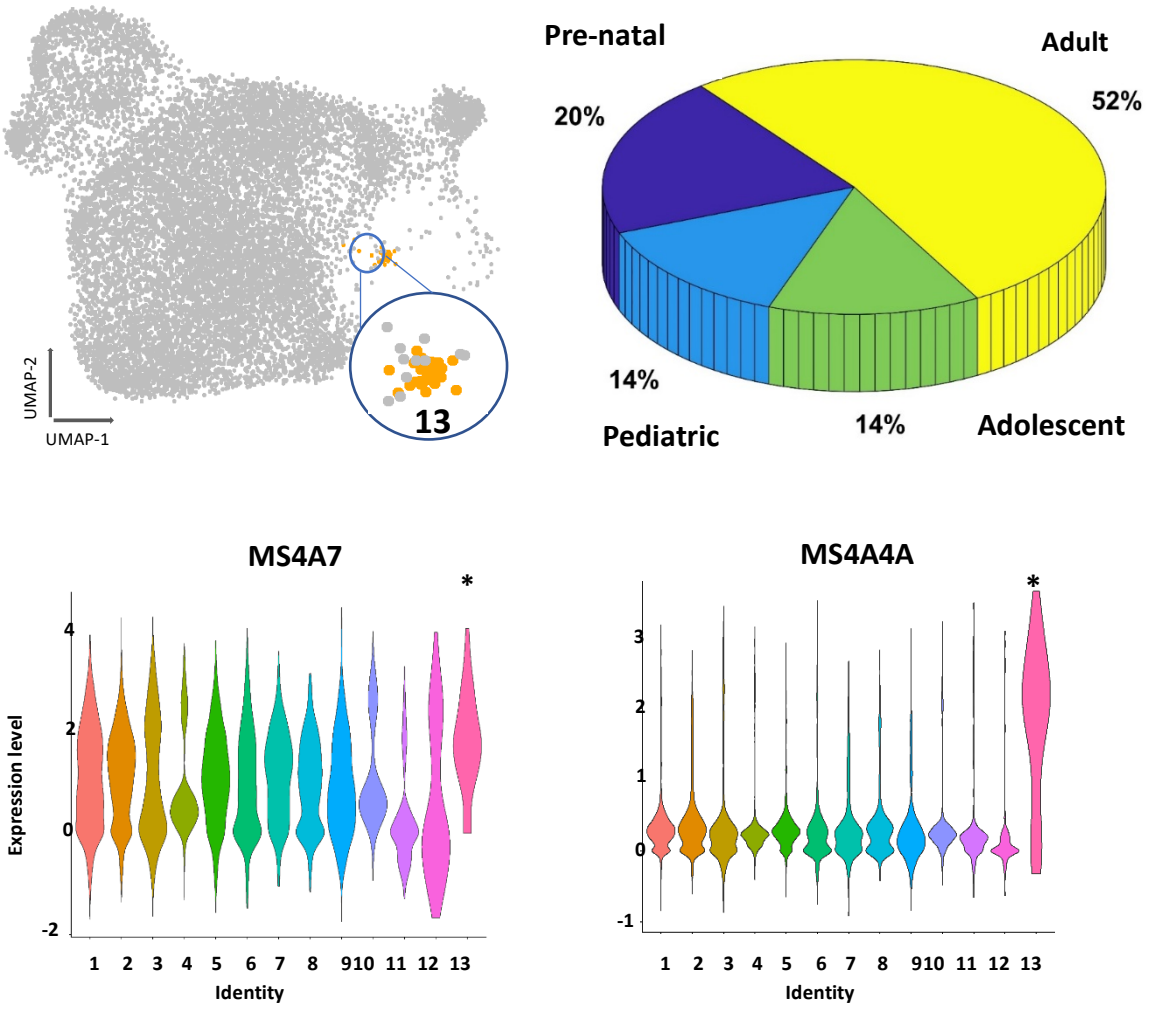

Figure 10. UMAP plot highlighting microglia originated from second wave of microglia development. Pie chart showing the contribution of microglia of each age to cluster 13. Each age is represented by a distinct color. Violin plots showing expression of MS4A4A and MS4A7 genes * adjusted p-value < 0.05 (Wilcox test).

Age-associated gene expression signatures of human microglia

To further investigate the differences between each developmental stage we grouped samples according to their age group and averaged the gene expression level of each sample in the groups. Next, we generated a Jaccard similarity matrix to measure the gene expression similarity at each age. The Jaccard similarity index ranges from 0 to 1, with 0 representing the lowest and 1 the greatest similarity. The analysis showed that pre-natal microglia were least similar to all other age groups (Figure 11A). Among the post-natal stages, adolescent microglia were the least similar compared to adult and pediatric cells, although the correlation coefficients of all post-natal samples were above 0.8 (high) (Figure 11A). Gene ontology analysis of the top 100 most variable genes in each age found that immune system processes, leukocyte activation, and antigen processing and presentation are upregulated in all developmental stages (Figure 11B). As this analysis measures only the most variable genes, this data suggests that different genes regulate the same pathways in each developmental stage. Of the pathways uniquely upregulated at each developmental stage we noted upregulation of stress response genes in adult cells, (Figure 11B), which may relate to their higher inflammatory capacity identified in Figure 2C. In adolescent cells there was an enrichment in the expression of metabolic genes, suggesting a greater metabolic activity of microglia at this developmental stage (Figure 11B). Pediatric microglia expressed high levels of genes involved in synaptic pruning, which is a prominent function of microglia at this time of development (Figure 11B). Finally, apoptotic pathways were among the most upregulated processes in pre-natal cells compared to all post-natal samples (Figure 11B), which could be explained by the importance of microglia in both clearing apoptotic debris and in inducing apoptosis of neuronal precursor cells in the embryonic brain [200].

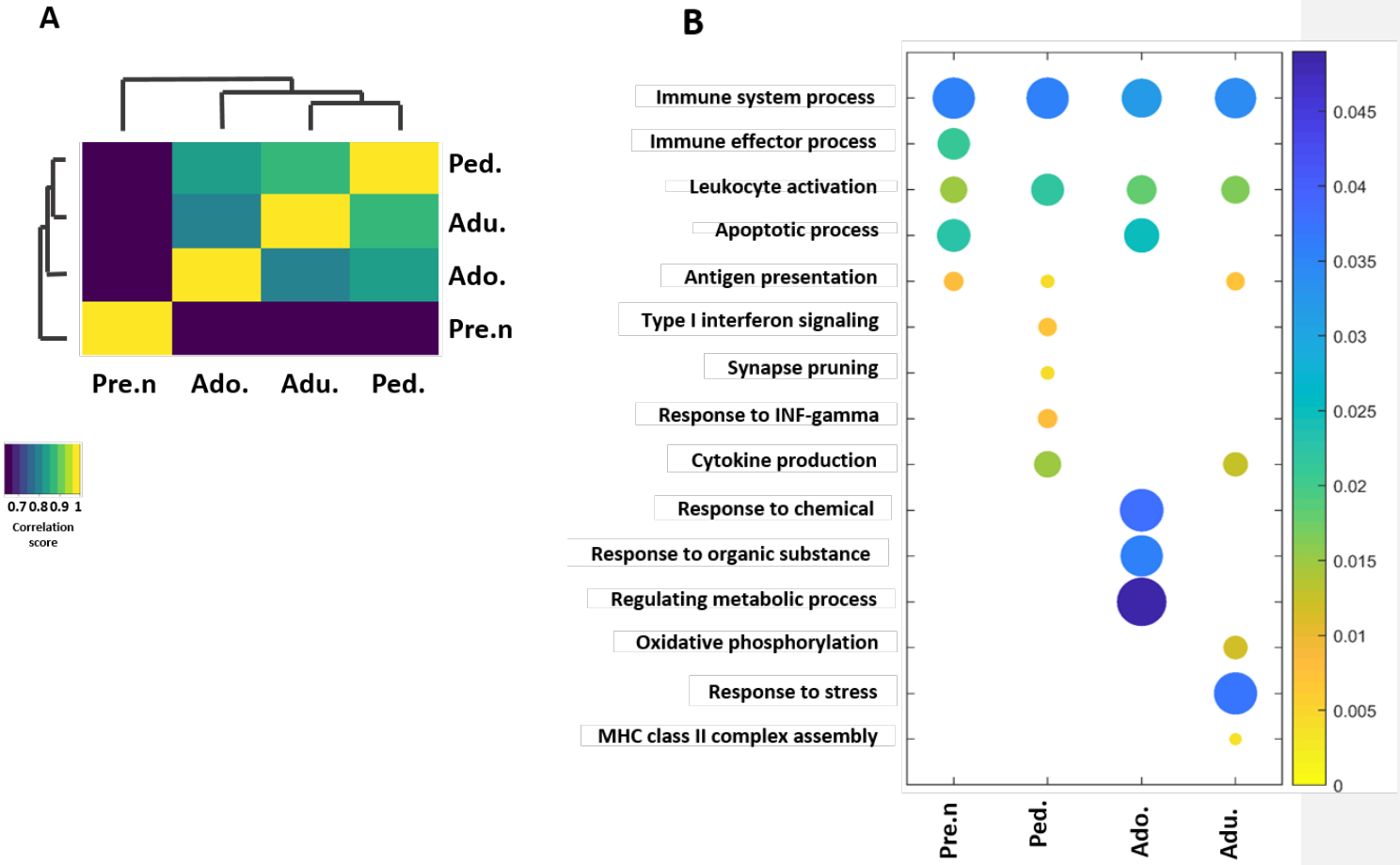

Figure 11. A) Hierarchal clustering of microglia at each age according to Jaccard similarity coefficient score which is represented by a color gradient, yellow (highest similarity) and dark blue (lowest similarity). B) Dot plot depicting the most affected biological processes of the top 100 highly variable genes for each age. The circle size indicates the number of genes present in each biological process. Statistical significance of terms is represented by color gradient, p-value of all terms is < 0.05. Pre.n = pre-natal, Ped. = Pediatric, Adol. = Adolescent, Adu. = Adult.

We next aimed to identify genes whose expression may correlate with the acquisition of a mature microglia phenotype. We identified two groups of genes, those whose expression decreased with age (Figure 12A) and those whose expression increased with age (Figure 13A). Gene ontology analysis of the top 100 most highly variable genes that were highest during embryogenesis and decreased over time (Figure 12B) showed that these genes were involved in cell apoptosis regulation, phagocytosis, and brain development (Figure 12B). One of the most up regulated genes in this group was fc fragment of IgG receptor I beta (*FCGR1B)*, a positive regulator of phagocytosis (Figure 12C), suggesting that human pre-natal microglia may have a greater phagocytic capacity than post-natal cells. Gene ontology analysis of the top 100 most highly variable genes that were lowest during embryogenesis and increased over time (Figure 13A) showed that these genes were involved in the positive regulation of *IL-17* and *IL-2* (Figure 13B). The IL-17 signaling pathway is involved in the pathogenesis of chronic inflammatory and autoimmune diseases [201]. C-X-C motif chemokine receptor 4 (*CXCR4*) another of the most upregulated genes in this group has a well-known function in microglia activation (Figure 13C) [202]. Overall, we found that human pre-natal microglia express a signature that indicates greater phagocytic capacity, while post-natal microglia appeared to be more inflammatory. Finally, microglia from the adolescent brain were more metabolically active than microglia at other developmental stages.

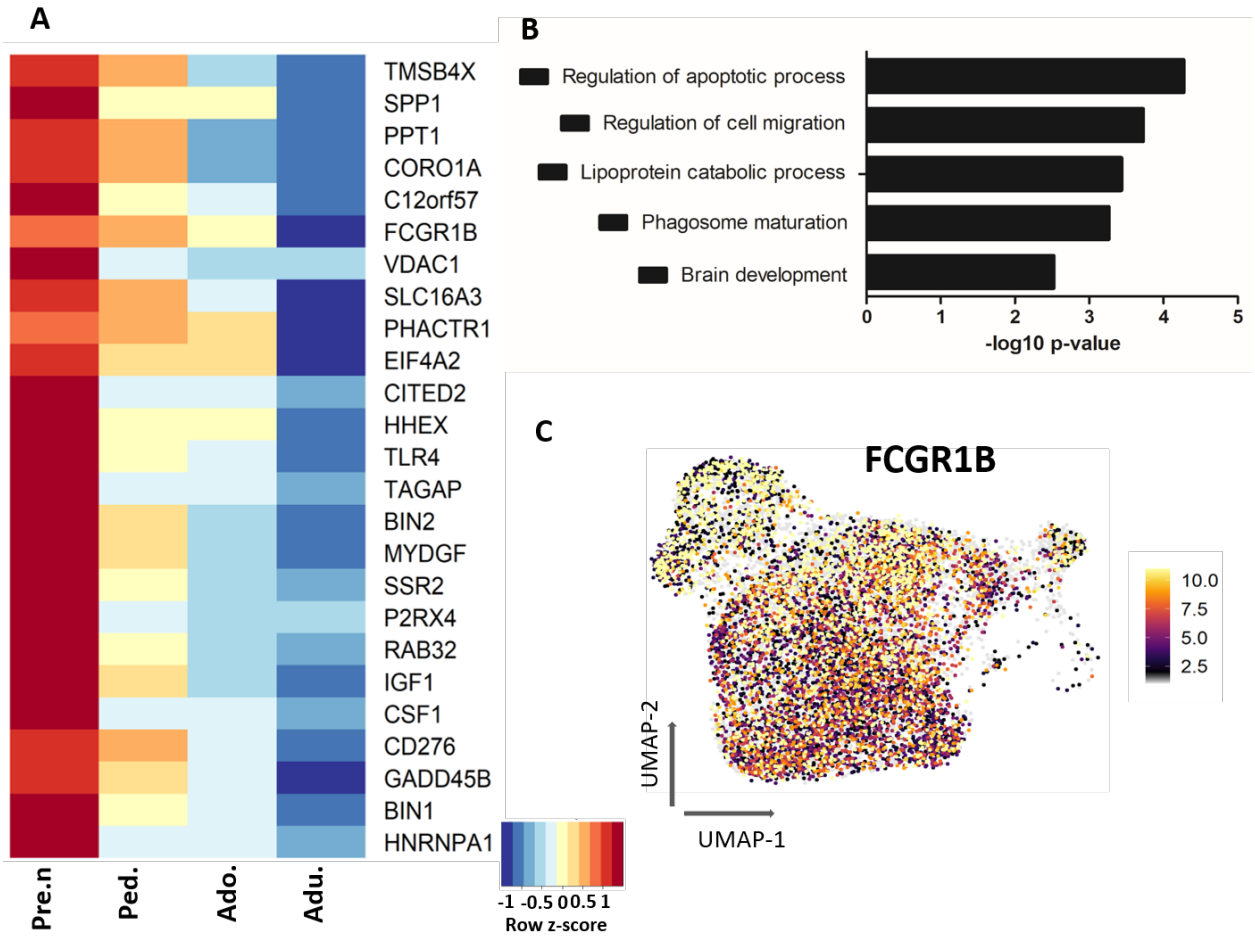

Figure 12. A) Heatmap showing expression of top 25 highly variable genes whose expression incrementally decreased with age. Red and blue color indicate up and down regulation of genes respectively. B) Gene ontology analysis of top 100 highly variable genes whose expression incrementally decreased with age. C) UMAP plot depicting normalized average expression of FCGR1B gene which has the highest expression in pre-natal cells and the lowest in adult cells. Pre.n = pre-natal, Ped. = Pediatric, Adol. = Adolescent, Adu. = Adult.

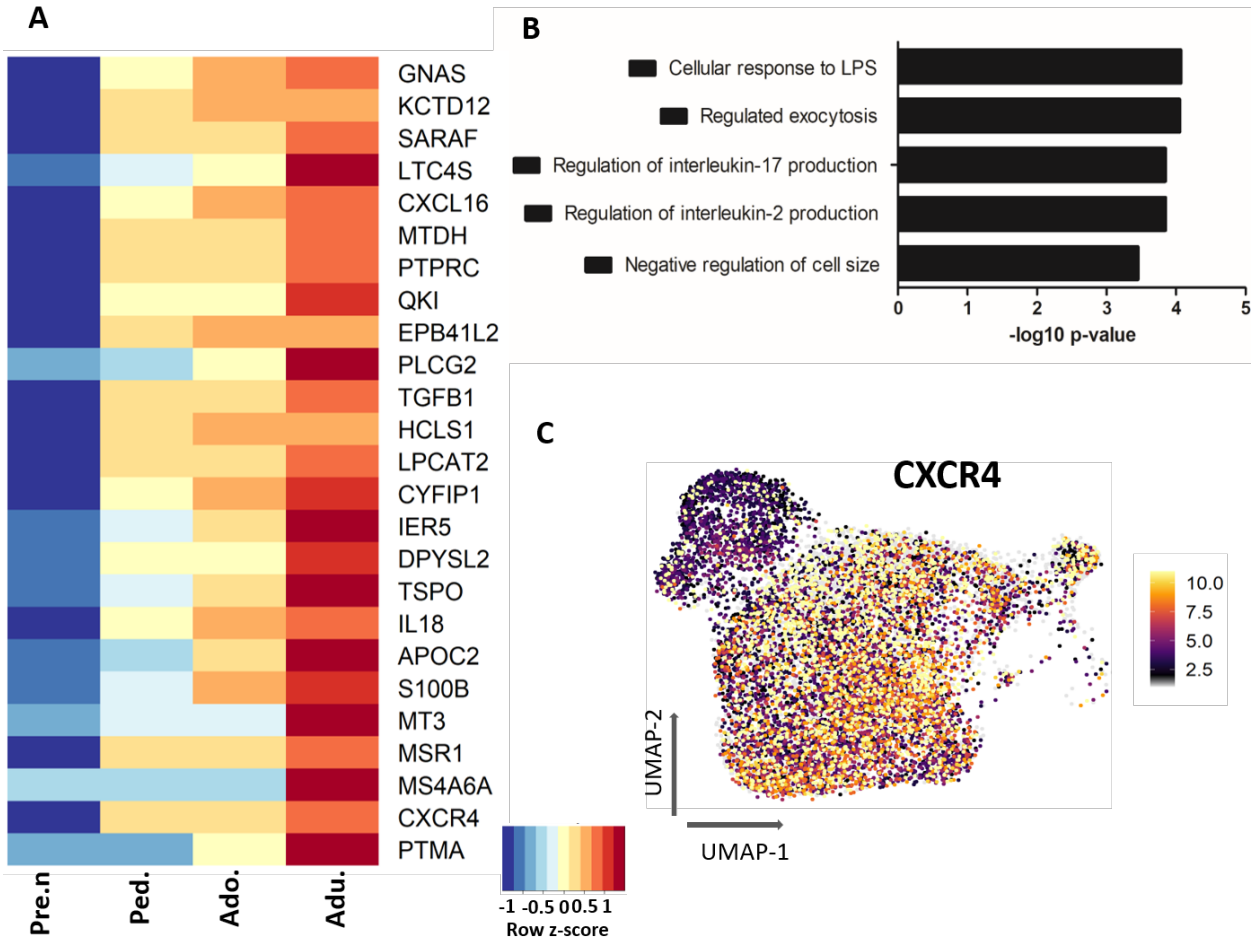

Figure 13. A) Heatmap showing expression of top 25 highly variable genes whose expression incrementally increased with age. Red and blue color indicate up and down regulation of genes respectively. B) Gene ontology analysis of top 100 highly variable genes whose expression incrementally increased with age. C) UMAP plot depicting normalized average expression of CXCR4 gene which has the lowest expression in pre-natal cells and the highest in the adult cells. Pre.n = pre-natal, Ped. = Pediatric, Adol. = Adolescent, Adu. = Adult.

Pre-natal microglia have a distinct transcription factor activity profile compared to post-natal microglia

Transcription factors (TFs) are the main regulators of developmental and cellular transitions, as they control the expression of key downstream target genes. TFs and their downstream targeted genes make up what is known as a gene regulatory network (GRN). To identify the TFs relevant to the maturation of microglia single cell regulatory network inference and clustering (SCENIC) was utilized. The SCENIC pipeline identifies putative GRNs involved in microglia maturation by measuring the expression of TFs and their downstream target genes. SCENIC analysis provides a measurement of activity for a given TF. We identified 142 TFs that potentially govern the activity of GRNs involved in microglia maturation. We measured both the transcriptional expression level of TFs in our transcriptomic dataset and the activity of these TFs using SCENIC analysis. We found that certain TFs were uniquely upregulated in individual developmental stages compared to all others (Figure 14A). The most expressed TFs for each age compared to other ages was SRY-box transcription factor 4 (*SOX4*) for pre-natal microglia, V-maf musculoaponeurotic fibrosarcoma oncogene homolog B (*MAFB*) for pediatric microglia, CCAAT enhancer binding protein delta (*CEBPD*) adolescent microglia, hypoxia-inducible factor 1-α (*HIF1A*) for adult microglia (Figure 14A). The high expression of *SOX4* in pre-natal microglia is consistent with the finding of Kracht et al., 2020, in which an upregulation of *SOX4* in the early gestational weeks of development was reported [126]. We did not observe any sex differences for the expression signature of TFs (data not shown).

As expression differences alone does not provide insight into TF activity, we next examined the activity level of the previously identified 142 TFs. SCENIC analysis similarly identified TFs with higher activity at each age, with the most significant differences found between pre-natal and post-natal cells (Figure 14B). Interestingly, the overall activity of most TFs was higher in pre-natal cells than post-natal cells with TF activity found to be similar among post-natal microglia (Figure 15). Of the TFs identified that could distinguish pre- and post-natal microglia, some had functions associated with pathways previously identified to be upregulated at specific ages. For example, activating transcription factor 4 (*ATF4)*, which has been shown to regulate the inflammatory signature of microglia [203], displayed higher activity in post-natal versus pre-natal microglia (Figure 16). TFs such as E2F transcription factors 4 (*E2F4)*, a cell cycle regulator, had higher

activity in pre-natal microglia, indicating a higher proliferative capacity versus post-natal cells (Figure 17). *SOX4* has previously been identified to control general cellular functions at early developmental stages as determined by Kracht et al., 2020 [126]. Among the post-natal microglia, we identify 'hotspots' of specific TF activity regulating gene expression in these cells (Figure 18A). In contrast to *ATF4* that uniformly regulated the expression of all post-natal microglia, TATA-box binding protein associated factor 1 (*TAF1*), CCCTC-binding factor (*CTCF*), nuclear factor, interleukin 3 regulated (*NFIL3*) and nuclear factor kappa B subunit 1 (*NFKB1*) regulated the transcriptomic expression of specific microglia populations (Figure 18B).

Altogether, our analysis reveals that each stage of human microglia development has specific TF content at the expression level, the activity of TFs broadly clusters microglia into pre-natal and post-natal populations. Pre-natal microglia have higher activity of TFs that control cell proliferation while adult specific TFs mainly control the immune signature of microglia.

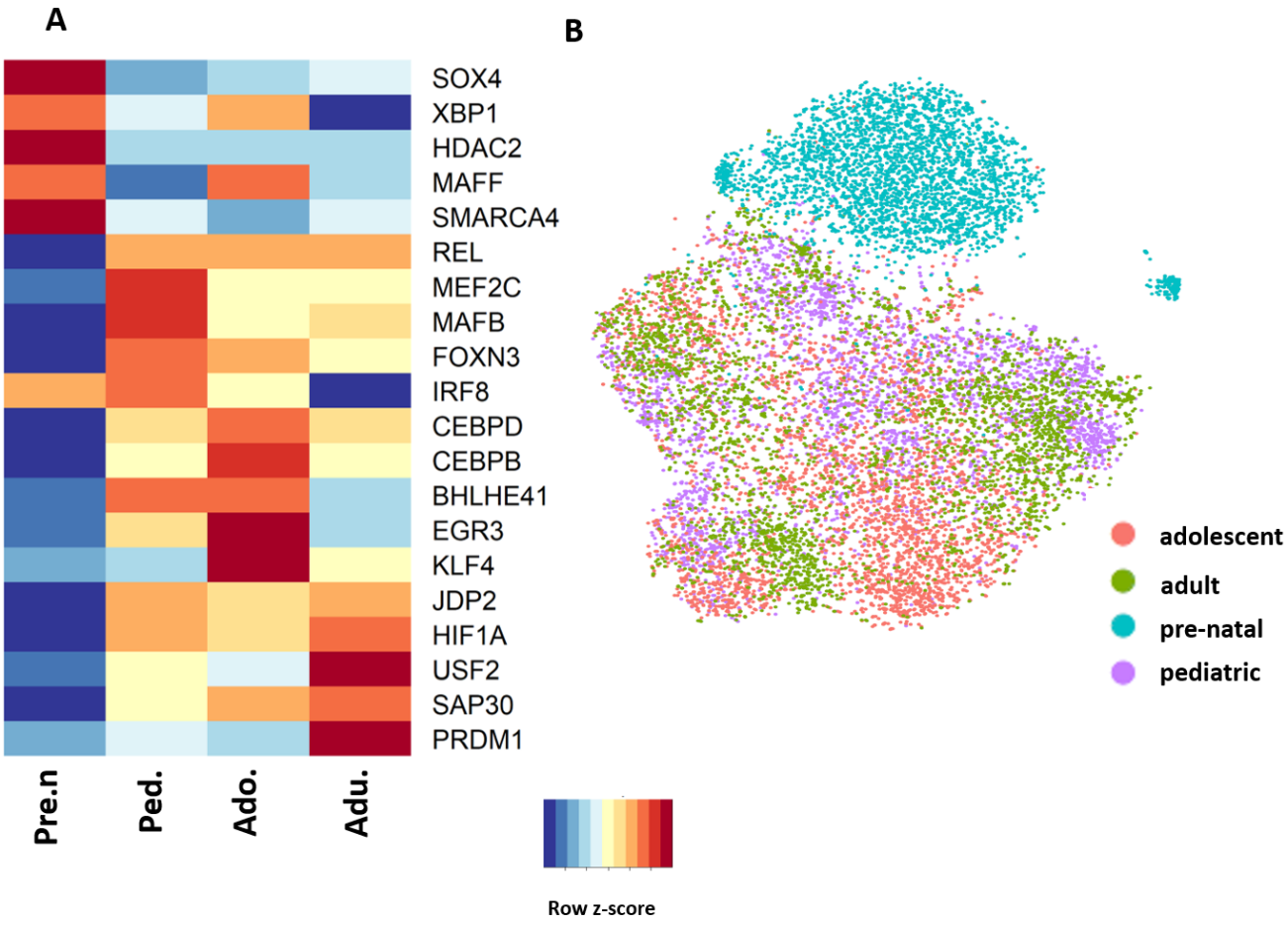

Figure 14. Heatmap depicting expression of top 5 most upregulated transcription factor per age. Red and blue color indicate up and down regulation of genes respectively. B) SCENIC plot depicting unbiased clustering of cells according to the activity of TFs identified. Each age is represented by a distinct color. Pre.n = pre-natal, Ped. = Pediatric, Adol. = Adolescent, Adu. = Adult.

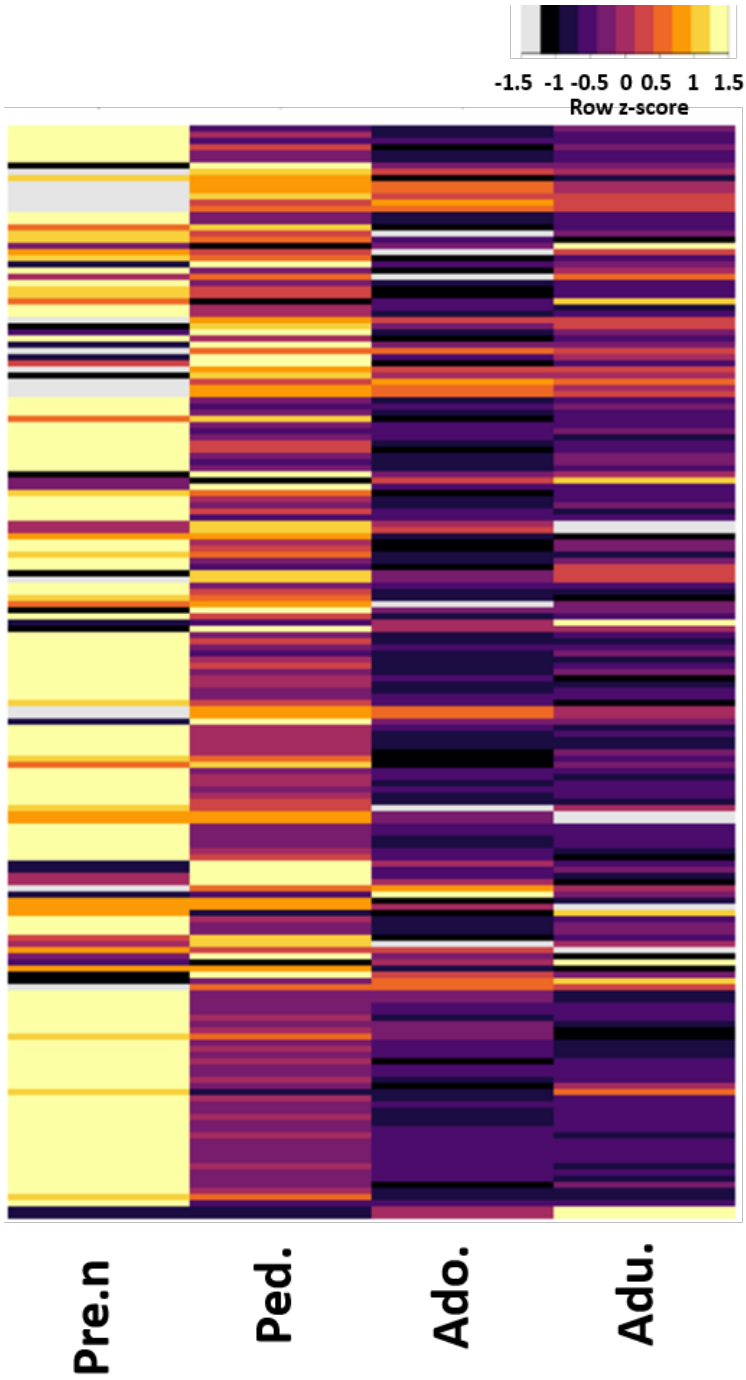

Figure 15. A) Heatmap showing the activity of 142 identified transcription factor during SCENIC analysis. The activity score of transcription factors is represented by color coded z-score. Pre.n = pre-natal, Ped. = Pediatric, Adol. = Adolescent, Adu. = Adult.

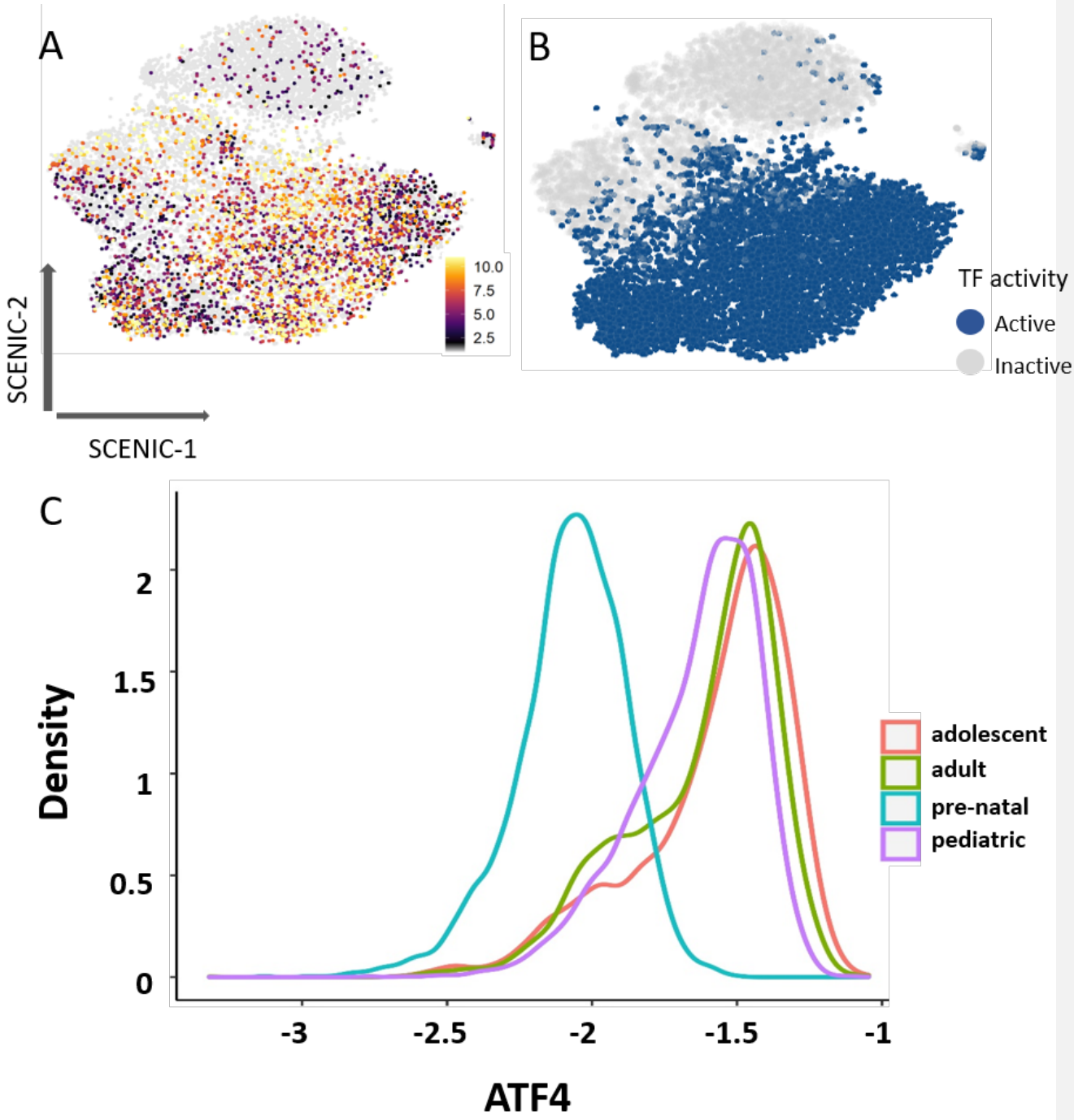

Figure 16. SCENIC plot representing mRNA expression, binary regulon activity, and kernel density AUC histogram for ATF4 TF. Expression of genes is represented by a color gradient. Activity is represented by a binary index in which blue denotes active and grey denotes inactive.

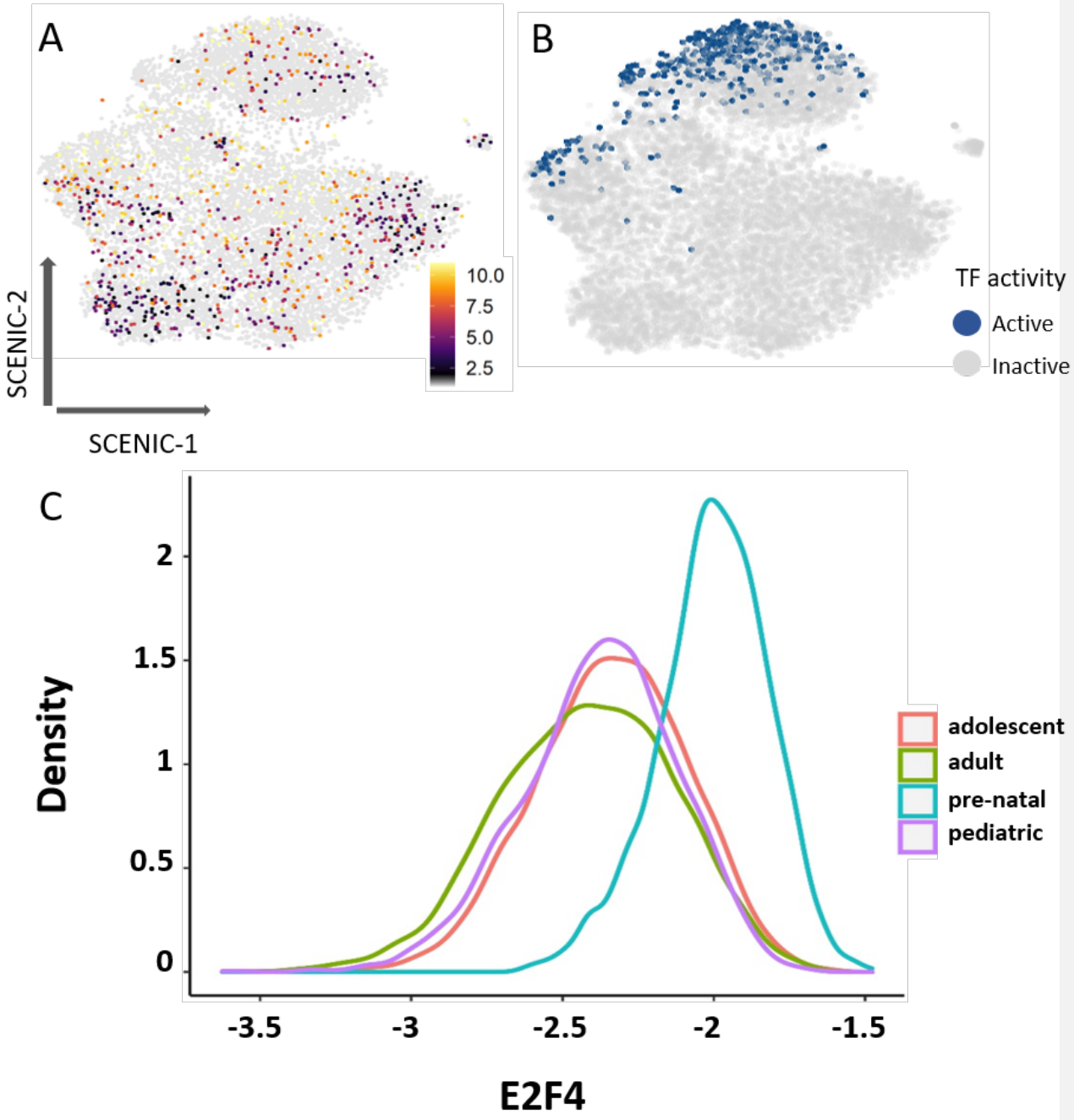

Figure 17. SCENIC plot representing mRNA expression, binary regulon activity, and kernel density AUC histogram for E2F4 TF. Expression of genes is represented by a color gradient. Activity is represented by a binary index in which blue denotes active and grey denotes inactive.

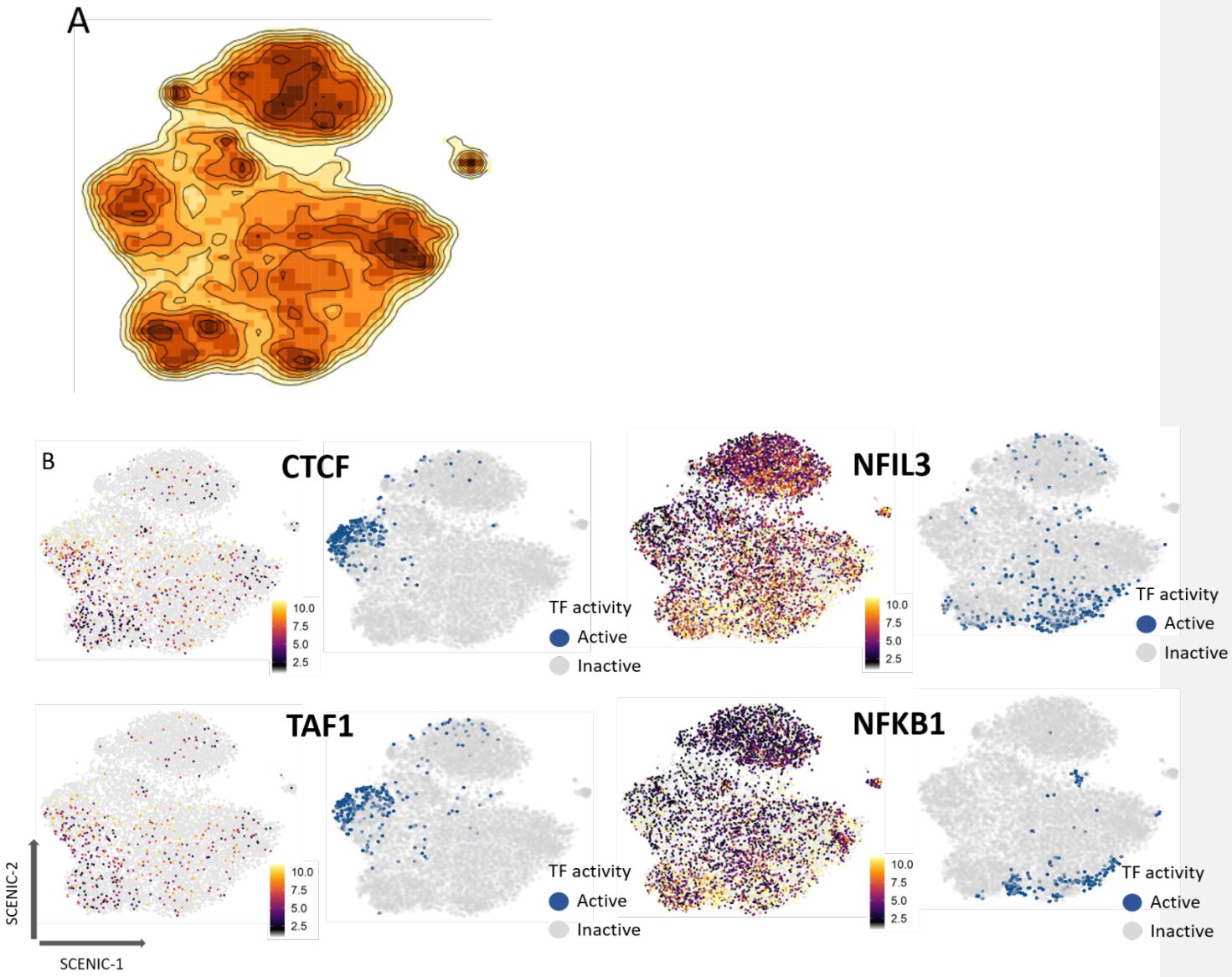

Figure 18. A) Density plot showing the activity map of TFs. Highly active and less active spots are represented by dark and light orange color respectively. B) SCENIC plot representing mRNA expression and binary regulon activity of selected TFs. Expression of genes is represented by a color gradient. Activity is represented by a binary index in which blue denotes active and grey denotes inactive.

Microglia do not progress along a clear developmental lineage as seen by pseudotime analysis

To further understand the maturation of human microglia over time, we performed a pseudotime trajectory analysis. Microglia did not align on the trajectory plot according to their developmental age, microglia from each age can be found disturbed evenly across pseudotime (Figure 19A). The shape and number of branches in the pseudotime trajectory plot were primarily driven by distinct microglia clusters previously identified in Figure 5A. We identified two transitional paths on the trajectory plot (Figure 19B). The first of these paths was a continuous transition of cells from cluster 7 to cluster 8 to cluster 10 (Figure 19C). Gene set enrichment analysis (GSEA) of the DEGs in these clusters showed that post translational modification of proteins was the most enriched term in clusters 7 and 8 (Figure 19D). For cluster 10, the most affected biological process was 'oxidative phosphorylation' (Figure 19D). The second path was formed by clusters 5 and 6 (Figure 19C). GSEA of DEGs for these clusters indicated that most of the upregulated genes in these microglia had roles in regulating cytokine mediated signaling (Figure 19D). In cluster 6, there were terms involved in nervous system development and neurogenesis (Figure 19D). To ensure that the pre-natal samples were not skewing the data and masking minor developmental differences between post-natal samples, the pre-natal dataset was removed and the pseudotime analysis was re-run. Similar results were observed (Figure 19E).

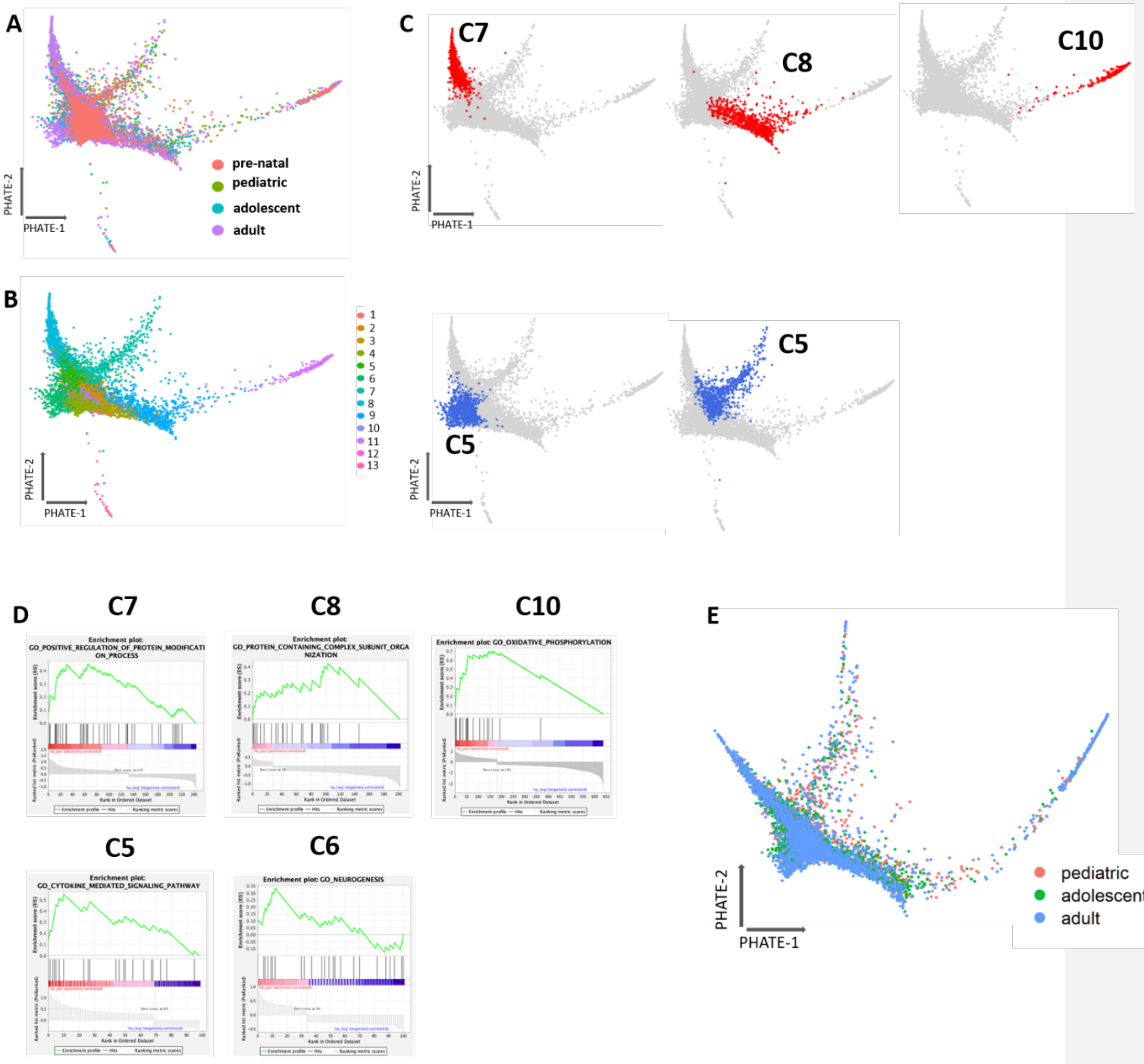

Figure 19. A) PHATE visualization for primary human microglia by age. B) PHATE visualization for primary human microglia by cluster. C) PHATE visualization for selected clusters. D) GSEA plot of the up regulated genes in clusters 7, 8, 10, 5 and 6. E) PHATE visualization for primary human post-natal microglia colored for each developmental stage.

Human microglia acquire a mature transcriptional signature faster than mouse microglia

Numerous equivalent mouse microglia datasets have been published recently, to understand the relevancy of findings in the murine system we compared our dataset to that of Hammond and colleagues as the time points used in their study were the most similar to ours [164]. Hammond et al used mouse microglia from embryonic day (E14.5), early postnatal day 4/5 (P4/P5), juvenile stage (P30), and adulthood (P100) tissue. We considered these samples equivalent to those of human pre-natal, pediatric, adolescent and adult time points, respectively [204]. Samples were analyzed separately and the average expression of each gene per time point was used to measure the correlation between age groups and a principal component analysis (PCA) was performed. The average of three adult human oligodendrocyte samples sequenced at the same time as the microglia was used to check for a batch effect between samples. The similarity of the samples was assessed at this step using Person correlation. This analysis indicated that there is a moderate similarity (correlation coefficient = ~0.5) between samples (Figure 20A). PCA analysis also confirmed that human oligodendrocyte sample was clustered with human microglia which indicated presence of batch effect between samples (Figure 20B). The idea of this sections was that similar cell types regardless of species should cluster together. Thus, clustering of human oligodendrocyte with human microglia confirmed presence of batch effect between samples. A combat algorithm was run to remove batch effect. Samples were found to have a high degree of similarity (correlation coefficient = ~0.8) (Figure 20C). According to the PCA plot, human oligodendrocytes clustered separately, indicating a lack of batch effect (Figure 20D). This plot revealed that human pre-natal samples had a distinct expression profile from the human post-natal samples (Figure 20D). E14.5 and P4/P5 mouse microglia clustered together but remained separate from the P30 and P100 microglia. These two early developmental stages of mouse microglia also clustered close to human pre-natal cells. These observations suggest that mouse P4/5 microglia have an expression profile similar to human and mouse pre-natal microglia (Figure 20D). Interestingly, human pediatric microglia clustered closely with human adolescent and adult samples. This contrasted with mouse pediatric microglia that clustered separately from mouse adolescent and adult microglia. We hypothesized that there is a delay in the maturation of mouse pediatric microglia compared to their human counterparts. To further explore this, we performed single sample gene set enrichment analysis (ssGSEA). We performed ssGSEA on our human microglia and on mouse microglia from

the Hammond et al study. Human microglia from Gosselin et al was used as a reference dataset to compare our human and mouse signatures with [205]. The ssGSEA revealed that human pediatric microglia from our study displayed the highest enrichment score with microglia from Gosselin et al. In contrast, in the mouse dataset P30 microglia had the highest enrichment score with cells from the Gosselin et al study (Figure 21). This finding suggests that mouse microglia require more time to develop an adult transcriptional signature than human microglia.

In summary, correlation analysis between human and mouse microglia samples across different stages of development suggests that, despite similarities between human and mouse microglia, cells tend to cluster in a species-specific manner rather than on their developmental age. In addition to this, we showed that human microglia acquire an adult transcriptional signature earlier than mouse microglia.

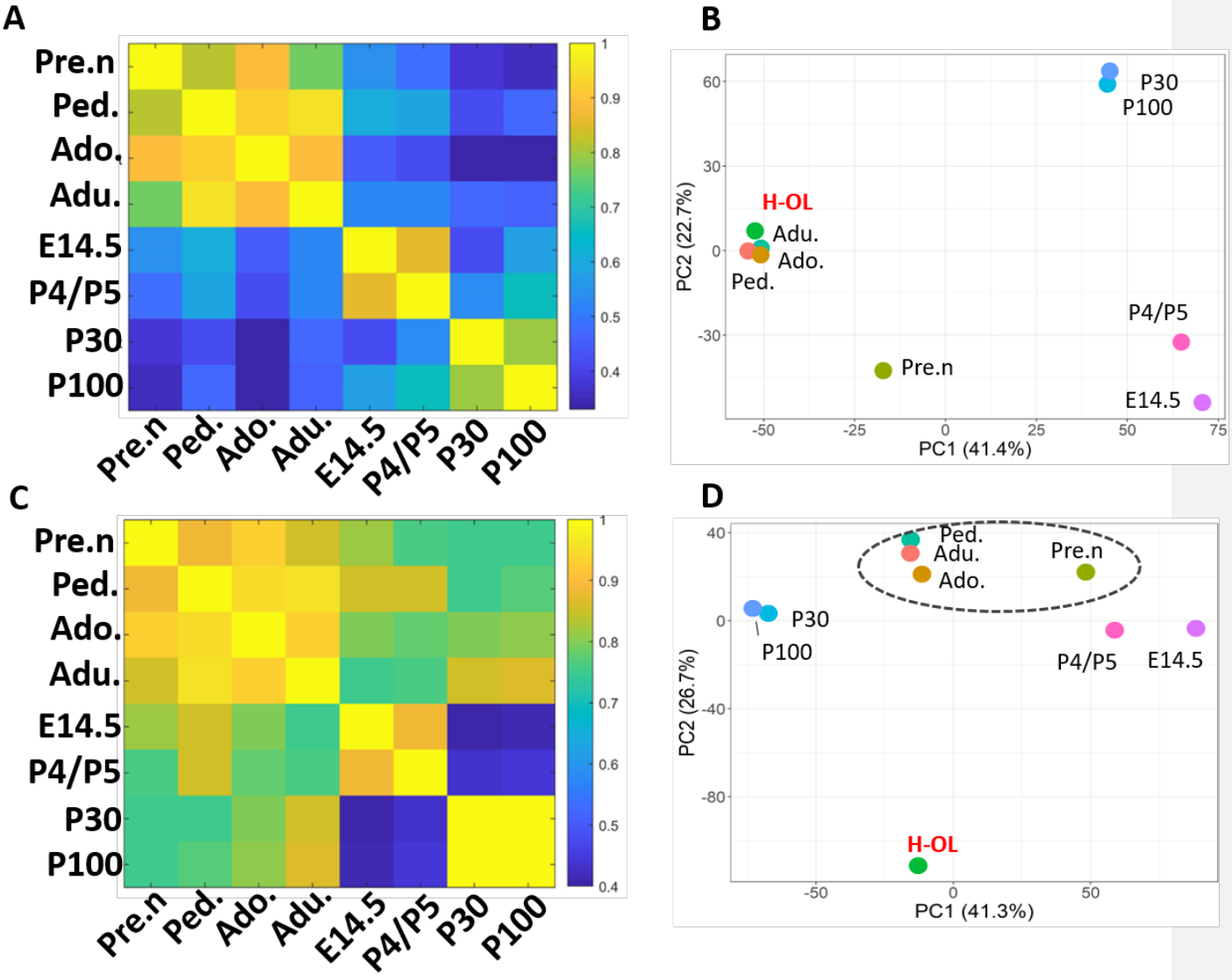

Figure 20. A) Heatmap showing Pearson correlation coefficient score of human and mouse microglia at different ages before batch effect correction, the score is represented by a color gradient in which yellow is the highest score (100%) and blue is lowest (40%). B) PCA plot of human and mouse microglia at different ages before batch effect correction. C) Heatmap showing Pearson correlation coefficient score of human and mouse microglia at different ages after batch effect correction, the score is represented by a color gradient in which yellow is the highest score (100%) and blue is lowest (40%). B) PCA plot of human and mouse microglia at different ages after batch effect correction. Pre.n = pre-natal, Ped. = Pediatric, Adol. = Adolescent, Adu. = Adult, H-OL = Human oligodendrocyte.

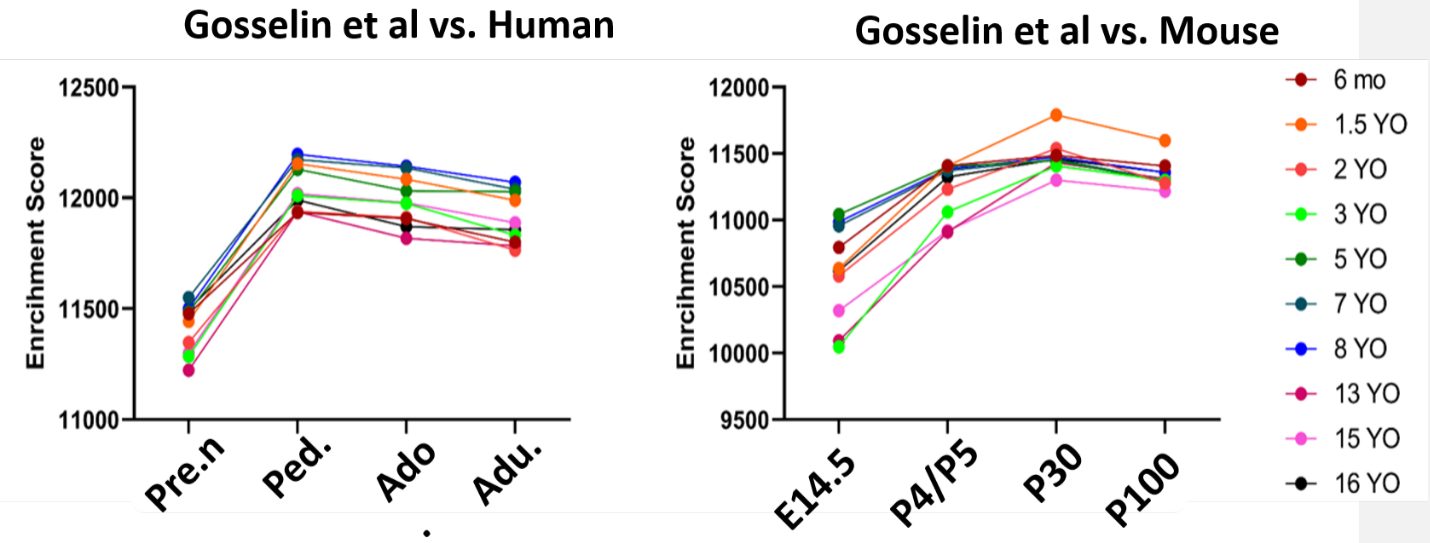

Figure 21. Line plot showing enrichment score resulting from ssGSEA between human and mouse microglia and reference dataset (Gosselin et al., 2016). Enrichment scores are represented along the Y-axis and age along the X-axis. Pre.n = Pre-natal, Ped. = Pediatric, Ado. = Adolescent, Adu. = Adult.

Chapter 4:

Discussion

The current study used high-throughput sequencing techniques to define the transcriptional landscape of human glial cells including OL lineage cells and microglia. The cells used were isolated from surgically resected brain tissue and sequenced immediately ex vivo. The tissue was isolated from donors covering a wide spectrum of ages. Among the ages included in our study were those with critically important developmental time points such as the early post-natal age in which a peak of myelination and synaptic pruning occurs [206]. The use of surgical tissue permitted the analysis of the full transcriptional content of whole cells, including cytoplasmic RNA.

We note that by employing the cell isolation procedure used here, OL-lineage cells and microglia constitute the majority of the cells isolated, followed by minor populations of lymphocytes and astrocytes. To date single cell nuclei staining data underrepresent the expected frequency of some glial cells like OL-lineage cells, especially from white matter samples. The observed paucity of neurons in our whole cell preparations could be explained in part because the samples were composed principally of white matter. We attribute the low number of astrocytes to the cell isolation procedure, particularly the Percoll gradient step. Therefore, the cell isolation protocols, and tissue dissociation methods appear to be important determining factors for the frequency of each cell type in the overall yield and is therefore a source of heterogeneity across studies. Other sources of variation in results across studies within the same species likely reflect samples being derived from distinct brain regions, different sequencing methodology, and/or the use of distinct bioinformatics analysis parameters.

As this study is focused on two of the three major glial cells of the CNS, in the following sections I will discuss our findings for each cell type separately.

Oligodendrocyte lineage cells:

The current analysis advances ongoing attempts to characterize populations of OLs at distinct stages of maturity and offers novel genetic targets for research studying demyelinating diseases. We focused on characterizing progenitor cells of the OL lineage using full microarray analysis to define more clearly the molecular properties that distinguish A2B5 antibody-selected cells ("pre-oligodendrocytes") from "mature OLs," as related to their place in the OL lineage [94,170–172],

and functional properties, as related to myelination potential and capacity to withstand injury. Previous studies compared the transcriptome profile of isolated adult human A2B5+ cells with the total dissociated cell population in the white matter, as well as astrocytes and myeloid cells isolated from this population, but not with the mature OL population [94,169].

Combination of our analyses using immunostaining on chamber slides and flow cytometry document that our starting population contained ~5%–15% A2B5+ cells, in line with previous reports [91,207,208], that the majority of these cells were O4+ [91,209], indicating they were committed to the OL lineage, and that the A2B5-reactive cells are effectively recovered by the immunomagnetic bead selection process. The intensity of A2B5 immunostaining was lower on bead-selected cells compared with cells examined prior to bead isolation, suggesting that the removal/reduction of epitopes recognized by the A2B5 antibody, steric hindrance of antibody binding by the immunomagnetic beads, and properties of the A2B5 antibody itself, contributed to the lack of complete cell identification by flow cytometry. The technical challenges regarding the use of an A2B5 antibody for cell isolation precluded carrying out our studies on immediately ex vivo cells.

Through use of a quantitative analytic system, we were able to demonstrate that the A2B5-selected (A+) population have a greater capacity to ensheath nanofibers than the non-selected A– population [168]. These observations extend our previous result that A+ cells have more extensive process outgrowth in dissociated cell cultures and show greater ensheathment of axons when added to cultures of rat-derived dorsal root ganglia. The nanofiber assay allowed us to document an increase in the mean length of segments ensheathed by A+ cells, as an indicator of myelination capacity. The nanofiber assay did not detect any significant difference in the mean number of segments formed per cell between A+ and A– populations. Nanofiber-OL cultures were assessed at 4 weeks; more prolonged cultures would be needed to assess the full potential of each of the cell populations to produce complete myelination.

Our transcriptomic analyses performed on cells at DIV1 indicated there were more genes upregulated in the A+ versus A– population. Upregulation of genes at DIV1 identified with the OL differentiation process were observed only in the A+ population, supporting that the A+

population reflects retained progenitor properties. *PTPRZ1*, the most robustly upregulated gene, inhibits OPC differentiation [210]. McClain et al showed that A2B5-selected cells exposed to the PTPRZ inhibitor bpV(phen), or lentiviral-shRNAi against PTPRZ, differentiate into OLs [211]. PDGFRA gene was upregulated in A+ cells at DIV1, but levels were significantly lower than those detected in fetal human brain-derived cells (15), consistent with observations using genetic linage tracking in the murine system [89]. We could not detect PDGFRA protein expression on DIV1 A+ cells using flow cytometry. The precise identity and function of cells shown to express PDGFRA transcripts in the adult human brain (Allen Brain Atlas, www.brain-map.org) remains to be defined. We cannot exclude that our isolation procedure resulted in depletion of these cells, as we have noted with astrocytes. Our findings that many OL lineage differentiation genes are comparably expressed between A+ and A– cell fractions is consistent with the A+ cells being late in the OL development pathway. We did not document whether absolute expression levels for all of these are downregulated in both cells types relative to fetal progenitors as observed with PDGFRα. The differential gene expression profile in the A+ cells is also distinct from the gene profiles identified in ex vivo or in vitro fetal human and murine studies [170–172,212], again supporting the distinct and late lineage properties of the human A2B5+ cells. In this regard, we find comparable expression of late myelin genes in the 2 populations, as did Sim et al [94,169]. We could not separately assess early (O4–) and later (O4+) lineage cells within the A2B5+ fractions.

Several pathways that we found to distinguish the A+ and A– populations would be relevant for functioning of these cell types both under physiologic conditions and under conditions encountered in active MS lesions. We observed differential expression of pathways (cellular development, cellular growth, and proliferation) that would favor enhanced process outgrowth and axon ensheathment as we have quantitated in our nanofiber-based assay comparing A+ and A– cells. For all these pathways, almost all DEGs were upregulated in the A+ population. Cell death/survival genes were upregulated in A+ cells, consistent with initial observations using an 84 apoptosis gene PCR pathway array (5). A+ cells are more susceptible to in vitro metabolic stress induced injury than are A– cells [213].

Our study of the most DEGs between the A+ and A– populations identified several genes usually attributed to immune system constituents, either myeloid or lymphocytic cells. Our cell

preparations do contain a detectable number of microglia in both the A+ and A– fractions although there were no differences between the fractions. Expression of some of these genes within the CNS has been reported [214–216]. Falcao et al reported the expression of multiple immune cell-associated genes by OL lineage cells in MS and its model experimental autoimmune encephalomyelitis [217]. IL-7 receptor (CD127), the most upregulated gene in DIV1 A+ cells, is usually associated with lymphoid cells. As stated, lymphocyte associated genes were more expressed in the A+ fraction. Our immunostaining and flow cytometry data directly indicate expression of CD127 on OLs. CD127 has previously been shown to be expressed in murine OL lineage cells [218] and we demonstrate expression on human OLs. The IL-7/IL-7R pathway has been shown to have cell survival promoting effect arising at least in part from its binding to various members of the anti-apoptotic BCL2 proteins [218]. The functional role of this pathway on promoting OL lineage cell survival and myelin maintenance properties remains to be established. Single nucleotide polymorphisms in IL-7 receptor have been implicated as susceptibility factors in multiple sclerosis [219].

In our study, we included a comparative analysis of A+ cells before and after being placed in dissociated cell culture for 6 days. After 6 DIV, a high percentage of initial A2B5-selected cells continued to express O4 and had extensive processes; the proportion of cells that were A2B5 antibody-reactive was reduced consistent with previous reports [94,169] and compatible with in vitro cell maturation having occurred. The total number of DEGs between cell types was markedly lower (i.e. 937) at DIV6 compared with DIV1 cells (i.e. 2094). We postulate this reflects initial increased active metabolism and ongoing active differentiation of the less mature OL lineage cells. Our postulate that the reduced differences over time between A+ and A– mainly reflect changes in the former would be consistent with the observation by Dugas et al that there was a remarkable similarity in gene expression between OLs generated in vitro and in vivo [170]. This remains to be tested in human studies when OLs derived from inducible progenitor stem cell sources are evaluated [220].

In the next part of the first chapter, we expanded the idea of characterizing OL lineage cells by explored transcriptional heterogeneity of the cells using more sophisticated tools like single cell RNA sequencing. Our result had significant correlation with the results reported for murine studies

in terms of maturity level of the identified cells [185]. We characterized three distinct cellular identities in OL lineage with differential abundance at different ages. In contrast to our MOL population for which we do not see a great heterogeneity as discussed in the literature [72], the transcriptomic profile of our l-OPC subpopulation, which were the only progenitor type identified in our adult samples, overlaps considerably with the signature of the OPC cluster from Jakel et al. (2019), with key top genes including SOX6, VCAN, MEGF11, HIF3A, and PTPRZ1 [72]. Such discrepancy might be due the bioinformatics approaches that we implemented in our study but we elected to focus first on characterizing the progenitor populations here.

In our analysis we were particularly interested in l-OPCs given they are most highly represented at time of peak myelination and l-OPCs appear to be the only OL progenitor population that is present in adulthood. Among the most affected biological processes by the highly expressed genes of this cell type only cell surface and ECM related terms were significant. Different cell surface molecules like of proteoglycans including chondroitin and heparin sulfate proteoglycans, and hyaluronan, as well as collagens, laminins, fibronectin, and tenascins were enriched in the most affected biological processes [221]. The interaction of cells with their immediate microenvironment through surface molecules greatly affect development of cells [222,223]. Interestingly, multiple chondroitin sulfate proteoglycans, including CSPG4, and VCAN, were expressed more highly in the pediatric l-OPCs compared to the adult l-OPCs. Surprisingly, one of the suggested underlying mechanism for low capacity of the mature in adult brain for remyelination is due to the scarcity of the ECM [222] or the increase in ECM stiffness [223]. In contrast we observed an increase in expression of ECM coding genes in l-OPCs. Chemotropic guidance cues netrin-1 (NTN1), semaphorins 5A and 5B (SEMA5A, SEMA5B), and SLIT1, as well as key receptor and downstream signaling components linked to these factors, including DSCAM, EPHB1, TRIO, CRMP1 and FYN [224–230] were among the most highly expressed genes in the lOPCs. Genes encoding proteins that influence ECM remodeling were also upregulated, including Tissue Inhibitor of Metalloproteinases 1 (TIMP1) [231] and SPARC-like protein 1 (SPARCL1) [232]. These observations underscore the importance of cell surface and ECM molecules during the dynamic process of myelinogenesis at the early post-natal ages and highlights ECM and surrounding environment of the cells is crucial for proper development of the cells. We have cross-referenced this data with rodent scRNA-seq data from healthy adult mouse

brain tissue [185], and found that indeed their OPC population uniquely expressed ECM-related molecules such as Cspg4, Fyn, Cspg5, Cntn1, Dscam, Sema5a, and Trio at the exclusion of MOLs, consistent with our findings. This was also the case in other datasets of the adult human control brain [72].

The importance of cell surface molecules in the biology of the OL lineage cells was also confirmed by exploring protein-protein interaction analysis. We revealed an up regulation of gene sets which are correlated with specific functions of each of characterized cell types. For example, for the l-OPCs we found up regulation of genes encoding cell surface molecules including neuroligins and neurexins (NLGN4X, NRXN1) and their interacting partner the leucine-rich repeat transmembrane protein LRRTM1 [233]. Moreover, for the e-OPC we unraveled up regulation of gene sets involved in OPC maturation and diversification during development including glutamate signaling, including metabotropic receptor GRM5, and AMPA type glutamate receptor subunits, GRIA2 and GRIA3 [234–236]. Finally, for the MOL identified protein network contained gene products which is necessary for OL survival such as OL survival, including the receptor GPR17 [237].

Besides cell surface molecules, biological processes such as lipid metabolism including cholesterol transport related terms were also significantly affected in l-OPCs. Cholesterol is required for the formation of lipid rafts [238], specialized plasma membrane microdomains that function as sites that focus transmembrane signal transduction and coordinate processes necessary for the initiation of myelination, such as cytoskeletal reorganization and recruitment of myelin-specific proteins (e.g., MBP and PLP1) [239]. The late myelin genes PLP1 and MBP, expressed in mature myelinating cells, were also upregulated in l-OPCs versus e-OPCs, consistent with their progression toward terminal differentiation and initial recruitment to early stages of myelin formation.

The combination of gene ontology and protein-protein interaction results suggest that cellular and extra cellular structure of l-OPC provide a microenvironment for l-OPC which make these cells prone to start myelination. Many of these processes are related through the activity of the tyrosine kinase FYN [240], a key gene we find significantly upregulated in l-OPCs compared to e-OPCs

and MOLs, which plays a central role in triggering OPC differentiation and promoting CNS myelination [230,241,242]. Previous studies reported significant expression of FYN during peak of myelination [243]. Our observation was in line with these reports in which we specifically reported uop regulation of FYN in pediatric l-OPCs compared to the adult l-OPCs consistent with recent finding of our lab in which we confirmed higher capacity of younger cells for remyelination (Luo et al., 2021- paper submitted). The relative upregulation of MBP and CNP expression in pediatric l-OPCs compared to adult l-OPCs suggests that these cells are undergoing active differentiation. The presence of l-OPCs in adult cerebral cortex was validated in situ using the RNAScope approach, and the transcripts of both TNR and VCAN genes were found to be expressed with high specificity by these OL progenitors.

We provided a description of the transcription factor landscape which have roles in the maturation of OL lineage cells. Our analysis revealed that SOX2 is the most central up regulated transcription factor in e-OPC and l-OPC compared to MOL has the highest number of direct targets. This appears consistent with its known role in maintaining stemness of multipotent progenitor cells [186]. In MOLs, SOX2 expression is markedly downregulated, as are many of the genes within its regulatory network. Considering the pivotal role of SOX2 for proper myelination [244], examining the downstream target genes and gene regulatory network of this transcription factor would be informative to understand the probable cause remyelination failure.

Even though transcriptomic content of the cells does not always lead to the same changes at the protein level, however, in our analysis we highlighted up regulation of a transcription factor which our lab had previously been identified presence of this gene at protein level. TCF7L2 RNA transcript is increased in l-OPCs, whose presence in pediatric tissue is 22.5 times higher than in the adult tissue (17.37% pediatric: 0.77% adult, Figure 3b). We observed that the myelin regulatory transcription factor TCF7L2 was predominantly detectible from full gestation to age 4 in humans by in situ immunohistochemistry [245]. This observation confirms there is a high correlation between our transcriptomic study and subsequent changes at protein level, although further experiments are required to validate our proposed gene sets in larger scale.
Overall, our work provides a valuable resource for the development of new stage specific markers of the OL-lineage, as well as potential targets for therapeutic interventions for demyelinating

diseases. Going forward, further studies based on these findings will investigate and identify novel contributions of these gene products to OL-lineage maturation and function.

In summary, our analysis of human brain tissue across a wide spectrum of ages, including the time of peak myelination, using a whole, live cell, scRNA-seq approach provides insight into the identity of subpopulations of OL-lineage cells that are distinct with respect to maturity and functional properties. This unbiased approach has identified novel genes whose role in the remyelination process remains to be further defined.

Microglia:

Next, we characterized the transcriptomic profile of microglia at a single cell level across pre-natal, pediatric, adolescent, and adult stages of human development. We identified a wide range of microglia transcriptional states during development which were associated with specific functions. Pre-natal cells were found to have a unique gene expression profile compared to post-natal cells, including a signature that suggests greater phagocytic capacity. Conversely, post-natal microglia displayed a continuum of gene expression, with only subtle differences between cells of different ages. Post-natal microglia exhibited a transcriptional signature indicating greater inflammatory capacity compared to pre-natal cells. We believe the distinct signature observed between pre- and post-natal cells is in response to changes in the brain microenvironment and not due to the existence of a predetermined microglia developmental program. We also explored the GRNs governing the differences between microglia of different ages and found that TF expression levels and activity differed the most between pre- and post-natal microglia. Despite high transcriptional similarity between human and mouse microglia of all age groups, microglia clustered more closely with the cells of their own species than with the other cells of the same age. Finally, we observed that human microglia acquire a mature signature more quickly than their mouse counterparts.

One of our primary objectives in this study was to determine if human microglia evolve transcriptionally over time. Our data suggests that microglia maturation does not follow a pre-determined developmental program, rather the cells acquire specific functional states likely as a result of changing microenvironments encountered over time. Previously, Kracht and colleagues studied the development of human pre-natal microglia at gestational week (GW) 9-18 and reported

that human pre-natal microglia acquired a mature phenotype by GW12 [126]. Microglia continued to develop up until GW18, at which point they were considered fully mature. In line with this observation, our pre-natal samples (GW 13-19) were not significantly different from post-natal microglia when subjected to pseudotime trajectory analysis. This result supports the idea that human microglia development starts at an early gestation timepoint and is completed by mid-gestation. Based on our data and that of Kracht et al, the differences between transcriptional states of microglia at various stages of development beyond GW18 appear to be in response to the changes in the surrounding CNS tissue as opposed to the existence of a predetermined microglia developmental program.

Given the significant differences between the pre- and post-natal CNS environment it was unsurprising to observe that the greatest separation between microglia of different ages came between pre- and post-natal microglia, also previously observed in mouse studies. The strongest suggested functional difference between pre- and post-natal microglia was that of pre-natal cells having a greater phagocytic capacity. Evidence from multiple models suggests that microglia display significant phagocytic activity early in brain development that is critical for the proper establishment of the CNS neuronal architecture. This relates to microglia-mediated regulation of neural progenitor cell (NPC) number, phagocytic clearance of synaptic material and the clearance of excess or dead neurons.

A comprehensive comparison of both human and mouse microglia is needed to better translate findings from mouse studies to basic human microglia biology and to understand the contribution of microglia to human disease. It has been shown that adult microglia from ten different species have some differences in their gene expression profile, though the core gene expression program in many species overlaps. Additional studies compared mouse and human microglia but limited their study to specific lists of genes. In our study, we compared the full transcriptional content of human and mouse microglia at specific ages and found a strong correlation between cells of both species at each age. Despite the similarity, human and mouse microglia exhibited a stronger correlation with the other developmental stages of their own species than with the corresponding developmental stage of the other. In addition, we observed a notable difference between human and mouse early post-natal microglia. Hammond and colleagues showed that mouse P4/P5

microglia have a more similar expression signature to pre-natal cells compared to the P30 and P100 microglia [164]. In contrast, human microglia of an equivalent age were found to be more similar to microglia of other post-natal stages (adolescent and adult) than to pre-natal microglia. This suggests that either intrinsic species differences and/or the significantly different environmental niches occupied by the species drives the more rapid acquisition of a mature signature by human microglia.

In our study, we found that human microglia do not exhibit distinct maturation stages but rather acquire transcriptional signatures in response to a continuously evolving brain microenvironment. Nonetheless microglia from each age point do display an enhancement of particular transcriptional states that suggest an importance of certain functions. For example, some microglial clusters had higher expression of inflammatory genes like IL1B and MSR1, which are well established drivers of pro-inflammatory cellular responses. These clusters were heavily enriched with the post-natal cells specifically adult cells. This observation might imply higher inflammatory signature of the adult human microglia compared to the pre-natal one. Moreover, we identified microglia that expressed the MS4A gene family, which has been introduced by Hammond et al. as a group of cells that express both microglia and macrophages markers [164]. They found this MS4A positive cluster of cells at early developmental stages in mice while in contrast, we identified these cells to be enriched in post-natal samples. In line with our data, a recent study suggests that these cells may come from a second wave of microglia development, in which the cells proliferate in the pre-natal liver before seeding the brain tissue.

We investigated the transcription factor (TF) expression and activity levels of microglia to supplement our transcriptional analysis. The TF content of microglia at different ages has been documented in mice in two separate studies. In a study of human microglia, Kracht and colleagues studied the TFs underlying the maturation of microglia from early gestational weeks (GWs) to later GWs. They found that gene expression programs switched from general cellular processes to microglia-specific functions during later gestational timepoints (GW 12-18). In our study, we found that at each age microglia had a moderately unique TF profile at the expression level. Even more noticeable, however, was at the activity level, for which the pre-natal microglia were distinct from the post-natal cells. For example, we found ATF4 to be highly active in the post-natal cells

as compared to pre-natal microglia. ATF4 is known to have a role in positively regulating the inflammatory signature of microglia. This observation suggests a higher inflammatory signature of post-natal microglia and is in agreement with our previous transcriptional findings. Conversely, we found increased activity of E2F4in the pre-natal microglia, which has been shown to be a cell cycle regulator. Increased activity of TFs involved in the cell cycle in the pre-natal microglia is in line with the well-documented higher proliferative capacity of microglia at this developmental stage, as seen in rodent models.

Here we provide a comprehensive single cell analysis of the transcriptional profile of human microglia at different ages. Further studies are needed to gain a better understanding of the molecular mechanisms that underlie human microglia development and to understand how the aging process may contribute to the loss of homeostatic microglia functions and/or the acquisition of pathological microglia phenotypes.

Chapter 5:

Conclusion and Summary

Conclusion:

Glial cells of the CNS including oligodendrocyte (OL) lineage cells and microglia have traditionally been considered static bystanders with neutral functions. However, a decade of research has revealed that both cells are critically important for normal CNS development and for maintaining CNS homeostasis into adulthood. OL lineage cells myelinate axonal fibers and therefore help facilitate saltatory conductance. Microglia are the primary brain-resident immune cell population that perform a wide range of immunological functions. Considering the critical function of these cells, any failure or damage to them can lead to an array of neurological disorders including MS, Alzheimer's disease, autism spectrum disorders, and Parkinson's disease. To better understand the function of these cells in disease we first need to understand how these cells develop in healthy brain tissue. Transcriptomic analyses of the cells can shed light on their functional properties. In the current thesis, using high throughput sequencing techniques we explored the temporal and spatial heterogeneity of OL lineage cells and characterized distinct OL lineage cells identities at a single cell resolution. We studied the transcriptomic and functional properties of OLs from different stages of human development including critical time points like early post-natal ages in which myelination peaks. The unbiased approach implemented in this study has identified novel sets of genes and molecular pathways the activity of which can be used to understand the role of these cells in brain homeostasis and disease. Moreover, we provided evidence of regional heterogeneity in the mature OL (MOL) population from the brain parenchyma, sub-ventricular zone, and spinal cord. Our observations suggested that there are multiple sub-types of MOLs across human CNS region with potential specific functions. We also uncovered that cells from the spinal cord have a distinct, more immunogenic transcriptomic signature compared to cells from elsewhere in the CNS.

Furthermore, we unveiled transcriptional heterogeneity of human microglia from embryonic life and into adulthood and confirmed there were multiple subtypes of microglia during human development although in general microglia display a gene expression continuum rather than very distinct and unique 'cellular subsets'. The identification of these microglial signatures provides a valuable source of information to aid our understanding of microglial functional diversity which may aid in the potential therapeutic manipulation of specific sub-types in disease situations. Through gene ontology analysis we also correlated the transcriptional landscape of cells at each

stage of development. Our observation indicated that pre-natal human microglia have a transcriptomic content which make them distinct from post-natal microglia, similar to published studies of murine microglia. We showed that the separation of pre- and post-natal microglia is not due to the existence of a pre-determined developmental program. In fact, microglia development finishes by the end of the second trimester. From that point onward expression changes of microglia are likely in response to changing the local microenvironment. In addition, by comparing our data with published murine datasets we show that despite similarities between human and mouse microglia, cells tend to cluster in a species-specific manner rather than according to their developmental age. Finally, we showed that human microglia acquire an adult transcriptional signature earlier than mouse microglia.

Altogether, the content of the current thesis provides a unique insight into the transcriptomic content of human glial cells at the single cell level from various stages of development. Here, we unraveled the dynamics of OL lineage cells during human development and from the critical developmental time points that had never been studied before in the human system. Moreover, for the first time, we provided evidence for regional heterogeneity of MOLs across human CNS regions. Characterizing temporal and regional heterogeneity different cell types of OL lineage cells and understanding their biology will shed light on the role of these cells in etiology of diseases which are associated with their malfunction. Furthermore, this knowledge might suggest these cells as novel targets for the treatment of MS.

For microglia, we provided a full perspective of human microglia development by having access to a unique dataset which covers wide range of ages from embryonic microglia up to adult cells. Providing documentation of microglia heterogeneity during development is critically important because these cells are indispensable player of proper CNS development. Such information will eventually lead to the identification of new targets for the treatment of neurodegenerative and neuro-inflammatory diseases. In addition, by comparing our human microglia dataset with murine microglia dataset we have provided valuable information regarding the basic biology and divergent species properties of the cells. These observations are of great interest specifically in the drive to translate studies done in mouse models to the human system and may lead to designing more thoughtful experiments for microglia related studies.

Future direction:

There are specific issues which need to be considered for future studies. The prediction of age and region enrichment gene expression profiles are based on scRNAseq data can be biased by technical limitations, such as differences in the viability of cell subpopulations following the tissue dissociation process. Moreover, bioinformatics approach might produce vague clustering results in a process called over clustering. In this process, mathematical algorithms underlying clustering produces clusters that are not true biological clusters [246]. Finally, the percentage of the genome covered by the scRNAseq technique needs to be considered as an important factor. There is a direct correlation between the number of genes that a technique can capture and the amount of information that can be extracted from the cells. This is also true for the length of the captured genes, so that techniques that cover the full length of genes reveal more information [247]. Considering these facts, in future experiments I would suggest the use of library preparation techniques such as SMART-seq2 which covers full-length of genes and also captures more genes per cell compared to 10X Chromium [247].

One potential yet important approach to continue this thesis is using publicly available single cell RNA-seq data sets of the neurodegenerative diseases like MS and AD to directly compare the transcriptional landscape of healthy microglia and OL lineage cells with the disease associated cell types. Moreover, the transcriptional landscape of the primary cells can be used to compare with the transcription signature of stem cell derived microglia and OLs to check the accuracy of their differentiation pathway. In addition, recruitment of bioinformatics tools such as NicheNet and CellPhoneDB provide a way to identify new receptor-ligand pairs from single-cell RNA sequencing data, which will serve as the starting point to dissect intercellular communications between microglia and OL lineage and their surrounding cellular niche that can then be studied in vitro and in vivo.

More importantly to substantiate these transcriptional observations functional experiments are needed to validate the finding in more detail. For example, we showed that pre-natal microglia displayed a transcriptional signature indicating a higher capacity for phagocytosis, this could further be validated by direct measurement of phagocytic activity in vitro. We also claimed that adult microglia have more inflammatory signature compared to the pre-natal cells. The validity of this claim can be confirmed by comparing the amount of secreted pro-inflammatory cytokines upon stimulating microglia with pro-inflammatory molecules. Staining techniques like

immunohistochemistry can also be used to check for the presence of proposed marker genes in our study. For OL lineage cells the myelination potential of human derived cells could be examined by grating them into the brains of mice with experimentally induced focal demyelinating injury. In this model we can see if progenitors or mature cells of different ages can myelinate axon fibers in vivo in different extent or not. In summary, while more work is needed in both the microglia and OL field we believe that the work presented here expands our knowledge regarding the biology of both cell types and can be used as a reliable reference for futures studies related to transcriptome content and functional diversity.

References:

1. Mestas J, Hughes CCW. Of Mice and Not Men: Differences between Mouse and Human Immunology. J Immunol. 2004;172: 2731–2738. doi:10.4049/jimmunol.172.5.2731
2. Vandamme T. Use of rodents as models of human diseases. J Pharm Bioallied Sci. Medknow Publications & Media Pvt Ltd; 2014;6: 2. doi:10.4103/0975-7406.124301
3. van der Worp HB, Howells DW, Sena ES, Porritt MJ, Rewell S, O'Collins V, et al. Can Animal Models of Disease Reliably Inform Human Studies? PLOS Med. Public Library of Science; 2010;7: e1000245. Available: https://doi.org/10.1371/journal.pmed.1000245
4. Christopher N, Brooks P. Antirheumatic medication in pregnancy. Br J Rheumatol. 1985;24: 282–90.
5. Stebbings R, Findlay L, Edwards C, Eastwood D, Bird C, North D, et al. "Cytokine Storm" in the Phase I Trial of Monoclonal Antibody TGN1412: Better Understanding the Causes to Improve PreClinical Testing of Immunotherapeutics. J Immunol. 2007;179: 3325–3331. doi:10.4049/jimmunol.179.5.3325
6. Seok J, Warren HS, Cuenca AG, Mindrinos MN, Baker H V, Xu W, et al. Genomic responses in mouse models poorly mimic human inflammatory diseases. Proc Natl Acad Sci. 2013;110: 3507–3512. doi:10.1073/pnas.1222878110
7. Butovsky O, Jedrychowski MP, Moore CS, Cialic R, Lanser AJ, Gabriely G, et al. Identification of a unique TGF-β–dependent molecular and functional signature in microglia. Nat Neurosci. Nature Publishing Group; 2014;17: 131–143. doi:10.1038/nn.3599
8. Masuda T, Sankowski R, Staszewski O, Böttcher C, Amann L, Sagar, et al. Spatial and temporal heterogeneity of mouse and human microglia at single-cell resolution. Nature. 2019;566: 388–392. doi:10.1038/s41586-019-0924-x
9. Sankowski R, Böttcher C, Masuda T, Geirsdottir L, Sagar, Sindram E, et al. Mapping microglia states in the human brain through the integration of high-dimensional techniques. Nat Neurosci. Springer US; 2019;22: 2098–2110. doi:10.1038/s41593-019-0532-y
10. Fields RD. White matter in learning, cognition and psychiatric disorders. Trends Neurosci. 2008;31: 361–370. doi:10.1016/j.tins.2008.04.001
11. Ramón y Cajal S. Contribución al conocimiento de la neuroglía del cerebro humano. Trab Lab Invest Biol. 1913;11: 255–315.
12. Ramon Ramón y Cajal S. Sobre un nuevo proceder de impregnación de la neuroglía y sus resultados en los centros nerviosos del hombre y animales. Trab Lab Invest Biol. 1913;11: 103–112.
13. Río-Hortega P del. Noticia de un nuevo y fácil método para la coloración de la neuroglia y el tejido conjuntivo. Trab Lab Invest Biol. 1918;15: 367–378.
14. Rio-Hortega P. Estudios sobre la neuroglía. La microglía y su transformación en células en bastoncito y cuerpos granuloadiposos. Trab Lab Invest Biol. 1920;18: 37–82.
15. Gill AS, Binder DK. Wilder Penfield, Pío Del Río-hortega, and the Discovery of Oligodendroglia. Neurosurgery. 2007;60: 940–948. doi:10.1227/01.NEU.0000255448.97730.34
16. Martínez-Cerdeño V, Noctor SC. Neural progenitor cell terminology. Front Neuroanat. 2018;12: 1–8. doi:10.3389/fnana.2018.00104

17. Lu QR, Sun T, Zhu Z, Ma N, Garcia M, Stiles CD, et al. Common Developmental Requirement for Olig Function Indicates a Motor Neuron/Oligodendrocyte Connection. Cell. 2002;109: 75–86. doi:10.1016/S0092-8674(02)00678-5
18. Arnett HA, Fancy SPJ, Alberta JA, Zhao C, Plant SR, Kaing S, et al. bHLH transcription factor Olig1 is required to repair demyelinated lesions in the CNS. Science (80-). 2004;306: 2111–2115. doi:10.1126/science.1103709
19. Paes de Faria J, Kessaris N, Andrew P, Richardson WD, Li H. New Olig1 null mice confirm a non-essential role for Olig1 in oligodendrocyte development. BMC Neurosci. 2014;15: 1–8. doi:10.1186/1471-2202-15-12
20. Zhou Q, Anderson DJ. The bHLH Transcription Factors OLIG2 and OLIG1 Couple Neuronal and Glial Subtype Specification. Cell. 2002;109: 61–73. doi:10.1016/S0092-8674(02)00677-3
21. Chapman H, Waclaw RR, Pei Z, Nakafuku M, Campbell K. The homeobox gene Gsx2 controls the timing of oligodendroglial fate specification in mouse lateral ganglionic eminence progenitors. Dev. 2012;140: 2289–2298. doi:10.1242/dev.091090
22. Nakatani H, Martin E, Hassani H, Clavairoly A, Maire CL, Viadieu A, et al. Ascl1/Mash1 promotes brain oligodendrogenesis during myelination and remyelination. J Neurosci. 2013;33: 9752–9768. doi:10.1523/JNEUROSCI.0805-13.2013
23. Sugimori M, Nagao M, Parras CM, Nakatani H, Lebel M, Guillemot F, et al. Ascl1 is required for oligodendrocyte development in the spinal cord. Development. 2008;135: 1271–1281. doi:10.1242/dev.015370
24. Douvaras P, Wang J, Zimmer M, Hanchuk S, O'Bara MA, Sadiq S, et al. Efficient generation of myelinating oligodendrocytes from primary progressive multiple sclerosis patients by induced pluripotent stem cells. Stem Cell Reports. The Authors; 2014;3: 250–259. doi:10.1016/j.stemcr.2014.06.012
25. Küspert M, Hammer A, Bösl MR, Wegner M. Olig2 regulates Sox10 expression in oligodendrocyte precursors through an evolutionary conserved distal enhancer. Nucleic Acids Res. 2011;39: 1280–1293. doi:10.1093/nar/gkq951
26. Weider M, Starost LJ, Groll K, Küspert M, Sock E, Wedel M, et al. Nfat/calcineurin signaling promotes oligodendrocyte differentiation and myelination by transcription factor network tuning. Nat Commun. Springer US; 2018;9: 1–16. doi:10.1038/s41467-018-03336-3
27. Samanta J, Kessler JA. Interactions between ID and OLIG proteins mediate the inhibitory effects of BMP4 on oligodendroglial differentiation. Development. 2004;131: 4131–4142. doi:10.1242/dev.01273
28. Liu A, Li J, Marin-Husstege M, Kageyama R, Fan Y, Gelinas C, et al. A molecular insight of Hes5-dependent inhibition of myelin gene expression: Old partners and new players. EMBO J. 2006;25: 4833–4842. doi:10.1038/sj.emboj.7601352
29. Baroti T, Zimmermann Y, Schillinger A, Liu L, Lommes P, Wegner M, et al. Transcription factors Sox5 and Sox6 exert direct and indirect influences on oligodendroglial migration in spinal cord and forebrain. Glia. 2016;64: 122–138. doi:10.1002/glia.22919
30. Stolt CC, Lommes P, Sock E, Chaboissier MC, Schedl A, Wegner M. The Sox9 transcription factor determines glial fate choice in the developing spinal cord. Genes Dev. 2003;17: 1677–1689. doi:10.1101/gad.259003
31. Klum S, Zaouter C, Alekseenko Z, Björklund ÅK, Hagey DW, Ericson J, et al.

Sequentially acting SOX proteins orchestrate astrocyte- and oligodendrocyte-specific gene expression. EMBO Rep. 2018;19: 1–14. doi:10.15252/embr.201846635
32. Kang P, Lee HK, Glasgow SM, Finley M, Donti T, Gaber ZB, et al. Sox9 and NFIA Coordinate a Transcriptional Regulatory Cascade during the Initiation of Gliogenesis. Neuron. Elsevier Inc.; 2012;74: 79–94. doi:10.1016/j.neuron.2012.01.024
33. Turnescu T, Arter J, Reiprich S, Tamm ER, Waisman A, Wegner M. Sox8 and Sox10 jointly maintain myelin gene expression in oligodendrocytes. Glia. 2018;66: 279–294. doi:10.1002/glia.23242
34. Chew LJ, Ming X, McEllin B, Dupree J, Hong E, Catron M, et al. Sox17 Regulates a Program of Oligodendrocyte Progenitor Cell Expansion and Differentiation during Development and Repair. Cell Rep. ElsevierCompany.; 2019;29: 3173-3186.e7. doi:10.1016/j.celrep.2019.10.121
35. Zhao C, Deng Y, Liu L, Yu K, Zhang L, Wang H, et al. Dual regulatory switch through interactions of Tcf7l2/Tcf4 with stage-specific partners propels oligodendroglial maturation. Nat Commun. Nature Publishing Group; 2016;7. doi:10.1038/ncomms10883
36. Wedel M, Fröb F, Elsesser O, Wittmann MT, Lie DC, Reis A, et al. Transcription factor Tcf4 is the preferred heterodimerization partner for Olig2 in oligodendrocytes and required for differentiation. Nucleic Acids Res. 2020;48: 4839–4857. doi:10.1093/nar/gkaa218
37. He Y, Dupree J, Wang J, Sandoval J, Li J, Liu H, et al. The Transcription Factor Yin Yang 1 Is Essential for Oligodendrocyte Progenitor Differentiation. Neuron. 2007;55: 217–230. doi:10.1016/j.neuron.2007.06.029
38. Weng Q, Chen Y, Wang H, Xu X, Yang B, He Q, et al. Dual-Mode Modulation of Smad Signaling by Smad-Interacting Protein Sip1 Is Required for Myelination in the Central Nervous System. Neuron. Elsevier Inc.; 2012;73: 713–728. doi:10.1016/j.neuron.2011.12.021
39. Aprato J, Sock E, Weider M, Elsesser O, Fröb F, Wegner M. Myrf guides target gene selection of transcription factor Sox10 during oligodendroglial development. Nucleic Acids Res. 2020;48: 1254–1270. doi:10.1093/nar/gkz1158
40. Elbaz B, Aaker JD, Isaac S, Kolarzyk A, Brugarolas P, Eden A, et al. Phosphorylation State of ZFP24 Controls Oligodendrocyte Differentiation. Cell Rep. ElsevierCompany.; 2018;23: 2254–2263. doi:10.1016/j.celrep.2018.04.089
41. Zhang C, Huang H, Chen Z, Zhang Z, Lu W, Qiu M. The transcription factor NKX2-2 regulates oligodendrocyte differentiation through domain-specific interactions with transcriptional corepressors. J Biol Chem. Â© 2020 ASBMB. Currently published by Elsevier Inc; originally published by American Society for Biochemistry and Molecular Biology.; 2020;295: 1879–1888. doi:10.1074/jbc.RA119.011163
42. Ehrlich M, Mozafari S, Glatza M, Starost L, Velychko S, Hallmann AL, et al. Rapid and efficient generation of oligodendrocytes from human induced pluripotent stem cells using transcription factors. Proc Natl Acad Sci U S A. 2017;114: E2243–E2252. doi:10.1073/pnas.1614412114
43. Cai J, Zhu Q, Zheng K, Li H, Qi Y, Cao Q, et al. Co-localization of Nkx6.2 and Nkx2.2 homeodomain proteins in differentiated myelinating oligodendrocytes. Glia. 2010;58: 458–468. doi:10.1002/glia.20937
44. Williamson JM, Lyons DA. Myelin Dynamics Throughout Life: An Ever-Changing Landscape? [Internet]. Frontiers in Cellular Neuroscience . 2018. p. 424. Available:

https://www.frontiersin.org/article/10.3389/fncel.2018.00424
45. Scantlebury N, Cunningham T, Dockstader C, Laughlin S, Gaetz W, Rockel C, et al. Relations between White Matter Maturation and Reaction Time in Childhood. J Int Neuropsychol Soc. 2013/10/29. Cambridge University Press; 2014;20: 99–112. doi:10.1017/S1355617713001148
46. Seidl AH. Regulation of conduction time along axons. Neuroscience. 2013/06/29. 2014;276: 126–134. doi:10.1016/j.neuroscience.2013.06.047
47. Scholz J, Klein MC, Behrens TEJ, Johansen-Berg H. Training induces changes in white-matter architecture. Nat Neurosci. 2009/10/11. 2009;12: 1370–1371. doi:10.1038/nn.2412
48. Sampaio-Baptista C, Khrapitchev AA, Foxley S, Schlagheck T, Scholz J, Jbabdi S, et al. Motor Skill Learning Induces Changes in White Matter Microstructure and Myelination. J Neurosci. 2013;33: 19499–19503. doi:10.1523/JNEUROSCI.3048-13.2013
49. Mount CW, Monje M. Wrapped to Adapt: Experience-Dependent Myelination. Neuron. 2017;95: 743–756. doi:10.1016/j.neuron.2017.07.009
50. Fields RD. A new mechanism of nervous system plasticity: activity-dependent myelination. Nat Rev Neurosci. 2015;16: 756–767. doi:10.1038/nrn4023
51. Franklin RJM, Ffrench-Constant C. Remyelination in the CNS: from biology to therapy. Nat Rev Neurosci. 2008;9: 839–855. doi:10.1038/nrn2480
52. Wang H, Allen ML, Grigg JJ, Noebels JL, Tempel BL. Hypomyelination alters K+ channel expression in mouse mutants shiverer and Trembler. Neuron. Cell Press; 1995;15: 1337–1347. doi:10.1016/0896-6273(95)90012-8
53. Hamada MS, Kole MHP. Myelin Loss and Axonal Ion Channel Adaptations Associated with Gray Matter Neuronal Hyperexcitability. J Neurosci. Society for Neuroscience; 2015;35: 7272–7286. doi:10.1523/JNEUROSCI.4747-14.2015
54. Felts PA, Baker TA, Smith KJ. Conduction in Segmentally Demyelinated Mammalian Central Axons. J Neurosci. Society for Neuroscience; 1997;17: 7267–7277. doi:10.1523/JNEUROSCI.17-19-07267.1997
55. Duncan ID, Marik RL, Broman AT, Heidari M. Thin myelin sheaths as the hallmark of remyelination persist over time and preserve axon function. Proc Natl Acad Sci. 2017;114: E9685–E9691. doi:10.1073/pnas.1714183114
56. Duncan ID, Radcliff AB, Heidari M, Kidd G, August BK, Wierenga LA. The adult oligodendrocyte can participate in remyelination. Proc Natl Acad Sci. 2018;115: E11807–E11816. doi:10.1073/pnas.1808064115
57. Irvine KA, Blakemore WF. Remyelination protects axons from demyelination-associated axon degeneration. Brain. 2008;131: 1464–1477. doi:10.1093/brain/awn080
58. Mei F, Lehmann-Horn K, Shen Y-AA, Rankin KA, Stebbins KJ, Lorrain DS, et al. Accelerated remyelination during inflammatory demyelination prevents axonal loss and improves functional recovery. Elife. eLife Sciences Publications, Ltd; 2016;5: e18246. doi:10.7554/eLife.18246
59. Schirmer L, Möbius W, Zhao C, Cruz-Herranz A, Ben Haim L, Cordano C, et al. Oligodendrocyte-encoded Kir4.1 function is required for axonal integrity. Elife. eLife Sciences Publications, Ltd; 2018;7: e36428. doi:10.7554/eLife.36428
60. Saab AS, Tzvetavona ID, Trevisiol A, Baltan S, Dibaj P, Kusch K, et al. Oligodendroglial NMDA Receptors Regulate Glucose Import and Axonal Energy Metabolism. Neuron. Elsevier; 2016;91: 119–132. doi:10.1016/j.neuron.2016.05.016
61. Micu I, Plemel JR, Caprariello A V, Nave K-A, Stys PK. Axo-myelinic

neurotransmission: a novel mode of cell signalling in the central nervous system. Nat Rev Neurosci. 2018;19: 49–58. doi:10.1038/nrn.2017.128
62. Guo C, Cho K-S, Li Y, Tchedre K, Antolik C, Ma J, et al. IGFBPL1 Regulates Axon Growth through IGF-1-mediated Signaling Cascades. Sci Rep. 2018;8: 2054. doi:10.1038/s41598-018-20463-5
63. Nikić I, Merkler D, Sorbara C, Brinkoetter M, Kreutzfeldt M, Bareyre FM, et al. A reversible form of axon damage in experimental autoimmune encephalomyelitis and multiple sclerosis. Nat Med. 2011;17: 495–499. doi:10.1038/nm.2324
64. Witte ME, Schumacher A-M, Mahler CF, Bewersdorf JP, Lehmitz J, Scheiter A, et al. Calcium Influx through Plasma-Membrane Nanoruptures Drives Axon Degeneration in a Model of Multiple Sclerosis. Neuron. 2019/01/24. Cell Press; 2019;101: 615-624.e5. doi:10.1016/j.neuron.2018.12.023
65. Crawford AH, Tripathi RB, Foerster S, McKenzie I, Kougioumtzidou E, Grist M, et al. Pre-Existing Mature Oligodendrocytes Do Not Contribute to Remyelination following Toxin-Induced Spinal Cord Demyelination. Am J Pathol. 2016/01/07. American Society for Investigative Pathology; 2016;186: 511–516. doi:10.1016/j.ajpath.2015.11.005
66. Wang S, Sdrulla AD, DiSibio G, Bush G, Nofziger D, Hicks C, et al. Notch Receptor Activation Inhibits Oligodendrocyte Differentiation. Neuron. 1998;21: 63–75. doi:10.1016/S0896-6273(00)80515-2
67. Windrem MS, Nunes MC, Rashbaum WK, Schwartz TH, Goodman RA, McKhann G, et al. Fetal and adult human oligodendrocyte progenitor cell isolates myelinate the congenitally dysmyelinated brain. Nat Med. 2004;10: 93–97. doi:10.1038/nm974
68. Fancy SPJ, Zhao C, Franklin RJM. Increased expression of Nkx2.2 and Olig2 identifies reactive oligodendrocyte progenitor cells responding to demyelination in the adult CNS. Mol Cell Neurosci. 2004;27: 247–254. doi:10.1016/j.mcn.2004.06.015
69. Emery B, Agalliu D, Cahoy JD, Watkins TA, Dugas JC, Mulinyawe SB, et al. Myelin Gene Regulatory Factor Is a Critical Transcriptional Regulator Required for CNS Myelination. Cell. 2009;138: 172–185. doi:10.1016/j.cell.2009.04.031
70. Zhao C, Ma D, Zawadzka M, Fancy SPJ, Elis-Williams L, Bouvier G, et al. Sox2 Sustains Recruitment of Oligodendrocyte Progenitor Cells following CNS Demyelination and Primes Them for Differentiation during Remyelination. J Neurosci. 2015;35: 11482–11499. doi:10.1523/JNEUROSCI.3655-14.2015
71. Messersmith DJ, Murtie JC, Le TQ, Frost EE, Armstrong RC. Fibroblast growth factor 2 (FGF2) and FGF receptor expression in an experimental demyelinating disease with extensive remyelination. J Neurosci Res. John Wiley & Sons, Inc.; 2000;62: 241–256. doi:10.1002/1097-4547(20001015)62:2<241::AID-JNR9>3.0.CO;2-D
72. Jäkel S, Agirre E, Mendanha Falcão A, van Bruggen D, Lee KW, Knuesel I, et al. Altered human oligodendrocyte heterogeneity in multiple sclerosis. Nature. Springer US; 2019;566: 543–547. doi:10.1038/s41586-019-0903-2
73. Franklin RJM, Ffrench-Constant C. Regenerating CNS myelin — from mechanisms to experimental medicines. Nat Rev Neurosci. 2017;18: 753–769. doi:10.1038/nrn.2017.136
74. Targett MP, Sussmant J, Scoldingt N, O'Leary MT, Compston DAS, Blakemore WF. Failure to achieve remyelination of demyelinated rat axons following transplantation of glial cells obtained from the adult human brain. Neuropathol Appl Neurobiol. John Wiley & Sons, Ltd; 1996;22: 199–206. doi:10.1111/j.1365-2990.1996.tb00895.x
75. Yeung MSY, Djelloul M, Steiner E, Bernard S, Salehpour M, Possnert G, et al. Dynamics

of oligodendrocyte generation in multiple sclerosis. Nature. 2019;566: 538–542. doi:10.1038/s41586-018-0842-3
76. ffrench-Constant C, Raff MC. Proliferating bipotential glial progenitor cells in adult rat optic nerve. Nature. 1986;319: 499–502. doi:10.1038/319499a0
77. Dimou L, Simon C, Kirchhoff F, Takebayashi H, Gotz M. Progeny of Olig2-Expressing Progenitors in the Gray and White Matter of the Adult Mouse Cerebral Cortex. J Neurosci. 2008;28: 10434–10442. doi:10.1523/JNEUROSCI.2831-08.2008
78. Simon C, Götz M, Dimou L. Progenitors in the adult cerebral cortex: Cell cycle properties and regulation by physiological stimuli and injury. Glia. John Wiley & Sons, Ltd; 2011;59: 869–881. doi:10.1002/glia.21156
79. Hughes EG, Kang SH, Fukaya M, Bergles DE. Oligodendrocyte progenitors balance growth with self-repulsion to achieve homeostasis in the adult brain. Nat Neurosci. 2013;16: 668–676. doi:10.1038/nn.3390
80. Bergles DE, Roberts JDB, Somogyi P, Jahr CE. Glutamatergic synapses on oligodendrocyte precursor cells in the hippocampus. Nature. 2000;405: 187–191. doi:10.1038/35012083
81. Sun W, Dietrich D. Synaptic integration by NG2 cells [Internet]. Frontiers in Cellular Neuroscience . 2013. p. 255. Available: https://www.frontiersin.org/article/10.3389/fncel.2013.00255
82. Birey F, Kloc M, Chavali M, Hussein I, Wilson M, Christoffel DJ, et al. Genetic and Stress-Induced Loss of NG2 Glia Triggers Emergence of Depressive-like Behaviors through Reduced Secretion of FGF2. Neuron. 2015;88: 941–956. doi:10.1016/j.neuron.2015.10.046
83. Djogo T, Robins SC, Schneider S, Kryzskaya D, Liu X, Mingay A, et al. Adult NG2-Glia Are Required for Median Eminence-Mediated Leptin Sensing and Body Weight Control. Cell Metab. Elsevier; 2016;23: 797–810. doi:10.1016/j.cmet.2016.04.013
84. Faber CL, Deem JD, Phan BA, Doan TP, Ogimoto K, Mirzadeh Z, et al. Leptin receptor neurons in the dorsomedial hypothalamus regulate diurnal patterns of feeding, locomotion, and metabolism. Elmquist JK, Wassum KM, editors. Elife. eLife Sciences Publications, Ltd; 2021;10: e63671. doi:10.7554/eLife.63671
85. Jäkel S, Dimou L. Glial Cells and Their Function in the Adult Brain: A Journey through the History of Their Ablation [Internet]. Frontiers in Cellular Neuroscience . 2017. p. 24. Available: https://www.frontiersin.org/article/10.3389/fncel.2017.00024
86. Manzoni C, Kia DA, Vandrovcova J, Hardy J, Wood NW, Lewis PA, et al. Genome, transcriptome and proteome: the rise of omics data and their integration in biomedical sciences. Brief Bioinform. Oxford University Press; 2018;19: 286–302. doi:10.1093/bib/bbw114
87. Cahoy JD, Emery B, Kaushal A, Foo LC, Zamanian JL, Christopherson KS, et al. A Transcriptome Database for Astrocytes, Neurons, and Oligodendrocytes: A New Resource for Understanding Brain Development and Function. J Neurosci. 2008;28: 264 LP – 278. doi:10.1523/JNEUROSCI.4178-07.2008
88. Zhang Y, Chen K, Sloan SA, Bennett ML, Scholze AR, O'Keeffe S, et al. An RNA-Sequencing Transcriptome and Splicing Database of Glia, Neurons, and Vascular Cells of the Cerebral Cortex. J Neurosci. 2014;34: 11929–11947. doi:10.1523/JNEUROSCI.1860-14.2014
89. Moyon S, Dubessy AL, Aigrot MS, Trotter M, Huang JK, Dauphinot L, et al.

Demyelination Causes Adult CNS Progenitors to Revert to an Immature State and Express Immune Cues That Support Their Migration. J Neurosci. 2015;35: 4–20. doi:10.1523/JNEUROSCI.0849-14.2015
90. Zeisel A, Munoz-Manchado AB, Codeluppi S, Lonnerberg P, La Manno G, Jureus A, et al. Cell types in the mouse cortex and hippocampus revealed by single-cell RNA-seq. Science (80-). 2015;347: 1138–1142. doi:10.1126/science.aaa1934
91. Marques S, Zeisel A, Codeluppi S, van Bruggen D, Mendanha Falcao A, Xiao L, et al. Oligodendrocyte heterogeneity in the mouse juvenile and adult central nervous system. Science (80-). 2016;352: 1326–1329. doi:10.1126/science.aaf6463
92. Marques S, van Bruggen D, Vanichkina DP, Floriddia EM, Munguba H, Väremo L, et al. Transcriptional Convergence of Oligodendrocyte Lineage Progenitors during Development. Dev Cell. 2018;46: 504-517.e7. doi:10.1016/j.devcel.2018.07.005
93. Chen R, Wu X, Jiang L, Zhang Y. Single-Cell RNA-Seq Reveals Hypothalamic Cell Diversity. Cell Rep. 2017;18: 3227–3241. doi:10.1016/j.celrep.2017.03.004
94. Sim FJ, Lang JK, Waldau B, Roy NS, Schwartz TE, Pilcher WH, et al. Complementary patterns of gene expression by human oligodendrocyte progenitors and their environment predict determinants of progenitor maintenance and differentiation. Ann Neurol. 2006;59: 763–779. doi:10.1002/ana.20812
95. Sim FJ, McClain CR, Schanz SJ, Protack TL, Windrem MS, Goldman SA. CD140a identifies a population of highly myelinogenic, migration-competent and efficiently engrafting human oligodendrocyte progenitor cells. Nat Biotechnol. 2011;29: 934–941. doi:10.1038/nbt.1972
96. Darmanis S, Sloan SA, Zhang Y, Enge M, Caneda C, Shuer LM, et al. A survey of human brain transcriptome diversity at the single cell level. Proc Natl Acad Sci. 2015;112: 7285–7290. doi:10.1073/pnas.1507125112
97. Spaethling JM, Na Y-J, Lee J, Ulyanova A V, Baltuch GH, Bell TJ, et al. Primary Cell Culture of Live Neurosurgically Resected Aged Adult Human Brain Cells and Single Cell Transcriptomics. Cell Rep. 2017;18: 791–803. doi:10.1016/j.celrep.2016.12.066
98. Habib N, Avraham-Davidi I, Basu A, Burks T, Shekhar K, Hofree M, et al. Massively parallel single-nucleus RNA-seq with DroNc-seq. Nat Methods. 2017;14: 955–958. doi:10.1038/nmeth.4407
99. La Manno G, Gyllborg D, Codeluppi S, Nishimura K, Salto C, Zeisel A, et al. Molecular Diversity of Midbrain Development in Mouse, Human, and Stem Cells. Cell. Cell Press; 2016;167: 566-580.e19. doi:10.1016/j.cell.2016.09.027
100. Lake BB, Chen S, Sos BC, Fan J, Kaeser GE, Yung YC, et al. Integrative single-cell analysis of transcriptional and epigenetic states in the human adult brain. Nat Biotechnol. 2018;36: 70–80. doi:10.1038/nbt.4038
101. Rio-Hortega P. THE MICROGLIA. Lancet. Elsevier; 1939;233: 1023–1026. doi:10.1016/S0140-6736(00)60571-8
102. Fujita S, Kitamura T. Origin of Brain Macrophages and the Nature of the So-Called Microglia BT - Malignant Lymphomas of the Nervous System: International Symposium. In: Jellinger K, Seitelberger F, editors. Berlin, Heidelberg: Springer Berlin Heidelberg; 1975. pp. 291–296. doi:10.1007/978-3-662-08456-4_51
103. Kitamura T, Miyake T, Fujita S. Genesis of resting microglia in the gray matter of mouse hippocampus. J Comp Neurol. John Wiley & Sons, Ltd; 1984;226: 421–433. doi:https://doi.org/10.1002/cne.902260310

104. De Groot CJA, Huppes W, Sminia T, Kraal G, Dijkstra CD. Determination of the origin and nature of brain macrophages and microglial cells in mouse central nervous system, using non-radioactive in situ hybridization and immunoperoxidase techniques. Glia. John Wiley & Sons, Ltd; 1992;6: 301–309. doi:https://doi.org/10.1002/glia.440060408
105. Matsumoto Y, Fujiwara M. Absence of donor-type major histocompatibility complex class I antigen-bearing microglia in the rat central nervous system of radiation bone marrow chimeras. J Neuroimmunol. Elsevier; 1987;17: 71–82. doi:10.1016/0165-5728(87)90032-4
106. Lassmann H, Schmied M, Vass K, Hickey WF. Bone marrow derived elements and resident microglia in brain inflammation. Glia. John Wiley & Sons, Ltd; 1993;7: 19–24. doi:https://doi.org/10.1002/glia.440070106
107. Priller J, Flügel A, Wehner T, Boentert M, Haas CA, Prinz M, et al. Targeting gene-modified hematopoietic cells to the central nervous system: Use of green fluorescent protein uncovers microglial engraftment. Nat Med. 2001;7: 1356–1361. doi:10.1038/nm1201-1356
108. Murabe Y, Sano Y. Morphological studies on neuroglia. Cell Tissue Res. 1982;225: 469–485. doi:10.1007/BF00214798
109. Hume DA, Perry VH, Gordon S. Immunohistochemical localization of a macrophage-specific antigen in developing mouse retina: phagocytosis of dying neurons and differentiation of microglial cells to form a regular array in the plexiform layers. J Cell Biol. The Rockefeller University Press; 1983;97: 253–257. doi:10.1083/jcb.97.1.253
110. Perry VH, Hume DA, Gordon S. Immunohistochemical localization of macrophages and microglia in the adult and developing mouse brain. Neuroscience. 1985;15: 313–326. doi:10.1016/0306-4522(85)90215-5
111. Akiyama H, McGeer PL. Brain microglia constitutively express β-2 integrins. J Neuroimmunol. Elsevier; 1990;30: 81–93. doi:10.1016/0165-5728(90)90055-R
112. Beers DR, Henkel JS, Xiao Q, Zhao W, Wang J, Yen AA, et al. Wild-type microglia extend survival in PU.1 knockout mice with familial amyotrophic lateral sclerosis. Proc Natl Acad Sci. 2006;103: 16021 LP – 16026. doi:10.1073/pnas.0607423103
113. van Furth R, Cohn ZA, Hirsch JG, Humphrey JH, Spector WG, Langevoort HL. The mononuclear phagocyte system: a new classification of macrophages, monocytes, and their precursor cells. Bull World Health Organ. 1972;46: 845–852. Available: https://pubmed.ncbi.nlm.nih.gov/4538544
114. Ginhoux F, Guilliams M. Tissue-Resident Macrophage Ontogeny and Homeostasis. Immunity. Elsevier; 2016;44: 439–449. doi:10.1016/j.immuni.2016.02.024
115. Prinz M, Jung S, Priller J. Microglia Biology: One Century of Evolving Concepts. Cell. Elsevier Inc.; 2019;179: 292–311. doi:10.1016/j.cell.2019.08.053
116. Ginhoux F, Greter M, Leboeuf M, Nandi S, See P, Gokhan S, et al. Fate Mapping Analysis Reveals That Adult Microglia Derive from Primitive Macrophages. Science (80-). 2010/10/21. 2010;330: 841–845. doi:10.1126/science.1194637
117. Mrdjen D, Pavlovic A, Hartmann FJ, Schreiner B, Utz SG, Leung BP, et al. High-Dimensional Single-Cell Mapping of Central Nervous System Immune Cells Reveals Distinct Myeloid Subsets in Health, Aging, and Disease. Immunity. Elsevier; 2018;48: 380-395.e6. doi:10.1016/j.immuni.2018.01.011
118. Schulz C, Perdiguero EG, Chorro L, Szabo-Rogers H, Cagnard N, Kierdorf K, et al. A Lineage of Myeloid Cells Independent of Myb and Hematopoietic Stem Cells. Science

(80-). 2012;336: 86–90. doi:10.1126/science.1219179
119. Goldmann T, Wieghofer P, Jordão MJC, Prutek F, Hagemeyer N, Frenzel K, et al. Origin, fate and dynamics of macrophages at central nervous system interfaces. Nat Immunol. 2016;17: 797–805. doi:10.1038/ni.3423
120. Lawson LJ, Perry VH, Dri P, Gordon S. Heterogeneity in the distribution and morphology of microglia in the normal adult mouse brain. Neuroscience. 1990;39: 151–170. doi:10.1016/0306-4522(90)90229-W
121. Grabert K, Michoel T, Karavolos MH, Clohisey S, Baillie JK, Stevens MP, et al. Microglial brain region−dependent diversity and selective regional sensitivities to aging. Nat Neurosci. 2016;19: 504–516. doi:10.1038/nn.4222
122. De S, Van Deren D, Peden E, Hockin M, Boulet A, Titen S, et al. Two distinct ontogenies confer heterogeneity to mouse brain microglia. Development. 2018;145. doi:10.1242/dev.152306
123. Hutchins KD, Dickson DW, Rashbaum WK, Lyman WD. Localization of morphologically distinct microglial populations in the developing human fetal brain: implications for ontogeny. Dev Brain Res. 1990;55: 95–102. doi:10.1016/0165-3806(90)90109-C
124. Menassa DA, Gomez-Nicola D. Microglial Dynamics During Human Brain Development. Front Immunol. 2018;9. doi:10.3389/fimmu.2018.01014
125. Rezaie P, Dean A, Male D, Ulfig N. Microglia in the Cerebral Wall of the Human Telencephalon at Second Trimester. Cereb Cortex. 2005;15: 938–949. doi:10.1093/cercor/bhh194
126. Kracht L, Borggrewe M, Eskandar S, Brouwer N, Chuva de Sousa Lopes SM, Laman JD, et al. Human fetal microglia acquire homeostatic immune-sensing properties early in development. Science (80-). 2020;369: 530–537. doi:10.1126/science.aba5906
127. Elmore MRP, Najafi AR, Koike MA, Dagher NN, Spangenberg EE, Rice RA, et al. Colony-Stimulating Factor 1 Receptor Signaling Is Necessary for Microglia Viability, Unmasking a Microglia Progenitor Cell in the Adult Brain. Neuron. 2014;82: 380–397. doi:https://doi.org/10.1016/j.neuron.2014.02.040
128. Wang Y, Szretter KJ, Vermi W, Gilfillan S, Rossini C, Cella M, et al. IL-34 is a tissue-restricted ligand of CSF1R required for the development of Langerhans cells and microglia. Nat Immunol. 2012;13: 753–760. doi:10.1038/ni.2360
129. Kana V, Desland FA, Casanova-Acebes M, Ayata P, Badimon A, Nabel E, et al. CSF-1 controls cerebellar microglia and is required for motor function and social interaction. J Exp Med. 2019;216: 2265–2281. doi:10.1084/jem.20182037
130. Utz SG, See P, Mildenberger W, Thion MS, Silvin A, Lutz M, et al. Early Fate Defines Microglia and Non-parenchymal Brain Macrophage Development. Cell. Elsevier Inc.; 2020;181: 557-573.e18. doi:10.1016/j.cell.2020.03.021
131. Askew K, Li K, Olmos-Alonso A, Garcia-Moreno F, Liang Y, Richardson P, et al. Coupled Proliferation and Apoptosis Maintain the Rapid Turnover of Microglia in the Adult Brain. Cell Rep. 2017;18: 391–405. doi:10.1016/j.celrep.2016.12.041
132. Nikodemova M, Kimyon RS, De I, Small AL, Collier LS, Watters JJ. Microglial numbers attain adult levels after undergoing a rapid decrease in cell number in the third postnatal week. J Neuroimmunol. Elsevier B.V.; 2015;278: 280–288. doi:10.1016/j.jneuroim.2014.11.018
133. Lawson LJ, Perry VH, Gordon S. Turnover of resident microglia in the normal adult

mouse brain. Neuroscience. 1992;48: 405–415. doi:https://doi.org/10.1016/0306-4522(92)90500-2
134. Bruttger J, Karram K, Wörtge S, Regen T, Marini F, Hoppmann N, et al. Genetic Cell Ablation Reveals Clusters of Local Self-Renewing Microglia in the Mammalian Central Nervous System. Immunity. 2015;43: 92–106. doi:10.1016/j.immuni.2015.06.012
135. Gomez-Nicola D, Perry VH. Microglial Dynamics and Role in the Healthy and Diseased Brain: A Paradigm of Functional Plasticity. Neurosci. SAGE Publications Inc STM; 2014;21: 169–184. doi:10.1177/1073858414530512
136. Hashimoto D, Chow A, Noizat C, Teo P, Beasley MB, Leboeuf M, et al. Tissue-Resident Macrophages Self-Maintain Locally throughout Adult Life with Minimal Contribution from Circulating Monocytes. Immunity. 2013;38: 792–804. doi:10.1016/j.immuni.2013.04.004
137. Tay TL, Mai D, Dautzenberg J, Fernández-Klett F, Lin G, Sagar, et al. A new fate mapping system reveals context-dependent random or clonal expansion of microglia. Nat Neurosci. 2017;20: 793–803. doi:10.1038/nn.4547
138. Matcovitch-Natan O, Winter DR, Giladi A, Vargas Aguilar S, Spinrad A, Sarrazin S, et al. Microglia development follows a stepwise program to regulate brain homeostasis. Science (80-). 2016;353: aad8670–aad8670. doi:10.1126/science.aad8670
139. Lenz KM, Nelson LH. Microglia and Beyond: Innate Immune Cells As Regulators of Brain Development and Behavioral Function [Internet]. Frontiers in Immunology . 2018. p. 698. Available: https://www.frontiersin.org/article/10.3389/fimmu.2018.00698
140. Bennett FC, Bennett ML, Yaqoob F, Mulinyawe SB, Grant GA, Hayden Gephart M, et al. A Combination of Ontogeny and CNS Environment Establishes Microglial Identity. Neuron. Elsevier; 2018;98: 1170-1183.e8. doi:10.1016/j.neuron.2018.05.014
141. Frost JL, Schafer DP. Microglia: Architects of the Developing Nervous System. Trends Cell Biol. Elsevier; 2016;26: 587–597. doi:10.1016/j.tcb.2016.02.006
142. Sedel F. Macrophage-Derived Tumor Necrosis Factor , an Early Developmental Signal for Motoneuron Death. J Neurosci. 2004;24: 2236–2246. doi:10.1523/JNEUROSCI.4464-03.2004
143. Tremblay M-È, Lowery RL, Majewska AK. Microglial Interactions with Synapses Are Modulated by Visual Experience. Dalva M, editor. PLoS Biol. Public Library of Science; 2010;8: e1000527. doi:10.1371/journal.pbio.1000527
144. Andoh M, Ikegaya Y, Koyama R. Synaptic Pruning by Microglia in Epilepsy. J Clin Med. 2019;8: 2170. doi:10.3390/jcm8122170
145. Xu Z-X, Kim GH, Tan J-W, Riso AE, Sun Y, Xu EY, et al. Elevated protein synthesis in microglia causes autism-like synaptic and behavioral aberrations. Nat Commun. 2020;11: 1797. doi:10.1038/s41467-020-15530-3
146. Sellgren CM, Gracias J, Watmuff B, Biag JD, Thanos JM, Whittredge PB, et al. Increased synapse elimination by microglia in schizophrenia patient-derived models of synaptic pruning. Nat Neurosci. Springer US; 2019;22: 374–385. doi:10.1038/s41593-018-0334-7
147. Ueno M, Fujita Y, Tanaka T, Nakamura Y, Kikuta J, Ishii M, et al. Layer V cortical neurons require microglial support for survival during postnatal development. Nat Neurosci. 2013;16: 543–551. doi:10.1038/nn.3358
148. Hagemeyer N, Hanft KM, Akriditou MA, Unger N, Park ES, Stanley ER, et al. Microglia contribute to normal myelinogenesis and to oligodendrocyte progenitor maintenance during adulthood. Acta Neuropathol. Springer Berlin Heidelberg; 2017;134: 441–458.

doi:10.1007/s00401-017-1747-1
149. Wlodarczyk A, Holtman IR, Krueger M, Yogev N, Bruttger J, Khorooshi R, et al. A novel microglial subset plays a key role in myelinogenesis in developing brain. EMBO J. 2017;36: 3292–3308. doi:10.15252/embj.201696056
150. Lloyd AF, Davies CL, Holloway RK, Labrak Y, Ireland G, Carradori D, et al. Central nervous system regeneration is driven by microglia necroptosis and repopulation. Nat Neurosci. 2019;22: 1046–1052. doi:10.1038/s41593-019-0418-z
151. Nimmerjahn A. Resting Microglial Cells Are Highly Dynamic Surveillants of Brain Parenchyma in Vivo. Science (80-). 2005;308: 1314–1318. doi:10.1126/science.1110647
152. Jung S, Aliberti J, Graemmel P, Sunshine MJ, Kreutzberg GW, Sher A, et al. Analysis of Fractalkine Receptor CX 3 CR1 Function by Targeted Deletion and Green Fluorescent Protein Reporter Gene Insertion. Mol Cell Biol. American Society for Microbiology; 2000;20: 4106–4114. doi:10.1128/MCB.20.11.4106-4114.2000
153. Tremblay M-E, Stevens B, Sierra A, Wake H, Bessis A, Nimmerjahn A. The Role of Microglia in the Healthy Brain. J Neurosci. 2011;31: 16064–16069. doi:10.1523/JNEUROSCI.4158-11.2011
154. Galloway DA, Phillips AEM, Owen DRJ, Moore CS. Phagocytosis in the Brain: Homeostasis and Disease [Internet]. Frontiers in Immunology . 2019. p. 790. Available: https://www.frontiersin.org/article/10.3389/fimmu.2019.00790
155. Fourgeaud L, Través PG, Tufail Y, Leal-Bailey H, Lew ED, Burrola PG, et al. TAM receptors regulate multiple features of microglial physiology. Nature. 2016;532: 240–244. doi:10.1038/nature17630
156. De Biase LM, Schuebel KE, Fusfeld ZH, Jair K, Hawes IA, Cimbro R, et al. Local Cues Establish and Maintain Region-Specific Phenotypes of Basal Ganglia Microglia. Neuron. Elsevier Inc.; 2017;95: 341-356.e6. doi:10.1016/j.neuron.2017.06.020
157. Masuda T, Prinz M. Microglia: A Unique Versatile Cell in the Central Nervous System. ACS Chem Neurosci. 2016;7: 428–434. doi:10.1021/acschemneuro.5b00317
158. Hanisch U-K. Functional diversity of microglia – how heterogeneous are they to begin with? [Internet]. Frontiers in Cellular Neuroscience . 2013. p. 65. Available: https://www.frontiersin.org/article/10.3389/fncel.2013.00065
159. Sharma K, Schmitt S, Bergner CG, Tyanova S, Kannaiyan N, Manrique-Hoyos N, et al. Cell type– and brain region–resolved mouse brain proteome. Nat Neurosci. 2015;18: 1819–1831. doi:10.1038/nn.4160
160. Ren L, Lubrich B, Biber K, Gebicke-Haerter PJ. Differential expression of inflammatory mediators in rat microglia cultured from different brain regions. Mol Brain Res. 1999;65: 198–205. doi:10.1016/S0169-328X(99)00016-9
161. Ayata P, Badimon A, Strasburger HJ, Duff MK, Montgomery SE, Loh Y-HE, et al. Epigenetic regulation of brain region-specific microglia clearance activity. Nat Neurosci. Springer US; 2018;21: 1049–1060. doi:10.1038/s41593-018-0192-3
162. Doorn KJ, Brevé JJP, Drukarch B, Boddeke HW, Huitinga I, Lucassen PJ, et al. Brain region-specific gene expression profiles in freshly isolated rat microglia [Internet]. Frontiers in Cellular Neuroscience . 2015. p. 84. Available: https://www.frontiersin.org/article/10.3389/fncel.2015.00084
163. Goldmann T, Zeller N, Raasch J, Kierdorf K, Frenzel K, Ketscher L, et al. <scp>USP</scp> 18 lack in microglia causes destructive interferonopathy of the mouse brain. EMBO J. 2015/04/20. BlackWell Publishing Ltd; 2015;34: 1612–1629.

doi:10.15252/embj.201490791
164. Hammond TR, Dufort C, Dissing-Olesen L, Giera S, Young A, Wysoker A, et al. Single-Cell RNA Sequencing of Microglia throughout the Mouse Lifespan and in the Injured Brain Reveals Complex Cell-State Changes. Immunity. Elsevier Inc.; 2019;50: 253-271.e6. doi:10.1016/j.immuni.2018.11.004
165. Li Q, Cheng Z, Zhou L, Darmanis S, Neff NF, Okamoto J, et al. Developmental Heterogeneity of Microglia and Brain Myeloid Cells Revealed by Deep Single-Cell RNA Sequencing. Neuron. Elsevier Inc.; 2019;101: 207-223.e10. doi:10.1016/j.neuron.2018.12.006
166. Keren-Shaul H, Spinrad A, Weiner A, Matcovitch-Natan O, Dvir-Szternfeld R, Ulland TK, et al. A Unique Microglia Type Associated with Restricting Development of Alzheimer's Disease. Cell. Elsevier; 2017;169: 1276-1290.e17. doi:10.1016/j.cell.2017.05.018
167. Olah M, Menon V, Habib N, Taga MF, Ma Y, Yung CJ, et al. Single cell RNA sequencing of human microglia uncovers a subset associated with Alzheimer's disease. Nat Commun. 2020;11: 6129. doi:10.1038/s41467-020-19737-2
168. Xu YKT, Chitsaz D, Brown RA, Cui QL, Dabarno MA, Antel JP, et al. Deep learning for high-throughput quantification of oligodendrocyte ensheathment at single-cell resolution. Commun Biol. 2019;2: 116. doi:10.1038/s42003-019-0356-z
169. Sim FJ, Windrem MS, Goldman SA. Fate determination of adult human glial progenitor cells. Neuron Glia Biol. 2009/10/07. Cambridge University Press; 2009;5: 45–55. doi:DOI: 10.1017/S1740925X09990317
170. Dugas JC, Tai YC, Speed TP, Ngai J, Barres BA. Functional Genomic Analysis of Oligodendrocyte Differentiation. J Neurosci. 2006;26: 10967 LP – 10983. doi:10.1523/JNEUROSCI.2572-06.2006
171. Cahoy JD, Emery B, Kaushal A, Foo LC, Zamanian JL, Christopherson KS, et al. A Transcriptome Database for Astrocytes, Neurons, and Oligodendrocytes: A New Resource for Understanding Brain Development and Function. J Neurosci. 2008;28: 264–278. doi:10.1523/JNEUROSCI.4178-07.2008
172. Ruffini F, Arbour N, Blain M, Olivier A, Antel JP. Distinctive Properties of Human Adult Brain-Derived Myelin Progenitor Cells. Am J Pathol. 2004;165: 2167–2175. doi:https://doi.org/10.1016/S0002-9440(10)63266-X
173. Cui Q-L, Kuhlmann T, Miron VE, Leong SY, Fang J, Gris P, et al. Oligodendrocyte Progenitor Cell Susceptibility to Injury in Multiple Sclerosis. Am J Pathol. 2013;183: 516–525. doi:https://doi.org/10.1016/j.ajpath.2013.04.016
174. Couturier CP, Ayyadhury S, Le PU, Nadaf J, Monlong J, Riva G, et al. Single-cell RNA-seq reveals that glioblastoma recapitulates a normal neurodevelopmental hierarchy. Nat Commun. 2020;11: 3406. doi:10.1038/s41467-020-17186-5
175. Ilicic T, Kim JK, Kolodziejczyk AA, Bagger FO, McCarthy DJ, Marioni JC, et al. Classification of low quality cells from single-cell RNA-seq data. Genome Biol. 2016;17: 29. doi:10.1186/s13059-016-0888-1
176. Stuart T, Butler A, Hoffman P, Hafemeister C, Papalexi E, Mauck WM, et al. Comprehensive Integration of Single-Cell Data. Cell. Elsevier Inc.; 2019;177: 1888-1902.e21. doi:10.1016/j.cell.2019.05.031
177. Haghverdi L, Büttner M, Wolf FA, Buettner F, Theis FJ. Diffusion pseudotime robustly reconstructs lineage branching. Nat Methods. 2016;13: 845–848. doi:10.1038/nmeth.3971

178. Moon KR, van Dijk D, Wang Z, Gigante S, Burkhardt DB, Chen WS, et al. Visualizing structure and transitions in high-dimensional biological data. Nat Biotechnol. 2019;37: 1482–1492. doi:10.1038/s41587-019-0336-3
179. Szklarczyk D, Franceschini A, Kuhn M, Simonovic M, Roth A, Minguez P, et al. The STRING database in 2011: Functional interaction networks of proteins, globally integrated and scored. Nucleic Acids Res. 2011;39: 561–568. doi:10.1093/nar/gkq973
180. Kuleshov M V, Jones MR, Rouillard AD, Fernandez NF, Duan Q, Wang Z, et al. Enrichr: a comprehensive gene set enrichment analysis web server 2016 update. Nucleic Acids Res. Oxford University Press; 2016;44: W90–W97. doi:10.1093/nar/gkw377
181. Saito R, Smoot ME, Ono K, Ruscheinski J, Wang P-L, Lotia S, et al. A travel guide to Cytoscape plugins. Nat Meth. Nature Publishing Group, a division of Macmillan Publishers Limited. All Rights Reserved.; 2012;9: 1069–1076. Available: http://dx.doi.org/10.1038/nmeth.2212
182. Scardoni G, Petterlini M, Laudanna C. Analyzing biological network parameters with CentiScaPe. Bioinformatics. 2009;25: 2857–2859. doi:10.1093/bioinformatics/btp517
183. Lambert SA, Jolma A, Campitelli LF, Das PK, Yin Y, Albu M, et al. The Human Transcription Factors. Cell. 2018;172: 650–665. doi:https://doi.org/10.1016/j.cell.2018.01.029
184. Miller RH. Regulation of oligodendrocyte development in the vertebrate CNS. Prog Neurobiol. 2002;67: 451–467. doi:10.1016/S0301-0082(02)00058-8
185. Artegiani B, Lyubimova A, Muraro M, van Es JH, van Oudenaarden A, Clevers H. A Single-Cell RNA Sequencing Study Reveals Cellular and Molecular Dynamics of the Hippocampal Neurogenic Niche. Cell Rep. 2017;21: 3271–3284. doi:10.1016/j.celrep.2017.11.050
186. Liu K, Lin B, Zhao M, Yang X, Chen M, Gao A, et al. The multiple roles for Sox2 in stem cell maintenance and tumorigenesis. Cell Signal. 2013;25: 1264–1271. doi:10.1016/j.cellsig.2013.02.013
187. Murtie JC, Macklin WB, Corfas G. Morphometric analysis of oligodendrocytes in the adult mouse frontal cortex. J Neurosci Res. John Wiley & Sons, Ltd; 2007;85: 2080–2086. doi:10.1002/jnr.21339
188. Vinet J, Lemieux P, Tamburri A, Tiesinga P, Scafidi J, Gallo V, et al. Subclasses of oligodendrocytes populate the mouse hippocampus. Eur J Neurosci. John Wiley & Sons, Ltd; 2010;31: 425–438. doi:10.1111/j.1460-9568.2010.07082.x
189. Chong SYC, Rosenberg SS, Fancy SPJ, Zhao C, Shen Y-AA, Hahn AT, et al. Neurite outgrowth inhibitor Nogo-A establishes spatial segregation and extent of oligodendrocyte myelination. Proc Natl Acad Sci. 2012;109: 1299–1304. doi:10.1073/pnas.1113540109
190. Floriddia EM, Lourenço T, Zhang S, van Bruggen D, Hilscher MM, Kukanja P, et al. Distinct oligodendrocyte populations have spatial preference and different responses to spinal cord injury. Nat Commun. 2020;11: 5860. doi:10.1038/s41467-020-19453-x
191. Hilscher MM, Langseth CM, Kukanja P, Yokota C, Floriddia E, Nilsson M, et al. Spatial cell type mapping of the oligodendrocyte lineage in the mouse juvenile and adult CNS with in situ sequencing. bioRxiv. 2021; 2021.06.04.447052. Available: https://doi.org/10.1101/2021.06.04.447052
192. Hayashi C, Suzuki N. Heterogeneity of Oligodendrocytes and Their Precursor Cells. In: Sango K, Yamauchi J, Ogata T, Susuki K, editors. Singapore: Springer Singapore; 2019. pp. 53–62. doi:10.1007/978-981-32-9636-7_5

193. van den Brink SC, Sage F, Vértesy Á, Spanjaard B, Peterson-Maduro J, Baron CS, et al. Single-cell sequencing reveals dissociation-induced gene expression in tissue subpopulations. Nat Methods. 2017;14: 935–936. doi:10.1038/nmeth.4437
194. Zappia L, Oshlack A. Clustering trees: a visualization for evaluating clusterings at multiple resolutions. Gigascience. 2018;7. doi:10.1093/gigascience/giy083
195. Aibar S, González-Blas CB, Moerman T, Huynh-Thu VA, Imrichova H, Hulselmans G, et al. SCENIC: single-cell regulatory network inference and clustering. Nat Methods. 2017;14: 1083–1086. doi:10.1038/nmeth.4463
196. Abbasi S, Sinha S, Labit E, Rosin NL, Yoon G, Rahmani W, et al. Distinct Regulatory Programs Control the Latent Regenerative Potential of Dermal Fibroblasts during Wound Healing. Cell Stem Cell. Elsevier; 2021;28: 581–583. doi:10.1016/j.stem.2021.02.004
197. Leek JT, Johnson WE, Parker HS, Jaffe AE, Storey JD. The sva package for removing batch effects and other unwanted variation in high-throughput experiments. Bioinformatics. 2012/01/17. Oxford University Press; 2012;28: 882–883. doi:10.1093/bioinformatics/bts034
198. Subramanian A, Tamayo P, Mootha VK, Mukherjee S, Ebert BL, Gillette MA, et al. Gene set enrichment analysis: A knowledge-based approach for interpreting genome-wide expression profiles. Proc Natl Acad Sci. 2005;102: 15545–15550. doi:10.1073/pnas.0506580102
199. Sanyal R, Polyak MJ, Zuccolo J, Puri M, Deng L, Roberts L, et al. MS4A4A: a novel cell surface marker for M2 macrophages and plasma cells. Immunol Cell Biol. 2017;95: 611–619. doi:10.1038/icb.2017.18
200. Marín-Teva JL, Dusart I, Colin C, Gervais A, van Rooijen N, Mallat M. Microglia Promote the Death of Developing Purkinje Cells. Neuron. 2004;41: 535–547. doi:10.1016/S0896-6273(04)00069-8
201. Milovanovic J, Arsenijevic A, Stojanovic B, Kanjevac T, Arsenijevic D, Radosavljevic G, et al. Interleukin-17 in Chronic Inflammatory Neurological Diseases. Front Immunol. 2020;11: 1–15. doi:10.3389/fimmu.2020.00947
202. Lipfert J, Ödemis V, Wagner D-C, Boltze J, Engele J. CXCR4 and CXCR7 form a functional receptor unit for SDF-1/CXCL12 in primary rodent microglia. Neuropathol Appl Neurobiol. John Wiley & Sons, Ltd; 2013;39: 667–680. doi:10.1111/nan.12015
203. Inoue T, Yamakage H, Tanaka M, Kusakabe T, Shimatsu A, Satoh-Asahara N. Oxytocin Suppresses Inflammatory Responses Induced by Lipopolysaccharide through Inhibition of the eIF-2α–ATF4 Pathway in Mouse Microglia. Cells. MDPI; 2019;8: 527. doi:10.3390/cells8060527
204. Dutta S, Sengupta P. Men and mice: Relating their ages. Life Sci. 2016;152: 244–248. doi:10.1016/j.lfs.2015.10.025
205. Gosselin D, Skola D, Coufal NG, Holtman IR, Schlachetzki JCM, Sajti E, et al. An environment-dependent transcriptional network specifies human microglia identity. Science (80-). 2017;356: 1248–1259. doi:10.1126/science.aal3222
206. Semple BD, Blomgren K, Gimlin K, Ferriero DM, Noble-Haeusslein LJ. Brain development in rodents and humans: Identifying benchmarks of maturation and vulnerability to injury across species. Prog Neurobiol. 2013;106–107: 1–16. doi:10.1016/j.pneurobio.2013.04.001
207. Roy NS, Wang S, Harrison-Restelli C, Benraiss A, Fraser RAR, Gravel M, et al. Identification, Isolation, and Promoter-Defined Separation of Mitotic Oligodendrocyte

Progenitor Cells from the Adult Human Subcortical White Matter. J Neurosci. 1999;19: 9986 LP – 9995. doi:10.1523/JNEUROSCI.19-22-09986.1999
208. Nunes MC, Roy NS, Keyoung HM, Goodman RR, McKhann G, Jiang L, et al. Identification and isolation of multipotential neural progenitor cells from the subcortical white matter of the adult human brain. Nat Med. 2003;9: 439–447. doi:10.1038/nm837
209. Leong SY, Rao VTS, Bin JM, Gris P, Sangaralingam M, Kennedy TE, et al. Heterogeneity of oligodendrocyte progenitor cells in adult human brain. Ann Clin Transl Neurol. 2014;1: 272–283. doi:10.1002/acn3.55
210. Kuboyama K, Fujikawa A, Suzuki R, Noda M. Inactivation of Protein Tyrosine Phosphatase Receptor Type Z by Pleiotrophin Promotes Remyelination through Activation of Differentiation of Oligodendrocyte Precursor Cells. J Neurosci. 2015;35: 12162 LP – 12171. doi:10.1523/JNEUROSCI.2127-15.2015
211. McClain CR, Sim FJ, Goldman SA. Pleiotrophin Suppression of Receptor Protein Tyrosine Phosphatase-β/ζ Maintains the Self-Renewal Competence of Fetal Human Oligodendrocyte Progenitor Cells. J Neurosci. 2012;32: 15066 LP – 15075. doi:10.1523/JNEUROSCI.1320-12.2012
212. Pol SU, Polanco JJ, Seidman RA, O'Bara MA, Shayya HJ, Dietz KC, et al. Network-Based Genomic Analysis of Human Oligodendrocyte Progenitor Differentiation. Stem Cell Reports. 2017;9: 710–723. doi:https://doi.org/10.1016/j.stemcr.2017.07.007
213. Rone MB, Cui Q-L, Fang J, Wang L-C, Zhang J, Khan D, et al. Oligodendrogliopathy in Multiple Sclerosis: Low Glycolytic Metabolic Rate Promotes Oligodendrocyte Survival. J Neurosci. 2016;36: 4698 LP – 4707. doi:10.1523/JNEUROSCI.4077-15.2016
214. Chamberlain AJ, Vander Jagt CJ, Hayes BJ, Khansefid M, Marett LC, Millen CA, et al. Extensive variation between tissues in allele specific expression in an outbred mammal. BMC Genomics. 2015;16: 993. doi:10.1186/s12864-015-2174-0
215. Paschalidis N, Iqbal AJ, Maione F, Wood EG, Perretti M, Flower RJ, et al. Modulation of experimental autoimmune encephalomyelitis by endogenous Annexin A1. J Neuroinflammation. 2009;6: 33. doi:10.1186/1742-2094-6-33
216. Nakahara J, Seiwa C, Tan-Takeuchi K, Gotoh M, Kishihara K, Ogawa M, et al. Involvement of CD45 in central nervous system myelination. Neurosci Lett. 2005;379: 116–121. doi:https://doi.org/10.1016/j.neulet.2004.12.066
217. Falcão AM, van Bruggen D, Marques S, Meijer M, Jäkel S, Agirre E, et al. Disease-specific oligodendrocyte lineage cells arise in multiple sclerosis. Nat Med. 2018;24: 1837–1844. doi:10.1038/s41591-018-0236-y
218. Arbelaez CA, Glatigny S, Duhen R, Eberl G, Oukka M, Bettelli E. IL-7/IL-7 Receptor Signaling Differentially Affects Effector CD4⁺ T Cell Subsets Involved in Experimental Autoimmune Encephalomyelitis. J Immunol. 2015;195: 1974 LP – 1983. doi:10.4049/jimmunol.1403135
219. Tavakolpour S. Interleukin 7 receptor polymorphisms and the risk of multiple sclerosis: A meta-analysis. Mult Scler Relat Disord. 2016;8: 66–73. doi:https://doi.org/10.1016/j.msard.2016.05.001
220. Ehrlich M, Mozafari S, Glatza M, Starost L, Velychko S, Hallmann A-L, et al. Rapid and efficient generation of oligodendrocytes from human induced pluripotent stem cells using transcription factors. Proc Natl Acad Sci. 2017;114: E2243 LP-E2252. doi:10.1073/pnas.1614412114
221. Gundelfinger ED, Frischknecht R, Choquet D, Heine M. Converting juvenile into adult

plasticity: a role for the brain's extracellular matrix. Eur J Neurosci. John Wiley & Sons, Ltd; 2010;31: 2156–2165. doi:10.1111/j.1460-9568.2010.07253.x
222. Colognato H, Tzvetanova ID. Glia unglued: How signals from the extracellular matrix regulate the development of myelinating glia. Dev Neurobiol. John Wiley & Sons, Ltd; 2011;71: 924–955. doi:10.1002/dneu.20966
223. Segel M, Neumann B, Hill MFE, Weber IP, Viscomi C, Zhao C, et al. Niche stiffness underlies the ageing of central nervous system progenitor cells. Nature. 2019;573: 130–134. doi:10.1038/s41586-019-1484-9
224. Brose K, Tessier-Lavigne M. Slit proteins: key regulators of axon guidance, axonal branching, and cell migration. Curr Opin Neurobiol. 2000;10: 95–102. doi:10.1016/S0959-4388(99)00066-5
225. DeGeer J, Kaplan A, Mattar P, Morabito M, Stochaj U, Kennedy TE, et al. Hsc70 chaperone activity underlies Trio GEF function in axon growth and guidance induced by netrin-1. J Cell Biol. 2015;210: 817–832. doi:10.1083/jcb.201505084
226. Püschel AW. The function of semaphorins during nervous system development. Front Biosci. Abteilung Molekularbiologie, Institut fur Allgemeine Zoologie und Genetik, Westfalische Wilhelms-Universität, Schlobplatz 5, 48149 Münster, Germany.; 2003;8: 1080. doi:10.2741/1080
227. Henderson NT, Dalva MB. EphBs and ephrin-Bs: Trans-synaptic organizers of synapse development and function. Mol Cell Neurosci. 2018;91: 108–121. doi:10.1016/j.mcn.2018.07.002
228. Sun KLW, Correia JP, Kennedy TE. Netrins: versatile extracellular cues with diverse functions. Development. 2011;138: 2153–2169. doi:10.1242/dev.044529
229. Norris AD, Sundararajan L, Morgan DE, Roberts ZJ, Lundquist EA. The UNC-6/Netrin receptors UNC-40/DCC and UNC-5 inhibit growth cone filopodial protrusion via UNC-73/Trio, Rac-like GTPases and UNC-33/CRMP. Development. 2014;141: 4395–4405. doi:10.1242/dev.110437
230. Rajasekharan S, Baker KA, Horn KE, Jarjour AA, Antel JP, Kennedy TE. Netrin 1 and Dcc regulate oligodendrocyte process branching and membrane extension via Fyn and RhoA. Development. 2009;136: 415–426. doi:10.1242/dev.018234
231. Grünwald B, Schoeps B, Krüger A. Recognizing the Molecular Multifunctionality and Interactome of TIMP-1. Trends Cell Biol. 2019;29: 6–19. doi:10.1016/j.tcb.2018.08.006
232. Jones E V, Bouvier DS. Astrocyte-Secreted Matricellular Proteins in CNS Remodelling during Development and Disease. Bernardinelli Y, editor. Neural Plast. Hindawi Publishing Corporation; 2014;2014: 1–12. doi:10.1155/2014/321209
233. Reissner C, Runkel F, Missler M. Neurexins. Genome Biol. 2013;14: 213. doi:10.1186/gb-2013-14-9-213
234. Deng W, Wang H, Rosenberg PA, Volpe JJ, Jensen FE. Role of metabotropic glutamate receptors in oligodendrocyte excitotoxicity and oxidative stress. Proc Natl Acad Sci. 2004;101: 7751–7756. doi:10.1073/pnas.0307850101
235. Luyt K, Váradi A, Durant CF, Molnár E. Oligodendroglial metabotropic glutamate receptors are developmentally regulated and involved in the prevention of apoptosis. J Neurochem. John Wiley & Sons, Ltd; 2006;99: 641–656. doi:10.1111/j.1471-4159.2006.04103.x
236. Spitzer SO, Sitnikov S, Kamen Y, Evans KA, Kronenberg-Versteeg D, Dietmann S, et al. Oligodendrocyte Progenitor Cells Become Regionally Diverse and Heterogeneous with

Age. Neuron. 2019;101: 459-471.e5. doi:10.1016/j.neuron.2018.12.020
237. Ou Z, Sun Y, Lin L, You N, Liu X, Li H, et al. Olig2-Targeted G-Protein-Coupled Receptor Gpr17 Regulates Oligodendrocyte Survival in Response to Lysolecithin-Induced Demyelination. J Neurosci. 2016;36: 10560–10573. doi:10.1523/JNEUROSCI.0898-16.2016
238. Lingwood D, Simons K. Lipid Rafts As a Membrane-Organizing Principle. Science (80-). 2010;327: 46–50. doi:10.1126/science.1174621
239. Simons M, Krämer E-M, Thiele C, Stoffel W, Trotter J. Assembly of Myelin by Association of Proteolipid Protein with Cholesterol- and Galactosylceramide-Rich Membrane Domains. J Cell Biol. 2000;151: 143–154. doi:10.1083/jcb.151.1.143
240. Mathews ES, Mawdsley DJ, Walker M, Hines JH, Pozzoli M, Appel B. Mutation of 3-Hydroxy-3-Methylglutaryl CoA Synthase I Reveals Requirements for Isoprenoid and Cholesterol Synthesis in Oligodendrocyte Migration Arrest, Axon Wrapping, and Myelin Gene Expression. J Neurosci. 2014;34: 3402–3412. doi:10.1523/JNEUROSCI.4587-13.2014
241. Peckham H, Giuffrida L, Wood R, Gonsalvez D, Ferner A, Kilpatrick TJ, et al. Fyn is an intermediate kinase that BDNF utilizes to promote oligodendrocyte myelination. Glia. John Wiley & Sons, Ltd; 2016;64: 255–269. doi:10.1002/glia.22927
242. Sperber BR, Boyle-Walsh ÉA, Engleka MJ, Gadue P, Peterson AC, Stein PL, et al. A Unique Role for Fyn in CNS Myelination. J Neurosci. 2001;21: 2039–2047. doi:10.1523/JNEUROSCI.21-06-02039.2001
243. Krämer E-M, Klein C, Koch T, Boytinck M, Trotter J. Compartmentation of Fyn Kinase with Glycosylphosphatidylinositol-anchored Molecules in Oligodendrocytes Facilitates Kinase Activation during Myelination. J Biol Chem. Elsevier; 1999;274: 29042–29049. doi:10.1074/jbc.274.41.29042
244. Zhang S, Zhu X, Gui X, Croteau C, Song L, Xu J, et al. Sox2 Is Essential for Oligodendroglial Proliferation and Differentiation during Postnatal Brain Myelination and CNS Remyelination. J Neurosci. 2018;38: 1802–1820. doi:10.1523/JNEUROSCI.1291-17.2018
245. Lürbke A, Hagemeier K, Cui Q-L, Metz I, Brück W, Antel J, et al. Limited TCF7L2 Expression in MS Lesions. PLoS One. Public Library of Science; 2013;8: e72822. Available: https://doi.org/10.1371/journal.pone.0072822
246. Kiselev VY, Andrews TS, Hemberg M. Challenges in unsupervised clustering of single-cell RNA-seq data. Nat Rev Genet. 2019;20: 273–282. doi:10.1038/s41576-018-0088-9
247. Wang X, He Y, Zhang Q, Ren X, Zhang Z. Direct Comparative Analyses of 10X Genomics Chromium and Smart-seq2. Genomics Proteomics Bioinformatics. 2021; In press. doi:10.1016/j.gpb.2020.02.005
{